TECHNISCHE UNIVERSITÄT MÜNCHEN

Lehrstuhl II für Organische Chemie – Institute for Advanced Study

Synthesis of highly active and selective peptides and peptidomimetics

Burkhardt Laufer

Vollständiger Abdruck der von der Fakultät für Chemie der Technischen Universität München zur Erlangung des akademischen Grades eines

Doktors der Naturwissenschaften

genehmigten Dissertation.

Vorsitzender: Univ.-Prof. Dr. Steffen J. Glaser

Prüfer der Dissertation:

1. Univ.-Prof. Dr. Dr. h.c. Horst Kessler
2. Univ.-Prof. Dr. Aphrodite Kapurniotu
3. Univ.-Prof. Dr. Michael Groll

Die Dissertation wurde am 08.10.2009 bei der Technischen Universität München eingereicht und durch die Fakultät für Chemie am 22.10. 2009 angenommen.

–

für Juliane

Wer nichts als die Chemie versteht,

versteht auch die nicht recht.

Georg Christoph Lichtenberg (Sudelbücher)

Die vorliegende Arbeit wurde im Zeitraum von März 2006 bis September 2009 am Department Chemie der Technischen Universität München unter Anleitung von Prof. Dr. Horst Kessler angefertigt.

Danksagung

Meinem Doktorvater, Herrn Prof. Dr. **Horst Kessler** danke ich für all die interessanten Themen, an denen ich während meiner Promotion arbeiten durfte. Vor allem aber, möchte ich ihm für die Unterstützung, viele anregende wissenschaftliche und private Diskussionen, seinen Humor und seine Einstellung zur Doktorandenausbildung, die weit über das akademische hinaus geht und viel Wert auf das menschliche legt, danken.

Meinen drei Mentoren im Bereich Synthese, Dr. **Sebastian Knör**, Dr. **Dominik Heckmann** und Prof. Dr. **Eric Biron** möchte ich auch nochmals herzlich danken. Ich habe von euch unglaublich viel gelernt. Danke vor allem aber auch für die schöne Zeit, die man über die Chemie hinaus miteinander hatte.

Dem NMR-Kompetenzteam, M. Sc. **Grit Kummerlöwe**, Dr. **Andreas O. Frank** und Dr. **Andreas Enthart** sei ebenfals herzlichst für all die Erklärungen und die Geduld mit einem dummen Synthetiker gedankt.

Meinen Laborkollegen Dipl. Chem. **Stefanie Neubauer**, M. Sc. **Florian Rechenmacher**, Dr. **Jayanta Chatterjee**, M. Sc. **Florian Opperer**, Dr. **Clemens Wagner**, Dr. **Timo Weide** und M. Sc. **Thomas Neubauer** möchte ich für die gute und oft äußerst amüsante Laboratmosphäre danken.

Für hervorragende Zusammenarbeit auf dem CXCR4-Projekt danke ich Dr. **Norman Koglin** und Dr. **Margret Schottelius**. Ebenso danke ich Dr. **Monica Lopez-Garcia**, Dr. **Luciana Marinelli**, Dr. **Ettore Novellino**, Dr. **Roland Stragies**, Dr. **Frank Osterkamp**, Dr. **Grit Zahn** und **Dörte Vossmeyer** für die gute Zusammenarbeit beim Integrin-Projekt.

Für die sehr nette und lehrreiche Betreuung, viel Unterstützung und philosophische Aspekte während der biologischen Tests in Leuven danke ich Dr. **Abdellah Benhida**, Dr. **Sabrina C. Grailly** und Prof. Dr. **Jean-Marie Saint-Rémy**.

Für meinen wunderbaren Aufenthalt in San Diego danke ich der ganzen Finn-Group, im Speziellen aber Dr. **Michael Baksh**, Dr. **Nicole F. Steinmetz**, **Vu Hong**, Prof. Dr. **M.G. Finn** und **Laurie Smith** sowie **Elisabeth A. Stein**.

Mein besonderer Dank gilt all den Freunden, die ich während meiner Arbeit im AK Kessler gefunden habe, für eine wunderbare Zeit, die ich im Arbeitskreis verbringen durfte (in chronologischer Reihenfolge):

The following publications resulted from the work of this Ph. D. thesis:

1. S. Knör, B. Laufer, H. Kessler. Efficient Enantionselective Synthesis of Condensed and Aromatic-Ring-Substituted Tyrosine Derivatives, *J. Org. Chem.* **2006**, *71 (15)*, 5625-5630.

2. S. Knör, A. Khrenov, B. Laufer, E. L. Saenko, C. A. E. Hauser, H. Kessler. Depelopment of a Peptidomimetic Ligand for Efficient Isolation and Purification of Factor VIII via Affinity Chromatography, *J. Med. Chem.* **2007**, *50 (18)*, 4329-4339.

3. S. Knör, A. Khrenov, B. Laufer, A. Benhida, S. C. Grailly, R. Schwaab, J. Oldenburg, N. Beaufort, V. Magdolen, J.-M. Saint-Rémy, E. L. Saenko, C. A. E. Hauser, H. Kessler. Efficient factor VIII affinity purification using a small synthetic ligand, *J. Thromb. Haem.* **2008**, *6 (3)*, 470-477.

4. D. Heckmann, A. Meyer, B. Laufer, G. Zahn, R. Stragies, H. Kessler. Rational design of highly active and selective ligands for the $\alpha5\beta1$ integrin receptor, *ChemBioChem* **2008**, *9 (9)*, 1397-1407.

5. G. Kummerlöwe, F. Halbach, B. Laufer, B. Luy. Precise Measurement of RDC's in water and DMSO based gels using a silicone rubber tube for tunable stretching, *Open Spectr. J.* **2008**, *2*, 29-33.

6. B. Laufer, J. Chatterjee, A. O. Frank, H. Kessler. Can *N*-methylated amino acids serve as substitutes for proline in conformational design of cyclic pentapeptides?, *J. Pept. Sci.* **2009**, *15 (3)*, 141-146.

7. D. Heckmann[*], B. Laufer[*], L. Marinelli, V. Limongelli, E. Novellino, G. Zahn, R. Stragies, H. Kessler. Breaking the Dogma of the Metal-Coordinating Carboxyl Group in Integrin Ligands: Introducing Hydroxamic Acids to the MIDAS to Tune Potency and Selectivity, *Angew. Chem. Int Ed.* **2009**, *48.* 4436-4440.

8. M. Schottelius[*], B. Laufer[*], H. Kessler, H.-J. Wester. Ligands for mapping $\alpha v \beta3$-integrin expression in vivo, *Acc. Chem. Res.*, *in press*.

The following patents resulted from the work of this Ph. D. thesis:

1. H.-J. Wester, N. Koglin, M. Schwaiger, H. Kessler, B. Laufer, O. Demmer, M. Anton, Cancer Imaging and Treatment, *PCT Int. Appl.* **2007** WO 2007096662.

---

[*] Equally contributing authors.

The following conference proceedings resulted from the work of this Ph. D. thesis:

1. B. Laufer, J. Chatterjee, A. O. Frank, H. Kessler. Making double-minded peptides strong-willed? The side-chain impact on the backbone conformation of N-methylated cyclic pentapeptides., *Adv. Exp. Med. Biol.* **2009**, *611*, 157-158.
2. S. Knör, B. Laufer, A. Khrenov, A. Benhida, S. C. Grailly, N. Beaufort, V. Magdolen, C. A. E. Hauser, E. L. Saenko, J.-M. Saint-Rémy, H. Kessler. Development of a small peptidomimetic affinity ligand for efficient purification of the large protein factor VIII, *Adv. Exp. Med. Biol.* **2009**, *611*, 151-152.

The following published poster abstracts resulted from the work of this Ph. D. thesis:

1. S. Knör, B. Laufer, A. Khrenov, A. Benhida, S. C. Grailly, N. Beaufort, V. Magdolen, C. A. E. Hauser, E. L. Saenko, J.-M. Saint-Rémy, H. Kessler. Development of a small molecule peptidomimetic affinity ligand for efficient purification of the large protein factor VIII, *Biopolymers* **2007**, *88 (4 Sp. Iss. SI)*, 582.
2. B. Laufer, J. Chatterjee, H. Kessler. Making double-minded peptides strong-willed? The side chain impact on the backbone conformation of N-methylated cyclic pentapeptides, *Biopolymers* **2007**, *88 (4 Sp. Iss. SI)*, 585.
3. H. Kessler, D. Heckmann, B. Laufer, E. Otto, G. Zahn, R. Stragies. New results in the RGD field, *J. Pept. Sci.* **2008**, *14 (8 Suppl. S.)*, 115-116.
4. B. Laufer, D. Heckmann, A. Meyer, L. Marinelli, S. Neubauer, G. Zahn, R. Stragies, H. Kessler. Rational Design of highly acitve and selective alpha 5 beta 1 integrin antagonists, *J. Pept. Sci.* **2008**, *14 (8 Suppl. S.)*, 144-145.
5. H. Kessler, D. Heckmann, B. Laufer, E. Otto, L. Marinelli, G. Zahn, R. Stragies. Unexpected new Results in the RGD Field, *Biopolymers* **2009**, *92 (4)*, 344.
6. B. Laufer, N. F. Steinmetz, V. Hong, M. Manchester, H. Kessler, M. G. Finn. Guiding VLP's the right Way: Coating of Virus Like Particles with Peptidic Integrin Ligands, *Biopolymers* **2009**, *92 (4)*, 323.

Abbreviations

Å	Ångstrom, 10^{-10} m
Ac	Acetyl-
ACN	Acetonitrile
ADDP	Azodicarboxylic dipiperidide
ADME	Absorption, distribution, metabolism, excretion
ADMIDAS	Adjacent metal induced adhesion site
Bn	Benzyl-
Boc	*tert*-Butyloxycarbonyl-
br.	Broad
Bu	Butyl
^{t}Bu	*tert*-Butyl
CAM	Cell adhesion molecule
Cbz	Benzyloxycarbonyl-
Conc.	Concentrated
COSY	Correlated spectroscopy
d	Doublet or days
δ	Chemical shift
1D, 2D, 3D	One / two / three- dimensional
DBU	1,8-Diazabicyclo[5.4.0]undec-7-ene
DCM	Dichloromethane
dd	Dublett of dubletts
dest.	Destilled
DDTC	Sodium *N,N*-diethyldithiocarbamate
DEAD	Diethyl azodicarboxylate
DIAD	Diisopropylazodicarboxylate
DIPEA	Diisopropylethylamine
DMA	*N,N*-Dimethylacetamide
DMAP	4-Dimethylaminopyridine
DMF	*N,N*-Dimethylformamide
DMSO	Dimethylsulfoxide
DPPA	Diphenylphosphoric acid azide
ECM	Extracellular matix
ESI-MS	Electrospray ionization mass spectrometry
Et	Ethyl-

FAK	Focal adhesion kinase
FV-XIII	Blood coagulation factors V-XIII
Fmoc	9-Fluorenylmethoxycarbonyl
Fn	Fibronectin
GC-MS	Gas chromatography mass spectroscopy
h	Hour
HATU	O-(7-Azabenzotriazol-1-yl)-N,N,N',N',-tetramethyluronium-hexafluorophosphat
HMBC	Heteronuclear multiple bond correlation
HMQC	Heteronuclear multiple quantum coherence
HMQC-COSY	Heteronuclear multiple quantum coherence with COSY-pulse sequence
HOAc	Acetic acid
HOAt	1-Hydroxy-7-azabenzotriazol
HOBt	1-Hydroxybenzotriazol
HPLC	High performance liquid chromatography
HSQC	Heteronuclear single quantum coherence
Hz	Hertz
H-Tic-OH	Tetrahydroisoquinolin-3-carbonxylic acid
IC	Inhibitory capacity
J	Scalar coupling constants
kDa	Kilodalton
KHMDS	Potassium hexamethyldisilazid
LC-MS	Liquid chromatography mass spectrometry
LIMBS	Ligand-induced metal ion dependent binding site
Ln	Laminin
m	Multiplett
M	Molar
Me	Methyl-
MeOH	Methanol
MHz	Megahertz
MIDAS	Metal ion dependent site
min.	Minutes
mL	Milliliter
mmol	Millimol
MS	Mass spectroscopy

MTBD	7-Methyl-1,5,7-triazabicyclo-[4.4.0]dec-5-en
MW	Molecular weight
$^N J$	Scalar coupling over n-bonds
N	Normal
NBS-Cl	*o*-Nitrobenzosulfonic acid chloride
NMM	*N*-Methylmorpholine
NMP	*N*-Methylpyrrolidone
NMR	Nuclear magnetic resonance
NOESY	Nuclear Overhauser enhancement spectroscopy
PBS	Phosphate buffered saline
Ph	Phenyl
ppm	Parts per million
q	Quartett
R_f	Retention factor
RGD	Arginine-Glycine-Aspartic acid
ROESY	Rotating frame nuclear Overhauser and exchange spectroscopy
R_t	Retention time
RT	Room temperature
s	Singulett
sat.	Saturated
SPPS	*Solid phase peptide synthesis*
t	Triplett
TBAF	Tributylammoniumfluorid
TBDPS	*Tert*.butyldiphenylsilyl
TBS	*Tert*.butyldimethylsilyl
TBTU	*O*-(1H-Benzotriazol-1-yl)-*N,N,N',N'*-tetramethyluronium-tetrafluoroborat
TCP	Tritylchlorid-Polystyrene-resin
TEA	Triethylamine
TFA	Trifluoroacetetic acid
TFE	Trifluoroethanol
THF	Tetrahydrofurane
TIPS	Triisopropylsilane
TLC	Thin layer chromatography
TMS	Trimethylsilyl-
TOCSY	Total correlation spectroscopy

UV	Ultraviolett
Vn	Vitronectin
vWF	*von Willebrand* Factor

Introduction

Peptides – as well as desoxyribonucleic acids (DNA) – can be considered as a code, life is using to write. While DNA is a rather simple code using only four different letters, proteins and peptides can be written out of 20 (or 22) different letters, the amino acids, respectively. It is quite tempting to consider this writing as simple as human writing. Nevertheless, it is not. Human writing is only two dimensional, it forms a kind of line, where words have a certain length and a height. Writing with peptides or proteins has to be seen in four dimensions: Three dimensions for the structure of the peptides or proteins and as a fourth dimension time, as peptides are made up out of the DNA code, fulfill their task and will be degraded enzymatically afterwards.

This fourth dimension gives nature a clear advantage compared with medicinal chemists as biological molecules do not have to fulfill the same standards, potential drugs need to have to be successful in clinical trials. Biological molecules are optimized towards the overall system. The latter ones expressed in the human body do not have to be as selective as a drug, as they are produced closely to their target and do not have any other "temptations" to bind to another binding pocket or to be bound unspecifically at e.g. serum albumin. Furthermore, they do not have to be enzymatically stable as their task will be fulfilled soon and they are wanted to be degraded afterwards not to cause any side effects. Finally, they do not have to be that active as there are no real competitors for the biological molecules since life does not try to compete with itself. At the early stages of embryogenesis, apoptosis competes against cell growth. Yet, even this process is not a real competition as it is a guided apoptosis for special cells not needed for the embryo and not a random cell death.

Due to all these advantages evolution paved the path for life to make things as simple as possible by "never changing a winning team". Consequently, structures that can be built up easily via enzymes in the human body are used for different purposes as often as possible only by subtle changes in the structure of the molecules, resulting in the so-called "privileged structures"[1,2]. For natural products, these structures can be found in e.g. the steroid backbone[3] (cholesterol, cholic acid, progesterone, testosterone, estradiol), benzodiazepines[1] or benzopyrans[4].

But there are also some peptides or peptide sequences that can be considered as privileged strucures[5]. The most famous representative of such a privileged sequence for cell adhesion is the RGD sequence which binds to integrin ligands and was misleadingly called "universal cell-recognition site"[6].
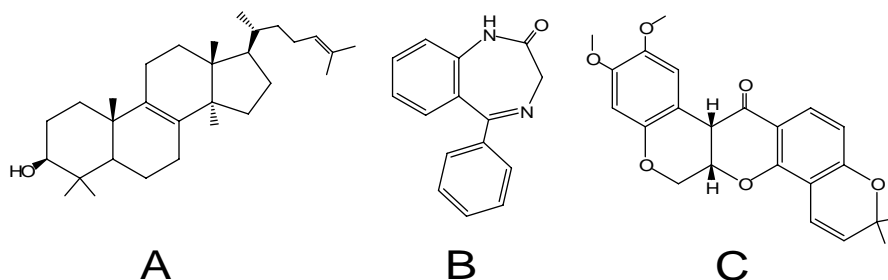
Figure 1: *Privileged structures used in medicinal chemistry. A: lanosterol, a member of the steroid family; B: 5-phenyl-1,4-benzodiazepin-2(3H)-one, a member of the benzodiazepine family; C: deguelin, a member of the benzopyran family.*

Using the RGD sequence in linear peptides only leads to unselective peptides which will be rapidly degraded by enzymes and only show poor biological activity[7]. On the other hand introduction of this sequence into cyclic penta- or hexapeptides can cause highly active and selective peptides that are stable towards degradation[8].

But in order to compete with nature a lot of things still have to be optimized as these cyclic compounds in most cases lack oral bioavailability and have to be given via injections which is highly unlikely in connection with normal drugs and will only be tolerated by pharmaceutical companies and afflicted patients for severe diseases such as e.g. anti-cancer therapeutics. To optimize compounds towards bioavailability or to screen just for compounds that might be orally available, C. A. Lipinski and D. F. Veber postulated some rules for properties, compounds should have to gain bioavailability[9,10]. These rules dramatically reduced the "chemical space" in which pharmaceutical companies searched for new lead structures for potential drugs. However, the finding that the natural product Cyclosporin A[11], a cyclic peptide containing eleven amino acids and seven *N*-methylated amide bonds violating all of the so-called Lipinski rules is bioavailable, focussed the attention on *N*-methylation of amide bonds to gain oral bioavailability[12].
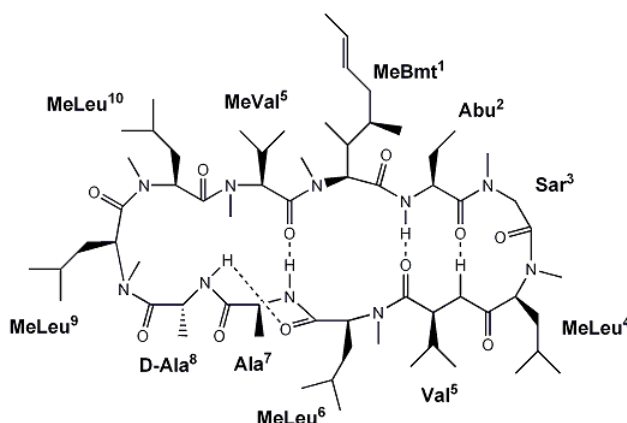
Figure 2: *Cyclosporin A[13].*

While the influence of cyclization on the structure of peptide sequences and also the influence of *N*-methylation towards the properties of the amide bonds have been known since many years[14-16] there is only little knowledge about the influence of *N*-methylated amide bonds on cyclic peptides[17,18].

Consequently, there is a high need for template structures to investigate the impact of *N*-methylation towards the effect on the structure and the bioavailability of such compounds and to try to make these influences predictable. Afterwards, these predictions will have to be transferred towards "real" peptide structures bearing side chain functionalities and to check if the template systems work.

A promising alternative to peptides is the synthesis of peptidomimetics. For this purpose only the pharmacophoric groups are kept while the rest of the amino acids can be replaced using any possibility that is desired or chemically achievable. Therefore peptidomimetics do not suffer from the restriction of having to use amino acids, they enlarge the possibilities of a fine-tuning of receptor selectivity, biological activity and pharmaco-kinetics dramatically by enabling diversity oriented synthesis. Additionally, the functionalization of these compounds for new applications such as surface coating or imaging becomes facilitated as functional groups can be introduced easily.
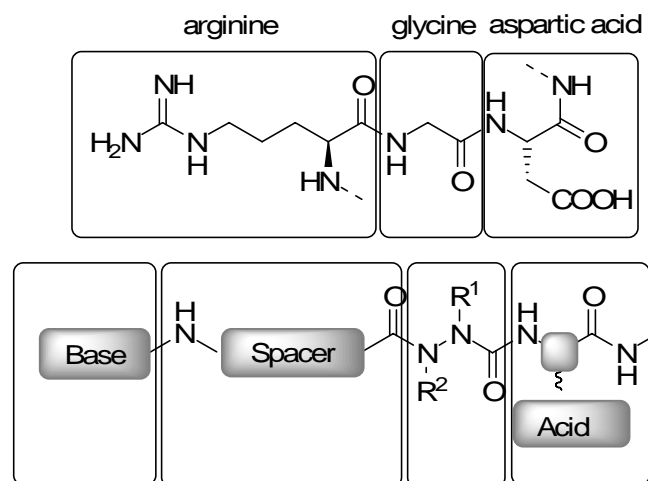
Figure 3: *Simplification of the RGD sequence (top) into four building blocks (bottom) with substitution of glycine by azaglycine.*

I   *N*-Methylation of Cyclic Peptides

I.1   *N-Methylated Template Structures*

I.1.1   Theoretical Background

I.1.1.1 Cyclic Peptides and Their Structural Properties

Many physiologically active peptides like hormones or neuro peptides have a relatively small active region consisting of four to five amino acids[14]. As structural changes in this region have the highest impact on biological activity, it's the main goal to fix the bioactive conformation according to the "key-lock-principle" of Emil Fischer saying that a ligand needs the ability to form a complex with its receptor[14,19-22]. On the other hand, the extended concept of „induced fit" proposes that receptors as well as hormones are capable to undergo conformational changes while complexation[23,24]. Using cyclisation of short peptide sequences enables fixation or stabilization of the biologically most active conformation and additionally adds enhanced metabolic stability as these cyclic peptides quite often do not fit any longer into the binding pockets of enzymes used for metabolism[22,25-27].
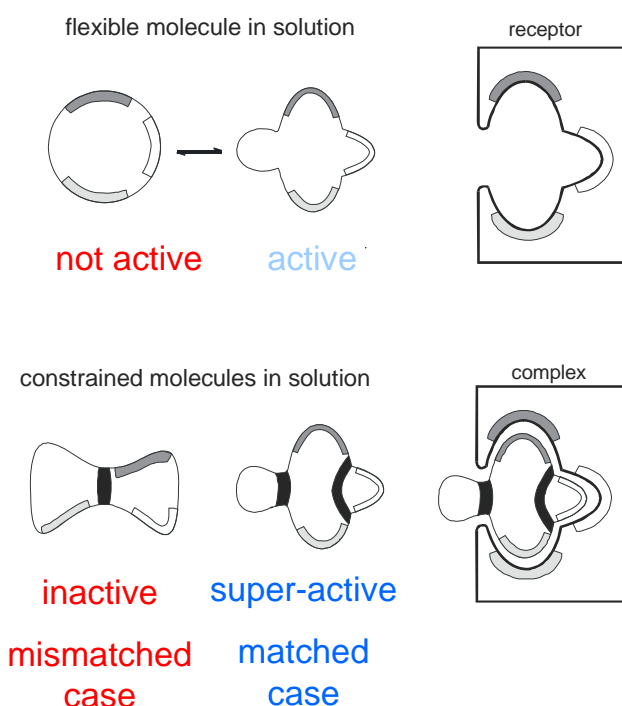
Figure 4*: Comparison of a flexible and a fixed molecule in solution[28].*

In most of the cases, cyclisation of peptides is performed through amide bonds or disulfide bridges via the cysteine side chain functionality. Depending on the position of the briding atoms in

the primary structure of the peptide, one speaks of head-to-tail-, backbone-, side-chain- or side-chain-backbone-cyclization[19,29-31].
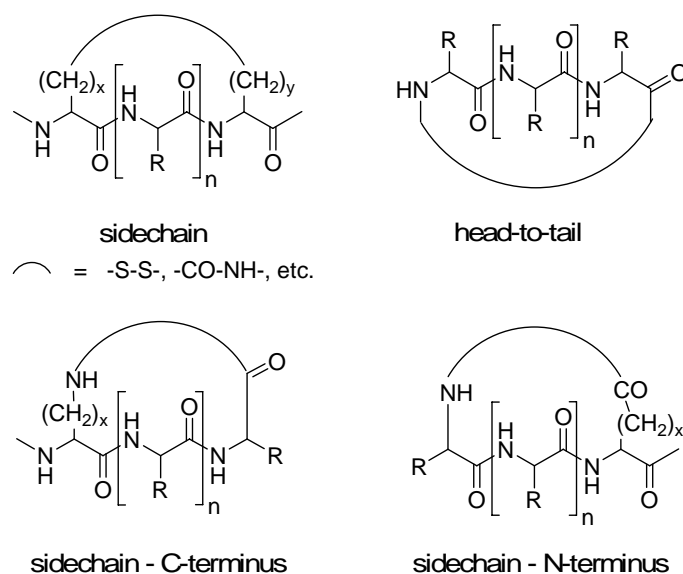
Figure 5: *Different kinds of cyclizations via amide bonds or disulfide bridges.*

However, the most intensively investigated cyclic peptides are the head-to-tail cyclized penta- and hexapeptides showing β- and γ-turn structures as their main features[14,32,33].

A typical β-turn is formed out of four amino acids having a hydrogen bond between the NH-group of the fourth amino acid (*i+3*) and the carbonyl group of the first amino acid (*i*) facilitating an antiparallel hairpin structure of the peptides (see Figure 6)[14].

For smaller acyclic and cyclic peptides, a γ-turn structure enables a hydrogen bond between the NH-group of the third (*i+2*) and the carbonyl group of the first amino acid (*i*)[14].

For β-turns, the structure is defined via the dihedral angles ϕ and ψ of (*i+1*) and (*i+2*) while for definition of a γ-turn the ϕ and ψ of (*i+1*) are sufficient[34]. Several different basic motives are known, just differing in their ϕ and ψ angles.

Table 1: *Φ- and Ψ-angles of ideal β-and γ-turn structures.*[35]

Turn structure	ϕ (i+1) [°]	ψ (i+1) [°]	ϕ (i+2) [°]	ψ (i+2) [°]
βI	-60	-30	-90	0
βI´	60	30	90	0
βII	-60	120	80	0
βII´	60	-120	-80	0
βVia	-60	120	-90	0
βVib	-120	120	-60	150
γ	70 - 85	-60 - (-70)		
γ$_i$	-70 - (-85)	60 - 70		

Figure 6: *β- and γ-turns as typical structure characteristic of cyclic peptides[35].*

For β-turn structures, the backbone structure of βI towards βI' or βII compared to βII', respectively, are mirror-symmetric to each other. While all other β-turn variations show a characteristic hydrogen bond between amino acids (*i*) and (*i+3*) and for γ-turns between the amino acids (*i*) and (*i+2*), the βVI-turn is a case apart as it forms a *cis* amide bond between (*i+1*) and (*i+2*) but no hydrogen bonding like the other turn structures. Additionally, it is known that in βII'-turns the (*i+1*) position normally is occupied by the D-amino acid residue[35,36].

I.1.1.2 Template Structures for Cyclic Penta- and Hexapeptides

Searching for preferred conformations - which are not necessarily rigid - a library of cyclic penta- and hexapeptides was synthesized by M. Kurz using all possible diastereomeric alanine peptides and investigated for the presence of conformational preferences using NMR spectroscopy[35].
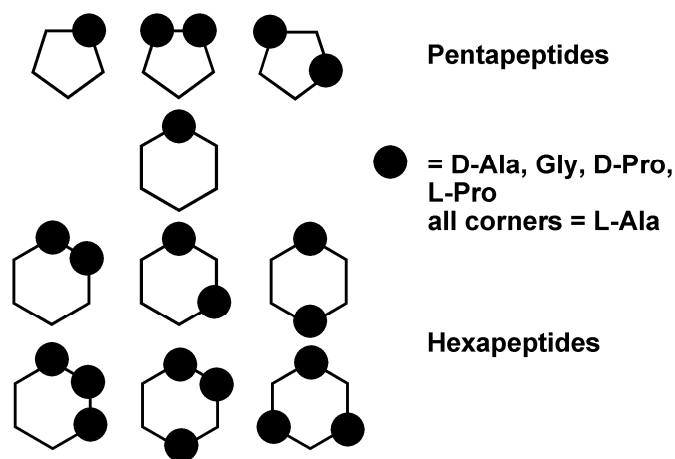
Figure 7*: Search for a preferred conformation. The configuration of the amino acids accounts for the spatial arrangement[35].*

In cyclic pentapeptides, one of the strongest preferences was found for *cyclo*(-D-Ala-Ala$_4$-) and *cyclo*(-D-Pro-Ala$_4$-). Hence, this molecule was considered as a conformational template meaning that a substitution of any alanine by any other amino acid except glycine or proline might exihibit a similar conformation[37,38]. In these peptides, the D-amino acid is found in the (*i+1*)-position of a βII'-turn allowing the formation of a γ-turn around Ala^3. The latter position is less well defined and often shows flexibility[8,37-40].

In cyclic hexapeptides conformation with two β-turns are often observed[36]. Again, if the cycle contains only one D-alanine or one D-proline, this residue prefers the (*i+1*)-position of a βII'-turn. The second β-turn can be found on the opposite side, often in fast equilibrium between βI and βII[41].

I.1.1.3 Synthesis of *N*-Methylated Amino Acids

The first *N*-methylated amino acid was reported by H. Lindenberg in 1875 describing the synthesis of a racemic mixture of *N*-methylated alanine[42]. In 1915, E. Fischer and W. Lipschitz were able to synthesize enantiomerically pure *N*-methylated amino acids[15]. Since then, many different methodologies for the synthesis of enantiomerically pure *N*-methylated amino acids have been described[43]. Nowadays, *N*-methylation is performed using Fmoc-protected amino acids to get products that can directly be used for solid phase synthesis. The most commonly used synthesis was reported by Freidinger *et al.*[44] where in a first step an oxazolidinone ring is formed using paraformaldehyd and *p*-toluol sulfonic acid under mild conditions. Afterwards, the resulting oxazolidin-5-one ring is cleaved under reductive conditions using triethylsilane and trifluoro acetic acid.
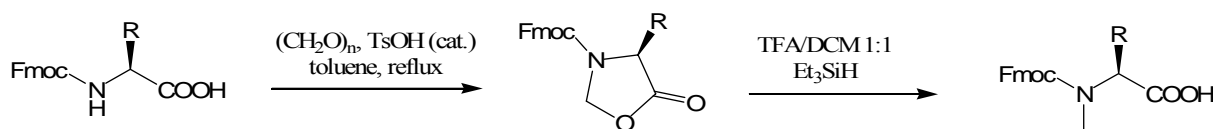
Scheme 1*: Synthesis of Fmoc-protected N-methylated amino acids.*

One crucial restriction for application of this procedure is the use of 50% TFA for the ring opening in the second step as most of the acid-labile side-chain protecting groups would be cleaved off under these conditions. This limits the procedure to amino acids not having any functional groups in their side chain or necessitates the use of different side-chain protecting groups.

Due to this fact, Biron et al. developed an optimized procedure for *N*-methylation on solid support based on the *N*-methylation procedure published by Miller and Scanlan[45-47]. In this procedure, the peptide is built up until the desired point of *N*-methylation. After Fmoc-deprotection, the free amine functionality is activated using *o*-nitrobenzosulfonic acid chloride (NBS-Cl).
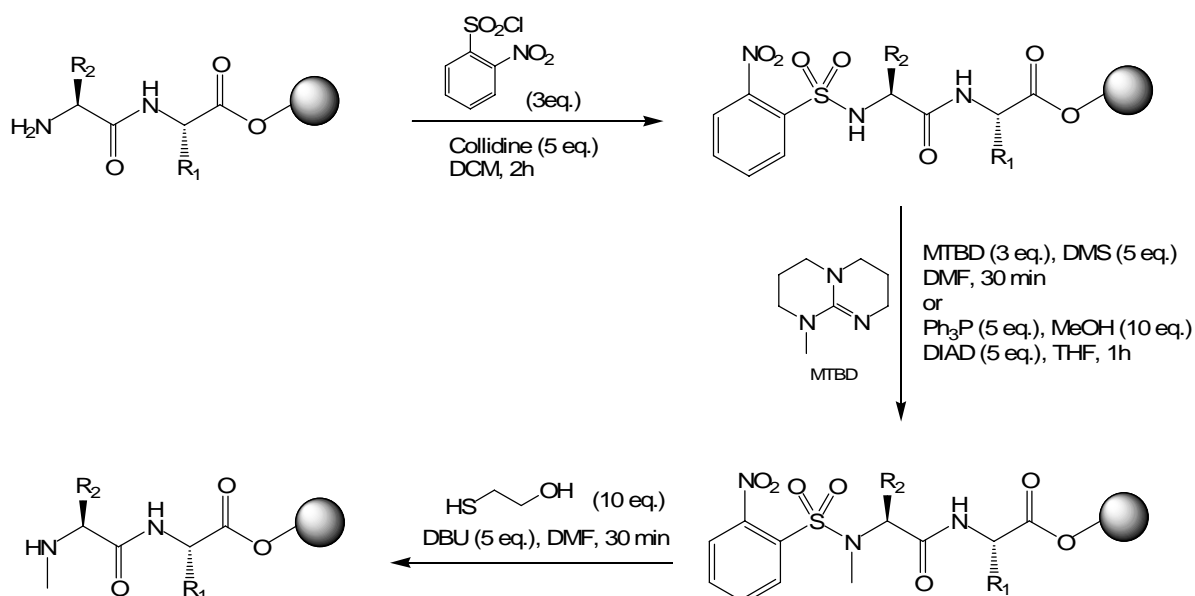
Scheme 2*: N-methylation of NBS-protected amino acids on solid support.*

Then, the *N*-alkylation can be performed using two different strategies: the sterically hindered base 7-methyl-1,5,7-triazabicyclo-[4.4.0]dec-5-en (MTBD) for deprotonation and dimethyl sulfat for *N*-methylation or the use of Mitsunobu conditions using methanol, triphenylphosphine and DEAD or DIAD for *N*-alkylation. Removal of the NBS-group can be performed by β-mercaptoethanol and DBU[47].

I.1.1.4 Influence of *N*-Methylation towards the Conformation and Bioavailability of Cyclic Pentapeptides

N-methylation of peptide bonds in the backbone of cyclic peptides can cause many different effects and has a great influence on the backbone flexibility[17]. *N*-methylation has a crucial effect on the conformation of the amide bond, too.
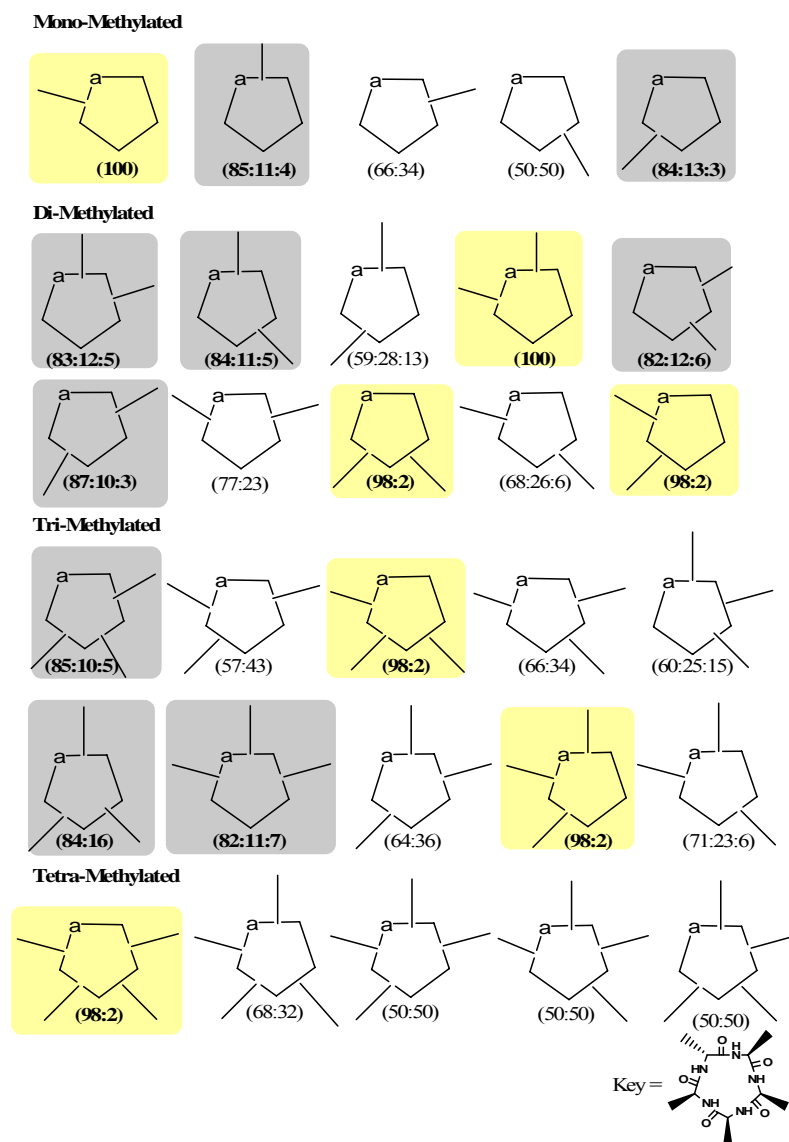
Figure 8*: Template structures for N-methylated cyclic pentapeptides[18,48]. Peptides with a preferred conformation of more than 90% are indicated in pale yellow, peptides with a preferred conformation of more than 80% are marked in grey.*

While for secondary amides the all-*trans* conformation is normally favored, *N*-methylation or *N*-alkylation induces a steric clash causing destabilization of the *trans*-conformation which results in a reduced energetic gap between *cis*- and *trans*-conformation[16,18,48]. As the *cis-trans*-isomerization at room temperature is quite slow relating to the NMR time scale, both

conformations can be seen in the NMR spectrum[49]. However, *N*-methylation sometimes can cause quite rigid turn structures limiting the conformational change[18].

To investigate the influence of *N*-methylation on the conformation of cyclic pentapeptides, a first library of template structures has been synthesized by Chatterjee *et al*.[18,48]. These template structures revealed that the position, where a *N*-methylated amide bond is introduced has dramatically different influences on the backbone conformation. While some compounds kept a population of 100% in the all-*trans* conformation, some showed a mixture of all-*trans*-conformation and conformations bearing one or two *cis*-amide-bonds. Finally, highly populated conformations could be found showing a *cis*-amide bond in their main conformation[17,18,48].

The possibility to adopt a *cis*-conformation could enable a new orientation of pharmacophoric side chain functionalities which could cause improved activity or selectivity[17]. In addition, *N*-methylation reduces the inter- and intramolecular hydrogen bonds resulting in an increased basicity and reduced polarity of the carbonyl group lacking the hydrogen bond[17].

To investigate, if these new orientations and pharmacophoric properties might have an influence on receptor selectivity, Chatterjee *et al.* synthesized a library of *N*-methylated hexapeptides based on the previously published peptide *cyclo*(-G-R-G-D-f-L-), that binds towards the integrin receptors $\alpha_{IIb}\beta_3$, $\alpha_V\beta_3$ and $\alpha_5\beta_1$[50]. Doing so, they were able to find a tri-*N*-methylated compound showing improved activity and highly improved receptor selectivity for $\alpha_{IIb}\beta_3$[51].

As mentioned before, Cyclosporin A – though violating all Lipinski rules – is orally available in man. These findings stimulated Biron *et al.* to perform a *N*-methyl-scan of the Veber-Hirschmann peptide that shows activity towards the somatostatin subtype receptors sst2 and sst5 but lacks oral availability[52]. In that case, one compound with mild and one compound with good bioavailability were found that still showed biological activity towards the somatostatin receptors[53].

I.1.2 *N*-Methylated Cyclic Hexapeptides as Template Structures for Spatial Screening and Oral Bioavailability

The following project was performed in cooperation with Dr. Jayanta Chatterjee. Biological testings have been performed by Oded Ovaid from the group of Prof. Dr. Amnon Hoffman at the Hebrew University of Jerusalem (Jerusalem, Israel). For a detailed assignment of the synthesized compounds towards the creators, please see experimental section.

I.1.2.1   *N*-Methylated Cyclic Hexapeptides as Template Structures

As described in the chapter before, *N*-methylation of amide bonds can enable bioavailability of peptides or result in new selectivity profiles[53]. But on the other hand, the reduced energy barrier between the *cis*- and *trans*-conformation of the amide bond can cause completely different conformations of the peptides compared to the non-*N*-methylated peptides. So, a highly active compound might become completely inactive as the necessary turn structure of the peptide backbone is destroyed. Additionally, it is possible, that several different conformations become feasible, which interchange slowly from one into the other. However, in medicinal chemistry, only one conformation – the active one – is welcome while an equilibrium of different conformations where only one is active is completely undesired.

As this equilibrium has a slow exchange rate, it can be monitored in the NMR time scale and the population of the different conformations can be given by the peak intensities. Here, it is important to remember that a high accuracy will only be given, if only one scan is performed before integration as otherwise the different relaxation times would have to be considered. Additionally, it's worth mentioning that all these measurements have to be kept correlated to the solvent as the character of the solvent can have a strong impact on the population of the different conformations[54].

As mentioned before, a library of template structures for *N*-methylated cyclic pentapeptides has recently been synthesized and investigated for preferred conformations[18]. However, this has not yet been done for cyclic hexapeptides, which, together with cyclic pentapeptides, are the most commonly used cyclic backbone structure in medicinal chemistry.

For non-*N*-methylated hexapeptides, it is known that peptides of the DL_5-type form two γ-turns which are determined by the sterical impact and the angles of the amino acid backbone and are additionally stabilized by hydrogen bonding between the CO of amino acid 6 and the NH of amino acid 2 and between CO of amino acid 3 and NH of amino acid 5 (if the D-residue is taken as amino acid 1). Due to that, the two NH-groups forming the hydrogen bonds point into the inner side of the cyclic peptide. This hypothesis can be supported easily by a temperature gradient in the NMR spectrometer as these protons should be more shielded from the solvent and, out of that, their chemical shift should be less temperature dependent than the other ones[55].
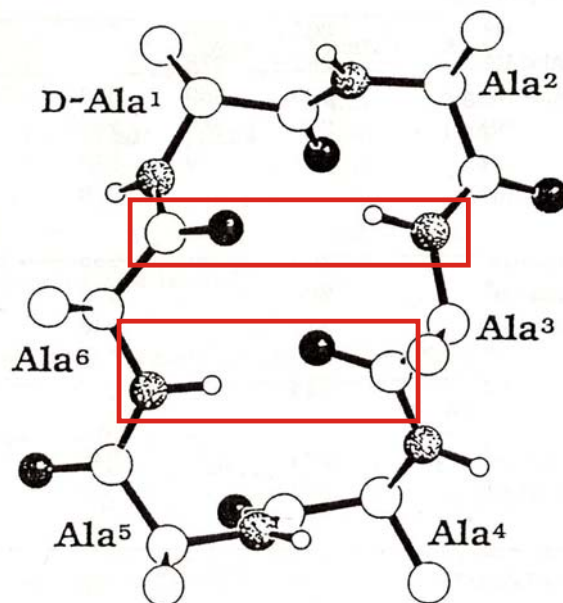
Figure 9*: Structure of cyclo(-a-A-A-A-A-A-)[35]. The two hydrogen bonds which form the β-turns are marked by a red square. The upper turn is a βII' while the lower turn in the molecule changes from βI to βII.*

So, if these two amide bonds were *N*-alkylated it could be expected that the turn structures might be destroyed or at least twisted. This would have a strong influence on the conformation of the hexapeptide while *N*-alkylation on the other positions should have a much lower impact. However, one should always keep in mind, that *N*-methylation can also result in formation of a *cis*-amide bond which could enable some completely new conformations that might become favored due to stabilizing turn structures which then could be formed.

I.1.2.1.1 Results and Discussion

I.1.2.1.1.1   Synthesis of the Peptide Library

Sequence optimization of peptides built up on solid support which are supposed to be cyclized afterwards is usually based on formation of a turn structure. If the sequence as a linear peptide already preforms the turn needed for cyclization, yields can be dramatically increased for the cyclic peptide and much weaker cyclization reagents can be used.

As for cyclic peptides the sequence can be started at every position of the peptide, the focus is set on pre-forming these turns by introducing the D-residue at the right position in the linear sequence[31]. However, for highly *N*-methylated cyclic peptides, the preformation of the turn structure has not the highest priority. For such peptides, it has to be taken into account that sequences like *NMe*AA-AA-SolidSupport tend to form diketopiperazines[56]. This formation results in cleavage of the peptide from solid supoort and out of that in a complete loss of the peptide.

Therefore, alternating sequences of "normal" amino acids and *N*-methylated amino acids should be avoided if possible.

Additionally, one has to take care that the sequence does not end with an *N*-methylated amino acid as this would result in a much more demanding cyclization and a higher demand for the coupling reagent. If coupling reagents like HATU can be used for cyclization such couplings are possible with good yields for sterically not too demanding amino acids. However, for the use of DPPA or PyBOP an *N*-methylated *N*-terminus should be avoided.

An additional problem arose for the library of *N*-methylated cyclic hexapeptides due to the fact that the retention time in the prep. HPLC while purification of the cyclized peptides is similar to the one of reacted HATU and HOAt. So, the use of these strong coupling reagents was not possible and DPPA which has a more unpolar character had to be chosen. This results in lower yields and additionally makes it impossible to end the sequence with an *N*-methylated alanine. So, in several cases sequences with alternating *N*-methylated and normal alanine could not be avoided leading to dramatically decreased yields and much more demanding purifications due to an increased number of side products.

I.1.2.1.1.2 Evaluation of the Populations of the different Conformations

As template structure for the *N*-methyl scan *cyclo*(-a-A-A-A-A-A-) was chosen as alanine is the simplest amino acid bearing stereoinformation and the side-chain does not introduce any unpredictable impacts like a charged residue which could form salt bridges or an aromatic residue which might be able to form π-π-interactions. In addition, *cyclo*(-a-A-A-A-A-A-) is known to form two stable β-turns[35] which facilitates the understanding of the results of the *N*-methyl scan.

In a first step, one *N*-methylation was varied through every position of the hexapeptide leading to six mono-methylated cyclic peptides (see figure 10). Out of these, three were found to have a main conformation which is populated with more than 90%, two of them even showed only one single conformation.

Mono-*N*-Methylated

Figure 10: *Template structures for mono-N-methylated cyclic hexapeptides. Numbers in bold are the compound numbers, numbers in italic represent the population of the different conformations. Hexapeptides with a favoured conformation (population of >90%) are highlighted in pale yellow.*

As expected, these three peptides have their *N*-methylations at positions, where the formation of the β-turn structures is not disturbed (*i* (the position of the D-residue), *i+1* and *i+4*), while for position *i+2* and *i+5*, where the NH is needed for the formation of hydrogen bridges which stabilize the turn structure, the introduction of a *N*-methyl group is disfavored. For compound **4**, the *N*-methylation is not at a position essential for the formation of hydrogen bridges. But, as was also shown for the pentapeptide library, this position is prone for the appearance of a *cis*-amide bond causing a 50/50 mixture between the all-trans conformation and one with one *cis*-amide bond for *cyclo*(-a-A-A-MeA-A-)[18] which might be also the case for the hexapeptide, as it nearly shows the same ratio of two conformations.

A direct comparison of the hexapeptides with the library of *N*-methylated cyclic pentapeptides[18,48] is tempting, but has to be performed carefully, as one should always keep in mind, that cyclic pentapeptides are much more flexible than cyclic hexapeptides as the γ-turn is not as stable as a β-turn. However, taking a look at the results found for the pentapeptides, it is obvious, that also the highest populated molecules were found with *N*-methylations at position *i*, *i+1* or *i+5*. For the other two positions, much lower populated conformations were found, as the formation of the β-turn is disturbed or the formation of a *cis*-amide bond is favored, respectively.

In the next step, two *N*-methylations were varied through the hexapeptide in all possible combinations leading to 14 different peptides (see figure 11). Out of these, 5 were found to have a main conformation which is more than 90% populated.

Di-*N*-Methylated
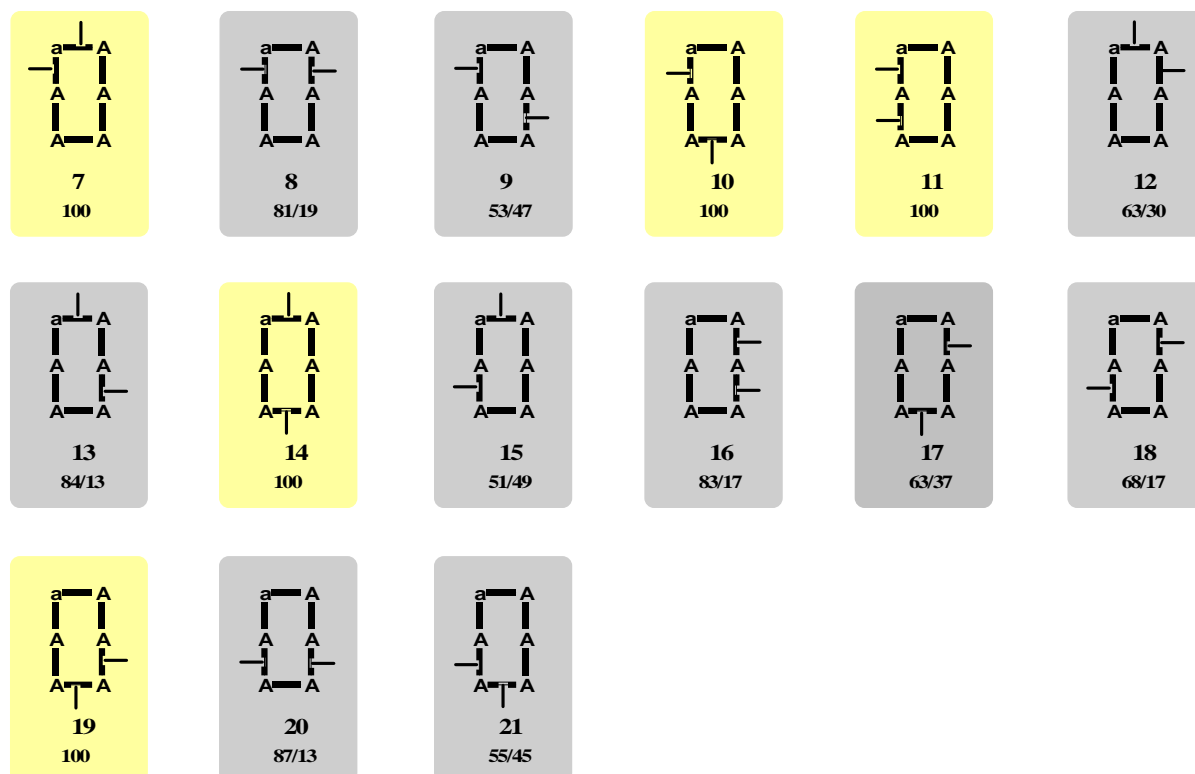
Figure 11*: Template structures for di-N-methylated cyclic hexapeptides. Numbers in bold are the compound numbers, numbers in italic represent the population of the different conformations. Hexapeptides with a favoured conformation (population of >90%) are highlighted in pale yellow.*

For the highly populated main conformation of compounds **7**, **10**, **14** and **19** the *N*-methylations were again found at positions not affecting the formation of the turn structures. However, for compound **11** this is not the case as it has an *N*-methylation at a position for an H-bond that is essential for the β-turn stabilization. This strongly indicates the presence of a *cis*-amide bond in the main conformation enabling the generation of different turn structures.

Again, these results are in good agreement with the pentapeptide library. There, only one di-*N*-methylated compound was found to show only one conformation having these alkylations at exactly the same positions like compound **7**[18,48]. The other highly populated conformations of this series are in agreement to compounds **11** and **19**.

Looking at the next set of *N*-methylated cyclic hexapeptides, the tri-*N*-methylated ones, six compounds can be found, showing highly populated main conformations, three of them showing only one single conformation in the 1D-^{1}H-NMR spectrum. Out of these six compounds, **24**, **28** and **34** again are in good agreement with the assumption, that *N*-methylations at positions not affecting the turn structures might be well tolerated.

Tri-*N*-Methylated
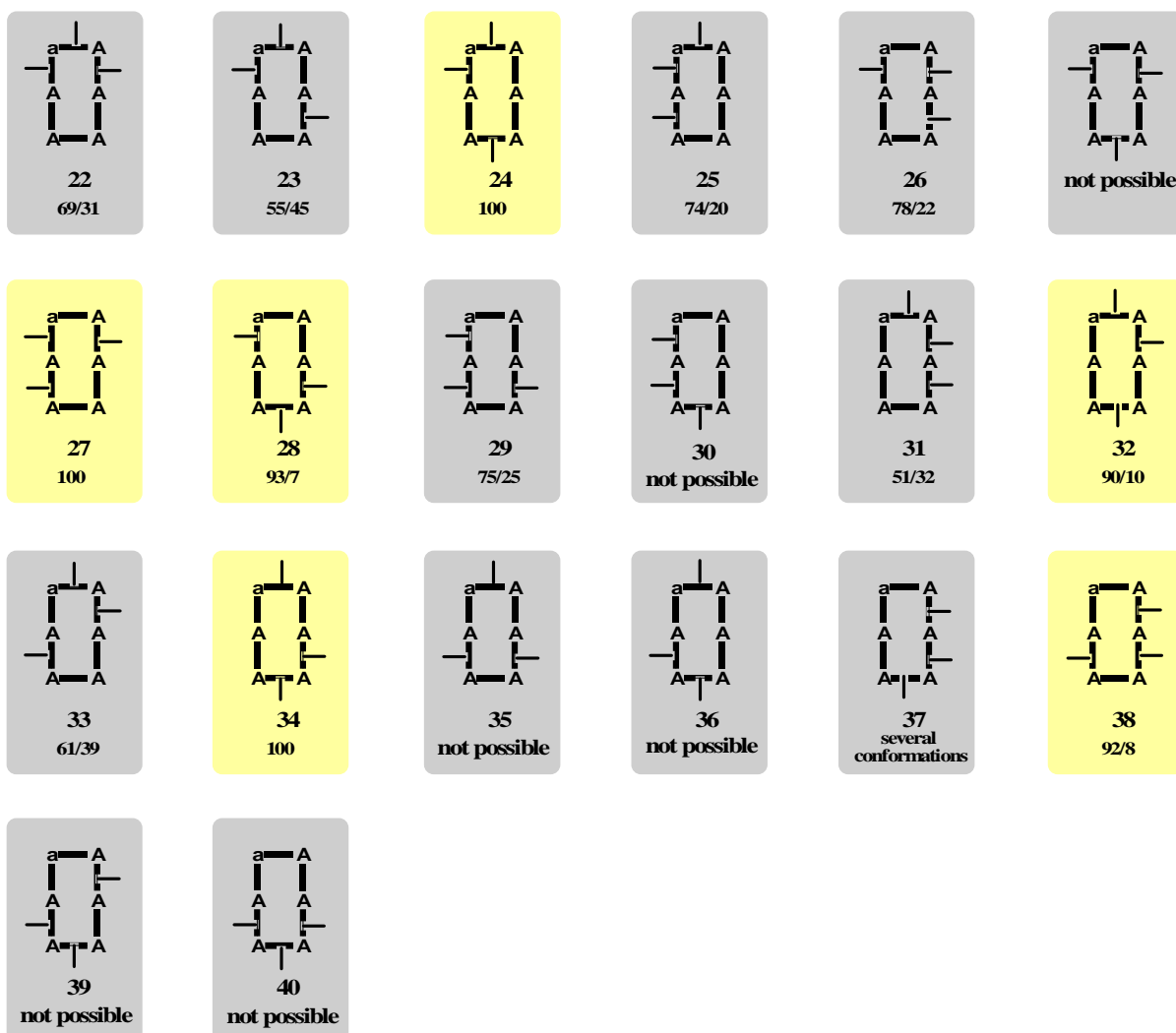
Figure 12: *Template structures for tri-N-methylated cyclic hexapeptides. Numbers in bold are the compound numbers, numbers in italic represent the population of the different conformations. Hexapeptides with a population of >90% are highlighted in pale yellow.*

However, three compounds (**27**, **32** and **38**) have their *N*-methylations at positions inhibiting the formation of the stabilizing hydrogen bonds for the turn structures. As the steric clash of the *N*-methyl group should be so high, that the amide bond has to evade by changing orientation, the angle for the formation of a β-turn should no longer exist. Typically, this would result in a set of several low populated conformations. Especially compound **38** should have disfavored conformations, as both NH-groups necessary for hydrogen bonding are not accessible. Nevertheless, this is not the case for all these compounds.

Taking a look at the behaviour of *N*-methylated cyclic pentapeptides[18,48], one tri-*N*-methylated compound can be found showing a similar *N*-methylation profile like **28** and also a highly populated main conformation. For this compound, *cyclo*(-Mea-A-A-MeA-MeA-), one *cis*-peptide bond was found for the main conformation. This is in good agreement to the consideration of

evasion to the steric clash as this *cis*-amide bond enables the formation of a γ-turn like structure at a different position in the molecule.

For the tetra-*N*-methylated cyclic hexapeptides only compound (**53**) was found showing a main conformation with a population of more than 90% (see figure 13). Again, the *N*-methylation pattern of this molecule is somehow surprising as both NH-groups necessary for the turn structure are not accessible for hydrogen bonding. However, this is again in a good agreement to the cyclic pentapeptides where *cyclo*(-Mea-A-MeA-MeA-MeA-) shows two *cis*-peptide bonds in its main conformation enabling the formation of a γ-turn like structure to stabilize the molecule.
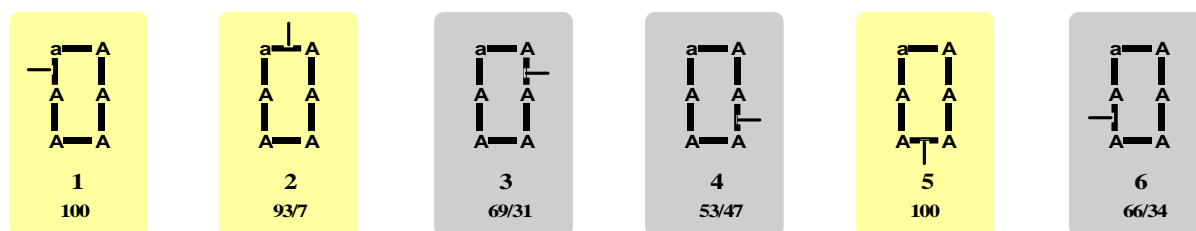
Tetra-*N*-Methylated

Figure 13: *Template structures for tetra-N-methylated cyclic hexapeptides. Numbers in bold are the compound numbers, numbers in italic represent the population of the different conformations. Hexapeptides with a population of >90% are highlighted in pale yellow.*

Finally, also the penta-*N*-methylated cyclic hexapeptides were synthesized. For *cyclo*(-Mea-MeA-MeA-MeA-A-MeA-) this was not possible as this sequence makes the formation of diketopiperazines possible which results in cleavage from solid support and a complete loss of product.

Nevertheless, five out of these six possible cyclic hexapeptides were successfully synthesized, but only one of them (**60**) showed a satisfyingly populated main conformation, which is still not highly enough populated to be of high interest for appliance in medicinal chemistry.

Penta-*N*-Methylated

Figure 15: *Template structures for penta-N-methylated cyclic hexapeptides. Numbers in bold are the compound numbers, numbers in italic represent the population of the different conformations.*

Summing up, it was possible to synthesize a library of *N*-methylated cyclic alanine hexapeptides and to screen them for sequences with only one or a highly populated main-conformation, useful for appliance as templates in medicinal chemistry. Out of the 60 synthesized compounds, 16 compounds were found to have a main conformation with a population of more than 90%.

I.1.2.2 The impact of *N*-methylation Towards Bioavailability of Cyclic Hexapeptides

One of the main goals in pharmaceutical drug research is the finding of highly selective and active drug candidates that are also orally available. While for cancer therapy and other severe diseases injections are tolerated as formulation for the drugs, this is absolutely not the case for "normal" diseases. Out of that, the predictability of the pharmaceutical properties of a potential drug candidate is one of the targets, medicinal chemists try to reach.

A first step into the right direction seemed to be the so-called Pfizer rules which were proposed by Lipinski and coworkers[9]. But, as was shown by Veber, these rules are not useful for all compounds and limit the chemical space dramatically[10]. As the number of peptidic drug candidates is currently increasing year by year, there is a high demand in understanding the properties, peptides need to have, to gain oral bioavailability.

One of the systems used to test for bioavailability is the so-called Caco-2 test which uses cell monolayers on permeable filters to study the transepithelial transport of drugs[57]. Here, the main focus is on studying whether a compound is actively or passively transported across the intestinal epithelium and – for the case of an active transport – to identify the relevant carrier[58]. These carriers can be the dipeptide carrier and P-glycoprotein in the case of Caco-2[59,60]. As was shown, best correlation to the in vivo situation is obtained for drugs being transported by passive transcellular route. Nevertheless, this route is less permeable in cell monolayers than in vivo but the data obtained so far indicate that the selectivity of this pathway is comparable to the in vivo situation[58].

However, one of the big challenges of this test system is the comparability of one test with another. So, unoptimized test conditions might compromise the value of the Caco-2 model as a permeation screening tool. Until now, no systematic studies comparing different experimental conditions have been performed defining an optimal solution to overcome the different issues associated with the use of saline aqueous buffer[61]. For the case that compounds are not soluble in the buffer system, 1% DMSO, dimethylacetamide (3%) or NMP (2.5%) can be added. However, these conditions do not imitate the in vivo situation properly any more[61].

Peptides normally gain cell permeability via paracellular transport via the so-called tight junctions. Paracellular transport is passive and result from diffusion, electrodiffusion, or osmosis down the gradient created by transcellular mechanisms[62]. The tight junction is an intracellular junctional structure mediating adhesion between epithelial cells which is required for epithelial cell function[63]. Until now, 30 different proteins have been described being associated to the tight junctions[64]. Nevertheless, the structure of the tight junctions is still unknown. Recently, the assumption that tight junctions are mainly formed by Claudin and Occludin has been posted by

several different groups[62,65] while also a combination of lipids and proteins forming a lipid-protein hybrid are discussed as model for tight junctions[66]. However, as long as no structure of the tight junctions is available, prediction of paracellular transport for different compounds is nearly impossible. Until now, it is only known, that for paracellular transport, ions or small hydrophilic molecules are preferred[67].

To give a first idea of the conditions, peptides might have to fulfill for transport via tight junctions, the hexapeptide library described above was tested for their permeability profile. As these compounds have very similar properties, it might be possible to gain some knowledge about structural or electronical features, cyclic peptides need to have to be able to pass this kind of a filter. So, all compounds were evaluated using the described Caco-2 test to classify them into permeable and un-permeable compounds.

I.1.2.2.1 Results and Discussion

All of the *N*-methylated cyclic hexapeptides of the library discussed above were tested for their passive transport via tight junctions by CaCo-2 test. From the series of the mono-*N*-methylated cyclic hexapeptides, no compound showed satisfying cell permeability (for exact results of the CaCo-2 testings, please see Experimental Section, Chapter IV.3.2). This might be due to a too high polarity or a "wrong" structure which does not fit into the tight junctions or to wrong electrochemical properties, as these compounds might be already too hydrophilic for paracellular transportation.
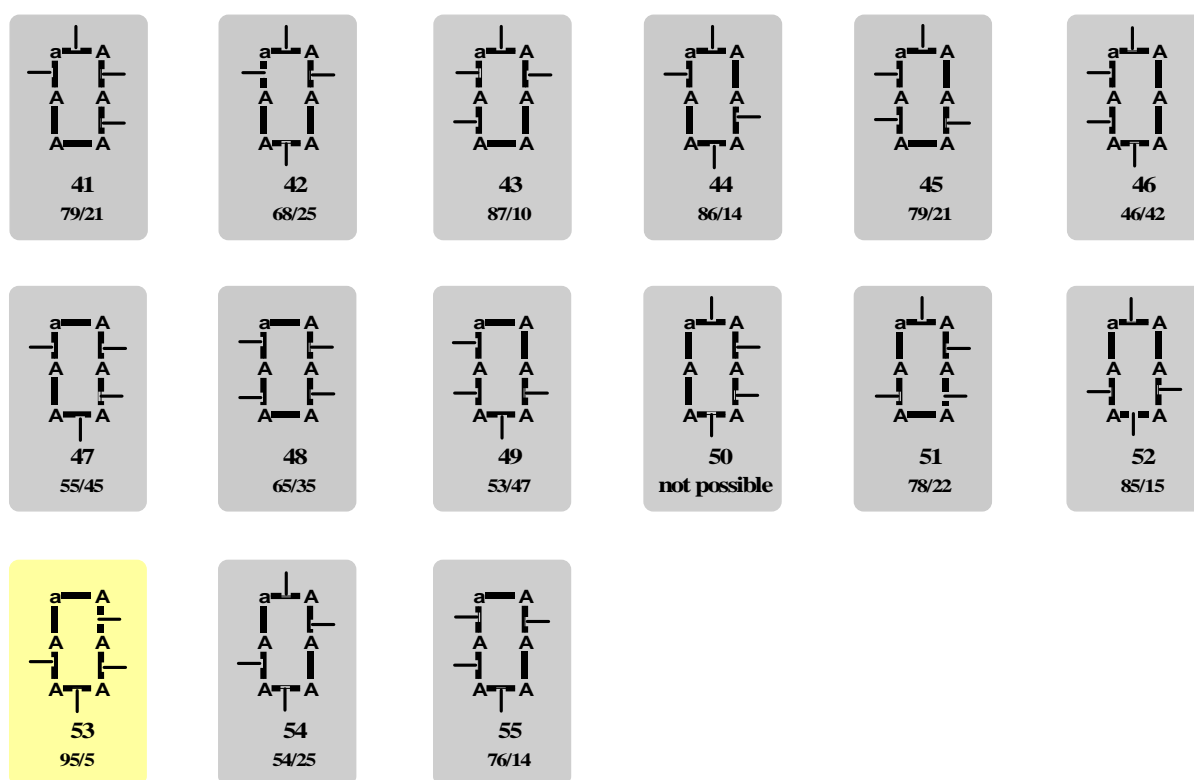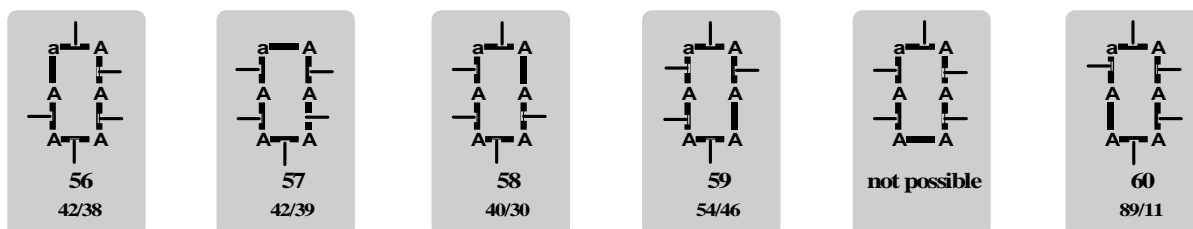
Mono-*N*-Methylated
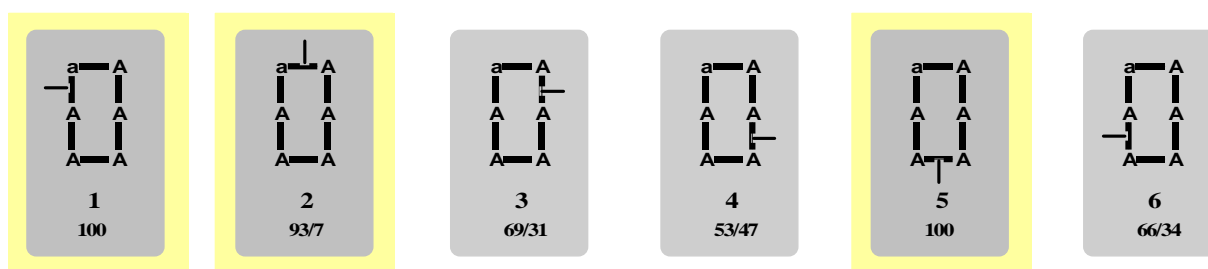
Figure 16: Template structures for mono-N-methylated cyclic hexapeptides. Numbers in bold are the compound numbers, numbers in italic represent the population of the different conformations. Hexapeptides with a population of >90% are highlighted with a pale yellow square behind the square. A grey square symbolizes a compound with no or nearly no permeability in CaCo2, pale red symbolizes good permeability and red symbolizes very good permeability.

For the di-*N*-methylated cyclic hexapeptides two compounds were found showing good passive transport properties (**10** and **17**) and two showing very good passive transportation through tight junctions (**11** and **21**, see figure 17). While compound **17** and **21** reveal two conformations in the NMR time scale in the 1D-¹H-spectrum in DMSO, the other two compounds show only one

conformation which makes them on one hand interesting candidates for the approach to understand the influence of the molecular structure towards passive transportation via tight junctions. On the other hand, they can be taken as useful template structures to further optimize the cellular uptake of drug candiates by introducing the *N*-methylation profile of one of the two template structures on the potential drug.

Di-*N*-Methylated
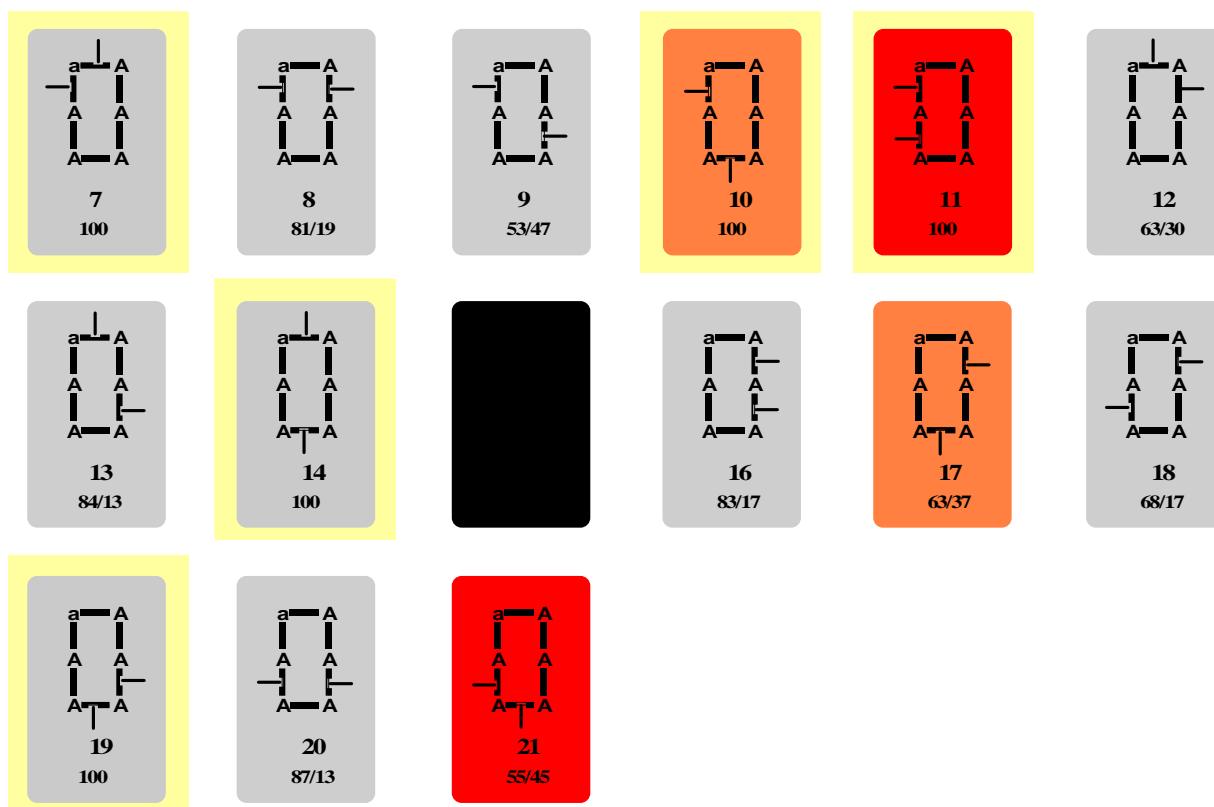
Figure 17: Template structures for di-N-methylated cyclic hexapeptides. Numbers in bold are the compound numbers, numbers in italic represent the population of the different conformations. Hexapeptides with a population of >90% are highlighted with a pale yellow square behind the square. A grey square symbolizes a compound with no or nearly no permeability in CaCo2, pale red symbolizes good permeability and red symbolizes very good permeability. The black structure stands for a compound that has not yet been tested.

Testing of the higher *N*-methylated cyclic hexapeptides are currently in progress. First results showed some tetra-*N*-methylated cyclic hexapeptides with very high permeability in Caco-2. For the results obtained for the higher *N*-methylated peptides see Experimental Section, Chapter IV.3.2.

I.1.3   *N*-Methylated Amino Acids as Substitutes for Proline in Cyclic Pentapeptides[68]

The following project was performed in cooperation with Dr. Andreas O. Frank and Dr. Jayanta Chatterjee for structure calculation.

I.1.3.1 Background

The presence of a tertiary amide bond both in *N*-methylated amino acids and proline containing peptides is tempting to consider that their corresponding stereo-impact on the peptide backbone might be similar. Although vivid explanations are available on the factors influencing the conformation of proline[39,40,69,70] and *N*-methylated amino acid containing peptides[18,48,51], there is a lack of a direct experimental comparison of peptides with *N*-methylated amino acids or prolines in peptides with otherwise identical constitution and configuration.

It is well known that proline markedly influences protein architecture due to its constrained five membered pyrrolidine ring[71] and acts as a reverse turn inducer in designed cyclic protein-epitope mimetics[72-75]. On the other hand, *N*-methylated amino acids are also able to induce turn structures[76] in cyclic peptides[17,48,73]. It was shown that both proline[14,77-79] and *N*-methylated amino acids[16,18,48] have the potential to introduce *cis*-peptide bonds into peptide sequences. However, in contrast to L-proline in which the φ angle is constrained to ca. -60° due to the pyrrolidine ring, *N*-methylated L-amino acids have much more flexibility, as the φ angle can vary between -100° and +60°[18]. Hence, it is not *a priori* predictable if mutual substitution of these structural units has a similar influence on the conformation.

Although *N*-methylation of amide bonds has been used in peptide chemistry for more than 130 years[42], introduction of proline or ring-derivatized prolines in peptidic sequences was the most popular method to induce turns or *cis*-peptide bonds in peptides since preparation of *N*-methylated amino acids on solid support came along with huge problems in their synthesis [80,81]. However, ring-derivatized prolines often need extensive synthesis or do not force adequately a molecule into a single preferred conformation[82]. Nowadays, the synthetic difficulties concerning *N*-methylated amino acids have been overcome and peptides including them are easily accessible[47,83]. Therefore, the question arose if it might be possible to replace a proline with an *N*-methylated amino acid without perturbing a favored conformation. In this case, one would regain the side-chain functionality which is lost in proline-type amino acids because of the five membered pyrrolidine ring. This side-chain could subsequently be used to improve the activity, selectivity or could act as a pharmacophore in the peptide.

I.1.3.2 Results and Discussion

For the comparison of proline and *N*-methylated amino acids, alanine was chosen as a template for *N*-methylation (because it is the simplest amino acid bearing stereoinformation) and the positions of *N*-methylated alanine (MeA) or proline in cyclic pentapeptides were screened (see figure 18). Afterwards, conformational equilibria were investigated by NMR spectroscopy. The use of alanine is reasonable, as in contrast to aromatic residues[84,85] or β-branched amino acids[86], the small side-chain of alanine has not such a great influence on the backbone conformation.
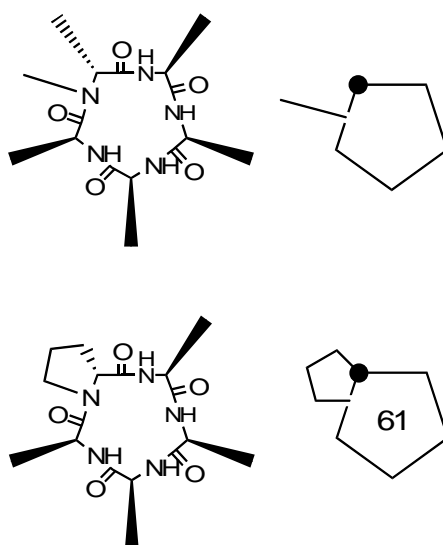
Figure 18: *cyclo(-Mea-A-A-A-A-) and cyclo(-p-A-A-A-A-)* **61** *shown as regular and schematic structures. The D-residue is marked as a black dot in the upper left corner. Small letters refer to a D-residue.*

The first comparison where only one *N*-methylation or one proline was varied led to the promising result that, in nearly every case, *N*-methylated alanine and proline show similar results with respect to the highest populated conformation and, in addition, are in good agreement concerning the *cis/trans*-ratios of amide bonds (see figure 19). Especially when introduced at the (*i*)-position (the position of the D-residue in the cyclic peptide) Me-D-alanine and D-proline both revealed only one highly populated conformation and both peptides are in the all-*trans*-conformation. Both structures possess a β-turn in the upper part which is introduced by the D-residue and a γ-turn in the lower part of the molecule, whereas the peptide bond between Ala^2 and Ala^3 is known to flip around its adjacent φ and ψ dihedral angles (flip of 180°)[18].
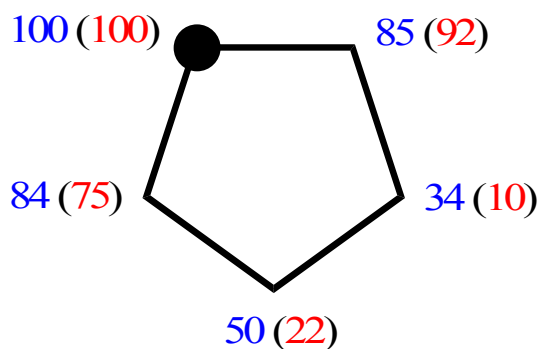
Figure 19*: Populations of the all-trans conformations for the peptides with one Me-alanine (proline) at the different positions in percent [%]. The remaining percentages are the populations containing a cis-peptide bond between the N-alkylated amino acid and the preceding one. The D-residue is marked as a black dot in the upper left corner.*

Also when being introduced in the (*i*+1)-position, the all-*trans* conformation is preferred in both cases with a population of 85% for the alanine and 92% for the proline peptide. It is worth mentioning that both peptides show a nearly identical structure what enables the replacement of one with another without changing the backbone conformation (see superposition in figure 20).
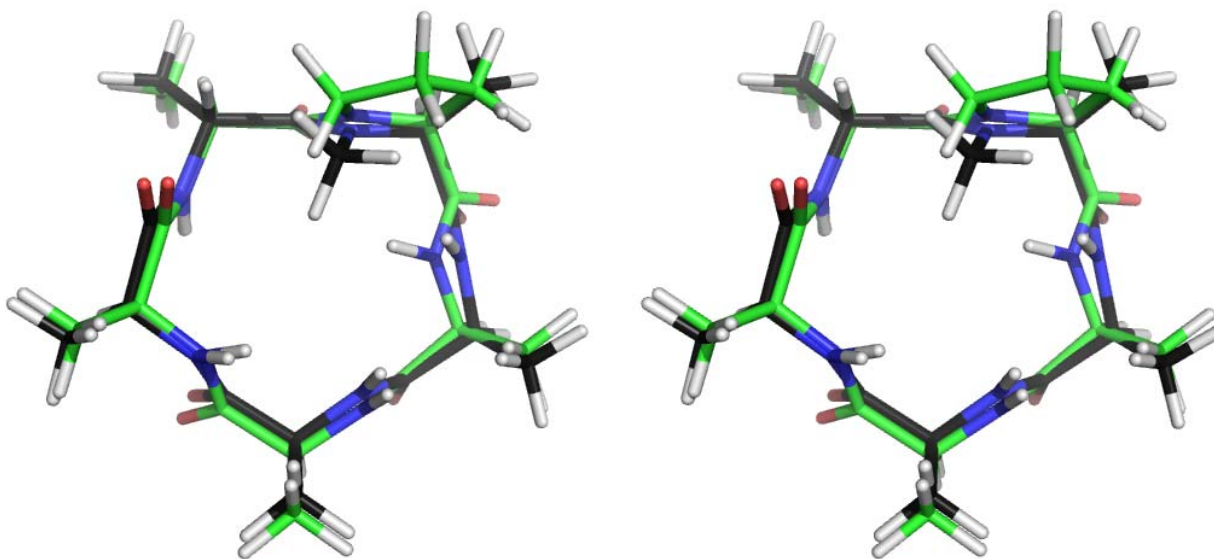
Figure 20*: Stereoview of the superposition of cyclo(-a-MeA-A-A-A-) and cyclo(-a-P-A-A-A-)* **62***.*

When the *N*-alkylated residue is introduced in the (*i*+2) or in the (*i*+3)-position, the all-*trans*-conformation is disfavored. Especially for proline, a *cis* peptide bond is preferred at the position of the *N*-alkylation finally resulting in a conformation with a population of about 90% for *cyclo*(-a-A-P-A-A-) **63** with a *cis* peptide bond at the position of proline. Being introduced at the (i+4)-position, the all-*trans* conformation is again favored. However, for *cyclo*(-a-A-A-A-*Me*A-), three conformations with a population of 84/13/3 are present where the two main populations

possess an all-*trans* conformation. *cyclo*(-a-A-A-A-P-) **65** also shows three conformations with a ratio of 75/19/6 where the main conformation also exhibits an all-*trans* arrangement.

To summarize, a MeAla has the ability to replace a single proline in cyclic pentapeptides without having an undesired impact on the backbone conformation. Furthermore, the *N*-methylated amino acid might be preferred because one regains the side-chain functionality which is lost when using proline. To prove this hypothesis, the Me-D-alanine in *cyclo*(-*Me*a-A-A-A-A-) was replaced with an *N*-methylated D-lysine and resulting in *cyclo*(-*Me*k-A-A-A-A-) **66** with a population of 100% (see figure 21). Another possibility to introduce functionalities into peptides is *N*-alkylation. For example, transitional sulfonamidic protection of the amine to be alkylated and subsequent alkylation under Mitsunobu conditions or halide displacement has been recently described by Demmer *et al*. [87].
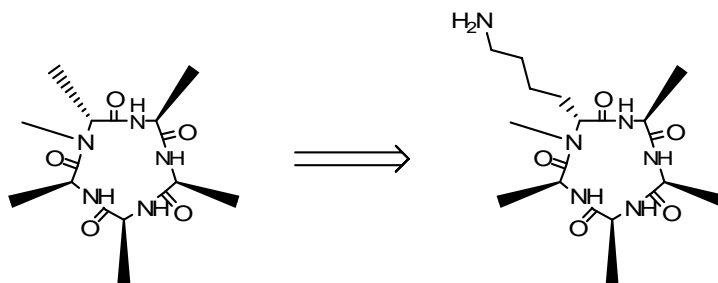
Figure 21*: cyclo(-Mea-A-A-A-A-) that shows an all-trans population of 100% was used as template for cyclo(-Mek-A-A-A-A-)* **66***. The generated peptide also revealed a population of 100% which serves as a hint that alanine can be used as a template for amino acids with a longer side-chain.*

While sequences containing two prolines are not well suited for application in medicinal chemistry as two of the possible side chain functionalities are lost, the incorporation of two *N*-methylated amino acids is preferable because all side chains can be used to gain activity or selectivity, respectively.

As in the case of *cyclo*(-a-A-A-*Me*A-A-) and *cyclo*(-a-A-A-P-A-) **64**, the differences for the populations between the all-*trans*-conformation and the conformation containing one *cis*-peptide bond were the lowest, the *N*-alkylated amino acid was fixed at the (*i*+3)-position and another proline or MeAla was rotated through the different positions of the cyclic pentapeptide. Thus, it was investigated if the presence of a second *N*-alkylated amino acid might alter the *cis/trans* equilibrium and finally the potential occurrence of new preferred conformations was tested.
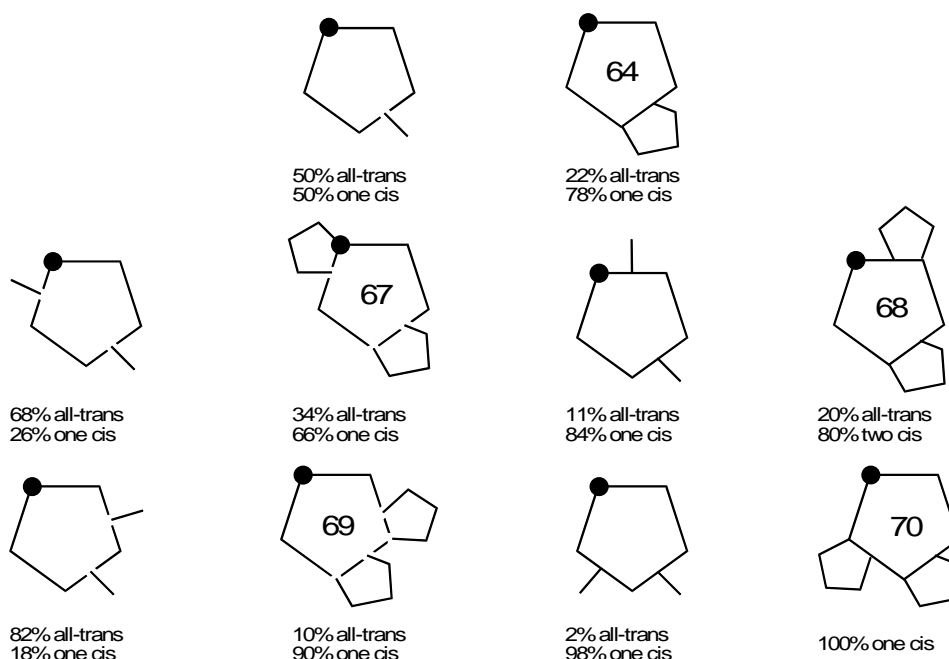
Figure 22: *Populations of the different conformations. The cis-amide bond occurs between an N-alkylated amino acid and the previous one. Two peptides revealed more than two conformations at the NMR time scale. In that case, only the two major conformations are given, leading to percentage statements that do not sum up to 100 %.*

As can bee seen in figure 22, there is a big population difference between *cyclo*(-p-A-A-P-A-) **67** and *cyclo*(-*Me*a-A-A-*Me*A-A-) since the latter shows a preference of the all-*trans* conformation with a population of 86% while in *cyclo*(-p-A-A-P-A-) **67** the conformation with one *cis*- and all other peptide bonds in *trans*-configuration is the highest populated conformation (~65%). For the two cyclic pentapeptides *cyclo*(-a-*Me*A-A-*Me*A-A-) and *cyclo*(-a-P-A-P-A-) **68**, the peptide with *N*-methylations prefers a highly populated conformation where one amide bond is in *cis* and the other *N*-alkylated amide bond is in *trans* conformation. In contrast, the cyclic peptide with two prolines shows a main population with two *cis*-amide bonds at the positions of the prolines. In the case of *cyclo*(-a-A-*Me*A-*Me*A-A-) and *cyclo*(-a-A-P-P-A-) **69**, the all-*trans* conformation is preferred for the peptide with the *N*-methylations while for the proline-peptide the conformation with one *cis*-amide bond is favored. For *cyclo*(-a-A-A-*Me*A-*Me*A-) and *cyclo*(-a-A-A-P-P-) **70**, both compounds show a preferred conformation which is highly populated bearing one *cis*-peptide bond between (i+3) and (i+4) (see superposition in figure 23).

In conclusion, structural features of a cyclic peptide are no longer predictable when two *N*-methylations or two prolines are present since peptides bearing more than one *N*-methylated amino acid often differ in their conformation compared to the proline containing analogues. One benefit of this finding is the fact that replacement of proline by an *N*-methylated amino acid most often results in a different structure which could be useful for the search for better candidates to fit into a binding pocket.
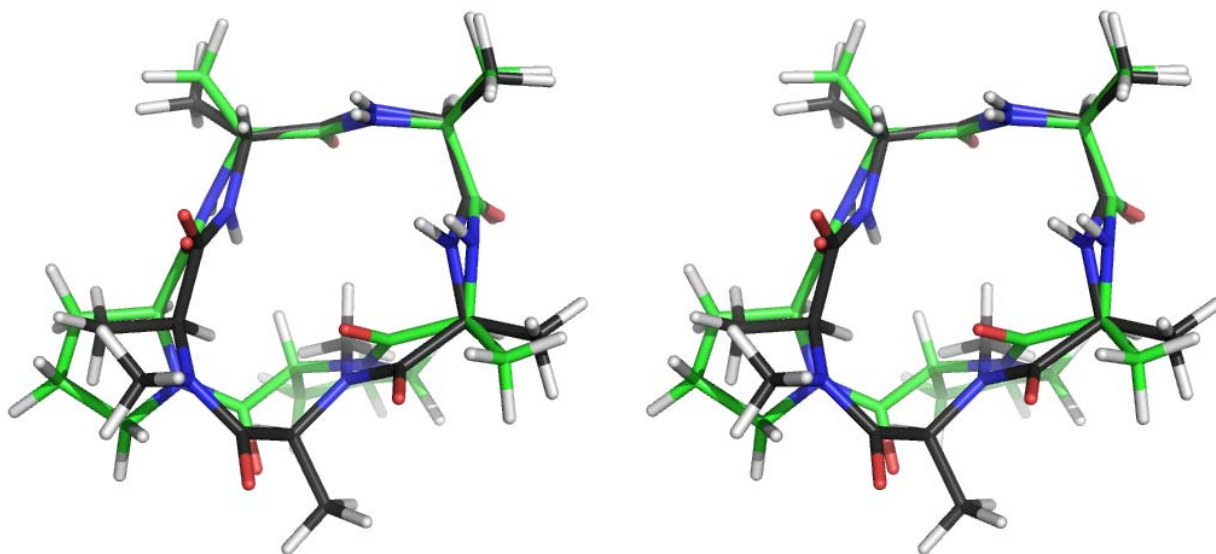
Figure 23*: Stereoview of the superposition of cyclo(-a-A-A-MeA-MeA-) and cyclo(-a-A-A-P-P-)* **70***. Small characters indicate a D-residue.*

Finally, the conformation of cyclic peptides when both, a proline and an *N*-methylated amino acid, are incorporated should be compared. In this study, proline was fixed at the *(i+3)*-position and the position of the *N*-alkylation were varied (and vice versa). The obtained set of compounds showed preferred conformations whereas the highest populated conformation of each peptide was in the range of 65-70% (see Table 2). Hence, it was decided not to go into further detail about *cis*- or *trans*-amide bond distributions as peptides that show such poor population preferences are of limited interest in medicinal chemistry.

Table 2*: Comparison of peptides, which contain one proline (or D-proline) and one N-methylated alanine (A´ for Me-L-Ala and a´ for Me-D-Ala). They are grouped in pairs in which both units are interchanged for each peptide. The populations of the dominating conformations are given.*
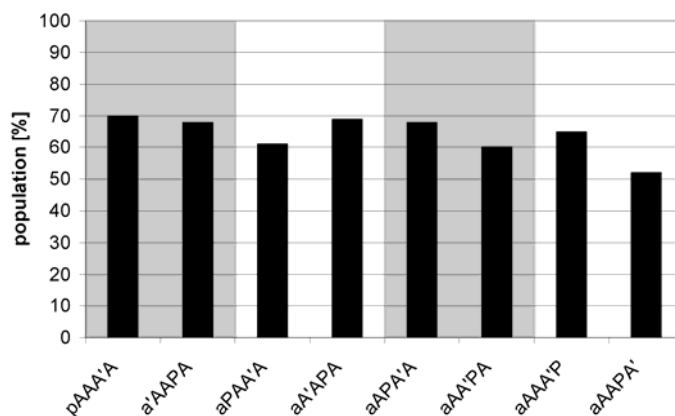
Summing up, it was possible to show that cyclic peptides containing one proline or one *N*-methylated amino acid reveal comparable conformational features. This allows substituting a

proline residue by an *N*-methylated amino acid without changing the overall conformation. Proline is often used as inducer of distinct conformations, e.g. turns or breaking helices. For conformational design it is also important to identify strongly preferred structures. Hence, the use of *N*-methylated amino acids allows for bringing additional side chain functionality into conformationally restricted (cyclic) peptides and therefore opens new perspectives for drug design. However, care should be taken when two prolines are to be replaced by *N*-methylated amino acids because the resulting structures might differ in their conformation. Finally, incorporation of one proline and one *N*-methylated amino acid into cyclic pentapeptides seems not to be useful since no strong preference of one single conformation was observed in the here demonstrated cases.

I.1.4 The Impact of Side-Chains on the Conformation of *N*-Methylated Cyclic Pentapeptides

I.1.4.1 Background

Introduction of mutations in proteins is the common way to explore the importance of the residues for protein-protein-interactions. However, it is not only the change of the side-chain functional groups but it is accompanied by conformational effects as well. Here, the latter effect is explored by substitution of a single amino acid by another. So, steric and electronic effects of the side chain with and without functional groups will not only influence the interaction with molecular reaction partners like e.g. receptors but also influence the conformation itself. In a first approximation, the backbone conformation of cyclic peptides is dominated by the sequence of D- and L-amino acids. Furthermore, the pattern of *N*-methylation also influences the structural properties[18].

The incorporation of *N*-methylated amino acids in cyclic peptides can have a strong impact on the structure and activity of peptides. The *N*-methylation of an amide bond increases the lipophilicity of the peptide and can lead to a more rigid structure[17]. Out of that, pharmacological features such as cell permeability or enzymatic stability can be increased and thinking of the principles of the Veber rules, the oral availability can be increased by the reduction of rotatable bonds[53]. In addition, higher receptor selectivity can be gained or agonists can be converted into antagonists[17,88-92].

In medicinal chemistry, one always tries to gain a preferred conformation which is as close as possible to the bioactive conformation of the natural ligands[14]. To avoid the time-consuming synthesis of large libraries, it is desirable to have template molecules that adopt a desired conformation. Having knowledge of the structure of the natural ligand, the template with the most similar backbone structure can be chosen whereas only the residues determining selectivity and activity have to be added. For non *N*-methylated cyclic peptides, a series of such templates or structure predictions are known, e.g. for cyclic pentapeptides of the DL_4 type[40,69,70,93]. Recently, also a large library of cyclic pentapeptides consisting of the sequence *cyclo*(-D-Ala-Ala$_4$-) was synthesized and the impact of several different degrees of *N*-methylation on the conformation were tested[18,48]. In contrast to the improvement of pharmacological features, it was shown that *N*-methylation additionally reduces the energy barrier between the *cis*- and *trans*-isomer which may result in an undesirable ratio shift between the preferred and the unwanted conformation.

I.1.4.2 Results and Discussion

In order to expand the latest conformation studies performed by Chatterjee *et al.*[18,48], the focus of this work was set on the influence of amino acid sidechain groups in respect of the backbone

structure of cyclic pentapeptides. To elucidate possible effects, the peptide *cyclo*(-a-A-A-MeA-A-) was chosen as starting template. Since it exhibits two equally populated conformations on the NMR timescale in DMSO (see Fig. 24), the peptide is sensitive to even minor changes in the stereo-electronic profile when introducing variable side-chains.
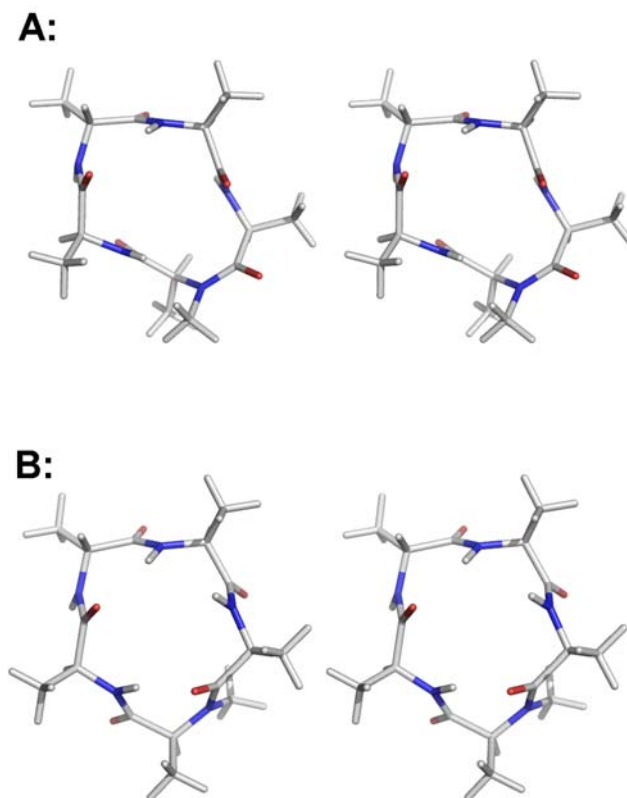
Figure 24*: Stereoview of the two different structures of cyclo(-a-A-A-MeA-A-). A: Structure of the peptide containing a cis-peptide bond between Ala³ and MeAla⁴. B: All-trans conformation of the peptide.*

To investigate the effect of side-chain bulk on the backbone conformation, each alanine of the peptide was substituted by hydrophobic (leucine, alanine), hydrophilic (aspartic acid, asparagine, serine), aromatic (phenylalanine, tryptophane) and β-branched (threonine, valine, isoleucine) amino acids, thus generating five positional isomers of each amino acid type.
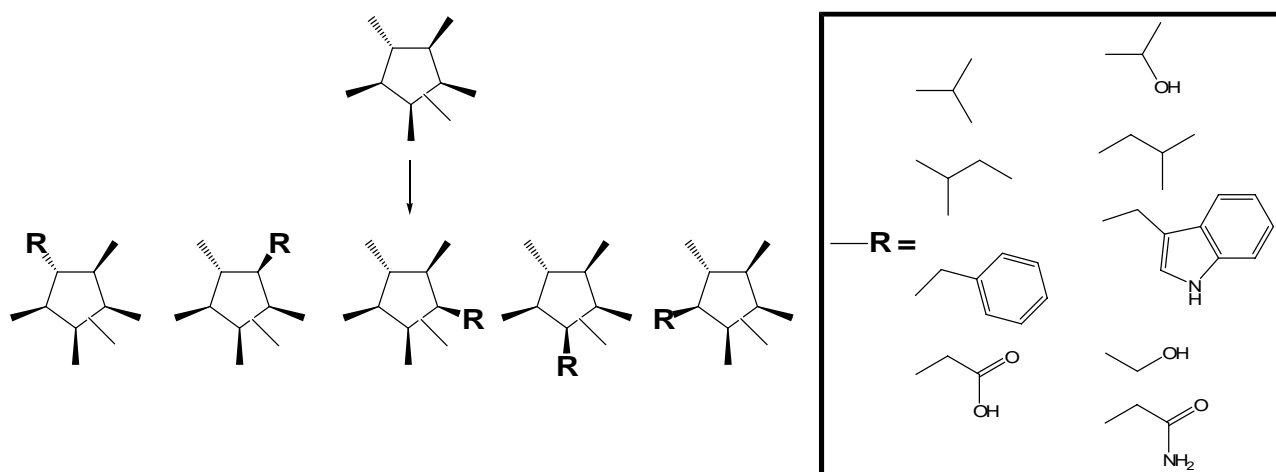
Figure 25*: Schematic overview of the synthesized library.*

After investigation of the synthesized 45 peptides, it was found that the preferred conformation of all peptides was the all-*trans* conformation. Regarding this, the sequence position of the amino acid substitution has a tremendous impact on the ratio of the different structures (Tab. 3).

Table 3*: Population of the all-trans conformation in [%].*
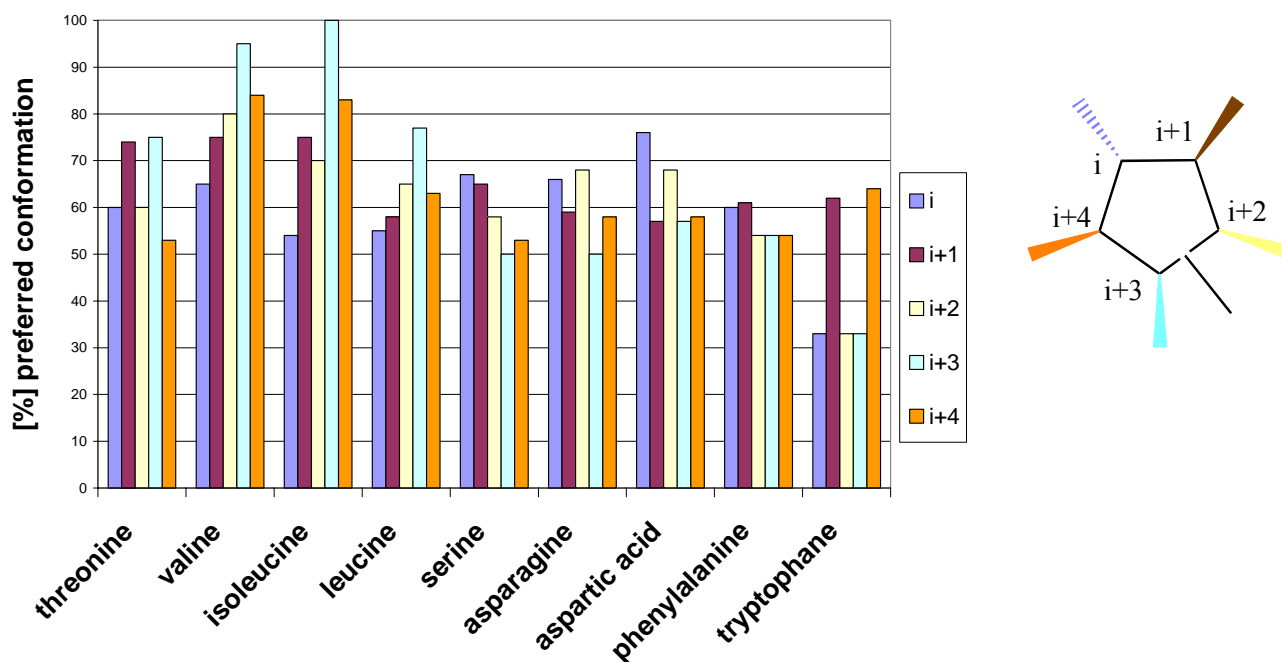
In a first approximation, it can be stated that all amino acids with a CH_2-group at the C^β-position only show subtle changes on the equilibrium of the two conformations. Solely leucine and tryptophane show a deviation at some positions.

Introduction of tryptophane seems to be completely disfavored at the (*i*)-position (the position of the D-residue), (*i*+2)- and (*i*+3)-position, where several low populated conformations were found.

For the other positions, (*i+1*) and (*i+4*), there is only a slight impact on the 50/50 structure ratio. This result is in good agreement with former studies which showed that tryptophane can stabilize β-hairpin structures when it is introduced at non-hydrogen binding positions[84,85]. Phenylalanine can be introduced at any position of the cyclic pentapeptide without having a strong influence on the ratio of the two different conformations (one *cis* and all-*trans*).

The incorporation of aliphatic side chain residues (both hydrophilic and hydrophobic) into the peptide does not lead to a significant augmentation of the *trans*- to *cis*-ratio with the exception that there is a slight increase of the all-*trans* conformation when a side-chain group is inserted at the (*i*)-position. This effect was observed especially for aspartic acid.

Opposed to the results presented so far, introduction of the β-branched amino acids threonine, valine and isoleucine caused dramatic changes of the 50/50 ratio of *trans*- to *cis*-conformation. Whereas nearly no influence was observed for the incorporation at the (*i*+1)-position the presence of a β-branched residue at all the other positions resulted in a strong preference of the all-*trans* conformation of the peptide. When the amino acids were introduced at the (*i*+2)-position, a *trans*- to *cis*-ratio of approximately 75/25 for all three amino acids was obtained. At the (*i*+3)-position, valine (80/20) and isoleucine (70/30) improved the population of the *trans*-conformation while the insertion of threonine does not show any significant effect. The highest impact on the ratio of the two conformations was observed at the (*i*+4)-position whereby valine (95/5) and isoleucine (100/0) showed a higher influence than threonine (75/25). At the *i*-position, threonine as well as all non-β-branched amino acids only slightly affects the *trans*/*cis*-ratio. In contrast, valine (84/16) and isoleucine (83/17) notably increase the population of the all-*trans* conformation.

An explanation for the stronger impact of valine and isoleucine on the backbone conformation compared to threonine may be found in the differing side-chain bulk. Having a van der Waals volume of 82.17 Å^3, threonine is not as sterically demanding as valine (89.32 Å^3) and isoleucine (101.87 Å^3) resulting in a higher degree of freedom of the peptide backbone.
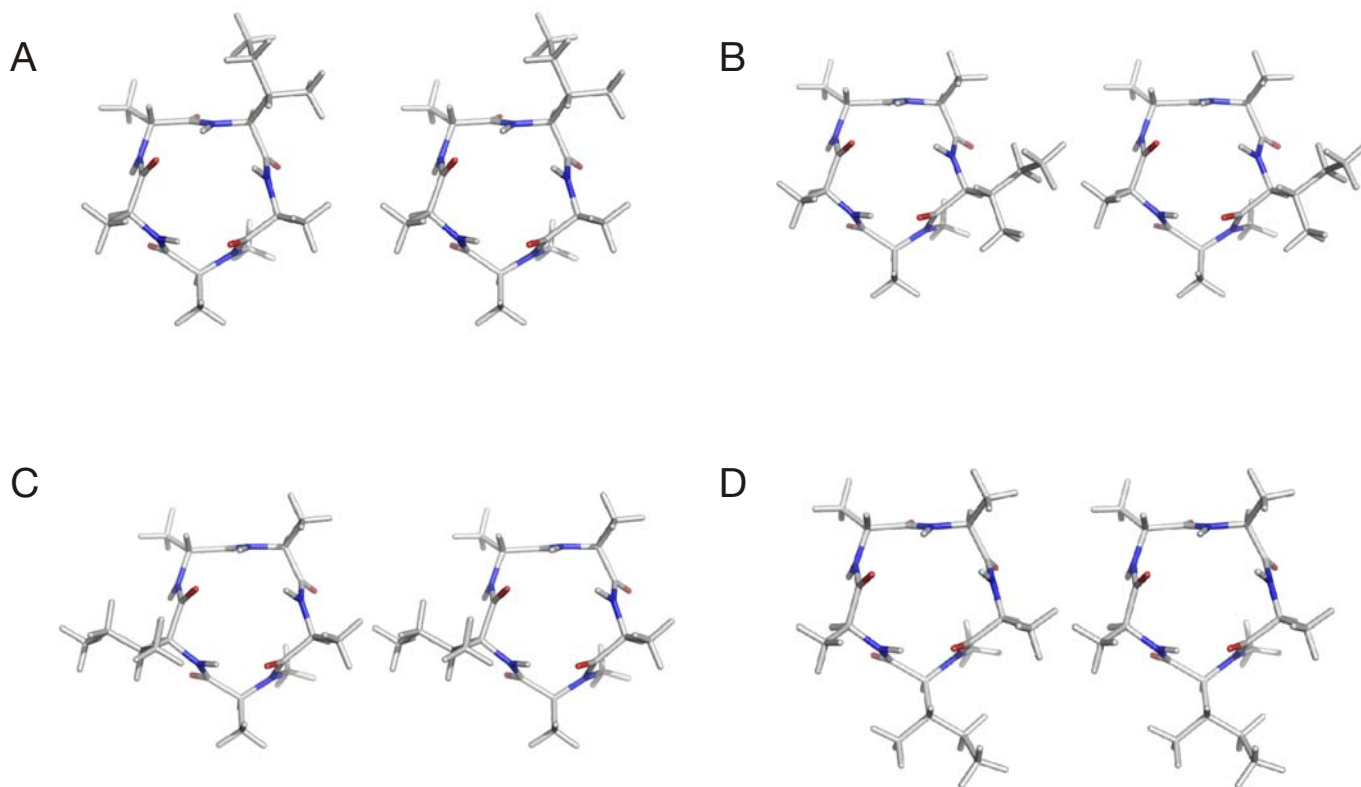
Figure 26*: Stereoview of the preferred conformations of the four peptides with one isoleucine in the sequence and a trans/cis-ratio of more than 70/30. A: cyclo(-a-I-A-MeA-A-)* **90***, B: cyclo(-a-A-I-MeA-A-)* **91***, C: cyclo(-a-A-A-MeA-I-)* **93***, D: cyclo(-a-A-A-MeI-A-)* **92**

Looking at the structures of the cyclic pentapeptides, one can see that the D-residue introduces a β-turn between the amino acids Ala[3] to Ala[5] (considering the nomenclature for turn-structures, where the D-residue is named as *i*+1, the turn is situated between *i*+3 (NH) and *i* (CO)). Furthermore, also a γ-turn between the amino acids Ala[3] to Ala[5] occurs (see figure 26 for the isoleucine peptides). The presence of a β-turn in a cyclic pentapeptide always imparts rigidity in the backbone conformation whereas a γ-turn allows higher flexibility. However, strong internal dynamics can be reduced or even removed via *N*-methylation. Because of an increased steric bulk in the neighborhood of adjacent C$^\alpha$'s, random flipping of the peptide bond is prevented[94]. Thus, a higher side-chain bulk located next to the *N*-methylated peptide bond incorporates rigidity into the backbone and results in a higher preference of the all-*trans*-conformation. Hence, a closed γ-turn and not a *cis*-peptide bond is found at this position. By help of this concept it becomes clear why threonine has the lowest impact of the three β-branched amino acids at the (*i*+4)-position whereas isoleucine has the strongest one. This observation also holds good for the (*i*) and (*i*+3)-position. Looking at the (*i*+2)-position, it seems that the volume of threonine is big enough to have the same effects as valine and isoleucine.

In summary, the impact of different amino acid side chains on the backbone conformation was demonstrated. Considering the methodology of "spatial screening", this procedure is based on the fact that for a given sequence of chirality the side-chains show no effect (in a first approximation)[38]. To verify this, the described test system was chosen to prove this approach as it is sensitive to smallest changes in energy. Out of the results obtained, it can be seen that, as long as no β-branched amino acids are used, the influence of side-chains is close to zero. However, if this is not the case, one has to take care about the applicability of the spatial screening system. Nevertheless, this screening method is useful as only the same functional groups in different spatial orientation are presented. Finding a hit, the conformation of this compound has to be determined anyway.

I.2   N-Methyl Scan and Ring Enlargement of CXCR4-Binding Peptides[95]

> Hier steh ich nun, ich armer Tor,
>
> und bin so klug, als wie zuvor.
>
> Johann Wolfgang von Goethe (Faust)

The following project was performed in cooperation with Dr. Norman Koglin and Dr. Margret Schottelius from the group of Prof. Dr. Hans-Jürgen Wester. All biological testings of the compounds synthesized in this project have been performed by them.

I.2.1   Background

I.2.1.1 The Chemokine Receptor CXCR4

Chemokines are chemotactic cytokines that can cause a guided migration of leucocytes. They are stimulated by inflammatory cytokines, growth factors and pathogenic stimuli[96,97]. The chemokine proteins have an average molecular weight of about 8-10 kDa and can be categorized into four groups depending on the position of the first two cysteins starting from the C-terminus: CXC, CC, C und CX3C[98].

Signalling through chemokines, which is performed by G protein-coupled receptors, can influence the mobility of cells in inflammation as well as transportation of hematopoietic stem cells (HSC), lymphocytes and dendritic dells[98,99].

Currently, the most investigated chemokine receptor is CXCR4[100], due to the fact that CXCR4 and its natural ligand CXCL12 (also called SDF-1, stromal derived factor 1) play an important role in HIV-infection, hematopoiosis, transportation of lymphocytes as well as in the development processes like organogenesis, vascularization and embryogenesis[97,98,101].

CXCR4 originally was cloned by several different groups as a chemokine receptor having an orphan status and named "fusin" or "LESTR"[102,103]. Later, the receptor could be found on most of the leukocyte types like, e.g. B-cells and on most of the T-lymphocytes, but only seldom on natural killer cells[104]. The discovery that SDF-1 is the natural ligand of Fusin/LESTR finally enabled the right classification as chemokine receptor CXCR4[105,106] .

CXCR4, like all chemokine receptors, constitutes a seven transmembrane domain receptor (7TM) that is bound to a heterotrimeric G-protein complex on the cytoplasmatic site. Signal transduction causes an activation of the G protein and of phospholipase C followed by an augmentation of the calcium concentration in the cytosol[107]. Furthermore, stimulation of CXCR4 can cause activation

of ERK-2 and PI 3-kinase. In contrast to other chemokine receptors, activation of these two signalling pathways holds much longer[107].
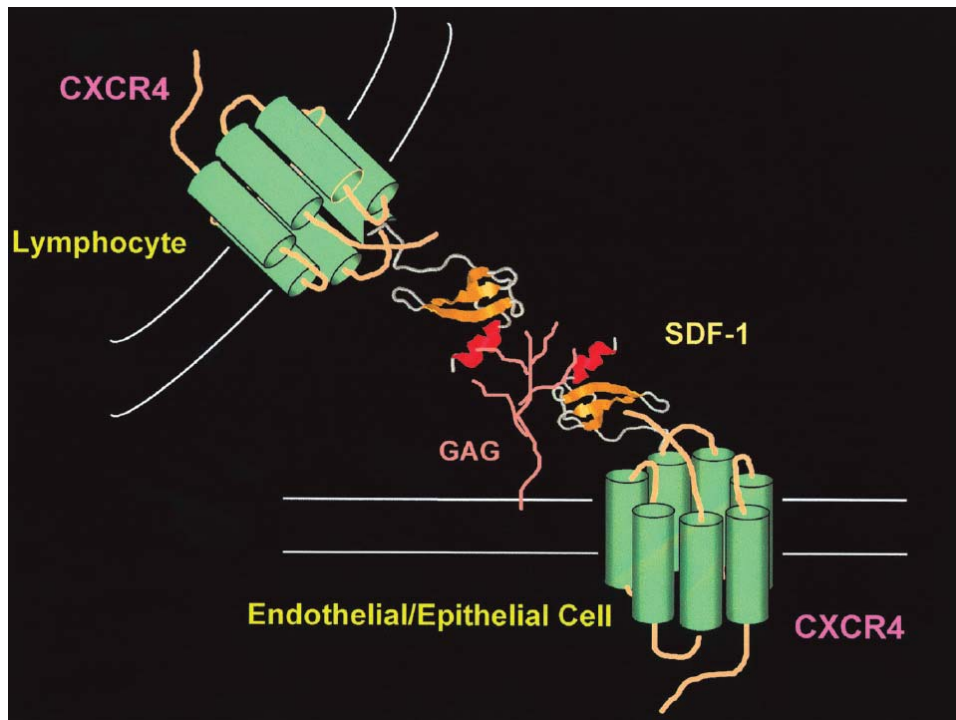
Figure 27: *Scheme of CXCR4 activation via SDF-1[100]. Reprinted by permission from Wiley Blackwell.*

In 1996, it was found that doses of CXCL12 can block HIV-1 cell penetration by binding to CXCR4[105,106]. *Feng et al.* could show that CXCR4 and CD4 are used by T-cell specific HIV-1 for *env*-mediated HIV-1 infection[108]. The finding that CXCR4 is a co-receptor for HIV dramatically potentiated research based on CXCR4 and SDF-1 which led to a much more detailed knowledge about the impact of CXCR4 and its ligand in immunology and embryology[100,109].

In 2001, Scotton *et al.* discovered that out of 14 chemokine receptors that were investigated, only CXCR4 is expressed on ovarian cancer cells[110]. Continuative research was able to prove that CXCL12 accelerates or improves the cancer cell growth of these cells even under unfavorable conditions[111]. Later onwards, these findings could also be shown for micro metastasis and colon carcinoma[112]. By now, CXCR4 is the most frequently found chemokine receptor on tumor cells, being proven to be overexpressed in 23 different types of cancer: B-CLL, AML, B-lineage ALL, intraocularic lymphoma,[113] non-Hodgkin-lymphoma, central follicle lymphoma, CML, multiple myeloma, pancreatic cancer,[114] prostatic cancer,[115] breast cancer,[116] ovarian cancer,[111,117] thyroid cancer, colorectal cancer, oral imbricated cancer, cervical cancer, neuroblastoma, renal cancer, glioma, astrozytoma,[118] rhabdomyomsarkoma,[119] melanoma and small cell lung carcinoma[101].

These findings gave hope to find a new starting point for cancer therapy as Zeelenberg *et al.* were able to fix CXCL12 on the endoplasmatic reticulum (ER) so that it can not reach the cell surface.

However, CXCR4 is still able to bind to this CXCL12 causing a retention in the ER inhibiting a CXCR4 expressing cell line to express its receptor on the cell surface[120].

A first therapy approach using the knowledge about CXCR4 and its ligand CXCL12 was shown by *Retz et al.* who were able to successfully inhibit metastasis of bladder cancer by giving doses of T140, a peptide originally developed by the group of *Nobutaka Fujii* to inhibit the infiltration of HIV-1[121].

I.2.1.2 The Development of FC131 by Fujii *et al.*

In 1992, the group of Nobutaka Fujii succeeded in finding a peptide called T22 which was developed out of the natural products Tachyplesin I and Polyphemusin II and is able to block HIV-1 infiltration into cells. Later, it was found that T22 is binding towards CXCR4 which is used as a co-receptor for this process[122].

		IC$_{50}$ (μM)		
		HIV-1 replication (NL4-3) in PBMC	12G5 binding in MOLT-4 cells	SDF-1α binding in MOLT-4 cells
Tachyplesin I	H$_2$N-Lys-Trp-Cys-Phe-Arg-Val-Cys-Ty-Arg-Gly-Ie-Cys-Tyr-Arg-Arg-Cys-Arg-CONH$_2$	4.0	2.9	0.10
Polyphemusin II	H$_2$N-Arg-Arg-Trp-Cys-Phe-Arg-Val-Cys-Tyr-Lys-Gly-Phe-Cys-Tyr-Arg-Lys-Cys-Arg-CONH$_2$	0.44	0.36	0.010
T22	H$_2$N-Arg-Arg-Trp-Cys-Tyr-Arg-Lys-Cys-Tyr-Lys-Gly-Tyr-Cys-Tyr-Arg-Lys-Cys-Arg-CONH$_2$	0.040	0.025	0.0020

Figure 28: *Development of T22 out of Tachyplesin and Polyphemusin.*[123]

Additional sequence optimization of the 18 amino acid long peptide lead to T140, a cyclic disulfide bridged peptide built up out of 14 amino acids which is able to inhibit HIV-1 binding with an IC$_{50}$ value of 2.5 nM showing only low cytotoxicity and improved enzymatic stability compared to T22[124-127]. Further sequence optimization based on the spatial screening methodology lead to FC131, *cyclo*(-Nal-Gly-D-Tyr-Arg-Arg-), which binds towards CXCR4 with an IC$_{50}$ value between 4.2 and 7.9 nM and shows high enzymatic stability[128-130].
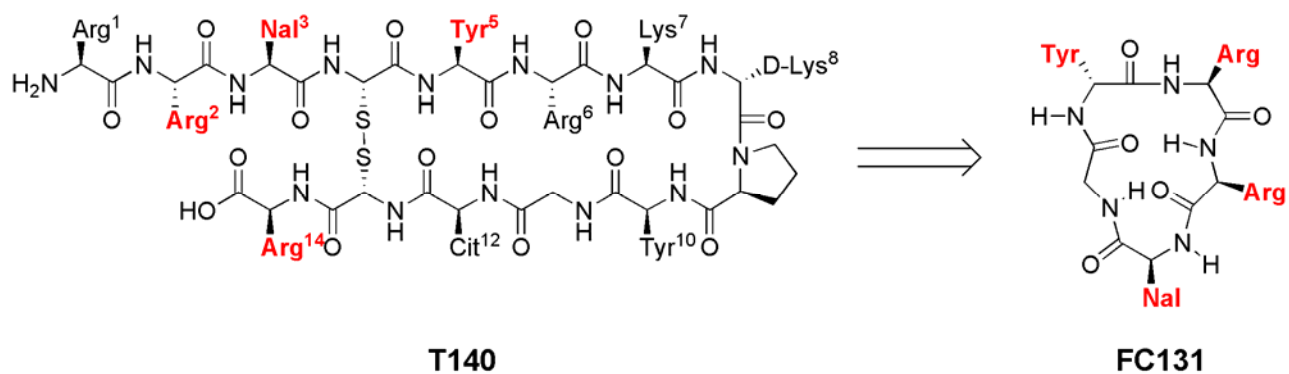
Figure 29: *Sequence optimization of T140 leading to FC131[131]. Amino acids highlighted in red are essential for biological activity.*

I.2.2 Results and Discussion

As can be seen in figure 29, the optimization of T140 to FC131 not really results in a peptide where the amino acids which are essential for biological activity are in the same position as in the parent peptide. So, the question arose, if it might be able to enlarge the pentapeptides into a hexapeptide structure and to improbe biological activity by doing so. On the other hand, it might be possible just shorten the "right part" of T140 (the cycle), as it binds into the binding pocket of CXCR4 with its C- and N-terminus and not the peptide cycle.

I.2.2.1 Ring enlargement of FC131 towards a cyclic hexapeptide and *N*-methylscan thereof

In a first approach, though being in contrast to the homology model of Luciana Marinelli for CXCR4, it was tried to introduce a sixth amino acid into the cyclic pentapeptide FC131 by introducing alanine, aza-glycine or lysine. Performance of a D-amino acid scan finally led to the cyclic hexapeptide *cyclo*(-y-R-R-Nal-A-G-) showing a binding affinity towards CXCR4 of 73 nmol[132]. This sequence was taken to perform a *N*-methyl scan in order to screen for a more active conformation. For the mono-*N*-methylated compounds, one compound -*cyclo*(-Mey-R-R-Nal-A-G-) **124**- with low activity towards CXCR4 was found, while all other mono-*N*-methylated compounds were completely inactive.

Mono-Methylated
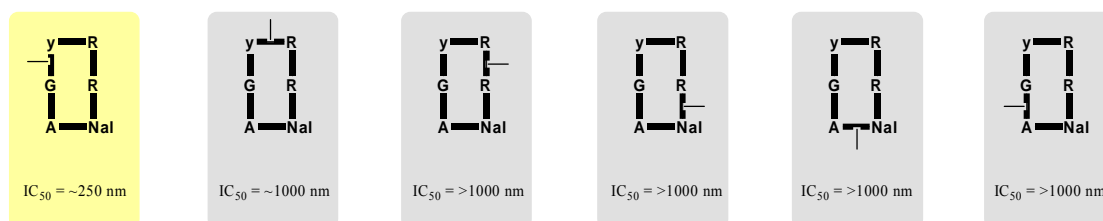
Figure 30*: Mono-N-methylated hexapeptides.*

The complete library of the di-*N*-methylated hexapeptides as well as the library for the tri-*N*-methylated hexapeptides and the partial library of the tetra-*N*-methylated hexapeptides resulted in no biological active compounds.

Di-Methylated

y|R G R A━Nal IC$_{50}$ = >1000 nm	y|R G R A━Nal IC$_{50}$ = >1000 nm	y|R G R A━Nal IC$_{50}$ = >1000 nm

IC$_{50}$ = >1000 nm (each panel)

Tri-Methylated

IC$_{50}$ = >1000 nm (each panel)

Tetra-Methylated

IC₅₀ =>1000 nm (×6, top row)

IC₅₀ =>1000 nm (×4, bottom row)

$IC_{50} => 1000\,nm$
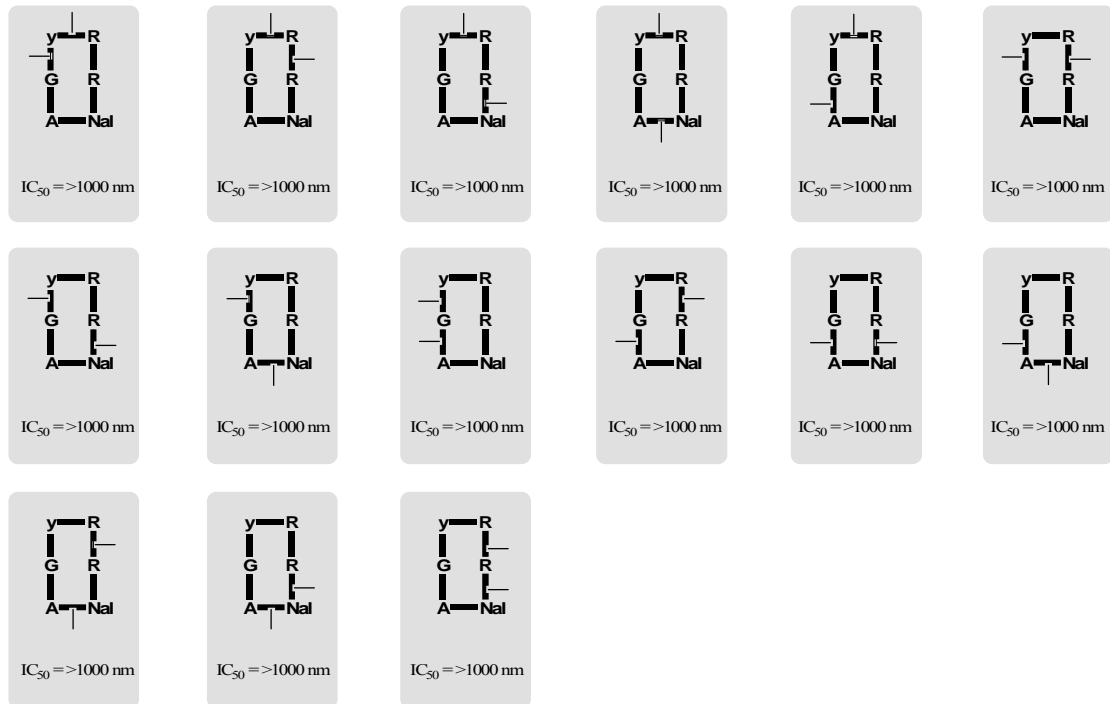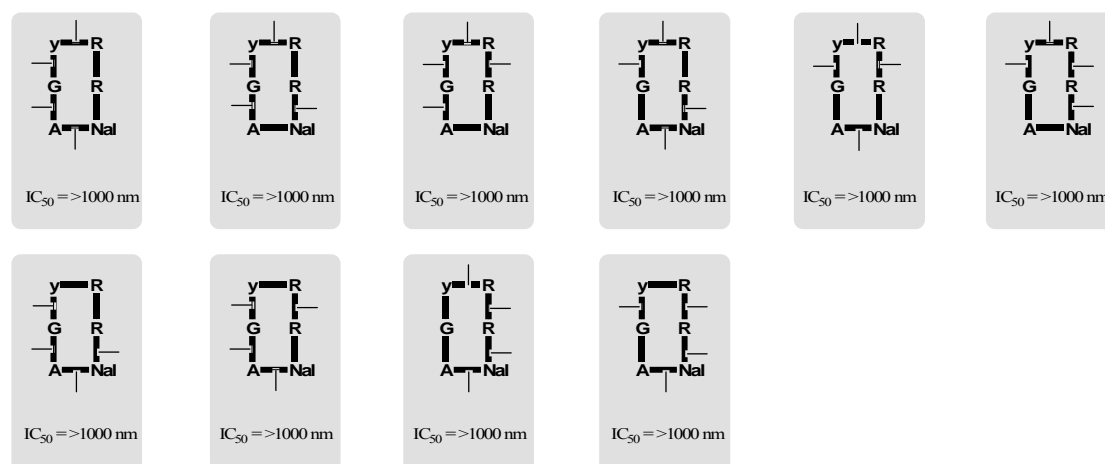
Figure 31: *Di-, tri- and tetra-N-methylated hexapeptides.*

I.2.2.2 Ring-Size Reduction Scan of T140

As the *N*-methyl-scan of the cyclic hexapeptid derived from FC131 did not result in any compound with acceptable biological activity towards CXCR4[95,132], it was decided to go back to the parent peptide T140. As can be seen in figure 32, all amino acids, needed for biological activity can be found between Arg^2 and Arg^6 as well as between Arg^{11} and Arg^{14}. So, it might be possible to cut out the sequence Lys^7-D-Lys^8-Pro^9-Tyr^{11} by directly coupling Arg^6 towards Arg^{11} and to leave out Arg^1 without loosing biological activity as it is supposed that T140 is binding with its tail and not the cycle into the binding pocket of CXCR4[133].
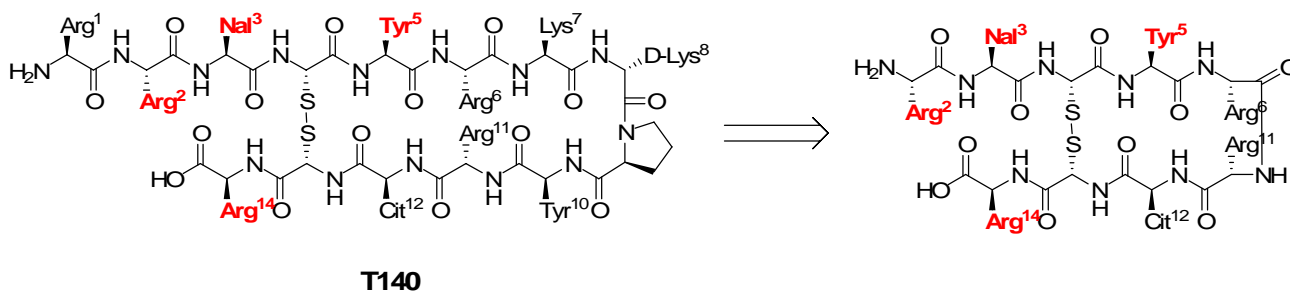
T140

Figure 32: *Shortening of T140. Amino acids highlighted in red are essential for biological activity.*

Surprisingly, the shortened disulfide bridged peptide without Lys^7-Tyr^{11} (**174**) didn't show any biological activity but the peptide also shortened by Arg^1 (**175**) again showed mild acitivity towards CXCR4. Also Arg^2 which was supposed to be needed for biological activity referring to Fujii and co-workers[131] could be truncated without decreasing the activity (**176**). Further truncation of Nal^3 (**177**) led – as expected - to a complete loss of the biological activity, which supports that the Nal side-chain is one of the four pharmacophoric groups in FC131 as was proposed by the group of Fujii[130].

Ic$_{50}$ [nM]	Compound No
>1000	174
400-500	175
400-500	176
>1000	177

```
     S————————S
     |        |
H2N-Arg-Arg-Nal-Cys-Tyr-Arg-Arg-Cit-Cys-Arg-OH

     S————————S
     |        |
H2N-Arg-Nal-Cys-Tyr-Arg-Arg-Cit-Cys-Arg-OH

     S————————S
     |        |
H2N-Nal-Cys-Tyr-Arg-Arg-Cit-Cys-Arg-OH

     S————————S
     |        |
H2N-Arg-Nal-Cys-Tyr-Arg-Arg-Cit-Cys-OH
```

Figure 33*: Shortening of T140.*

As also the D-amino acid-scan of compound **175** didn't result in any more active compound, the optimization of the T140 molecule had to be given. An alanine-scan, which would have normally been performed to figure out the biological active amino acids was useless, as the relevant amino acids were also known and also the biological active penta- and hexapeptides had been already investigated. Nevertheless, it was possible to reduce the size of T140 from a 14-mer to a heptamer by creating a new peptide **175**, not described in literature yet and by retaining some of the biological activity.

	IC$_{50}$ [nM]	Compound No
S————————S | | H$_2$N-Arg-Nal-Cys-Tyr-Arg-Arg-Cit-Cys-Arg-OH	400-500	175
S————————S | | H$_2$N-**arg**-Nal-Cys-Tyr-Arg-Arg-Cit-Cys-Arg-OH	>1000	178
S————————S | | H$_2$N-Arg-**nal**-Cys-Tyr-Arg-Arg-Cit-Cys-Arg-OH	>1000	179
S————————S | | H$_2$N-Arg-Nal-**cys**-Tyr-Arg-Arg-Cit-Cys-Arg-OH	>1000	180
S————————S | | H$_2$N-Arg-Nal-Cys-**tyr**-Arg-Arg-Cit-Cys-Arg-OH	>1000	181
S————————S | | H$_2$N-Arg-Nal-Cys-Tyr-**arg**-Arg-Cit-Cys-Arg-OH	>1000	182
S————————S | | H$_2$N-Arg-Nal-Cys-Tyr-Arg-**arg**-Cit-Cys-Arg-OH	>1000	183
S————————S | | H$_2$N-Arg-Nal-Cys-Tyr-Arg-Arg-**cit**-Cys-Arg-OH	>1000	184
S————————S | | H$_2$N-Arg-Nal-Cys-Tyr-Arg-Arg-Cit-**cys**-Arg-OH	>1000	185
S————————S | | H$_2$N-Arg-Nal-Cys-Tyr-Arg-Arg-Cit-Cys-**arg**-OH	>1000	186

Figure 34: *D-amino acid scan of the shortened T140 peptide.*

II Peptidomimetics

II.1 Peptidomimetics for Purification of FVIII[134,135]

Publier dans un petit journal ne veut pas dire petit résultat.

Ce qui compte, c'est que les gens l'essayent pour dire que ça marche!

(Dr. Abdellah Benhida, Katholic University Leuven, Belgium)

The following project was performed in cooperation with Dr. Sebastian Knör for the synthetic part. Biological testings have been performed in cooperation with Dr. Alexey Khrenov and Prof. Dr. Evgueni L. Saenko at the University of Maryland (MD, USA) and Dr. Abdellah Benhida, Dr. Sabrina C. Grailly and Prof. Dr. Jean-Marie Saint-Rémy at the Katholic University Leuven (Belgium). For a detailed assignment of the work performed, please see experimental section.

II.1.1 Background

II.1.1.1 The Blood Coagulation Factor VIII (FVIII)

The FVIII molecule (~330 kDa, 2332 amino acid residues) is a secretory glycoprotein consisting of three homologous A domains, two homologous C domains and the unique B domain, which are arranged in the order of A1-A2-B-A3-C1-C2[136,137]. The large B domain is not important for the FVIII procoagulant activity[138] but recent studies demonstrated its role in protecting the activated form of FVIII from proteolytic inactivation[139]. Prior to its secretion into plasma, FVIII is processed intracellularly to a series of noncovalently associated, metal(II)-linked heterodimers by cleavage at the B-A3 junction[140-142]. The cleavage generates the heavy chain (HC) consisting of the A1, A2 and B domains and the light chain (LC) composed of the A3, C1 and C2 domains[141,143]. The resulting protein varies in size due to additional cleavages within the B domain, giving molecules with different length[136,144].

As a cofactor of the intrinsic blood coagulation, FVIII interacts with a variety of other proteins. After secretion into plasma, FVIII binds towards the von Willebrand Factor (vWF) with high affinity in an inactive form through its A3 and C2 domains as well as the C1 domain[145,146] which protects it against proteolysis[147,148] and increases the half life of FVIII in plasma from 2-3 hours to 12-14 hours[149,150].

A crystal structure of the complete Factor VIII has not yet been reported and only model structures have been calculated based on the several subdomains that were crystallized so far[151]. The best crystal structure available so far was reported in 2008 by Shen *et al.* showing a

heterodimer of the B-domain deleted Factor VIII. As the function of the B-domain is only to stabilize the FVIII structure and has no influence on biological activity, this is the first structure of a fully active FVIII[152].
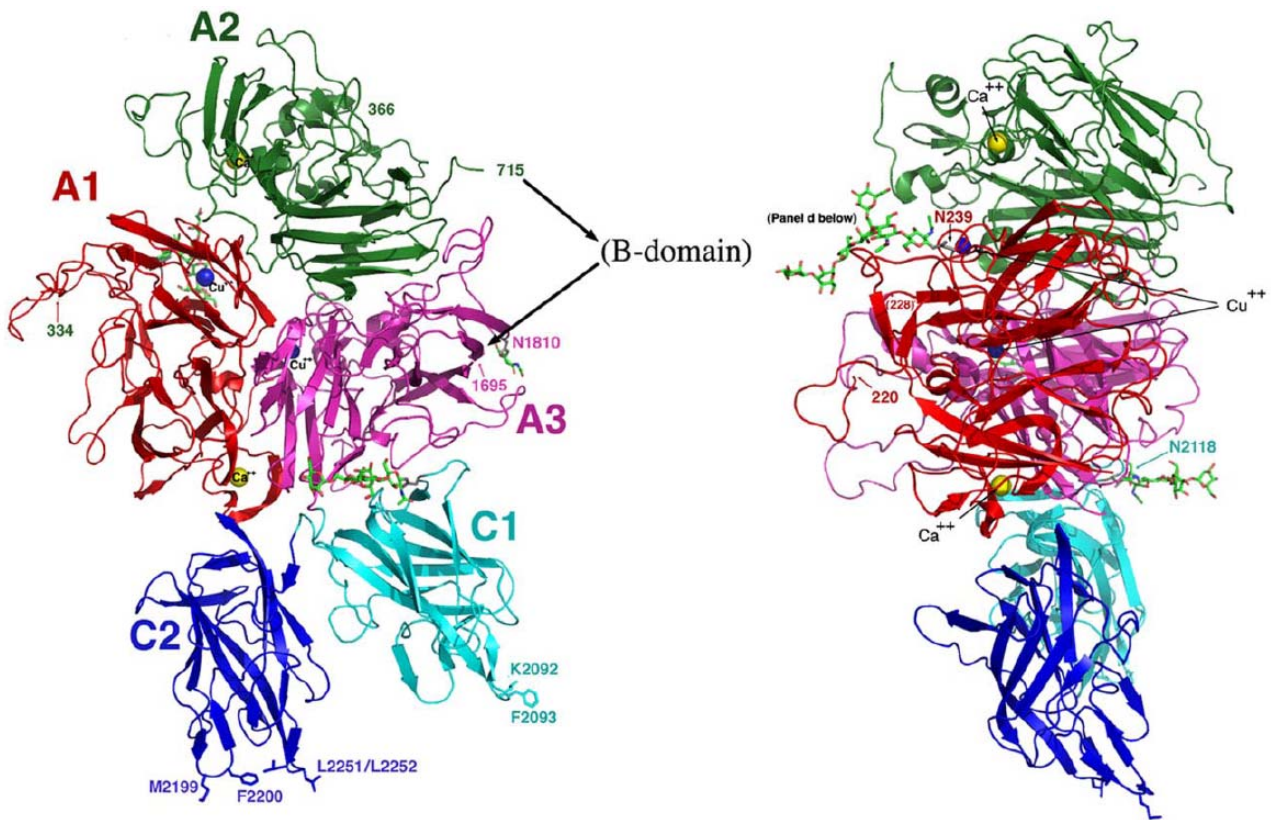
Figure 35: *Crystal structure of the B-domain deleted FVIII heterodimer[152]. This research was originally published in Blood: B. W. Shen et al., The tertiary structure and domain organization of coagulation factor VIII, Blood 2008, 111 (3), 1240-1247. © the American Society of Hematology.*

Factor VIII is an essential component of the intrinsic blood coagulation pathway circulating in blood in complex with von Willebrand factor (vWF), which protects and stabilizes it[153-157]. The intrinsic pathway (also termed contact activation pathway) is activated when blood comes into contact with sub-endothelial connective tissues or with negatively charged surfaces that are exposed as a result of tissue damage. Though the extrinsic pathway is much faster in fibrinogen activation than the intrinsic pathway, the intrinsic one is considered as the more important of the two pathways. The pathway involves the clotting factors VIII (FVIII), IX (FIX), X (FX), XI (FXI), and XII (FXII). Also required are the proteins prekallikrein (PK) and high-molecular-weight kininogen (HMWK), as well as calcium ions (Ca^{2+}) and phospholipids (PL) secreted from platelets[158-161].

The intrinsic pathway is initiated by binding of PK, HMWK, FXI and FXII to a sub-endothelial surface exposed by an injury[158-161]. The assemblage results in conversion of prekallikrein to kallikrein, which in turn activates FXII to the activated form FXIIa. Factor XIIa is then able to hydrolyze more prekallikrein to kallikrein, establishing a reciprocal activation cascade. There is

also evidence that the FXII can autoactivate, which makes the pathway self-amplifying[162-164]. FXIIa in turn activates FXI to FXIa, which, in the presence of Ca^{2+}, then activates FIX to FIXa. Factor IX is a proenzyme that contains vitamin K-dependent γ-carboxy-glutamate (*gla*) residues, whose serine protease activity is activated following Ca^{2+} binding to these *gla* residues. Several of the serine proteases of the cascade (thrombin, FVII, FIX, and FX) are *gla*-containing proenzymes.
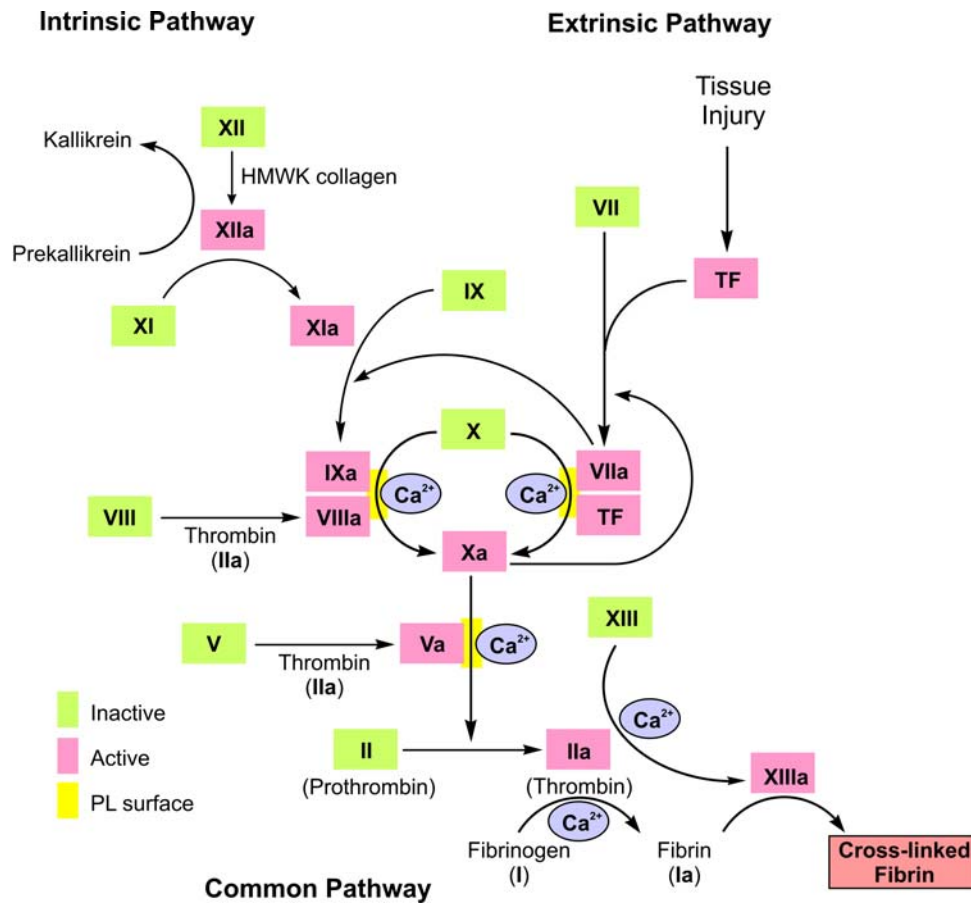
Figure 36: *Simplified illustration of the clotting cascade[165]. (PL: phospholipid, HMWK: high molecular weight kininogen)*

The intrinsic pathway ultimately activates FX, a process which can also be triggered by the extrinsic pathway[158-161]. The activation of FXa requires assembly of the intrinsic tenase (also termed Xase) complex (FVIIIa/FIXa/FX) on the surface of activated platelets which activates FX to FXa in presence of Ca^{2+}. The role of FVIIIa in this process is to act as a receptor for FIXa and FX and as a cofactor of FIXa and FX[166-168]. The activation of FVIII to FVIIIa occurs in the presence of diminutive quantities of thrombin. As the concentration of thrombin increases, FVIIIa is cleaved by thrombin and inactivated.

Additional control of FVIIIa activity is performed by activated protein C (APC) which is an important cofactor inhibitor[169]. It degrades FVIIIa (and also FVa) and is activated by thrombin in presence of thrombomodulin and requires its coenzyme protein S (PS) to function. The dual

action of thrombin (FVIII activation and deactivation) ensures a limited extent of the tenase complex formation[167].

II.1.1.2 Haemophilia A – The Royal Disease

Haemophilia A is one of the most common and severe bleeding disorders[170]. The inoffical name "Royal Disease" arose from the prevalence of the disease in the royal families of England, Spain, Germany and Russia, as a result of Queen Victoria of England (1819-1901) being a carrier. The marriage of Queen Victoria and Prince Albert marked the beginning of haemophilia in the British royal line. Queen Victoria had nine children and as English royal family members married into royalty of other countries, the disease eventually infected most of the royal houses of Europe[170].

Haemophilia A is the result of an X-linked inherited deficiency of FVIII function leading either to reduced FVIII levels or to a dysfunction of FVIII. Due to the X-linked inheritance, haemophilia A affects mostly males as illustrated in (figure 37)[166,171,172].
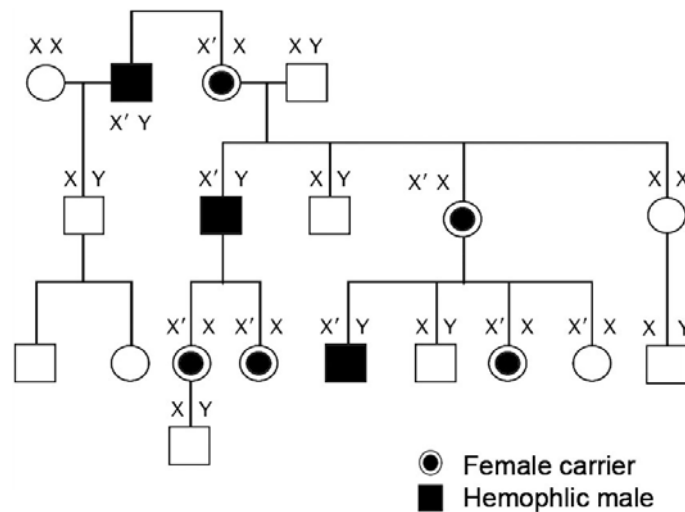
Figure 37: *Inheritance of haemophilia A[165].* **X'** *symbolizes the X-chromosome with the inherited deficiency.*

A lot of mutations can cause haemophilia A. Around 150 different point mutations have been characterized in the factor VIII gene in haemophilia A and the incidence of haemophilia A is approximately one in 5000 males, not varying appreciably between populations[166,170,173,174]. The disease is classified with respect to the FVIII blood level as mild (5-40% of normal), moderate (1-5% of normal) and severe (<1% of normal).

The severe form of the disease is characterized by spontaneous bleedings, as well as uncontrollable bleedings in case of trauma or surgery. Other clinical hallmarks are acute recurrent painful haemarthroses, which can progress to chronic arthropathy characterized by progressive destruction of the cartilage and the adjacent bone, muscle haematoma, intracerebral haemorrhages and haematuria[173].

Current treatment of haemophilia A is performed using infusions of FVIII (replacement therapy), either purified from human blood plasma (plasma-derived FVIII; pdFVIII) or expressed in recombinant cells (recombinant FVIII; rFVIII), normalizing the clotting process and stopping or preventing bleeding[161,175,176]. Out of that, survival and well-being of people with haemophilia depends on the supply of safe therapeutic products[177]. So, numerous haemophilia patients have been infected with HIV-1 or hepatitis C virus *via* injections of contaminated plasma-derived FVIII preparations in the past[170,175,178]. Due to these infections, safety of pdFVIII products has been continuously improved during the last decades[175]. However, isolation of the factor VIII gene in 1984 opened new opportunities for treatment by preparation of recombinant FVIII[179-182]. Nevertheless, rFVIII - as biotechnologically derived product produced by cell culture - carries the risk of transmitting infectious agents[183]. So, about 25% of the first-generation rFVIII concentrates were positive for transfusion-transmitted viruses from contaminated human serum albumin, which is added as stabilizer[184]. Due to this drawback, second-generation rFVIII products do not have added albumin any longer and use sucrose or other non-human derived material as a stabilizer instead[185].

However, as long as human albumin is added to the cell culture media and monoclonal antibodies (mAbs) are used as ligands in affinity purification there is a risk of transfusing pathogens left. Especially transmissible spongiform encephalopathies and new variants of Creutzfeldt-Jakob disease as well as previously unknown pathogens, including new murine viruses, may contaminate today's rFVIII products[183,186]. Consequently, there is a great demand for novel procedures avoiding such components in order to develop the next generation of recombinant FVIII products.

Besides product safety, financial aspects are major factors in the development of new FVIII products. While 88% of the safer but more expensive rFVIII is consumed in Europe and North America, the majority of the world's population with haemophilia is reliant on blood products or does not receive any treatment at all due to economic reasons[175-178].

II.1.1.3 Purification of FVIII

The purification of FVIII remains a challenging task. It involves a complex sequence of different purification techniques such as affinity chromatography[187], ion-exchange chromatography and virus inactivation[188-195]. Nowadays, all recombinant FVIII preparations and many plasma-derived FVIII products are purified via immunoaffinity chromatography employing mAbs as ligands[185,196,197]. Nevertheless, the application of protein ligands in affinity chromatography is very expensive and several problems limit their application[198-201]: Antibodies are known to be eluted along with the product contaminating or inactivating it or even evoking immune

responses[188,193,201]. As biologically derived products, they show lot-to-lot variation and they may be contaminated with e.g. host DNA, viruses or prions which can be transfused to the product[200]. Their high fragility shortens the column life and they suffer from low binding capacities, limited life cycles and low scale-up potential[198,200,201]. Moreover, because of the very strong binding of antibody ligands to FVIII, the procedure requires harsh conditions for elution of the protein which can harm both, the target protein and the ligand.

Synthetic ligands like peptides so far had only little application in affinity separation. Recently, two independent groups reported the development of oligo- and polypeptides as affinity ligands for factor VIII. In 2004, Kelley *et al*.[202,203] published the isolation of a 27 amino acid sequence using phage display techniques. The cyclic polypeptide is currently used in the manufacturing of ReFacto AF (Wyeth), a third-generation product[194]. Another promising effort was reported by the group of Jungbauer that found a series of octapeptides derived from a combinatorial library using spot technology on cellulose sheets showing high affinity towards FVIII. Via immobilization, this ligands could be used to purify FVIII from diluted plasma[204,205]. Nevertheless, the application of oligo- and polypeptides is associated with several problems restricting their use, especially their high sensitivity towards enzymatic degradation[198,201] significantly limiting their application for raw materials such as serum or cell culture extracts as these contain enzymes. Anyway, peptidic ligands are promising lead structures for the development of small non-peptidic molecules. Such compounds could have the potential to reduce production costs and to improve the safety of current and future FVIIII products.

II.1.2 Results and Discussion

As peptides seemed to be a promising target to find new highly active and selective compounds as affinity ligands for purification of FVIII several different aspects had to be considered. Such affinity ligands not only have to be highly active and selective, they also need the ability to give high loading densities on the affinity column to give quantitative retention of the desired molecules. Additionally, the affinity ligand has to be stable towards enzymatic degradation so that the column has a life cycle as long as possible and also can be cleaned under harsh conditions between the purification cycles.

II.1.2.1 Lead Optimization of EYHSWEYC

Starting from the best peptidic FVIII binder EYHSWEYC out of the library published by the group of Jungbauer, optimization via Ala-Scan and D-amino-acid-scan - performed by Sebastian Knör - led to the two highly active peptides YCVWEY and WEYC[134,135,206]. While the newly generated hexapeptide was able to bind 98% of the FVIII bound by the lead structure published by

Jungbauer, WEYC only was able to bind 65%. But, synthesizing a ligand supposed to be used as affinity ligand on a column, two aspects have to optimized: Target binding and loading density on solid support. Considering loading density, WEYC was much better as the hexapeptide compensating its lower binding affinity by higher loading density.
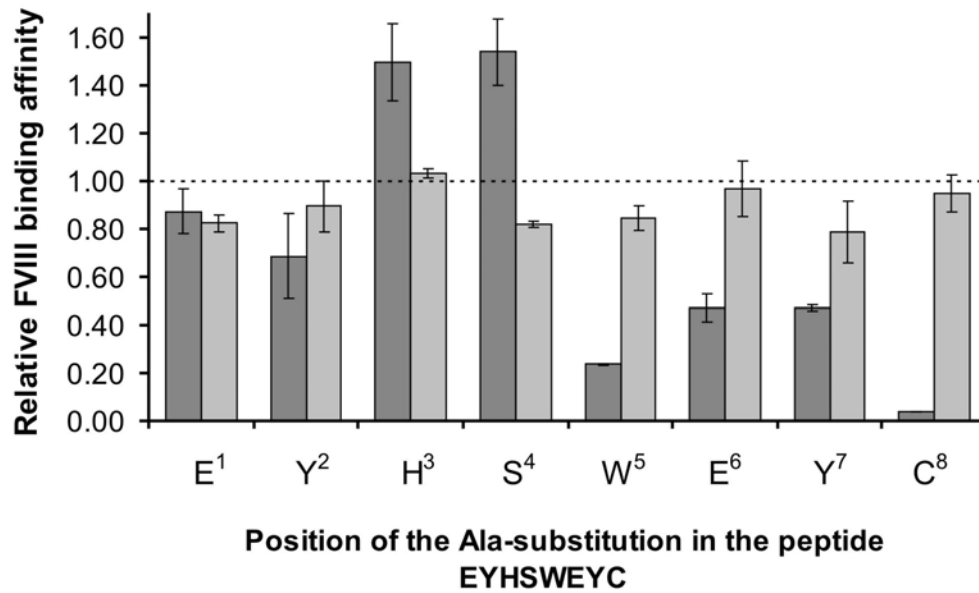
Figure 38*: Alanine-scan and D-amino-acid-scan of EYHSWEYC. Dark grey bars symbolize substitution by Alanine, light grey bars symbolize substitution by the corresponding D-amino acid. The value 1.0 gives the biological activity of the parent peptide.*

Nevertheless, the parent peptide EYHSWEYC and the shortened peptide WEYC showed poor stability towards enzymatic degradation (see figure 39) , performed with proteinase K and human serum (single donor). As an incubation time of about one hour is required for the loading of FVIII on an affinity column, further optimization of the peptide had to be performed to transform the active peptide WEYC into an active and stable peptidomimetic.
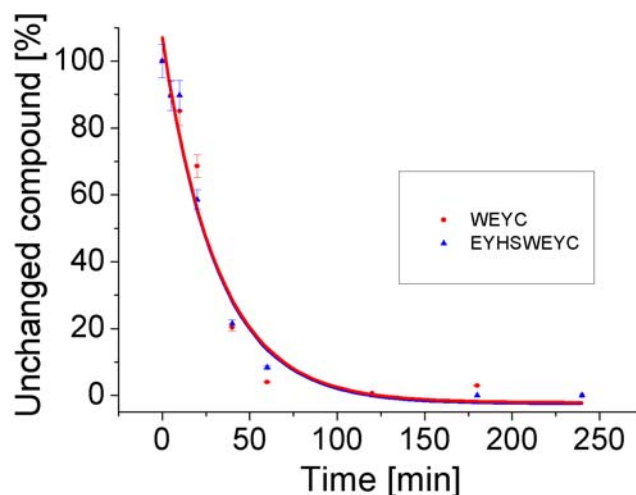
Figure 39*: Serum stability testing using human serum.*

II.1.2.2 From WEYC to the Peptidomimetic C141

To protect the ligand from metabolism by endopeptidases the N-terminal amino-group of tryptophan was cut off by using 3-(1*H*-indol-3-yl)-propanonic acid instead of tryptophan (**B**). Additionally, it was tested, if it might be possible to shorten the 3-(1*H*-indol-3-yl)-propanonic acid to a 3-(1*H*-indol-3-yl)-acetic acid (3-IAA) (**C**). As these compounds still might have been able to be cleaved (Glu-Tyr is a cleavage site for MMP3), reduction of the amide bond between glutamic acid and tyrosine finally led to (3-IAA)Eψ[CH$_2$NH]YC, called **C141**. This compound proved to be completely stable towards enzymatic degradation.
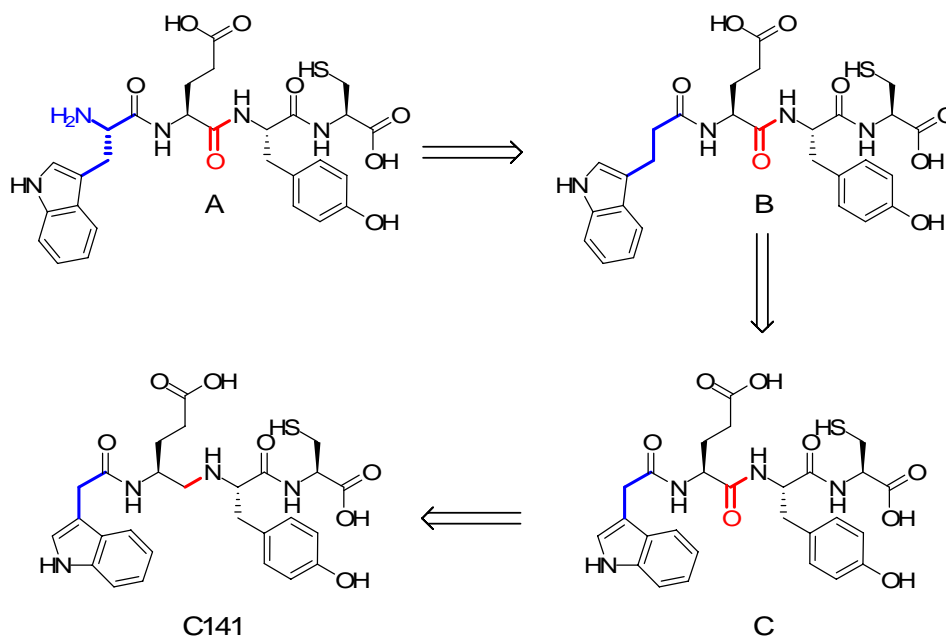
Figure 40*: Optimization of WEYC towards the peptidomimetic C141*

Fortunately, also the loading density of C141 on solid support was good enough to be useful for purification purposes of FVIII as it revealed to be much better than for the tetrapeptide WEYC.
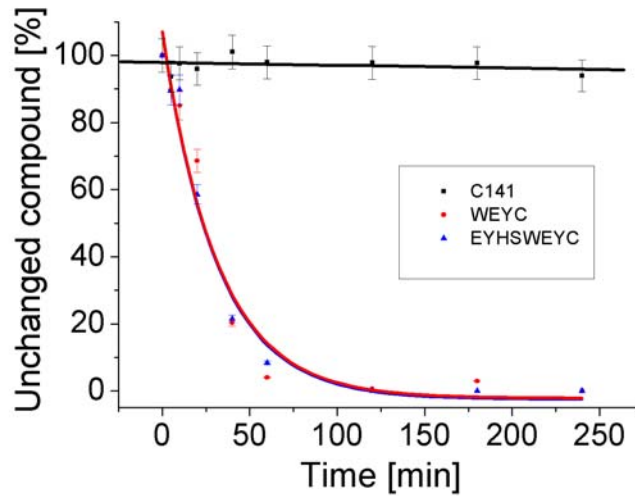
Figure 41: *Serum stability testing using human serum.*

II.1.2.3 Biological Activity of C141

II.1.2.3.1 Binding Studies Using C141-Coated ToyoPearl Resin

For the use as an affinity ligand, C141 had to be bound on solid support. For this purpose, ToyoPearl resin was chosen. This resin has an epoxy-functionality on the surface enabling a ring-opening reaction with the nucleophilic thiol-functionality of the cystein side-chain under mild conditions. The obtained affinity resin proved to be stable under mild basic and acidic conditions and to have long-term stability in ethanol. Only by freezing the affinity resin, a bleeding from the column could be proven via mass spectrometry which might be due to shear forces crushing the resin by ice crystals.

Nevertheless, a suitable affinity resin for purification purposes of FVIII has to bind the full-length plasma-derived FVIII (pdFVIII) which is glycosylated as well as to the full-length recombinant FVIII molecules (FL-rFVIII) and B-domain deleted rFVIII (BDD-rFVIII). To confirm its suitability for all kinds of FVIII products, Kogenate® FS, a FL-rFVIII, and ReFacto®, a BDD-rFVIII, were chosen for this assay. Under standard conditions, both recombinant proteins displayed binding similar to that of pdFVIII proving the general applicability of C141-coated resin.

Table 4*: Binding of C141 towards different FVIII preparations.*

FVIII formulation	FVIII bound to C141-resin [%]
Kogenate® FS (FL-rFVIII)	93
Re-Facto® (BDD-rFVIII)	92
pdFVIII	76

As a small drawback, it was shown that C141 is not able to bind FVIII in the presence of von Willebrand Factor which limits the use of C141 as affinity ligand as many different FVIII preparations are made in combination with von Willebrand Factor to stabilize FVIII and also explains the lower binding towards pdFVIII.

II.1.2.3.2 Effects of Ligand Density towards FVIII Binding

The ability to capture proteins with an affinity resin greatly depends on ligand properties as well as on its concentration on the resin.[207] To determine the effects of the latter, resins of different loading density of C141 were prepared to measure the ability to capture FVIII.

As expected, an increase of ligand density resulted in an increase of FVIII adsorption. However, there is a minimum concentration of about 5 to 10 µmol ligand per mL resin (depending on the nature of the ligand) which is crucial for efficient binding and saturation was observed at high loading densities. Another limit was found for the maximum of reachable ligand density where the minimized compounds C141 readily immobilized up to 40 µmol/mL. At these high loading densities, the small peptidomimetic bound almost 90% of the applied FVIII.
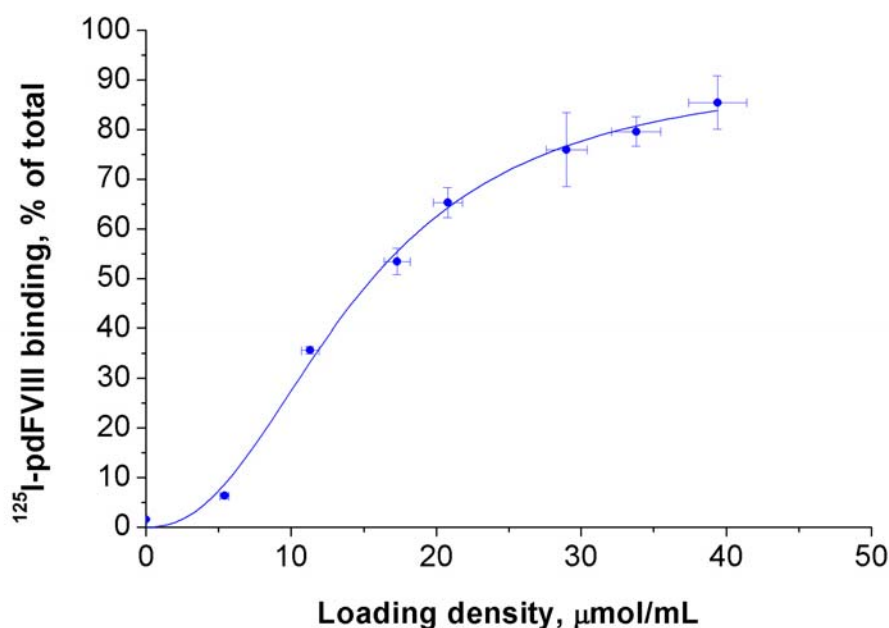
Figure 42*: Binding of FVIII correlated to the loading density of C141.*

II.1.2.3.3 Localization of the Binding Site in FVIII

An epitope mapping was performed to localize the binding site in FVIII of the new ligands[165]. For this purpose, L-[^{35}S]methionine-labeled rFVIII fragments had been expressed to measure the radioactivity of the FVIII bound to the different ligands. Binding of the following FVIII fragments and domains to immobilized ligands was tested: heavy chain (HC) (A1a1A2a2; FVIII$_{1-758}$), A1a1 (FVIII$_{1-398}$), a1A2a2 (FVIII$_{318-758}$), B domain, light chain (LC) (FVIII$_{1637-2332}$), a3A3C1 (FVIII$_{1637-2173}$), C2 (FVIII$_{2170-2332}$).

Table 5: *Mapping of recombinant FVIII epitopes. The strength of binding of ligand-coated resins to different recombinant FVIII epitopes is valuated as: (++) very strong binding; (+) significant binding; (—) no or minimal binding.*

Ligand	HC	A1a1	a1A2a2	B	LC	a3A3C1	C2
ydwacy	—	—	—	—	+	—	++
(3-IAA)EYC	—	—	—	—	+	+	++
(3-IAA)Eψ[CH$_2$NH]YC (**C141**)	—	—	—	—	+	+	—
YCAWEY	+	—	+	—	+	—	—
YCTWEY	+	+	—	—	+	—	—
YCVWEY	+	—	—	—	+	—	+
ECYYEHWS	—	—	—	—	—	—	—

To some extend, the obtained results were somewhat surprising. As shown in table 5, the studies indicated a strong binding to the light chain of FVIII for the fully retro-inverso peptide ydwacy as well as for the small ligands (3-IAA)EYC and (3-IAA)Eψ[CH$_2$NH]YC (**C141**). Moreover, among all FVIII fragments tested, only the a3A3C1 polypeptide showed a distinct binding to ligand **C141**-coated resin, whereas ligand (3-IAA)EYC-coated resin strongly bound the C2 domain, and to a lesser extent the a3A3C1 polypeptide.

In contrast, the hexapeptides were found to bind to both, the light chain and the heavy chain. The scrambled peptide ECYYEHWS was used as a negative control. It did not show binding to any of the FVIII fragments, verifying the accuracy of the experiment performed.

Considering the high homology between the A domains among each other and the C domains among each other, this might result in multiple similar binding sites on FVIII and explain the results obtained.

II.1.2.3.4 Affinity purification using C141

To demonstrate the potential of **C141** as ligand for FVIII affinity purification, sample purification from cell-conditioned fetal bovine serum (FBS)-containing Dulbecco's Modified Eagle Medium (DMEM) was performed. Affinity purification *via* **C141**-coated resin was achieved using two buffers varying only in their NaCl content which is an indication that the interaction between FVIII and the evaluated peptides has predominantly ionic character, as observed for various antibodies before. 0.1 M NaCl was used for FVIII adsorption and elution was done under very mild conditions applying 0.6 M NaCl at pH 6.8 to give sharp elution peaks (figure 44 and figure 45; left-hand panels). The pH of the buffers was furthermore adjusted to 6.8 as the slightly acidic condition were found to give a better elution threshold, and as FVIII is generally more stable under these conditions.
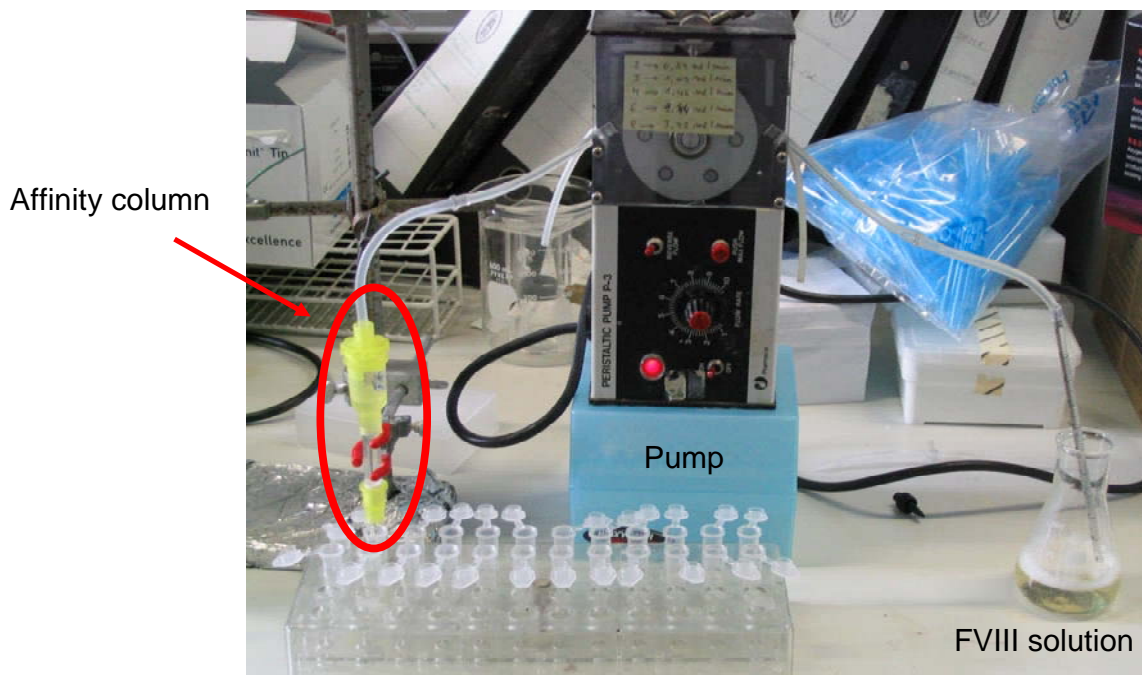
Figure 43: *Affinity column coated with C141connected to a membrane pump for purification of FVIII.*

As a positive control, binding and elution of pure pdFVIII was carried out, resulting in high FVIII column retention (~90%). Analysis of the flow-through and wash fractions by SDS-PAGE followed by silver staining and Western blotting revealed only traces of FVIII in those fractions. In the FVIII-rich eluate, the heterogeneous 230-90 kDa heavy chain bands and the ~80 kDa light chain doublet bands were visually distinguished. In addition, traces of proteolytic bands (~73 kDa, ~50 kDa, ~43 kDa) were found, from which the ~50 kDa band (A1 domain) was strongly reactive against mAb C5 in the blot.
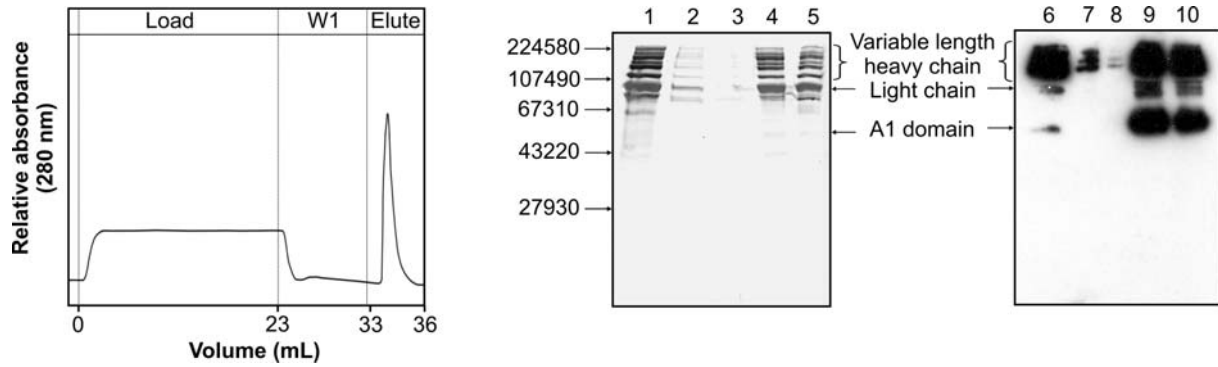
Figure 44: *Adsorption and elution of pure pdFVIII. 0.5 mg of pdFVIII were applied to 1 mL of resin. Samples from different purification fractions (see profile in left-hand panel) were analyzed by 10% SDS-PAGE followed by silver staining (middle panel) or Western blotting (right-hand panel) using mAbs C5 and 413 against FVIII. Lanes 1, 6: pure FVIII; Lanes 2, 7: source solution with pure FVIII for the column; Lanes 3, 8: flow-through fraction; Lanes 4, 5, 9, 10: elution fraction with 0.6 M NaCl.*

To test the C141-coated resin in a typical application, a purification of pdFVIII from cell-conditioned FBS-containing DMEM, which was spiked with prepurified pdFVIII, was performed showing retention of 89% and the vast majority of contaminant proteins were eluted with the flow-through containing only traces of FVIII.
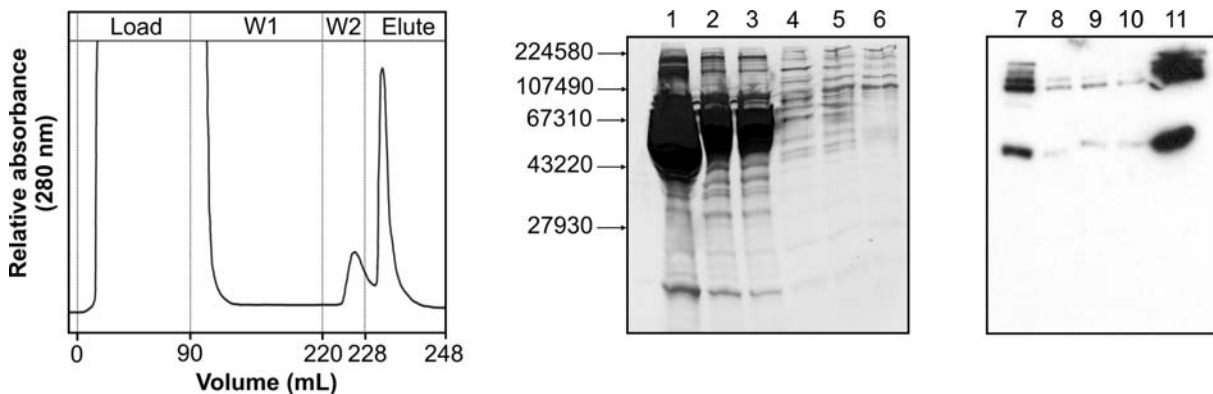
Figure 45: *Purification of pdFVIII diluted in cell-conditioned FBS-containing DMEM. 0.5 mg of pdFVIII were applied to 1 mL of resin. Samples from different purification fractions (see profile in left-hand panels) were analyzed by 10% SDS-PAGE followed by silver staining (middle panel) or Western blotting (right-hand panel) using mAbs C5 and 413 against FVIII. Lane 1: media; Lanes 2, 7: media with FVIII for column; Lanes 3, 8: flow-through fraction (W1); Lanes 4, 5, 9, 10: wash fractions (W2) with 0.2 M NaCl; Lanes 6, 11: elution fraction with 0.6 M NaCl.*

The purification was further optimized by additional washing with buffer containing 0.2 M NaCl thereby eluting additional contaminating proteins without losing FVIII. Altogether, contaminant proteins, presented in vast excess to FVIII in source solutions were successfully removed to

achieve a 63-fold FVIII concentration. Functional activity of eluted FVIII samples was confirmed by a one-stage clotting assay.

II.1.2.3.5 FVIII Activity in Presence of Unbound Ligands

For every affinity column, a so-called bleeding, which means an elution of the affinity ligand from the column, can not be completely excluded. Due to this reason, the activity of isolated pdFVIII in presence of increasing amounts of free ligands has to be determined to assure, that also FVIII preparations with a small amount of free affinity ligand can be used for treatment of patients. The activity of FVIII was measured using a chromogenic assay, enabling the measurement of only active FVIII in comparison to an ELISA experiment, where all of the FVIII would be measured (active and inactive). This experiment proved that there is no inhibitory effect of the ligands on FVIII function up to a vast ($\sim 10^8$ fold) excess of the ligands. The same results were obtained for the scrambled peptide which was used as control.
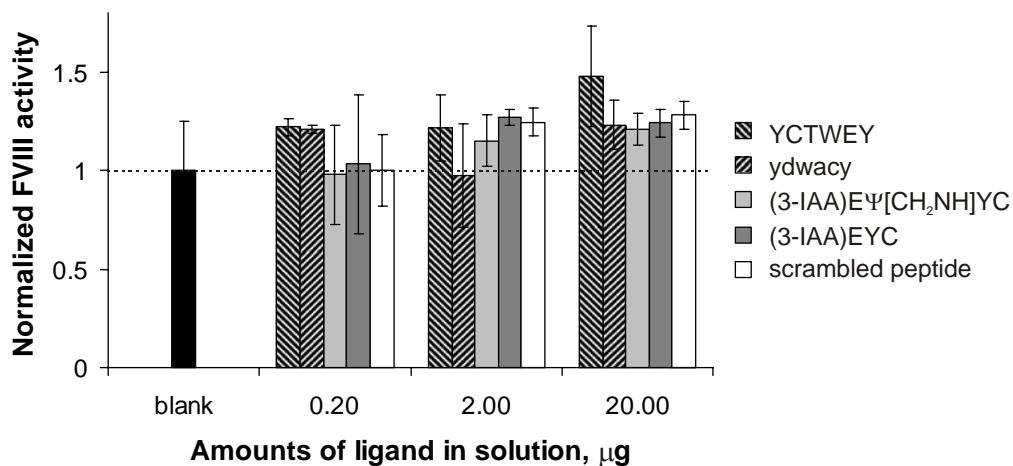
Figure 46: *Effect of dissolved ligands on the procoagulant activity of pdFVIII. FVIII was exposed to variable amounts of different ligands or scrambled peptide prior to determination of FVIIII activity by chromogenic assay. Values are normalized to those measured for a control sample without added ligand.*

Additionally, it was found that FVIII in combination with the free ligand seems to have a higher activity than the sample without the ligand. While this finding seems to be surprising for the first moment, it has to be taken into account that all samples have to be incubated for several hours before the activity is measured. So, also for the blank sample with only FVIII, a decrease of activity due to the lability of FVIII has to be considered. So, the free affinity ligands do not increase the activity of FVIII but seem to prevent degradation of the protein in solution.

II.1.2.4 Solution-Phase Synthesis of C141

As the peptidomimetic C141 had successfully fulfilled all requirements for a FVIII affinity ligand, a solution phase synthesis was developed to allow a cost efficient production in preparative scale for further experiments.

Usually, synthesis of peptides from the C-terminus to the N-terminus is the most common strategy[208]. But, in this special case, the inverse direction seemed to be more favorable: In peptide synthesis the cysteine side chain is most preferably protected with a trityl (Trt) group as this group is easily removable under acidic conditions[209]. In case of a C to N synthesis cysteine would be introduced in the first step. This is not recommended for a multi-step synthesis including several washing and chromatography columns as the cysteine side-chain protecting group is acid prone. Besides, the cysteine itself is quite sensitive towards racemization[210]. The main disadvantage of the N to C direction is the risk of racemization by oxazolone formation[211,212]. Nevertheless, this requires a *C*-activated *N*-acylamino acid, an arrangement which is not present in the N to C procedure for the synthesis of C141 as described below.

Synthesis started from 3-indolylacetic acid. The indole nitrogen was protected with a *tert*-butyloxycarbonyl (Boc) group in a three-step reaction sequence according to literature procedures: The indole acetic acid was transformed into its methyl ester by treatment with $SOCl_2$ in MeOH and the indole nitrogen subsequently protected with a Boc group by reacting with *tert*-butyl dicarbonate and 4-dimethyl aminopyridine (DMAP)[213] in acetonitrile to achieve **187**[214-216]. Saponification then yielded the desired indolylacetic acid **188** in 70% overall yield.
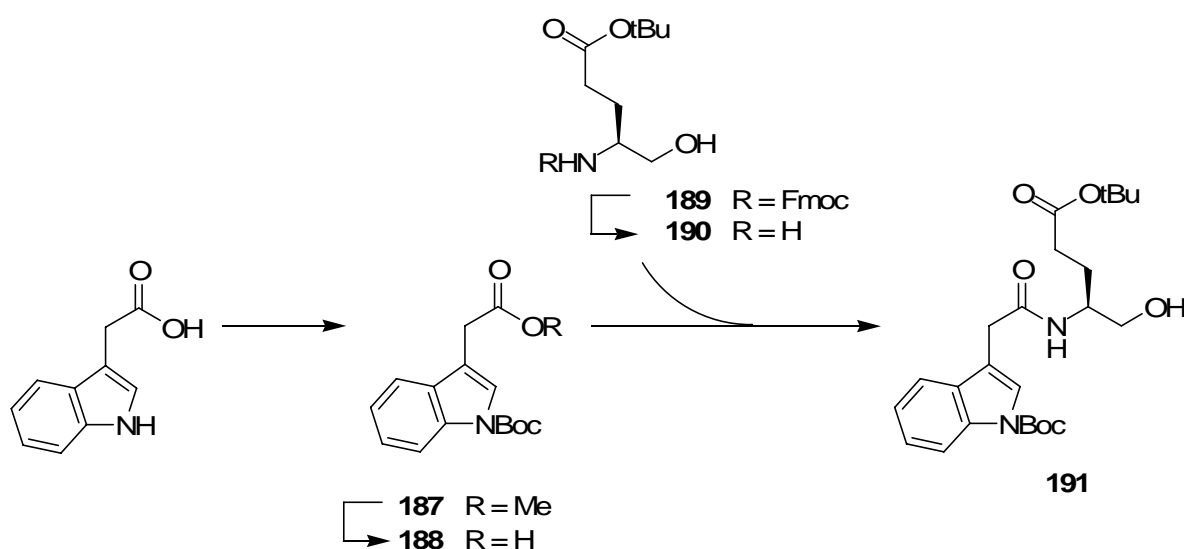
Scheme 3: *Synthesis of the N-substituted glutamol **191**.*

The conversion to **191** was achieved by coupling **188** to the side-chain-protected glutamol **190** using 1-hydroxybenzotriazol (HOBt) and *O*-(benzotriazol-1-yl)-*N,N,N',N'*-tetramethyluronium tetrafluoroborate (TBTU) as coupling reagents. **190** was readily available from commercial Fmoc-

glutamic acid(OtBu) which was reduced by NaBH₄ to give **189**, which was afterwards treated with piperidin and could be used without further purification. For the coupling to **188** a protection of the free hydroxyl functionality in **190** was not necessary and the reaction proceeded cleanly to give the *N*-substituted glutamol **191** in 95% yield. The reduced peptide bond linking the glutamic acid- and tyrosine residue in the target compound **C141** was formed by a reductive alkylation of the corresponding aldehyde **192** and commercially available Tyr(*t*Bu)OMe (scheme 4) to give **193**.
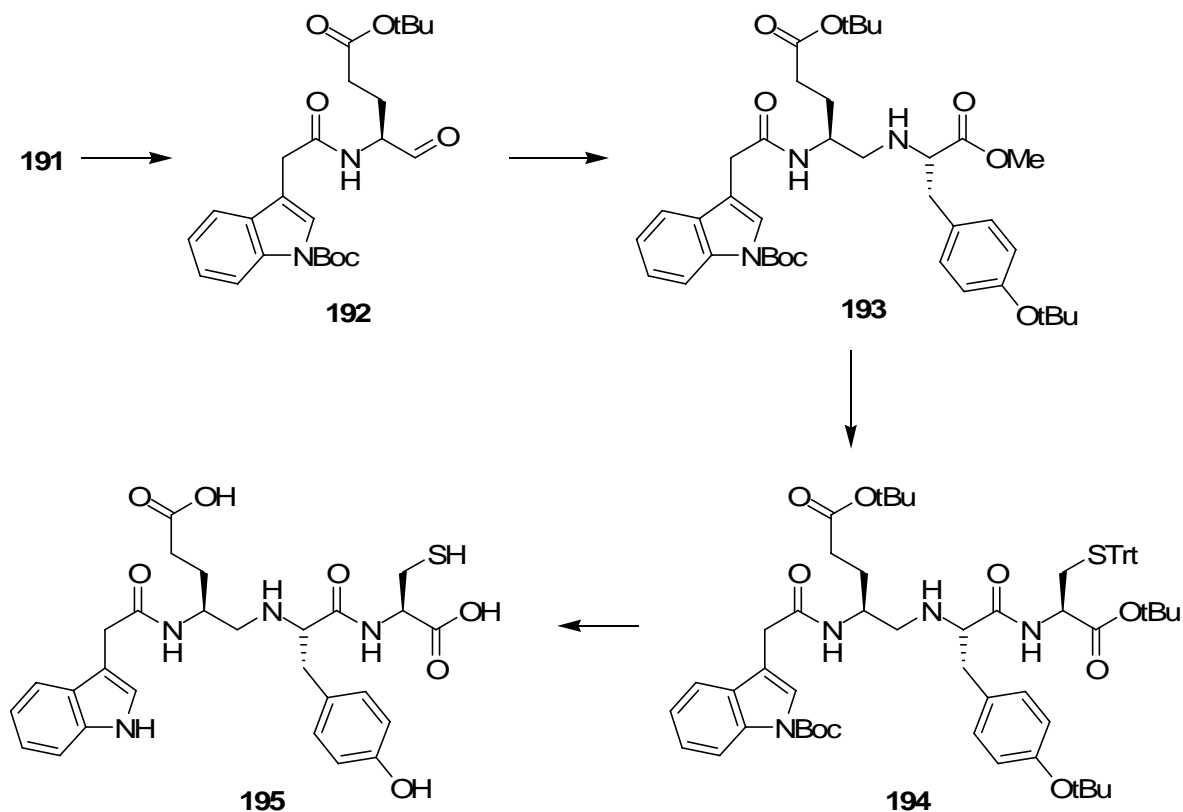
Scheme 4: *Synthesis of* **C141** *(195)*.

Due to the basic reaction conditions during the aldehyde formation by Swern oxidation[217,218] using the strong base *N,N*-diisopropylethylamine (DIPEA)[219,220] for the synthesis of the secondary amine **193** led to an inseparable 8:2 mixture of diastereomeric isomers due to racemization of the highly sensitive aminoaldehyde **192**. Also the further transformation to the imine by treating with Tyr(O*t*Bu)OMe*HCl was done in presence of DIPEA and MgSO₄[221]. Racemization was completely overcome by the use of Dess-Martin periodinane oxidation[222-224] instead of Swern oxidation and short preformation of the imine *in-situ* in absence of base rapidly followed by addition of the reducing agent. This procedure gave the desired secondary amine **193** in 75% yield over two steps. The methyl ester in **193** was cleaved by saponification using LiOH and the resulting free acid was coupled to Cys(Trt)O*t*Bu*HCl[225] in the presence of HOBt/TBTU and the mild base 2,4,6-collidine to yield **194** (83% yield, two steps). Although the applied cysteine *tert*-butyl ester is not commercially available it was favored over the commercial methyl ester as it is readily

synthesizable[225] and it allows a one-step deprotection of **194** to the desired free peptidomimetic **195** under acidic conditions.

The final deprotection and purification is the critical step in terms of an economic production of **195**. Therefore, we concentrated on the optimization of the deprotection reaction in order to reduce byproduct formation to circumvent a purification of the final product. The key to minimize side product formation was to avoid a sudden high concentration of *tert*-butyl cations as it occurs if **195** is directly treated with the cleavage mixture (75% trifluoroacetic acid (TFA), 10% triisopropylsilane (TIPS), 10% ethane dithiol, 5% H_2O)[226]. Thus, the problem was solved by suspending the protected peptidomimetic in a vigorously stirred mixture of the scavengers and slow addition of TFA over a period of 8 hours to give a final concentration of 75% of TFA by using a syringe pump. This procedure helped to significantly reduce the byproduct formation (typically 15% as determined by HPLC) to obtain the final peptidomimetic **C141** (**195**) in 98% yield (purity >95%) after precipitation in ice-cold ether/pentane.

II.1.3 Asymmetric Synthesis of Condensed and Aromatic Ring-Substituted Tyrosine Derivatives[227]

The following project was performed in cooperation with Dr. Sebastian Knör. For a detailed assignment of the synthesized compounds towards the creators, please see experimental section.

II.1.3.1 Background

Naturally occuring (proteinogenic) amino acids provide limited variation in size and shape while introduction of unusual substituents allows a systematic study of structure-activity relationships (SAR). Modified unnatural amino acids can bear new side chain functionalities to enable new synthetic routes not possible with natural amino acids like click-chemistry[228] or to form bicyclic or polycyclic constrained amino acids[229,230]. Beyond that, unnatural amino acids have been found to significantly improve the biological properties of numerous biologically active peptides and peptido-mimetics, *e.g.* by limiting conformational flexibility, enhancing enzymatic stability, improving pharmaco-dynamics or bioavailability[231-233]. Especially modified aromatic amino acids are important structural features in various pharmaceuticals which are currently under development or have already been introduced into the market. Among the latter are, for example, the broad-spectrum antibiotics Ampicillin® and Amoxicillin® which contain D-phenylglycine and D-4-hydroxyphenylglycine moieties and Nafarelin® a luteinising hormone releasing hormone (LHRH) analogue for treatment of endometrioses comprising a D-2-naphthylalanine residue[227].

As was found for the octapeptide EYHSWEYC for affinity purification of FVIII, the phenolic hydroxyl group of the tyrosine residues (Tyr^2 and Tyr^7) is important for ligand binding affinity as the corresponding phenylalanine derivatives led to a dramatically lower binding affinity. Additionally, the preference of larger aromatic systems in the position of Tyr^2 and Tyr^7 was found in several examples[165]. Out of that, substitution of tyrosine by analogues bearing both, an expanded aromatic system as well as the phenolic hydroxyl group, would be interesting in terms of optimizing the binding properties.

In the past few years several groups have reported strategies for the synthesis of aromatic substituted phenylalanines, tryptophans and naphthylalanines[234-237]. As there was no synthesis for easy accessable tyrosine derivatives described in literature, there was also a general interest in creating such unnatural amino acids as non-proteinogenic amino acids play an important role in drug development.

II.1.3.2 Results and Discussion

First, a general three-step procedure for the synthesis of enantiomerically pure 3-aryl-substituted L-tyrosine analogues *via* a Suzuki-type cross coupling reaction was developed. A second approach was used to extend the aromatic residue, in which the condensed 2-naphthylalanine analogue of tyrosine was synthesized *via* unselective hydrogenation of the corresponding α-enamide and enantioselective cleavage of the racemic mixture using acylase I as key step[238].

II.1.3.2.1 Synthesis of 3-Aryl-Substituted Tyrosine Derivatives
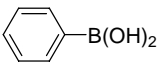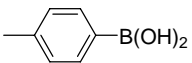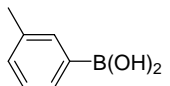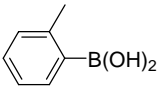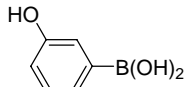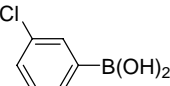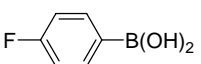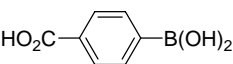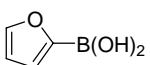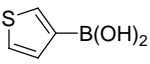
The synthesis of 3-aryl-substituted L-tyrosine derivatives started with commercially available L-3-iodo-tyrosine. The amino function was protected with Boc to ensure stability under Suzuki coupling conditions (scheme 5).
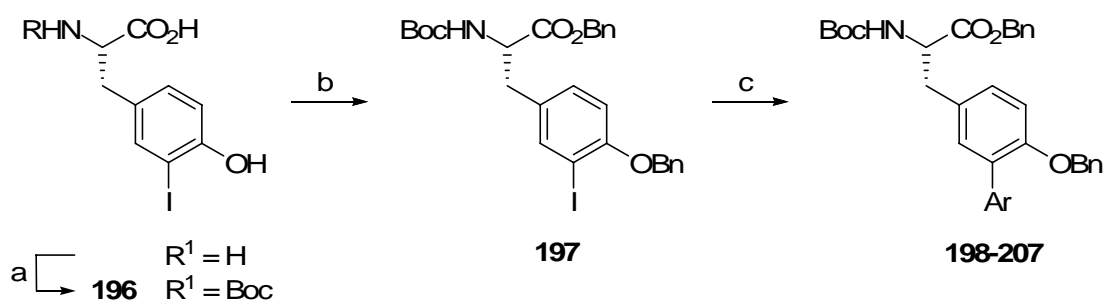
Scheme 5: *Synthesis of 3-aryl-substituted tyrosine derivatives.*

As suspected, attempts to use the commercially available compound or **196** directly for Suzuki couplings without any protecting groups failed, probably due to complexation of palladium by the neighboring free phenolic hydroxyl group after insertion into the carbon-iodine bond. For standard peptide coupling purposes, both in solution or solid phase, a protection of the phenolic side chain is generally not crucial. Thus, the phenolic side chain and the carboxylic acid were protected in one step as a benzyl ether and benzyl ester (b). This procedure avoids an additional protection and deprotection step as both groups can be removed simultaneously by hydrogenation, but offers the opportunity of a selective saponification of the benzyl ester when a side chain protection is needed. The benzyl protection was performed under mild conditions using sodium carbonate as base to give the fully protected amino acid **197** in 93% yield and without loss of enantiomeric purity.

Table 6: *Suzuki cross coupling of **197** with arylboronic acids.*

Compound	Ar-B(OH)$_2$	Yield (%)
198		95
199		93
200		79
201		70
202		80
203		39
204		94
205		92
206		99
207		45

For Suzuki cross couplings, PdOAc$_2$/P(*o*-tolyl)$_3$ was used as catalyst and sodium carbonate as base, a system which has proven to give good results in similar systems[234,235,237]. Thus, a series of 3-aryl-substituted tyrosine derivatives were synthesized in moderate to high yields using a variety of activated and deactivated phenylboronic acids as well as heteroaromatic boronic acids. Formation of the dimeric homo coupling product was found to be generally less than 2% as measured by HPLC-MS, except for the 3-chloro-phenylboronic acid where higher amounts of this side product were formed.

II.1.3.2.2 Enantionselective Synthesis of 4-Hydroxynaphthyl Alanine

Although a procedure for the enantioselecitve synthesis for 4-hydroxynaphthyl alanine was already described and proven to be quite efficient, the high costs for the catalyst limit the scope of this procedure, especially if both enantiomers, the L- and the D-form, are needed[227]. Therefore,

a new approach was developed offering a synthesis of both enantiomers. For this purpose, aldehyde **208** was condensed with Cbz-α-phosphonoglycine trimethyl ester to give the (*Z*)-dehydroamino acid **209** (*Z/E*>95/5) in 87% yield. To avoid decomposition, triethylamine had to be added to the eluent for column chromatography.
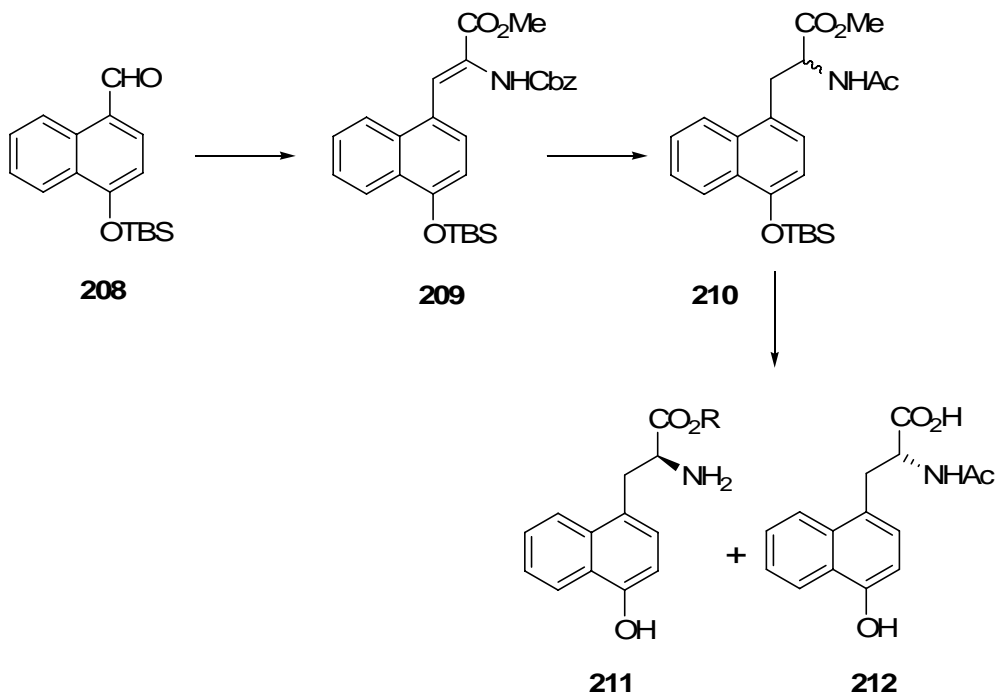
Scheme 6: *Synthesis of H-(*D/L*)-(4-hydroxy)Nal-OH.*

Then, hydrogenation was carried out using palladium on charcoal as catalyst leading to a simultaneous hydrogenation of the double bond and cleavage of the Cbz protection group. The reaction was monitored by TLC and mass spectroscopy and quenched after complete conversion to the saturated free amine (4 h) as prolonged reaction times (18 h) led to partial hydrogenation of the naphthalene residue. The resulting racemic mixture was directly acetylated by treating with acetic acid anhydride in presence of triethylamine to yield **210** in 76% yield over two steps.

Subjecting the fully protected compound **210** to enzymatic resolution led to an unseparable product mixture due to a partial loss of the TBS group and partial cleavage of the methyl ester. Thus, both protecting groups were removed prior to the resolution improving the solubility in aqueous conditions. To avoid additional separation steps, a one-pot procedure was developed: the TBS ether and the methyl ester were subsequently cleaved and the racemic mixture was resolved using acylase I to give the L-isomer **211** as free amine, while the D-isomer **212** remained in the *N*-acetylated form which was easily separated by extraction in high purity (93% by HPLC analysis). Unfortunately, isolation of the free L-amino acid **211** by crystallization failed, so it was converted to the corresponding methyl ester **213** and isolated by extraction (90% purity by HPLC

analysis). Further purification by column chromatography gave the pure enantiomer **213** and **214** (96%ee) in high yields (41% over four steps and 46% over three steps, respectively).
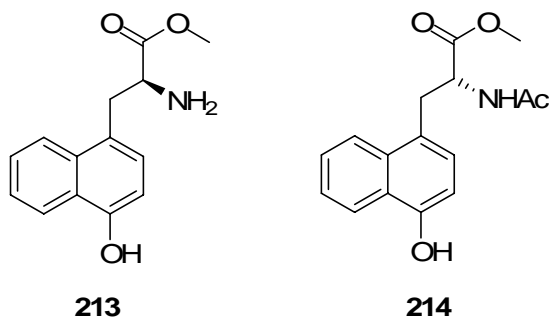
Scheme 7: *The final compounds **213** and **214**.*

The incorporation of these two compounds into FVIII-binding affinity ligands succeeded, but the biological activity was not enhanced so that the insertion of a synthetically demanding building block was avoided for the further optimization for FVIII ligands.

II.2 Integrin Ligands

II.2.1 Background

II.2.1.1 Integrins

In 1986, the term "integrin" was introduced by Tamkun *et al.* to emphasize the role of the adhesion receptor proteins of the extracellular matrix (ECM) as an integral membrane complex involved in the transmembrane association between the extracellular matrix and the cytoskeleton[239]. These cell surface receptors are essential integrators and mediators of ECM-dependent communication.

In the 1980s, first adhesion receptors of the integrin family were identified as being involved in cell adhesion to ECM as well as platelet aggregation, homing of leucocytes and immune response. The finding of fibronectin being an ECM protein which is strongly involved in cell adhesion led to the identification of the arginine-glycine-aspartic acid (RGD) sequence as pivotal recognition motif of integrin binding[7]. This facilitated the identification of the fibronectin and vitronectin receptors using affinity chromatography with affinity columns, coated with RGD containing peptide sequences[240,241]. By mistake, the RGD sequence was initially called "universal recognition motif" which was owed to the fact that fibronectin as well as vitronectin, fibrinogen, laminin, osteopontin etc. bind to this sequence. But, by now, many different recognition motifs are known from several natural integrin ligands[242]. Finally, molecular cloning and sequencing led to a classification of these receptors together with other adhesion receptors such as the platelet fibrinogen receptor, the *very late antigens* (VLAs) and *leucocyte-function associated antigen* (LFA) as one family of adhesion receptors[243]. Nowadays, integrins are known to play important roles in a variety of biological processes as well as in various pathological processes such as inflammation, vascular homeostasis, thrombosis, restenosis, bone resorption, cardiovascular disorders, cancer invasion, metastasis and tumor angiogenesis[244-246].

II.2.1.1.1 Integrin Structure

Integrins constitute a family of $\alpha\beta$ heterodimeric, type I transmembrane proteins with large extracellular (700-1100 residues) and short cytoplasmic domains (30-50 residues), which are linked by a short transmembrane region[247]. Until now, 18 α and 8 β subunits have been identified forming 24 heterodimers, each with distinct ligand binding properties, able to perform inside-out and outside-in signaling[239,242].
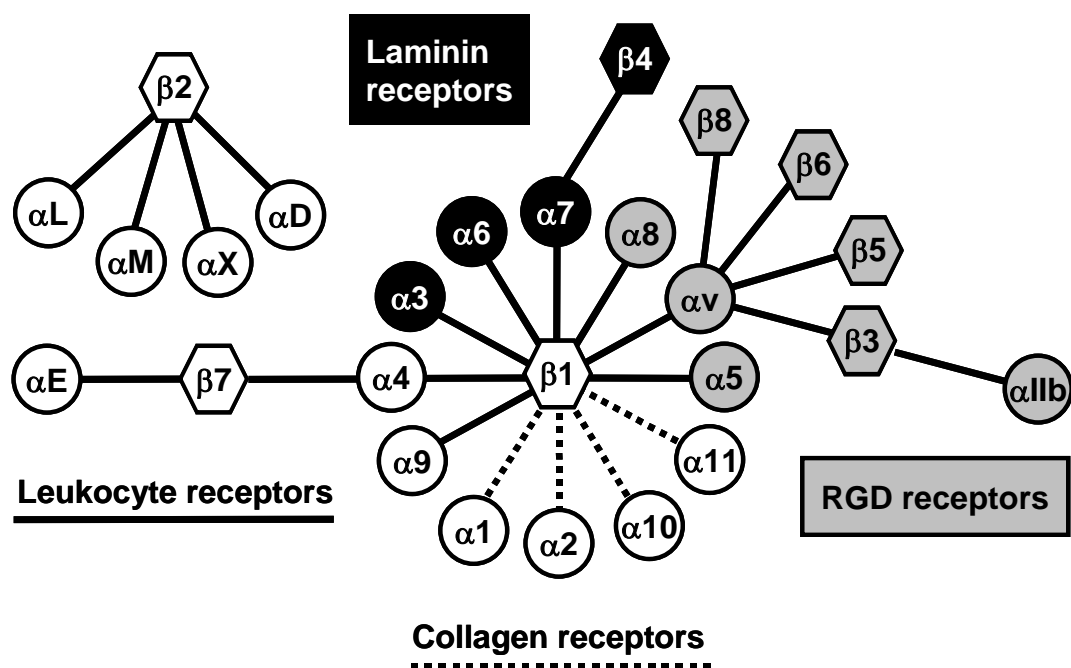
Figure 47: *The integrin family: RGD receptors, laminin receptors, leukocyte receptors and collagen receptors.*

First structure elucidations of integrins were performed by electron microscopy showing a 28 nm long molecule of a 8 x 12 nm globular head group and two 2 x 20 nm rod-like tails for $\alpha 5\beta 1$[248]. In 2001, the group of M. A. Arnaout was able to crystallize the headgroup of $\alpha v\beta 3$, shortly followed by the crystal structure of the headgroup in association with Cilengitide[249,250]. As could be shown by the crystal structure, both integrin subunits have a recognizable domain structure.
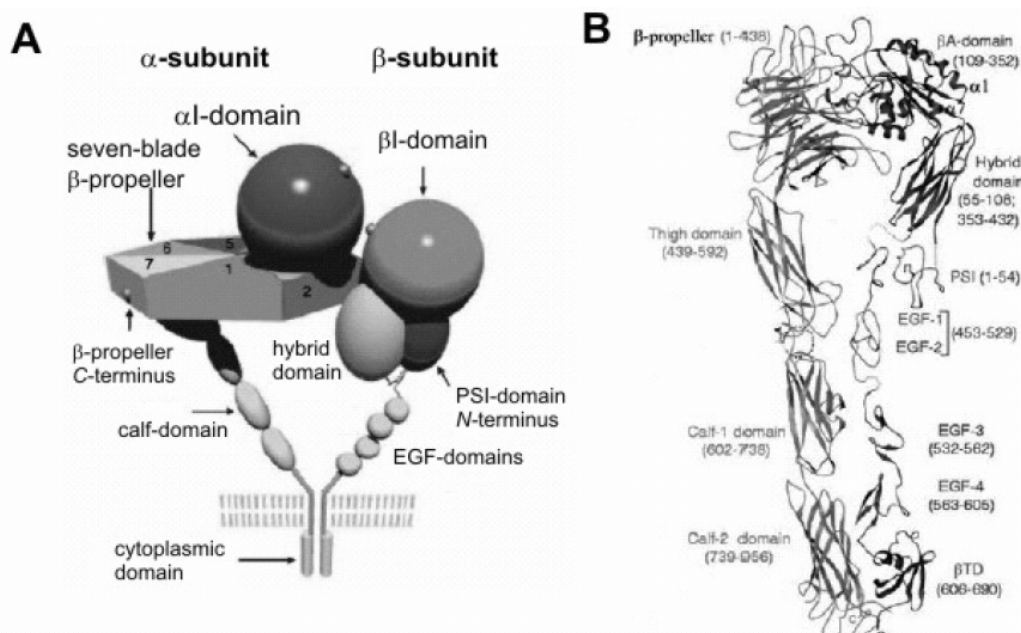
Figure 48: *Comparison of the schematic domain structure A with the ribbon drawing of the X-ray structure of $\alpha v\beta 3$[249]. B shows a straightened model. The αI-domain is not present in $\alpha v\beta 3$.*

The two subunits assemble in an ovoid-like shape consisting of a 9 x 6 x 4.5 nm head and two almost parallel tails. Except for the RGD-dependent integrins, a ~200 residue long module homologous with the cation-binding A-domain of von Willebrand factor, a so-called αA-domain or αI-domain (inserted domain), can be found, which is inserted into a seven-blade β-propeller. Also in the β-subunit, an A-domain like polypeptide – βI, 243 residues in β3 – which is looping out from a unique immunoglobulin (Ig)-like "hybrid"-domain (133 residues in β3) is present.

The tail of the αv-subunit is composed of three β-sandwich domains: one Ig-like "thigh" domain and two very similar domains that form the "calf" module. The β3-tail consists of a PSI module that can be found in several protein families like plexins, semaphorins or integrins[251], four cysteine-rich, epidermal-growth-factor (EGF)-like domains and a β-tail domain (βTD). In the originally obtained crystal structure (opposite to the straightened model in Figure 48), the tails of both subunits are folded back in a ~135° angle, resulting in a V-shape with a kink between the thigh-domain and the calf module of αv. Newer calculations now assume that integrins appear to be extended even in their resting state[252].

The binding site for RGD ligands is located at the interface of the β-propeller domain of the αv subunit and the βI-domain of the β-3 subunit. The β-propeller is formed from the amino terminus, seven fold ~60 residue long sequence repeats of αv and consists of seven radially arranged "blades", each being formed by a four-stranded antiparallel sheet. Each of these seven blades reveals a unique consensus sequence with three aromatic residues per blade, all pointing towards the center of the propeller, forming a "cage"-like hydrophobic cavity. This space is occupied by Arg^{261} of the β-subunit which stabilizes the αβ-heterodimer by cation-π-interaction.

The other part of the binding site, the βI-domain, is inserted into the B-C-loop of the β3-hybrid domain and adapts a so-called *Rossmann-fold* structure which also found in G-proteins as nucleotide binding motif[253]. This motif consists of a central six-stranded β-sheet surrounded by eight helices and three binding sited for divalent cations (like Ca^{2+}, Mg^{2+}, Mn^{2+}, etc.) dependent on the used buffer. In a cleft at the top of the central β-strand, a *metal ion dependent adhesion site* (MIDAS) motif is set which is only occupied by a metal ion in the protein-ligand complex in contrast to the unbound, inactive αvβ3. The MIDAS is flanked by the ADMIDAS, the *adjacent MIDAS*, which is occupied by a metal ion in bound as well as in unbound state. The conformational change induced by the binding event also unfolds another metal ion binding site, *ligand induced metal binding site* (LIMBS), where binding of a metal ion might stabilize the ligand-bound conformation of the integrin[250].

Still, there is much discussion going on about the nature of the divalent ions and their effects. While Mg^{2+} and particularly Mn^{2+} seem to have a strong agonistic effect on the activity of integrin

$\alpha5\beta1$ and $\alpha v\beta3$, Ca^{2+} reveals an antagonistic effect, while Ca^{2+} was not found to be inhibitory for αIIb$\beta3$[254,255].

II.2.1.1.2 Mechanisms of Integrin Activation and Signal Transduction via Integrins

Recent results gave rise to several theories concerning the mode of activation and conformational changes of the heterodimer on the way of ligand binding. To summarize, although it has been much debated whether a transition to an extended conformation precedes or follows activation, integrins appear to have an extended structure even in their resting state[252,254,256,257]. The former idea of a bent conformation might be owed to the fact that integrins can revert to fully or partially bent forms under certain conditions that favor it, such as in adhesion to substrates in EM or in crystals[252].
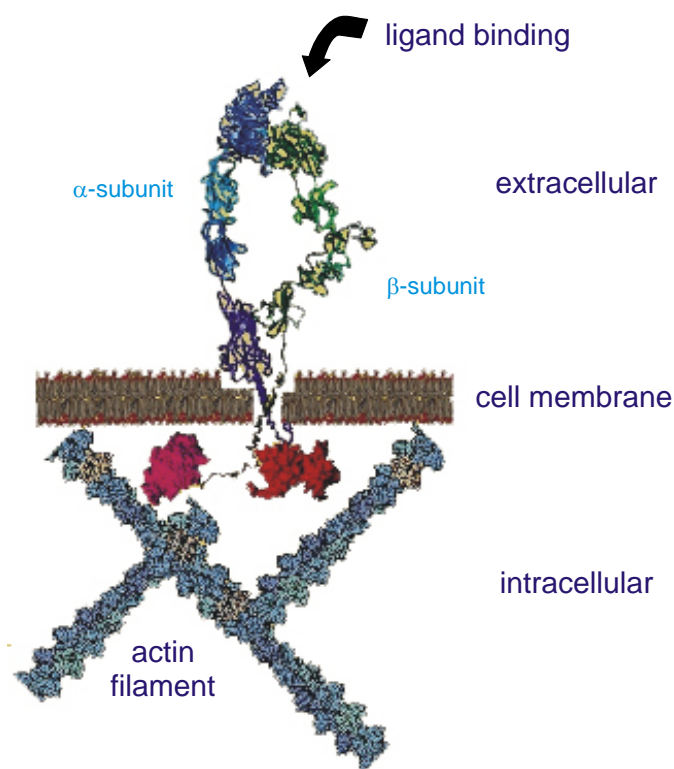
Figure 49: *An integrin receptor in the fully extended conformation.*

Recently, the structure of the integrin αIIb$\beta3$ transmembrane complex was solved using transmembrane domains in bicelles proving the hypothesis of the dissociation and association of the α and β subunits while transmembrane signalling[258,259]. The two transmembrane helices of the integrin heterodimer are essential in signalling events as linkers between the extracellular and intracellular domains. Hence, several groups have published different theories and calculations about the role of the transmembrane domain in signalling[259].
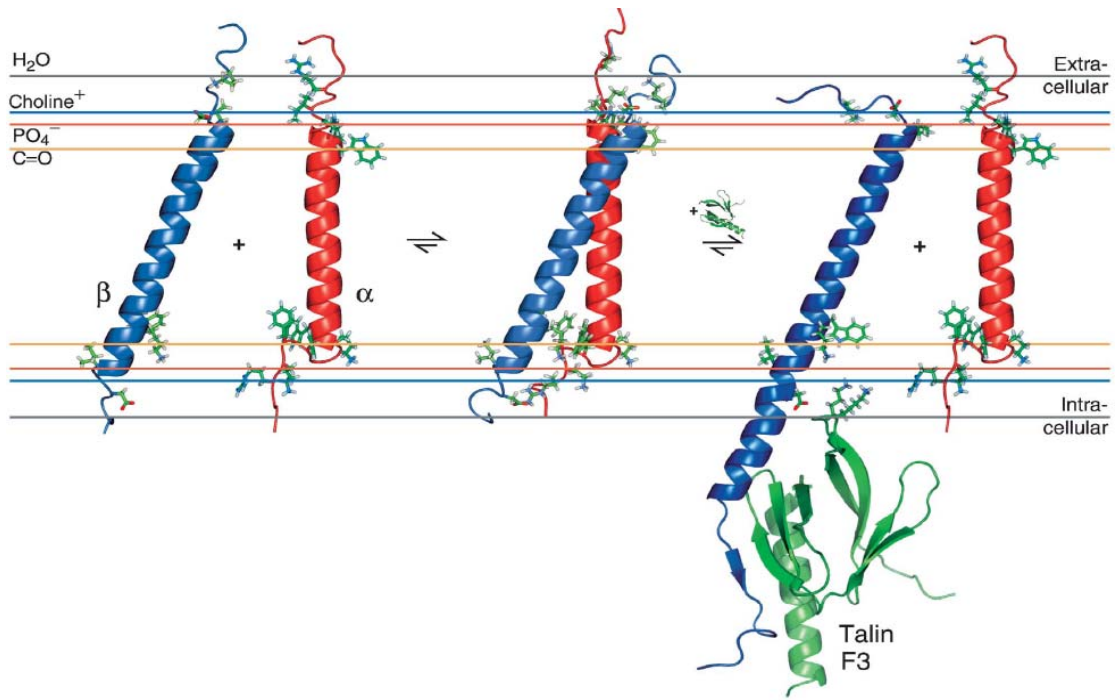
Figure 50: *Predicted orientations of the αIIb and β3 transmembrane segments in their monomeric and associated states[258]. Reprinted by permission from Nature Publishing Group, license number 2227041120343.*

Although the intracellular domains of the integrin subunits are relatively small, they are able to recruit a high number of proteins involved in the construction and anchorage of the cytoskeleton (actin stressfibers) and in various signalling pathways. Clustering of active integrins in focal adhesion points induces binding of the proteins talin (see figure 50), paxilin and vinculin, which connect the integrins to the actin cytoskeleton. Additionally, the integrin clusters bind and activate various tyrosine kinases such as focal adhesion kinase (FAK), integrin-linked kinase (ILK) or Fyn. Upon ligation of integrins with the ECM, focal adhesion kinase undergoes auto-phosphorylation at Tyr[397] enabling it to bind other kinases such as Src, which phosphorylate FAK at further tyrosine residues. A high number of proteins are accommodated in this signalling process, some of them acting as kinases or scaffolds while some of them are not yet fully understood.
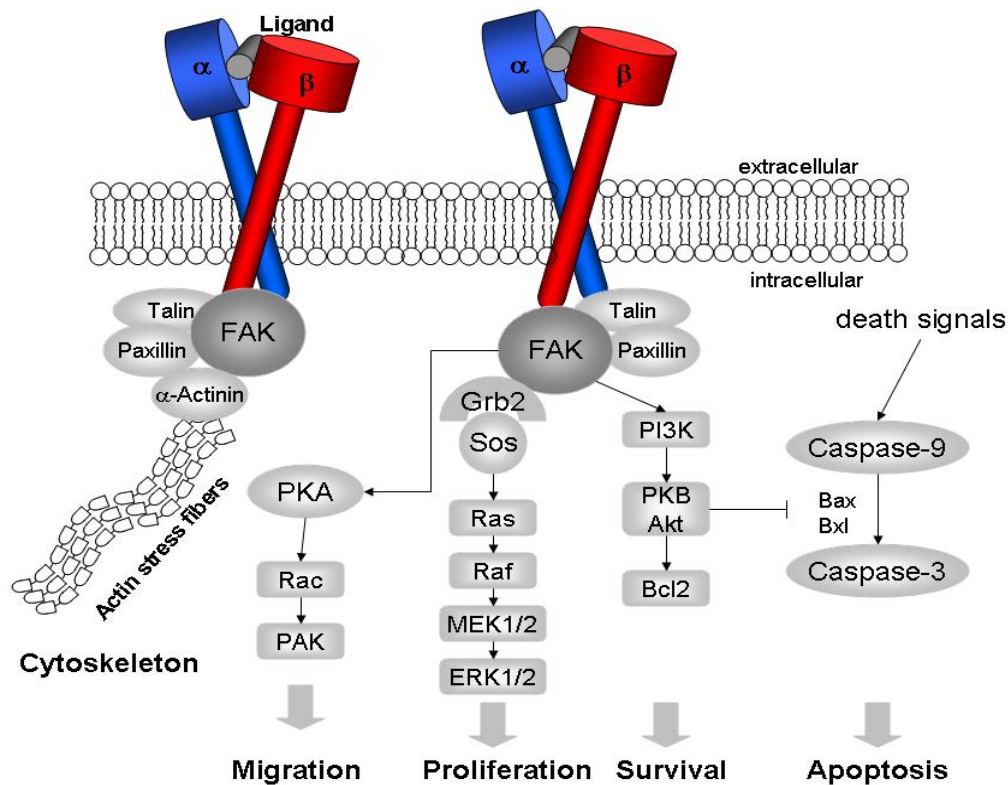
Figure 51*: Integrin-dependent signalling pathways[260].*

Several signalling pathways follow after this phosphorylation: Binding of the Grb2-Sos-complex activates the Ras-cascade activating the extracellular regulated kinases (ERKs). These are known to activate transcription factors regulating progression through G_1 phase of the cell cycle and contribute to cell growth. Also serine/threonine kinase PKB is activated by FAK via phosphatidylinositol-3-kinase. PKB itself phosphorylates and so inactivates proapoptotic molecules such as Bad, Bax and caspase-9.

If cells lose attachment to the matrix, they undergo apoptosis, a phenomenon referred to as "anoikis" (homelessness). This process is very important for the integrity of tissue as it prevents cells that lost their surrounding to establish themselves at inappropriate locations.

The exact mechanism of activation of the nuclear factor kB (NF-kB) is still under investigation. NF-kB is a key transcription factor for the regulation of immune and inflammatory response also promoting cell survival by induction of the expression of anti-apoptotic molecules[261]. It is also supposed that unligated integrins can actively recruit pro-apoptotic molecules such as caspase-8, which is called integrin-mediated death (IMD)[262].

All of the mechanisms mentioned above for signal transduction contribute to the *outside-in* signalling, that allow cells to react on changes referring to their binding to the ECM. For the corresponding *inside-out* signalling, there is still a debate going on about the mechanism of how such a signal might be performed. Nevertheless, there is strong evidence that integrin activation is at least partly regulated by GTPases such as Ras and Rap-1[263,264]. Additionally, recent results

indicate that interactions between different integrins present on the cell surface can strongly influence the adhesive functions of individual receptors, which is referred to as integrin "cross-talk"[265].

II.2.1.1.3 Ligand Binding to Integrins

In integrins without I-domain such as $\alpha v \beta 3$, $\alpha v \beta 5$, $\alpha 5 \beta 1$ and $\alpha IIb\beta 3$, the ligand binding site is located between the β-propeller of the α-subunit and the βI-domain of the β-subunit. In figure 52 binding modes of the RGD containing peptide Cilengitide in the integrin $\alpha v \beta 3$ and the binding mode of Tirofiban in $\alpha IIb\beta 3$ based on crystallographic data can be seen[253,254].
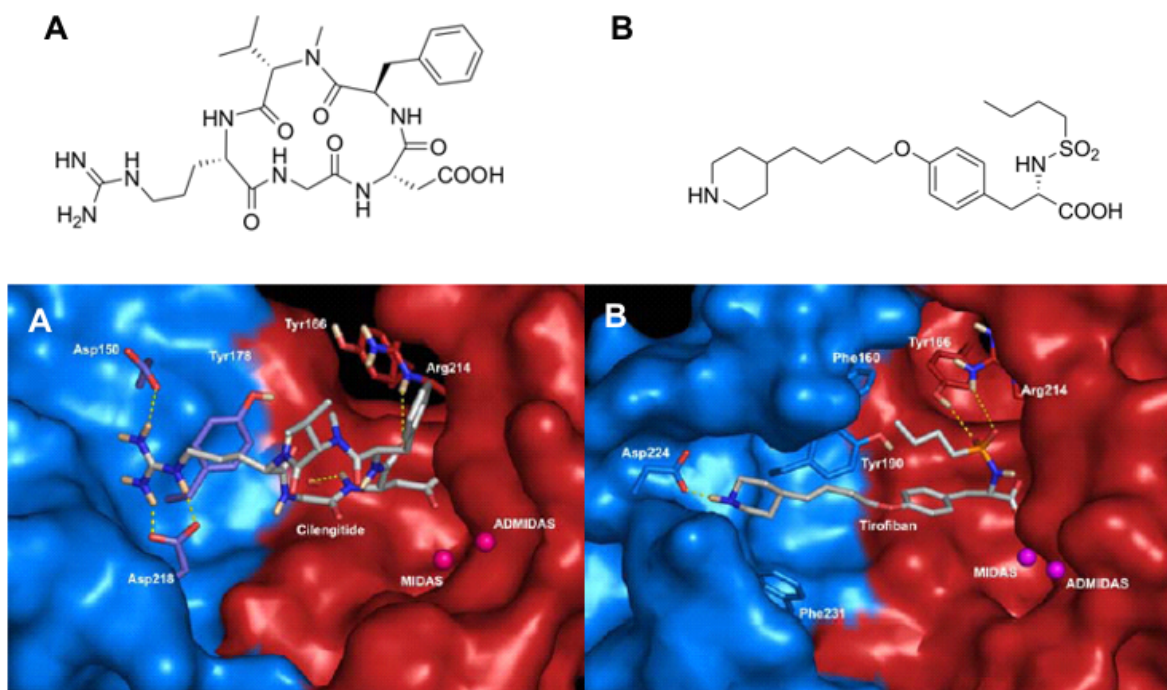
Figure 52: *Comparison of ligand binding in $\alpha v \beta 3$ and $\alpha IIb\beta 3$. A: Cilengitide in $\alpha v \beta 3$; B: Tirofiban in $\alpha IIb\beta 3$ as derived from crystal structures*[266].

As can be seen in figure 52, the guanidinium group of Cilengitide, *cyclo*(-R-G-D-f-MeV-), is fixed inside a narrow groove formed by the D3-A3- and D4-A4-loops of the β-propeller of αv by a bidentate salt bridge to (αv)-Asp[218] at the bottom of the groove and by an additional salt bridge with (αv)-Asp[150] at the rear. The side-chain carboxylate group of the Asp of the ligand primarily forms the contacts between the Asp and the βI-domain, protruding into a cleft between the βI-loops A'-$\alpha 1$ and C'-$\alpha 3$. This carboxylate function coordinates the metal ion at the MIDAS in βI and is also involved in hydrogen bonding towards the backbone amide proton ($\beta 3$)-Asn[215] and the backbone carbonyl of ($\beta 3$)-Arg[216] and the side-chain of ($\beta 3$)-Arg[214]. A week π-π-interaction with ($\beta 3$)-Tyr[122] is contributed by the D-phenylalanine of Cilengitide. Glycine does not interact with the

receptor but enables the formation of a γ-turn and acts as a spacer as extensive SAR studies revealed that the optimal distance between Arg-C^ζ and the Asp-C^β should be about 14 Å[267].

Tirofiban binds to αIIbβ3 in a very similar way as Cilengitide. The carboxylate group of the tyrosine scaffold coordinates the metal ion at the MIDAS while the piperidine moiety mimics the guanidyl group of arginine, forming a salt bridge with the (αIIb)Asp[224]. Opposite to the αv subunit, the aspartic acid residue binding to the piperidine moiety is more immersed in the receptor, leading to a longer groove in the β-propeller. Out of that, ligands, optimized for αIIbβ3 have to be elongated to be able to reach both anchoring points for which about 16 Å are required. Another difference between αIIbβ3 and αvβ3 is the more hydrophobic environment caused by (αIIb)Phe[160] and (αIIb)Tyr[190] as well as the replacement of (αv)Asp[218] by (αIIb)Phe[231]. Into this hydrophobic cleft, the *n*-butyl side chain of the sulfonamide can bind, while the sulfonamide itself is positioned by two hydrogen bonds with the (β3)Tyr[166]-hydroxyl function and the guanidine group of (β3)Arg[214].

II.2.1.2 Integrin Ligands

Over the past decades, integrins have been a promising target for medicinal chemistry. Since the recognition of the RGD-sequence as one of the crucial integrin binding sequences, a vast number of new ligands has been synthesized. While the monoclonal antibodies target a certain epitope on the receptor, peptides as well as small-molecule ligands mimic the natural ligands like e.g. fibronectin.

Figure 53: *Development of integrin ligands starting from proteins and resulting in small molecule ligands.*

II.2.1.2.1 Natural Integrin Ligands

Extracellular matrix proteins as fibronectin, vitronectin or fibrinogen are the most abundant class of integrin ligands. From these ligands, fibronectin has an outstanding role as it is widely expressed by multiple cell types and is critically important in vertebrate development[268].

Figure 54: *Schematic representation of fibronectin fragments. The three types of repeating homologous of which each subunit consists are termed Fn-I (blue rectangles), Fn-II (ovals) and Fn-III (yellow squares) repeats.*

Usually, fibronectin (Fn) exists as a dimer of two nearly identical subunits of about 250 kDa, linked covalently near their *C*-termini by a pair of disulfide bridges. The monomers consist of three types of repeating units: Fn-I, Fn-II and Fn-III (see figure 54).

Fibronectin is a soluble and abundant constituent of plasma and other body fluids. An assembly of soluble fibronectin on cell surfaces results in insoluble, associated fibronectin which becomes part of the ECM, a process referred to as *fibronectin fibrillogenesis* and depending on the self-association of fibronectin molecules directed by multiple binding sites along the molecule[269]. Especially the integrin $\alpha5\beta1$ has been found to be critical for this process as it can be inhibited by anti-$\alpha5\beta1$ antibodies as well as other antagonists. By mutagenesis studies, the binding site of Fn has been tracked down to the RGD sequence, which is mainly responsible for fibronectin binding and assembly. But, additional binding sites as the "synergy site" PHSRN have been identified, promoting binding of $\alpha5\beta1$ apparently via interaction with the $\alpha5$ subunit. Additional binding sites could be identified in the N-terminal region of Fn, which seem to be distinct from those generated in response to ligation with the RGD sequence[268].

II.2.1.2.2 Synthetic Ligands

The pioneering observation that integrins – especially $\alpha v\beta3$ and $\alpha5\beta1$ – are hallmarks of metastatic cancer and seriously involved in the process of tumor angiogenesis turned them into attractive targets for cancer therapy. Especially the subtype $\alpha5\beta1$ has recently been drawn into the focus of research due to its genuine role in angionesis which was found by a reevaluation of the integrin receptors[270]. Before that, most of the effort spent on the design of integrin ligands concerned the integrin receptors $\alpha IIb\beta3$ and $\alpha v\beta3$ as inhibition of the platelet receptor $\alpha IIb\beta3$ seems to be a promising way to inhibit fibrinogen-dependent platelet aggregation for the

treatment of thrombosis. On the other hand, up to now, $\alpha v\beta3$ was the main target of angiogenic cancer therapy. The main issue for the development of such ligands besides high activity is to gain selectivity as the prospect of strong adverse effects by non-selective ligands is present. Due to the crystal structures and homology models for different integrin receptors, the process of ligand design was generally accelerated yielding highly active and selective compounds.

Table 7: *Selected integrin ligands.*

Entry	Structure	IC_{50} [nM]	Reference
1 **Cilengitide**		0.5 ($\alpha v\beta3$) 70 ($\alpha v\beta5$) 860 ($\alpha IIb\beta3$)	[233]
2		2.6 ($\alpha v\beta3$) 280 ($\alpha v\beta5$) 8300 ($\alpha IIb\beta3$)	[271]
3		8 ($\alpha v\beta3$) 5170 ($\alpha v\beta5$) 4230 ($\alpha IIb\beta3$)	[272]
5		0.1 ($\alpha v\beta3$) 10 ($\alpha v\beta5$) 35000 ($\alpha IIb\beta3$)	[273]
6 **Tirofiban**		36 ($\alpha IIb\beta3$)	[274]
7		30 ($\alpha v\beta3$) 140 ($\alpha v\beta5$) 7800 ($\alpha5\beta1$) >20000 ($\alpha IIb\beta3$)	[275]

8 SJ749		49 (αvβ3)	[276]
		>100000 (αIIbβ3)	
		0.2 (α5β1)	
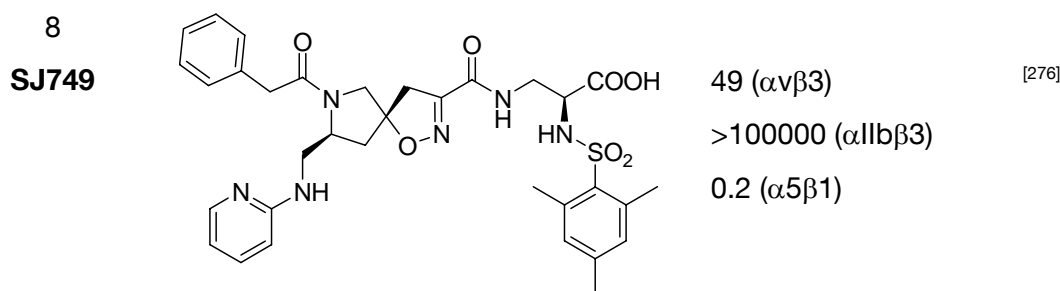
As can seen in table 7, all ligands share some general similarities: The guanidyl group of the arginine side chain of RGD is mimicked by a basic moiety and a carboxylate group represents the aspartic acid attached to a more or less rigid scaffold that arranges them in the appropriate three-dimensional manner. In most of the cases, an aromatic residue in the vicinity of the carboxylate improves properties by additional π-π-interactions with the receptor.

Tirofiban is an αIIbβ3 inhibitor authorized as drug for the treatment of angina pectoris and myocardial infarct[274]. Also the monoclonal antibody Abciximab, a fragment of a chimeric monoclonal antibody against αIIbβ3, is an approved drug, but lacks selectivity while showing higher receptor affinity than Tirofiban[277]. The αvβ3 antagonist Cilengitide is currently in clinical phase III trials for patients with glioblastoma multiforme, metastatic prostate cancer and lymphoma[278]. SJ749 was the first selective ligand reported for α5β1, enabling the set-up of the homology model calculated by Marinelli *et al.*[276,279].

II.2.1.3 The Role of the Integrins αvβ3 and α5β1

The integrins αvβ3, αvβ5 and α5β1 were found to be primarily expressed on activated endothelial cells what turned them into attractive targets for anti-angiogenic cancer therapy[280]. Originally, the integrin αvβ3 was found to be the one involved in tumor angiogenesis, as it could be shown that blocking of αvβ3 by monoclonal antibodies or peptides can suppress cornea vascularization, hypoxia-induced retinal neovascularization and tumor angiogenesis in mouse models[8,281-283]. Additionally, it was found that ligation of αvβ3 to the ECM activates proliferation and anti-apoptotic pathways such EFK-activation[284], NF-κB activation[285], increase in the Bcl-2/Bax ratio[286] and blocking of activator-caspase 8[287]. The integrin αvβ3 was also found to be activated by *vascular endothelial growth factor* (VEGF), enhancing ligand binding, cell adhesion and migration[288]. Though all these results sounded quite promising, the phenotype of β3 or β5 knockout mice (viable, fertile) displays a rather dispensable role in contrast to α5 knockout, which is lethal at E5[289]. Beyond that, β3-negative mice displayed an enhanced postnatal angiogenesis in response to hypoxia and VEGF which means the opposite of the desired result[290,291]. Additional results showed that also αv-deficient mice undergo extensive developmental vasculogenesis and angiogenesis[289]. The results raised the question if αvβ3 might regulate angiogenesis in a positive

or negative manner or if it might be possible, that other integrins have the ability to replace the function of $\alpha v \beta 3^{[270]}$.

These results also question the use of $\alpha v \beta 3$-binding antibodies or peptides and especially raise the question if these might act as antagonists or unwanted as agonists. The answer to these questions is further complicated as one has to consider the impact of integrin activation on different integrin types, the integrin "cross-talk"[265]. It was shown, that the binding of $\alpha v \beta 3$ by selective antibodies or a peptidic inhibitor not only inhibits cell migration on vitronectin, but also on fibronectin in the presence of $\alpha 5 \beta 1^{[292]}$. Similar results were obtained with a mutated $\beta 3$ subunit, indicating a modulation of $\alpha 5 \beta 1$ activity by $\alpha v \beta 3$. Additionally, concentration might have a strong impact, if an integrin ligand acts as agonist or as antagonist, as small picomolar doses of an RGD peptide increased binding affinity of $\alpha v \beta 3$ towards vitronectin, fibronectin and fibrinogen while higher doses up to 10 μM resulted in a dramatic loss of affinity[255].

Considering the success of e.g. Cilengitide in clinical trials, this might be due to the fact, that this compound is not really selective for $\alpha v \beta 3$, but is also highly active for $\alpha v \beta 5$ and $\alpha 5 \beta 1$ so inhibiting the replacement of one integrin receptor with another[233,278]. This might be a promising strategy as results indicate a certain ambivalent effect of $\alpha v \beta 3$ and $\alpha 5 \beta 1$ in anti-angiogenetic therapy as $\alpha 5 \beta 1$ was also found to induce angiogenesis in vitro while anti $\alpha 5$ antibodies suppressed VEGF-induced tumor angiogenesis in both chick embryo and murine models[293-295]. Engagement of $\alpha 5 \beta 1$ to fibronectin promotes proliferation via the NF-κB pathway and PKA / caspase 8 suppression while blocking of $\alpha 5 \beta 1$ via antibodies resulted in caspase 8 induced apoptosis due to sustained PKA activation[266]. So, $\alpha 5 \beta 1$ has been moved into the focus of drug development due to its pro-angiogenic function. A major step towards the synthesis of highly selective compounds for a5b1 was the setup of a homology model of $\alpha 5 \beta 1$ based on the crystal structure of $\alpha v \beta 3$ and the first slightly selective $\alpha 5 \beta 1$ integrin ligand SJ749[250,276,279]. So, first ligands showing a promising selectivity against $\alpha v \beta 3$ and good activity for $\alpha 5 \beta 1$ have recently been published[296,297].

II.2.1.4 Surface coating using integrin ligands

Coating of biomaterials for enhanced biocompatibility and improved ingrowth of implant materials is an important issue in medicine as most of the commonly used materials (polymers, ceramics, metals, etc.) are non-toxic, have sufficient mechanical stability and elasticity and are stable towards enzymatic degradation but often show graft rejection, inflammations, infection, local tissue wasting, implant encapsulation as well as thrombosis and embolization[298,299]. The demands on ligands used for coating of such implants are quite high as they should be able to endure the sterilization process of the implant before insertion into patients, should be stable towards degradation and metabolism in organisms, have to be non-toxic and must not cause any immune responses. Out of that, ECM proteins can be used for this purpose, but show all the

disadvantages listed above[300,301]. Also the use of antibodies and linear peptides though being reported to give very good results, are not the best choice as they are prone to degradation and once again can cause immune reactions[302,303].

As was shown by several groups, coating of different surfaces (e.g. PMMA[304], hydroxyapatite[302], titanium[305]) using RGD-containing proteins, peptides or RGD-based peptidomimetics can attract osteoblast causing improved bone formation.

A successful ligand for surface coating should be very specific for the desired integrin subtype of the adhering cells avoiding side effects from binding other cells, such as platelets via αIIbβ3. A spacer unit should provide a minimal distance between the ligand and the surface to avoid folding of the spacer unit but should also give enough distance from the surface that cells can easily bind towards the ligand. Finally, an anchor functionality is needed for ionic or covalent attachment of the ligand on the surface.
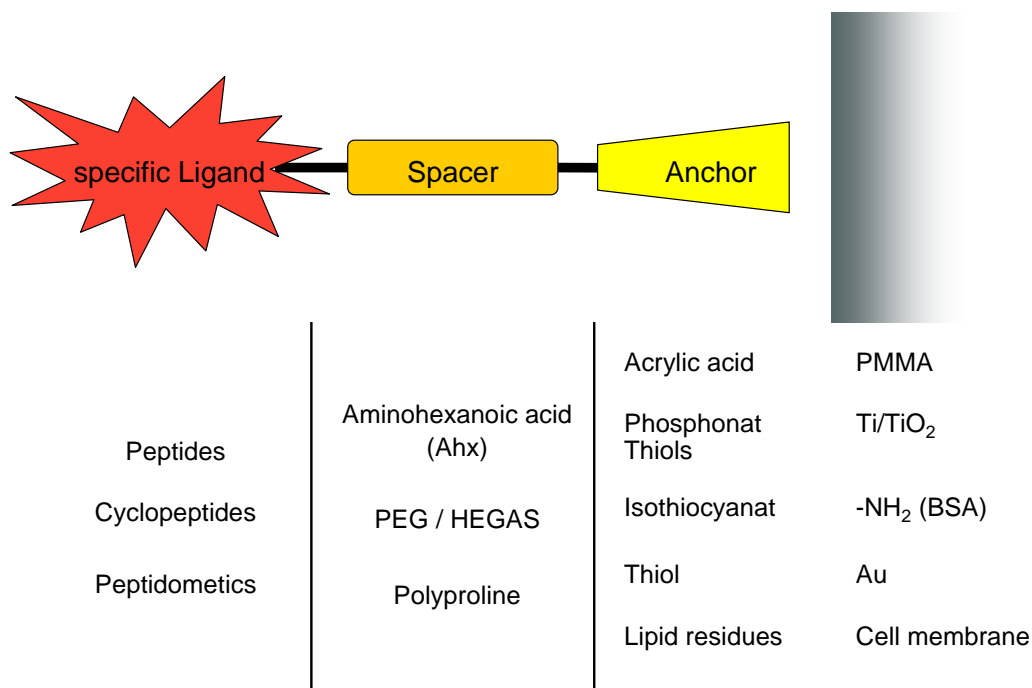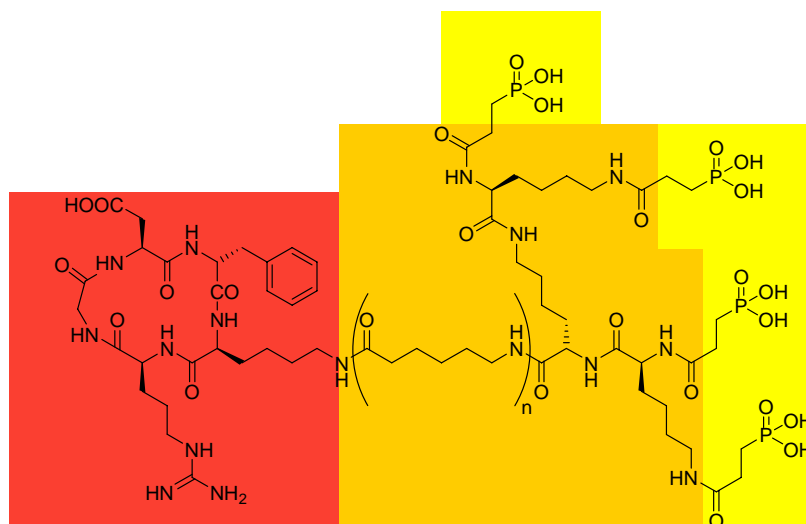
Figure 55*: Scheme (A) and example (B) of the ligand-spacer-anchor system required for surface coating.*

For *cyclo*(-R-G-D-f-V-), the parent peptide of Cilengitide, substitution of valine by lysine or glutamic acid retains full integrin-binding capacity while providing a functional group in the side-chain for the attachment of the spacer and anchor unit. This peptide was chosen because of its potency towards $\alpha v \beta 3$ and selectivity against $\alpha IIb \beta 3$, an important feature to avoid thrombosis as a result of platelet activation on the implant surface. For coating of titanium surfaces, coating with phosphonate groups as anchor has proven to result in extremely stable connections between the surface and the ligand[306-308]. In comparison to a single thiol anchor gave a higher immobilization densitiy for multimeric phosphonate and a stable anchoring.

II.2.2 Synthesis of highly active and selective α5β1 integrin ligands[309]

The following project was performed in cooperation with Dr. Roland Stragies, Dr. Grit Zahn and Dörte Vossmeyer, Jerini AG, Berlin, who performed the biological testings. Docking studies have been performed by Dr. Axel Meyer.

The pioneering observation that the αvβ3, αvβ5 and α5β1 integrin subtypes are essential for tumor angionesis and can be successfully inhibited by small-molecule ligands turned them into attractive targets for pharmaceutical research[260,281,283,310]. Until now, a large number of peptidic[129,233,282] and non-peptidic[271,311] ligands have been developed which are all related to the common recognition motif RGD. However, observations that mice lacking αv integrins show extensive angiogenesis while mice lacking β3 or β5 integrins show no significant effects, seriously challenged the status of αvβ3 and αvβ5 as pro-angiogenic integrins[270,289,312]. In contrast, the pro-angiogenic role drew α5β1 into the focus of research and led to increasing demand for selective α5β1 ligands[295]. However, the design of α5β1 ligands is handicapped by the lack of structural information about the receptor. Publication of a first ligand showing mild selectivity towards α5β1 by Smallheer *et al.*[276] enabled Marinelli *et al.*[279] in 2005 to create a homology model of α5β1. This model is based on the X-ray structure of αvβ3 in complex with Cilengitide[250] and uses the high sequence similarity of >50% between αvβ3 and α5β1. First results with ligands based on the tyrosine scaffold of SJ749 led to highly active α5β1 ligands with up to 300 fold selectivity against αvβ3[296,297].

II.2.2.1 Results and Discussion

As the tyrosine-backbone, derived from SJ749, resulted in highly active but only slightly selective compounds, there was a high need for a new approach to gain ligands for α5β1 with high selectivity and activity[297]. Simplification of the RGD sequence based on the homology model of Marinelli et al.[279] led to four building blocks, which had to be optimized to gain selectivity: The acid functionality mimicking the aspartic acid, which should be sterically demanding to gain selectivity against αvβ3, a glycine or aza-glycine for the glycine of the RGD-sequence, a spacer unit to mimic the unpolar part of the side-chain of arginine and a basic moiety to mimic the guanidyl residue of the arginine side-chain.
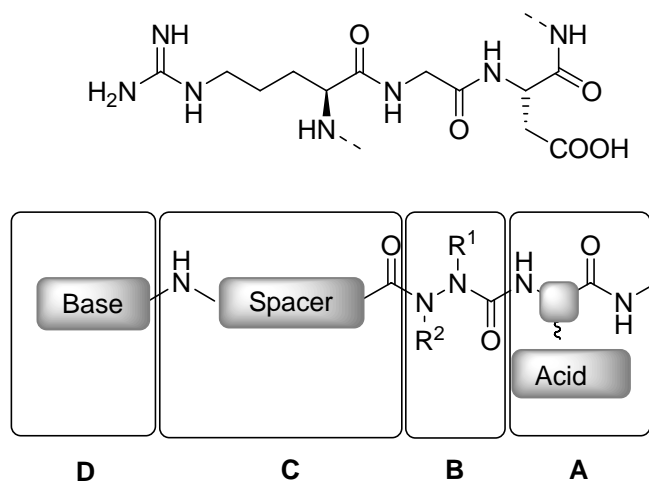
Figure 56: *Simplification of the RGD-sequence towards four building blocks.*

While for αvβ3-ligands a β-amino acid with a prolonged main chain is favored due to the longer binding pocket, a shorter chain length gives selectivity for α5β1. In this case, the use of a "normal" amino acid backbone can be applied.

As sterically demanding side-chain for the acid-building block, 2,6-dimethyl-4-isopropoxy-benzoic acid **214** was chosen which is easily accessible from 4-bromo-3,5-dimethylphenol by alkylation (**213**) followed a bromine lithium exchange reaction with CO_2.
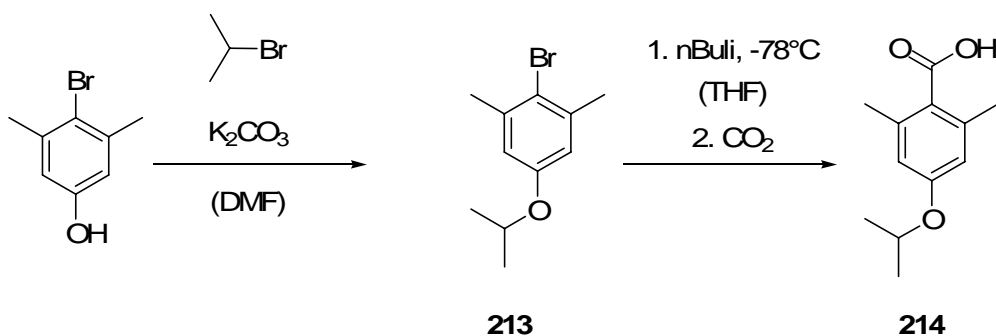
Scheme 8: *Synthesis of 2,6-dimethyl-4-isopropoxy-benzoic acid **214**.*

Synthesis of the aza-glycine was performed using activation of Fmoc-protected hydrazine by phosgene to give **215** which could be directly used for solid phase synthesis of the desired ligands without any further purification[313].
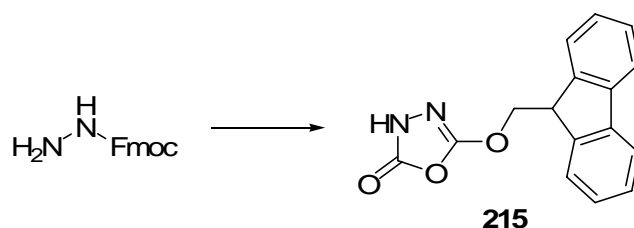
Scheme 9: *Synthesis of the aza-glycineprecursor **215**.*
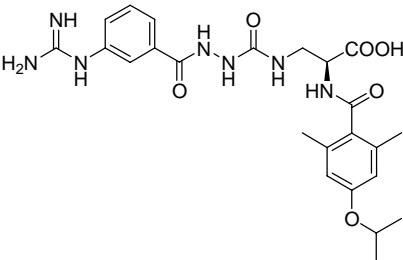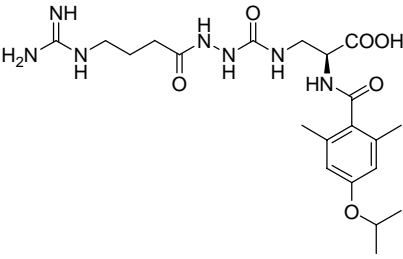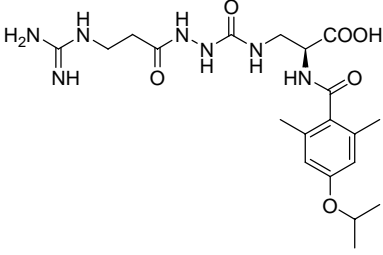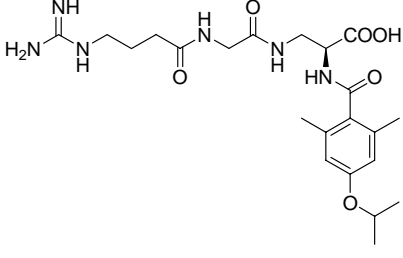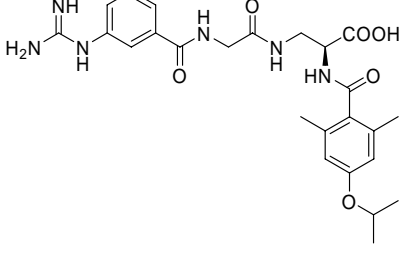
Synthesis of the ligands was performed on TCP resin loaded with Fmoc-,Alloc-orthogonally protected 2-(*S*),3-diamino propionic acid providing the essential carboxylic function and the α-amido-substitution which was found to be crucial for α5β1 selectivity. After Fmoc-deprotection, the amino-functionality was acylated with 2,6-dimethyl-4-isopropoxy-benzoic acid **214** to give **216**. After Pd-catalyzed Alloc-deprotection, either the aza-glycine was introduced via precursor **215** or Fmoc-protected glycine to give **216-X**. The spacer unit was then coupled to the unprotected hydrazine and the guanidinium group introduced via *N,N*'-di-Boc-1*H*-pyrazole-1-carboxamidine. Cleavage and Boc deprotection afforded the aza-glycine ligands **216-XRF** in satisfying yields.
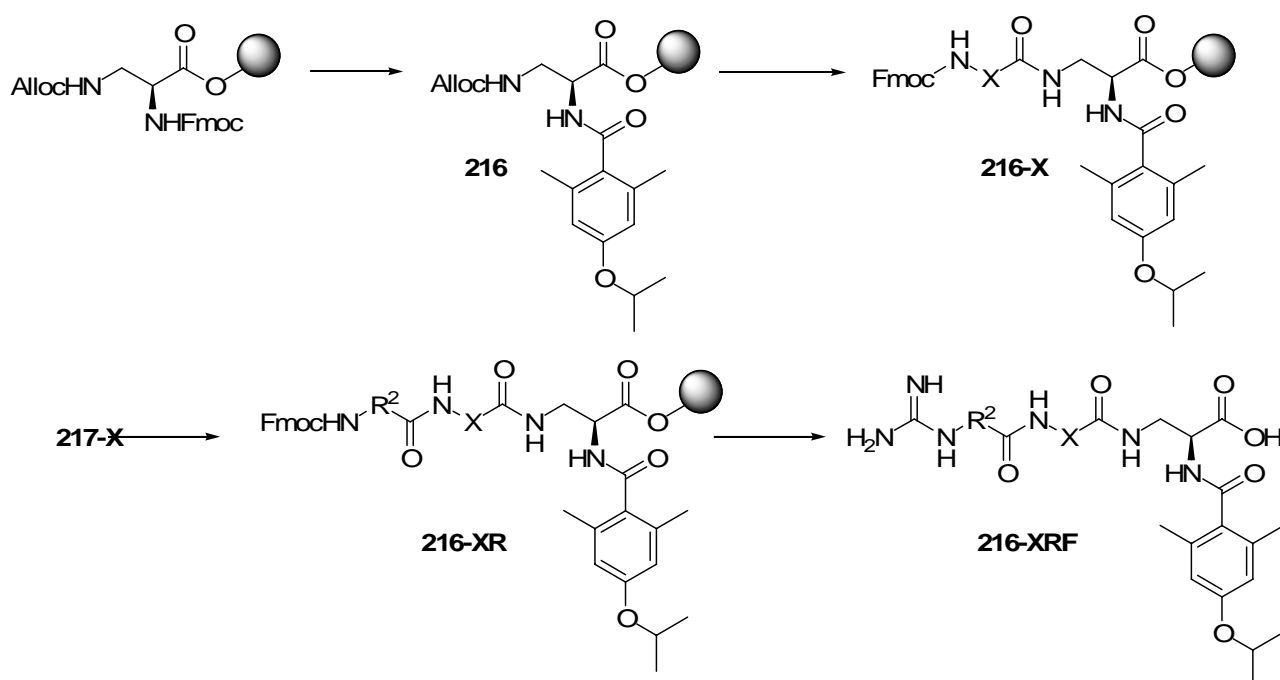
Scheme 10*: Synthesis of aza-glycine ligands on TCP resin*.

As can be seen in table 8, the combination of all features responsible for α5β1-selectivity (S-configured α-amino acid as carrier of the carboxyl moiety and aromatic amide with ortho-dimethyl-substitution pattern) resulted in highly active and selective compounds.

Table 8: *Biological activities of ligands based on the aza-glycine and the glycine scaffold.*

Compound	Structure	IC_{50}(α5β1) [nM]	IC_{50}(αvβ3) [nM]
217		0.96	>4750
218		3.3	>20000
219		34	>20000
220		1.5	>20000
221		0.86	9600

All compounds show a dramatically increased selectivity for α5β1 in comparison to the previously used tyrosine-based compounds[309] which might be caused by the reduced flexibility of the diacylhydrazone backbone. The lower activity for α5β1 for compound **219** compared to **218** proves that the total length of the ligand cannot be reduced. Substitution of aza-glycine with glycine shows only little effect on the high affinities.

Figure 57 demonstrates the fit of compound **217** into the α5β1 receptor and the main interactions with the binding pocket. The high selectivity of the ligand should be the result of an enhanced rigidity of the scaffold, which strongly disfavours the placement of the aromatic amide outside the receptor in αvβ3.
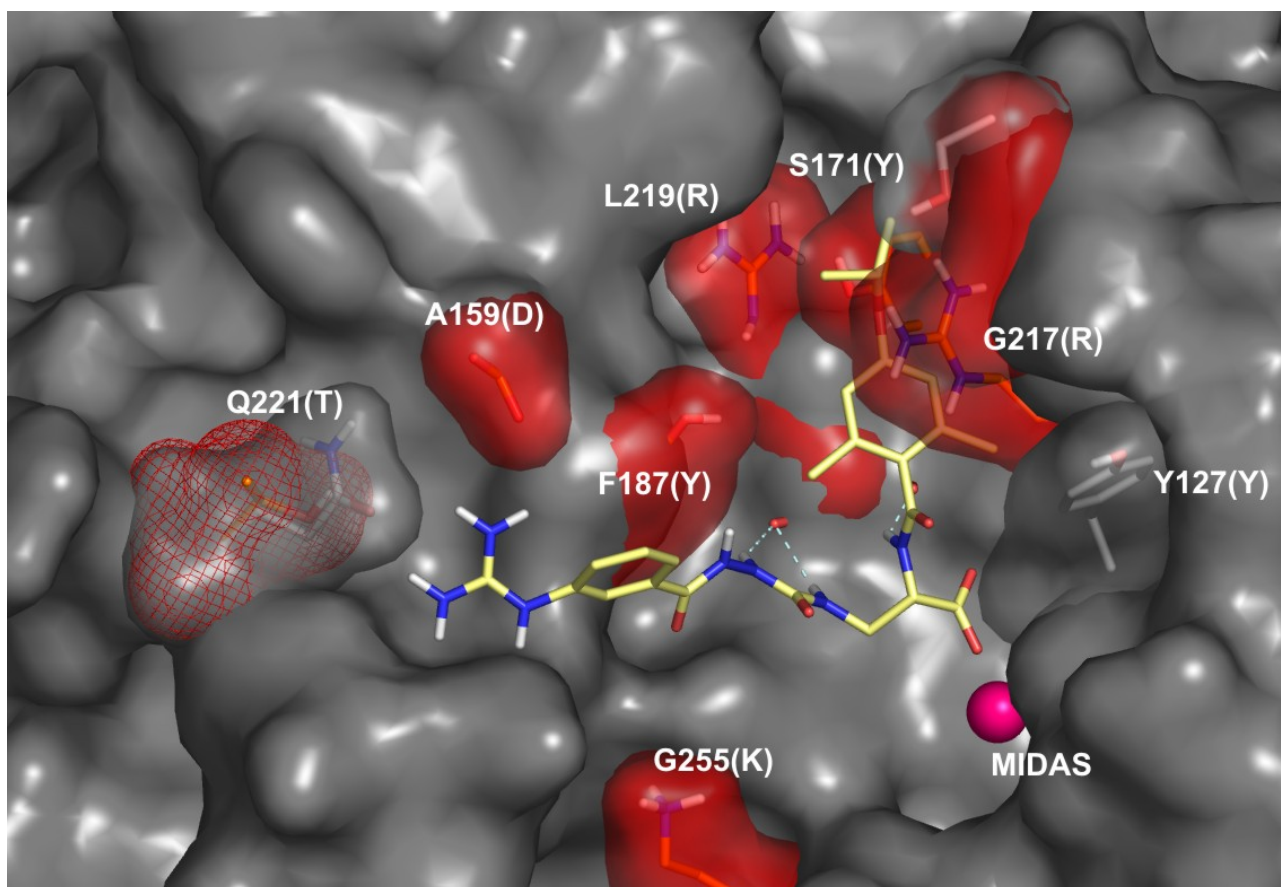
Figure 57*: Superposition of the binding pocket of the Conolly surface of α5β1 (grey) and αvβ3 (red) with ligand **217** docked into it.*

In the face of the growing importance of selective α5β1 ligands, the introduction of a new backbone for the synthesis of highly selective and active ligands succeeded in yielding compounds that display affinities in the low nanomolar range and below. Furthermore, the selectivity against αvβ3 exceedes 10^4 fold, which reveals the levevl of the most selective α5β1 ligands described in literature so far. These antagonists represent promising lead structures for antiangiogenic therapy of cancer and age-related macular degeneration.

II.2.3 Hydroxamic acids as a new class of integrin ligands[314]

The following project was performed in cooperation with Dr. Dominik Heckmann. For a detailed assignment of the synthesized compounds towards the creators, please see material and methods section. Biological testings have been performed by Dr. Roland Stragies, Dr. Grit Zahn and Dörte Vossmeyer, Jerini AG, Berlin. Docking studies have been performed by Dr. Ettore Novellino, Dr. Vittorio Limongelli and Dr. Luciana Marinelli (Università di Napoli "Federico II", Italy).

The application of RGD-based drugs is hampered by poor pharmacological properties which may to some extend be the result of the zwitterionic nature of the RGD motif. The improvement of pharmacological parameters has been subject of recent efforts, mainly by alteration of the polarity and rigidity of the scaffold, the nature of the basic moiety and synthesis of prodrugs[129,315,316].

While the guanidine group of arginine has been substituted by countless basic heterocycles during the process of designing peptidomimetics, the carboxylic acid functionality of the aspartate is the most conserved feature of all known integrin ligands up to now.

The acid functionality is involved in the crucial coordination of the bivalent metal cation at the MIDAS site, which is present in all integrins[317]. Although the nature of the metal ion is not yet fully determined, the importance of the cation-carboxylate interaction is undoubted[254,255]. Even though this site seems to be very sensible towards modifications as several attempts to substitue the carboxylate by tetrazole or sulfonic acids failed in the past, hydroxamic acids should be promising candidates leading to another binding mode and thus altering the selectivity profile.

Hydroxamic acids have the opportunity to coordinate metals in a bi-or mono-dentate fashion depending on the environment and are also known to possess good coordination properties towards many different ions[318,319].

II.2.3.1 Results and Discussion

Synthesis of the ligands started from the commercially available Boc-protected tyrosine methyl ester. The homologue β-amino acid was prepared from Boc-Tyr(Bn)-OH via Arndt-Eistert homologisation[320].

222   **223**
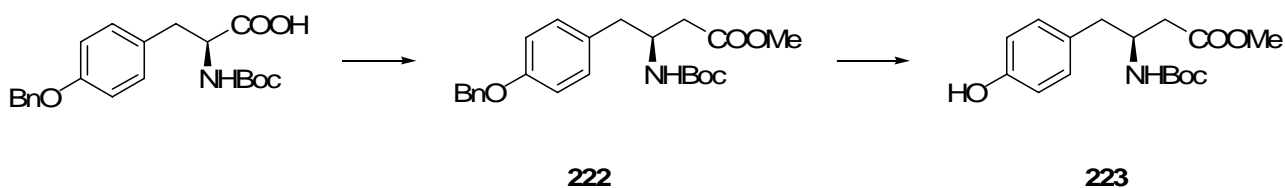
Scheme 11: *Synthesis of Boc-Tyr(Bn)-OH via Arndt-Eistert reaction.*

To enable a Mitsunobu reaction type alkylation of the tyrosine, the basic moiety has to be synthesized as aminoalcohol which was achieved via nucleophilic substitution of 2-bromopyridine.
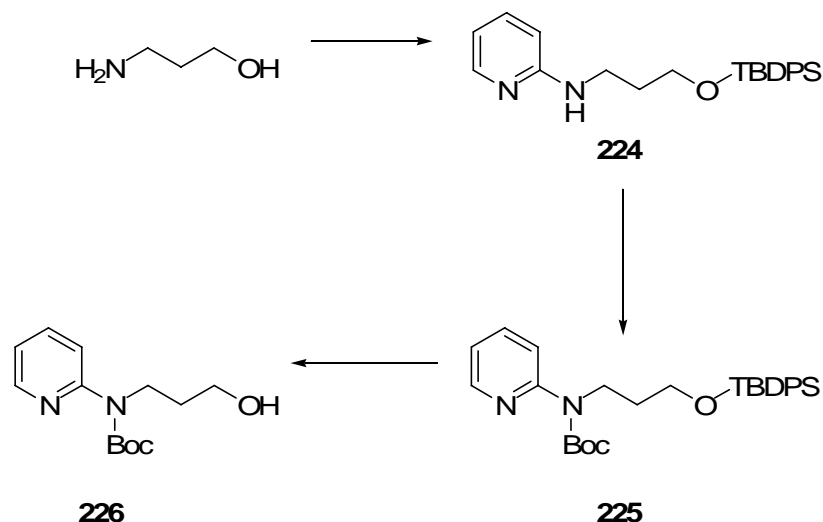
Scheme 12: *Synthesis of the amino alcohol building block.*

To enhance the yields of the Mitsunobu reaction, the aminopyridine was Boc-protected. For this purpose, the alcohol functionality had to be protected with TBDMS first following the Boc-protection of the amino function using Boc-anhydride, triethylamine with catalytic amounts of DMAP in DCM. Desilylation with TBAF gave the pure pyridinylaminoalcohol in good yield.
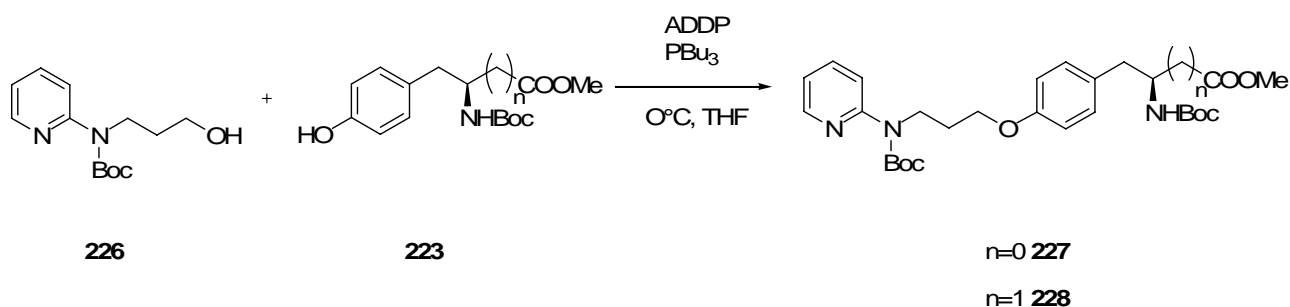
Scheme 13: *Synthesis of the ligand precursors via Mitsunobu-reaction.*

The Mitsunobu type alkylation of the tyrosine-hydroxyl group was performed by slow addition of azodicarboxylic dipiperidide (ADDP) via syringe pump to a solution of the educts with tributylphosphine.

n = 0 **227**

n = 1 **228**

n = 0:
R^1 = COPh, **229** R^2 = OH, **230** R^2 = NHOH
R^1 = COMes, **231** R^2 = OH, **232** R^2 = NHOH
R^1 = SO$_2$Ph, **233** R^2 = OH, **234** R^2 = NHOH
R^1 = SO$_2$Mes **235** R^2 = OH, **236** R^2 = NHOH
R^1 = COp(C$_6$H$_4$)OiPr, **237** R^2 = OH, **238** R^2 = NHOH
n = 1:
R^1 = COPh, **239** R^2 = OH, **240** R^2 = NHOH
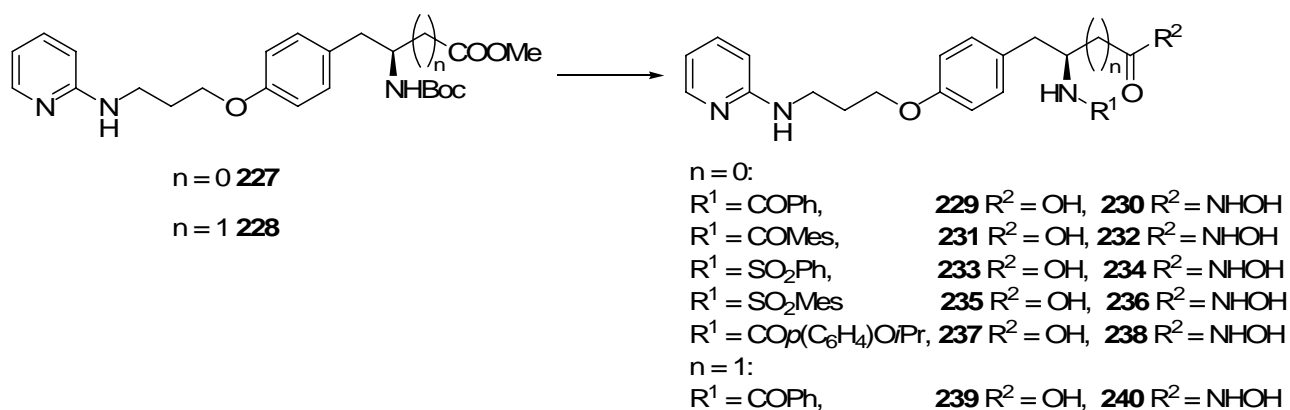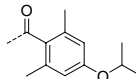
Scheme 14: *Synthesis of hydroxamic acid and carboxylic ligands.*

After Boc-deprotection with diluted aqueous HCl in dioxane, the resulting amines were acylated either with aromatic carboxylic acids or sulfonyl chlorides according to the desired selectivity profile. While saponification with LiOH in methanol/water gave the carboxylic acids, a feasible way to prepare the corresponding hydroxamic acids was the addition of an excess of hydroxylamine to the saponification mixture.

First, ligands **229** and **230** were examined as proof of principle and it was observed that for **230**, the IC$_{50}$ towards α5β1 increased while the corresponding value for αvβ3 decreased if compared to the nearly biselective carboxylic acid derivative.

Table 9: *IC$_{50}$ values of the integrin ligands for α5β1 and αvβ3.*

Compound	R^2	n	R^1	IC$_{50}$ [nM] α5β1	IC$_{50}$ [nM] αvβ3
229	-OH			243	207
230	-NHOH	0		2470	14
231	-OH			2.5	703
232	-NHOH	0		1244	72
233	-OH			284	1.9
234	-NHOH	0		296	11
235	-OH			46	3.4
236	-NHOH	0		132	4.8

237	-OH			1	279
238	-NHOH	0		40	13.5
239	-OH			264	1.2
240	-NHOH	1		4500	12

The spatial orientation of the aromatic moiety in vicinity to the carboxylic acid is determining for the selectivity of the ligand, a mesitylene carboxamide leading to $\alpha5\beta1$ selectivity while a sulfonamide group yields biselective ligands[296,297,309]. Out of that, it was expected that substitution of the carboxylate by a hydroxamate should have a high impact on the positioning of this group. So, five more pairs of ligands sharing the 2-aminopyridine group as basic moiety were synthesized and evaluated for their activity and selectivity profile. Furthermore, one of these pairs was prepared with an $\alpha v\beta3$ selective ligand based on an elongated β-homotyrosine.
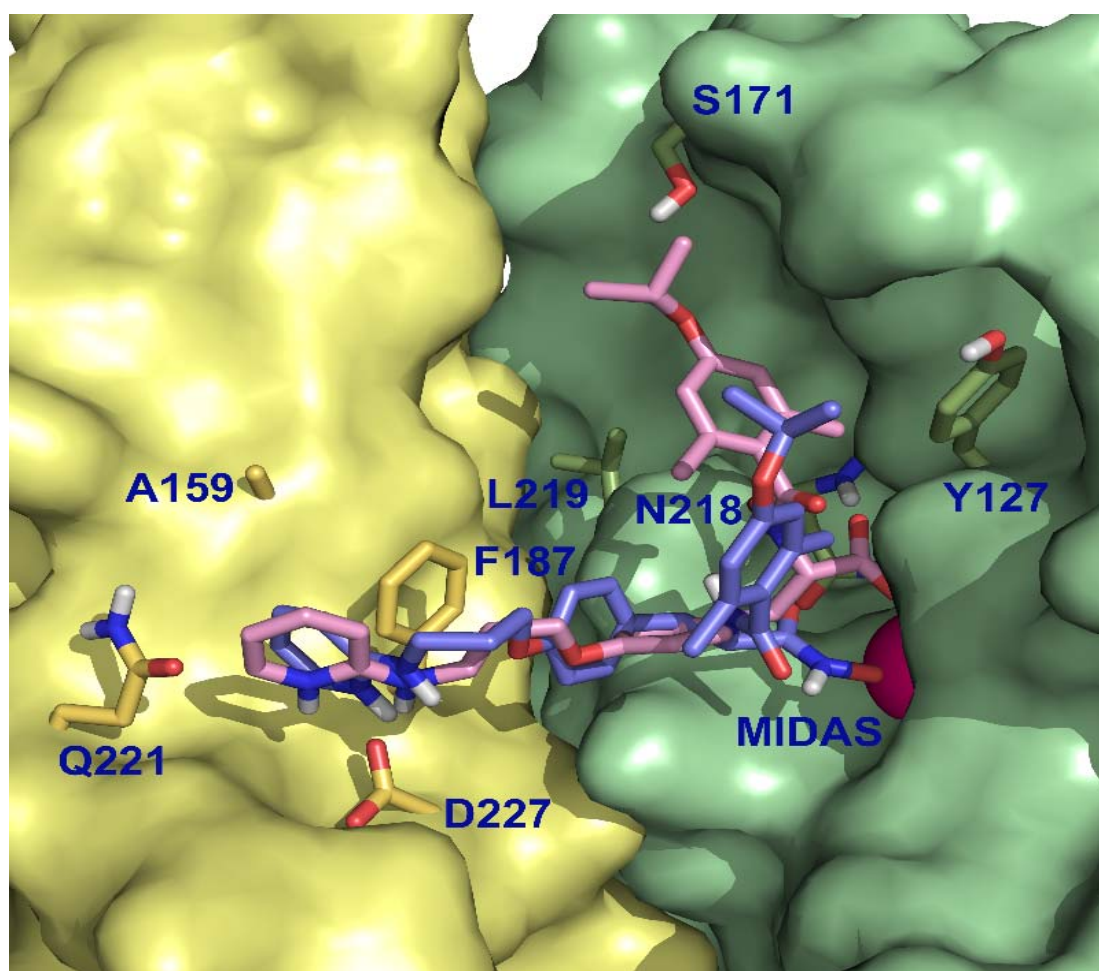
Figure 58: *Binding modes superimposition of **238** (blue) docked in the $\alpha v\beta3$ and **237** (pink) docked in $\alpha5\beta1$. In the figure, only the surface of $\alpha5\beta1$ is shown for clarity reason.*

Figure 58 shows the superimposition of the binding modes of **237** and **238**. The results in table 9 outline that in **237**, the replacement of the carboxylic group by the hydroxamate moiety allows **238** to regain the activity for αvβ3 receptor. A downshifting of the isopropyloxyphenyl moiety is observed for the hydroxamate derivative accounting for the activity for αvβ3. Moreover, as a result of the structural difference between the carboxylic and hydroxamic acids (the latter has a larger distance between the metal-coordinating oxygen atoms), the distance between the metal coordinating oxygen and the bulky substituent in the α-position is greater in **238** than in **237**. Out of that, the coordination made by the hydroxamate compound **238** allows a shifting of the isopropyloxyphenyl moiety towards the α subunit and an orientation that allows the isopropoxyphenl group to form hydrophobic interactions with (β3)-Tyr[122].

The inverted selectivity of compound **238** with respect to **237** seems to be a consequence of the increased distance between the acidic and the basic groups as a result of the presence of the hydroxamate moiety. This increased distance is favored by the binding pocket of αvβ3 which is longer than the one of α5β1 and normally prefers β-amino acids as backbone structures, as the mutation of (αv)-Thr[212] to (α5)-Gln[221] in the α5β1 receptor reduces the space available for the binding of the ligand's basic moiety which results in a preference of shorter chain lengths for the α5β1 receptor.

A second series started from precursor **241**, which was transformed into the derivatives **242**-**247** to investigate whether other derivatives of carboxylic acids and hydroxamic acids are capable of integrin binding. Table 10 shows the outstanding high affinity of the hydroxamic acid **243** in contrast to the other derivatives.

242 R = OMe
243 R = NHOH
244 R = OH
245 R = NH$_2$
246 R = NH$_2$NH$_2$
247 R = NHCH$_3$OH
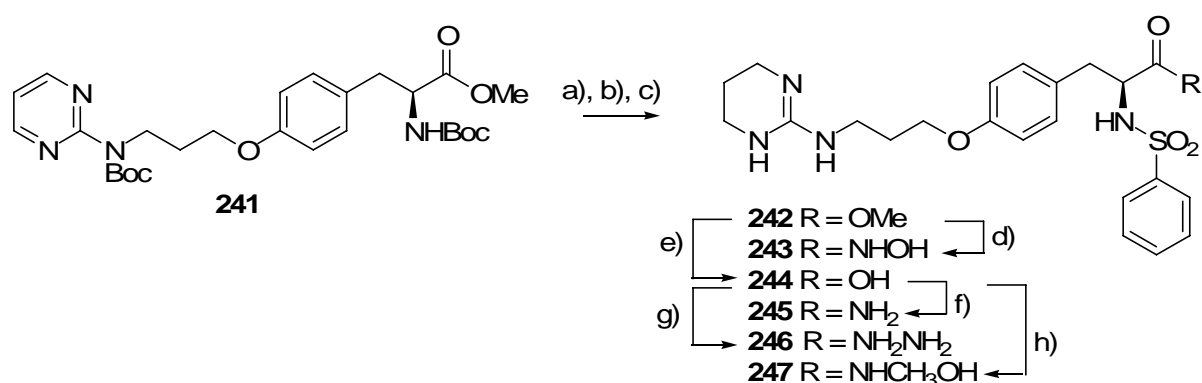
Scheme 15*: Synthesis of the second library.*

It is remarkably, that despite of their reduced acidity, hydroxamic acids are still able to complex the MIDAS metal efficiently. The low affinity for **246** is the result of the substitution of the MIDAS binding oxygen by a hydrazone NH$_2$ group with poor coordination properties. An even more

drastic effect can be observed for the amide **245**. Similar to **246**, a residual binding affinity can be still observed for the methyl ester **242**. The sensibility of the binding mode towards additional substituents is demonstrated by the low affinity of the *N*-methylated hydroxamic acid **247**.

Table 10: *IC$_{50}$ values of integrin ligands on $\alpha5\beta1$ and $\alpha v\beta3$.*
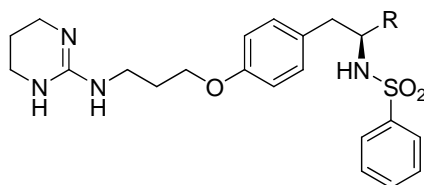
Compound	R	IC$_{50}$ [nM] $\alpha5\beta1$	IC$_{50}$ [nM] $\alpha v\beta3$
242	-COOMe	2366	419
243	-CONHOH	85	5.3
244	-COOH	79	4.2
245	-CONH$_2$	>20000	>1000
246	-CONHNH$_2$	9000	290
247	-CONCH$_3$OH	5216	359

Summing up, the first successful replacement of the ubiquitous carboxylic acid function in integrin ligands has been performed. The results indicate a shift of the selectivity profile from $\alpha5\beta1$-selective ligands towards $\alpha v\beta3$ ligands. So, hydroxamic acids could be used for new lead structures for $\alpha v\beta3$-selective ligands with improved pharmacophoric properties.

II.2.4 Integrin Ligands for Surface Coating

II.2.4.1 Integrin Ligands for Interversicle Cross-Linking

The following project was performed in cooperation with Hans-Jürgen Musiol from the group of Prof. Dr. Luis Moroder (Max-Planck Institut für Biochemie, Martinsried). Biological testings will be performed by Dr. Peter C. Seitz from the group of Prof. Dr. Motomu Tanaka at the University of Heidelberg.

Several different models have been designed as models to study cell adhesion using substrates composed of polyacrylamide gels or alkylsiloxanes functionalized by deposition of RGD peptides[321,322]. Also synthetic oligo(ethylene-glycol)thiolates modified by linear RGD-containing peptides have allowed preparation of self-assembled monolayers (SAM) with a controlled density of the functional ligands that promoted the bovine endothelial cell attachment and spreading[323]. Recently, Hu *et al.* published cyclic RGD lipopeptide binding towards αIIbβ3 which was able to anchor in membranes and could be used as a membrane-anchored integrin ligand[324]. In 2001, a RGD-lipopeptide based on *cyclo*(RGDfK) was published by Marchi-Artzner *et al.* which was able to be inserted into artificial membranes and selectively adhered endothelial cells[325].

For further studies on integrin αIIbβ3, a lipopeptide for coating/insertion into artificial membranes was synthesized based on the work of Hu *et al.*[324].

II.2.4.1.1 Results and Discussion

Synthesis of cyclo(-G-R(PBf)-G-D(tBu)-f-K(Cbz)-) **248** was performed using standard solid phase synthesis[326,327]. After cyclisation using HATU/HOBt and DIPEA[328], the Cbz protecting group was removed via hydrogenation using H$_2$ and Pd on charcoal to obtain **249**.

(RS)-3-*tert*.-Butyldithio-1,2-di-myristoyloxypropane was reduced by PBu$_3$ to give **250** which was added to N$^\varepsilon$(Mal>βAla)-Ahx-Gly-Gly-OH **251** to give the lipid anchor **252** for the RGD peptide.
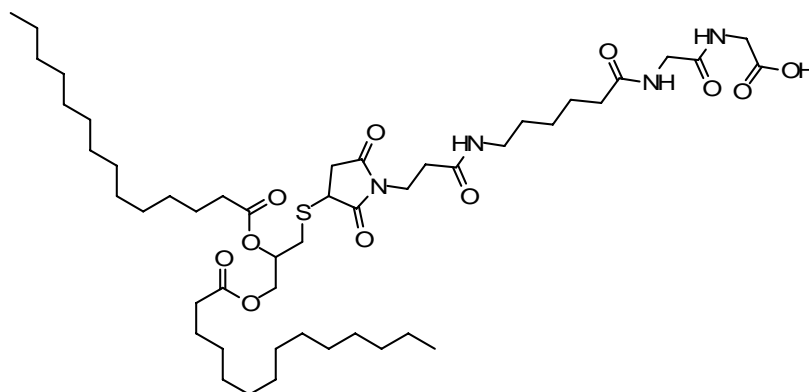
Figure 59: *The lipid anchor **252**.*

To obtain the final lipopeptide, the lipid anchor **252** was dissolved in freshly degassed argon-saturated DMF and coupled to **249** using HATU/HOAt. After cleavage of the protecting groups using 95% TFA, the compound was purified by precipitation using acetonitril/water to give the pure final product **253**.
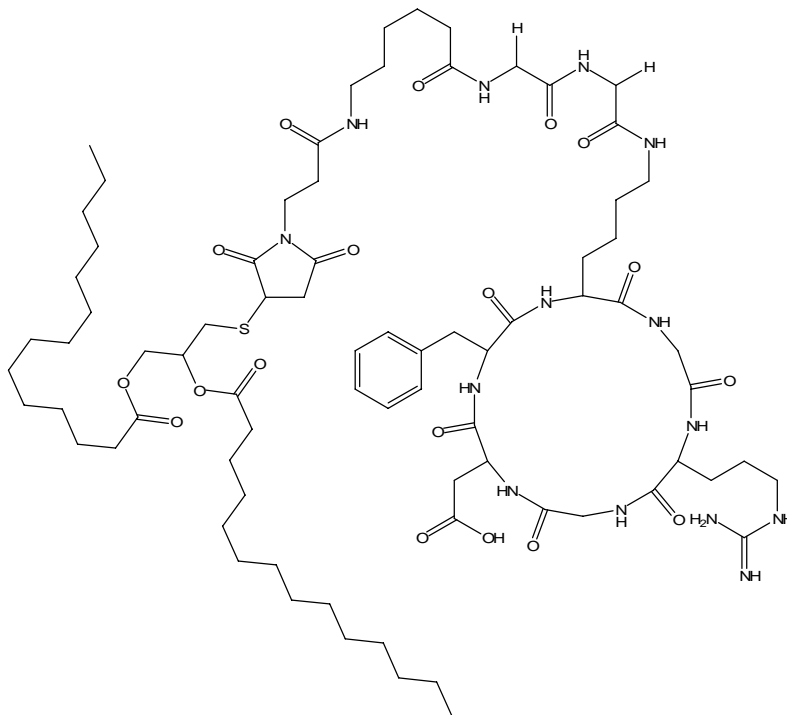
Figure 60: *The lipopeptide **253**.*

Biological testings in the Tanaka-group are still in progress.

II.2.4.2 Coating of Virus Like Particles

The following project was performed in cooperation with Vu Hong from the group of Prof. Dr. M.G. Finn at the Scripps Research Institue (La Jolla, Ca, USA). Biological testings have been performed by Dr. Nicole F. Steinmetz from the group of Prof. Dr. M. Manchester at the Scripps Research Institute (La Jolla, Ca, USA).

Targeting therapies or imaging modalities specifically to areas of disease while avoiding healthy tissue is an important goal in medicine. Virus like particles (VLPs) have been developed as nanomaterials for biomedical applications: they display many features that make them uniquely for such a development. They serve as polyvalent building blocks, provide a stable and well-characterized surface that can be used for many different chemical reactions[329,330]. Furthermore, they contain no replicative genetic information and can be produced recombinantly in large scale[331,332]. Thus, virus like particles present a safe and effective vaccine platform for inducing potent B- and T-cell responses and already two prophylactic virus-like particle vaccines (Gardasil™ and Cervavix™) have been registered for human use[331,333].
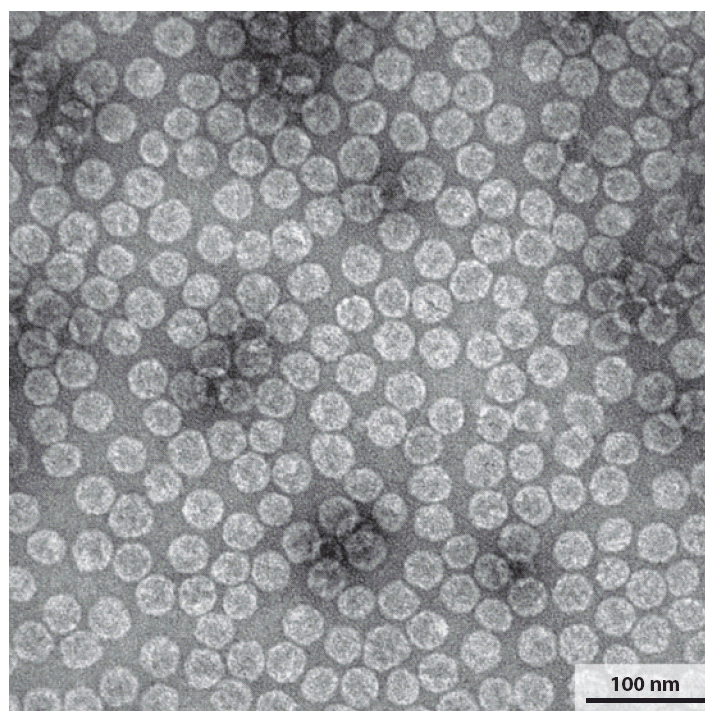
Figure 61: *Electron micrograph of purified recombinantly expressed VLPs derived from the RNA phage Qβ[333].*

Currently, VLPs are mainly used for vaccine concepts causing immune responses in the human body or for first imaging studies using MR[334]. However, VLPs still suffer from unselectivity concerning internalization if only a type of specific cells has to be attacked, as some VLPs internalize into every cell, while others do not internalize in any cell. As was shown recently,

PEGylation of VLPs can inhibit unselective internalization[335]. But still, there is a lack of selectivity for getting VLPs into cells.

Nevertheless, viruses often use integrins for attachment and internalization processed on human cells[336]. As was recently reported, αv integrins, especially αvβ3 and αvβ5[337], are needed for cell entry and gene delivery of adenovirus[338], while for human parvovirus B19 β1 integrin, especially α5β1 is essential as a co-receptor for viral entry[339]. Also for bacterium *yersinia pestis*, it was proven, that internalization into epithelial cells is performed by Invasin[340,341], which is binding towards β1-integrins[342,343].

Based on this knowledge, it should be possible to gain internalization of virus like particles into cells using integrin ligands as keys to open the way into the cell.

II.2.4.2.1 Results and Discussion

II.2.4.2.1.1 Synthesis of Cilengitide-Coated Virus Like Particles

As αvβ3, αvβ5 as well as α5β1 are reported to be receptors or co-receptors for virus internalization, Cilengitide, *cyclo*(-R-G-D-f-MeV-), was chosen as starting structure, as it shows subnanomolar activity towards αvβ3 and low nanomolar activity for αvβ5 and α5β1[233]. To gain a side chain functionality for attachment of a spacer and an anchor, the *N*-methylated valine was replaced by a *N*-methylated lysine to give **254**.

As unspecific internalization of virus like particles can be avoided by PEGylation[335] and it also improves the water solubility of the attached ligands, a PEG spacer with eleven units was chosen as spacer between the virus particle and the integrin ligand.

In a first step, the azide functionalized PEG was derivatized by attachment of an alkyne functionality giving **255** using NaH and propargyl bromide in DMF.
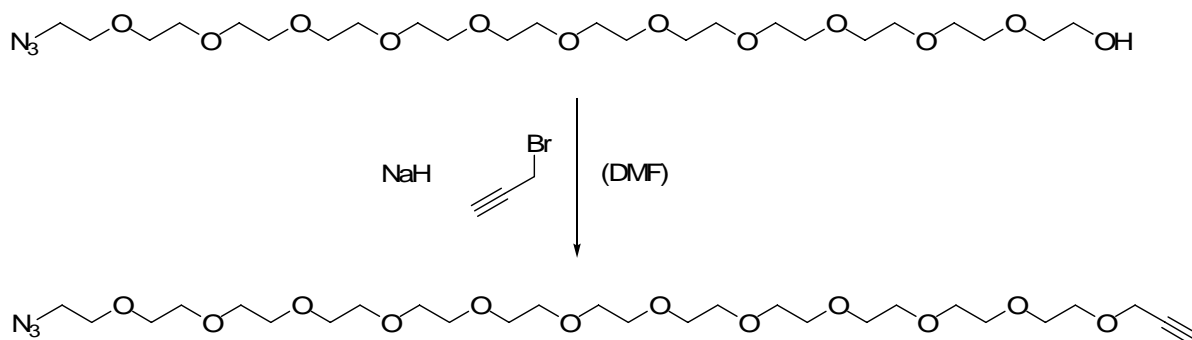
Scheme 16: *Synthesis of **255**.*

Reduction of the azide functionality of **255** with triphenyl phosphine in THF and argon atmosphere led to the amino functionalized product **256**.
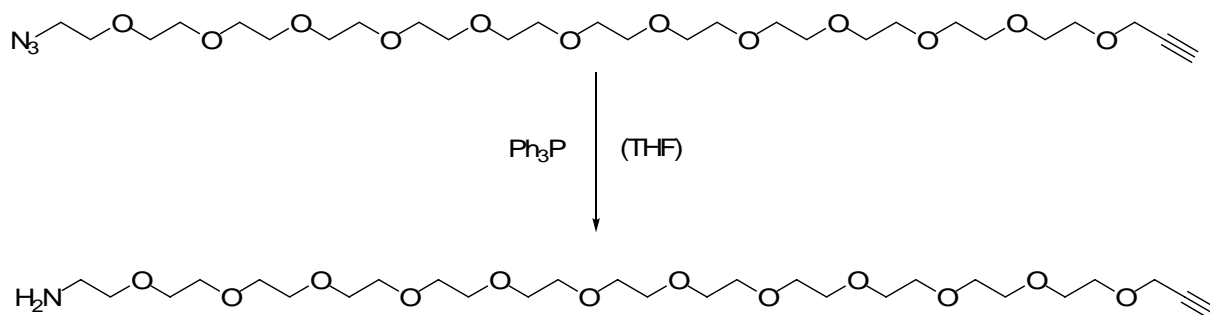
Scheme 17: *Reduction of 255 to gain 256.*

To introduce an acid functionality for the attachment of the lysine derivatized Cilengitide, succinic anhydride was added to a solution of **256** in acetonitrile to yield **257**.
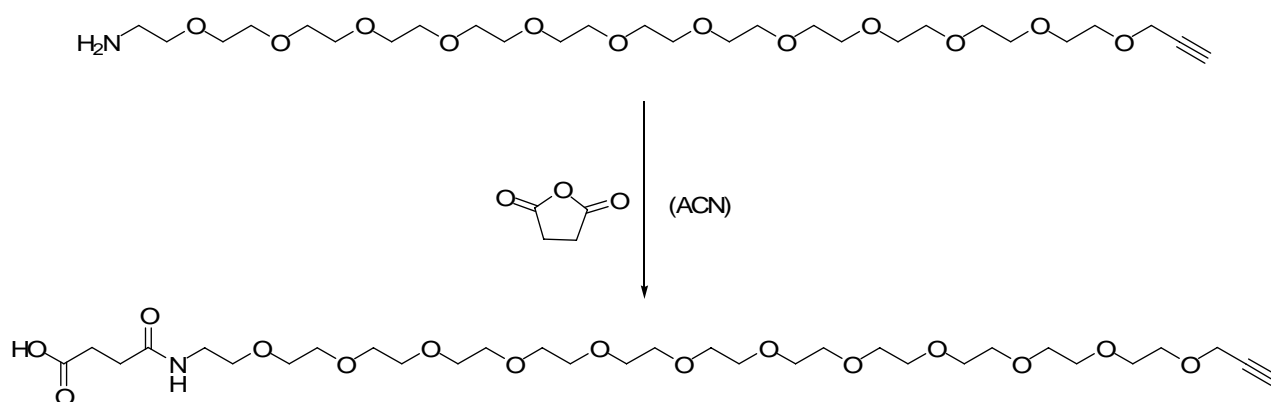
Scheme 18: *Introduction of a carboxylic acid functionality via reaction with succinic anhydride.*

Coupling of the PEG spacer **257** with the lysine derivatized and partially side-chain protected Cilengitide **254** was performed in DMF with HCTU as coupling reagent and DIPEA as base to give the protected integrin ligand **258**. Cleavage of the side-chain protecting groups was performed with 95% TFA, 2.5% TIPS and 2.5% water yielding the affinity ligand **259** as final product.
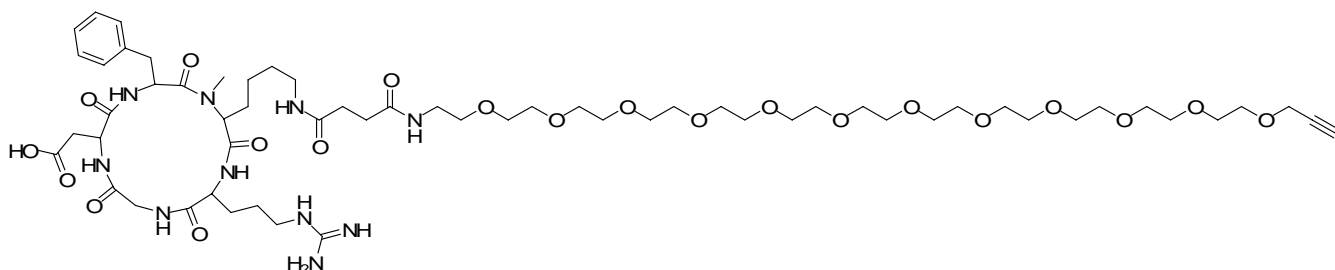
Figure 62: *The deprotected integrin ligand 259.*

As virus like particle for internalization experiments, a Qβ coat protein[344] was chosen, as it is known not to internalize into any cells. Isolation and purification of the VLP was performed as described in the literature by Kaltgrad *et al.*[345]. For fluorescence analysis of the internalization of the VLP, Alexa568 was attached as a strong fluorophor.

To enable attachment of the integrin ligand via click-reaction, the VLP was coated with azide groups by the use of azide *N*-hydroxysuccinimide ester[346]. Afterwards, click reaction was performed in water using an optimized procedure with sodium ascorbate as reducing agent for Cu[II] to give the final virus like particle. On each subunit, an average coating of 2-4 integrin ligands could shown via MALDI (4 adressable azide functionalities per subunit, 180 identical subunits) leading to about 410 ligands for the whole VLP while 10% of the free positions were coated with Alexa568 which results in 70 for the whole particle.
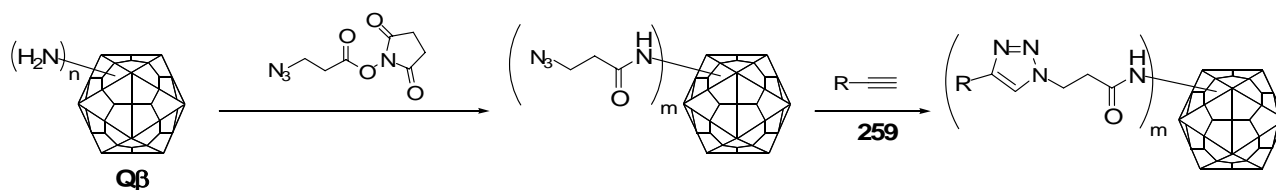
Scheme 19*: Click-reaction of the integrin ligand with the VLP.*

II.2.4.2.1.2 Biological Evaluation

In a first step, three different cell lines were used to prove binding/internalization of the coated VLPs towards the different integrin ligands. For this purpose, MCF-7-cells (breast cancer cells) overexpressing $\alpha 5\beta 1$, HT-29-cells (colon cancer cells) overexpressing $\alpha v\beta 5$ and HeLa-cells (cervical cancer cells) overexpressing $\alpha v\beta 3$ and $\alpha v\beta 5$ were used. This set of cells allows to test target-selectivity and –specificity on the VLP for different integrin combinations.

First confocal imaging studies using HeLa cells were conducted for which ligand-coated VLPs were incubated with living cells for three hours in medium and fixed prior to analysis. Imaging suggests internalization of the VLP-ligand complexes, thus confirming specificity for the integrins $\alpha v\beta 3$ and $\alpha v\beta 5$ (figure 63). For quantitative analysis flow cytometry was conducted.
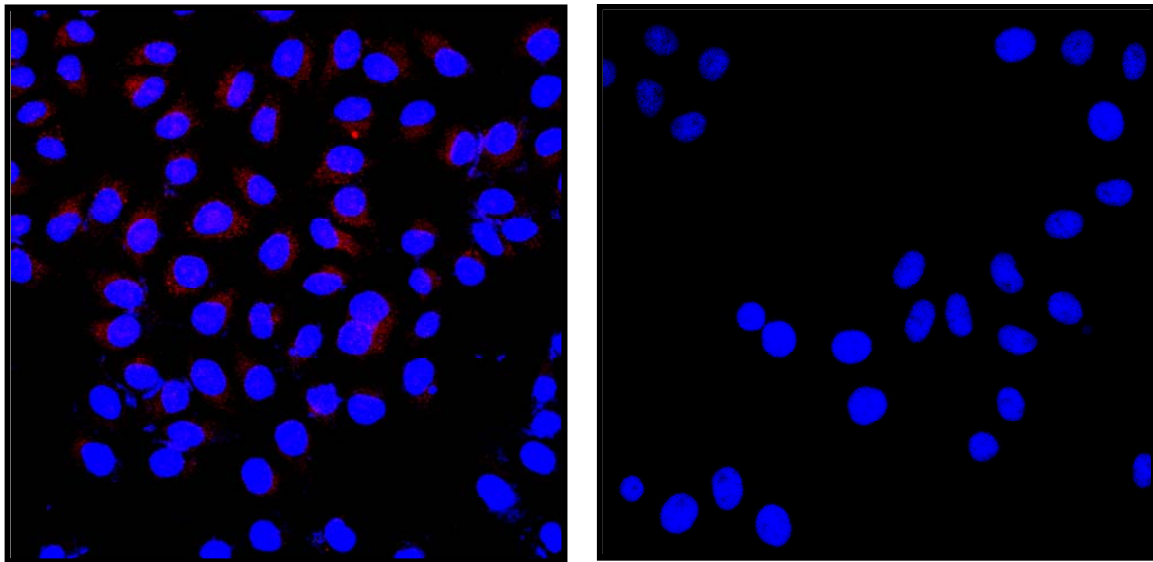
Qbeta-P.7-RGD/A568   HeLa

Figure 63: *Fluorescence images of HeLa-cells with coated VLPs (left) and only HeLa-cells (right). The Alexa568 label on the VLPs is indicated in red.*

To analyze the specificity towards the different integrin combinations all three cell lines were used. VLPs which were decorated with the PEG spacer only were used as negative control. Flow cytometry studies confirmed that the target VLP-ligand formulation indeed was taken up by all three cell lines tested. This confirms specificity towards $\alpha v \beta 3$, $\alpha v \beta 5$ and $\alpha 5 \beta 1$.
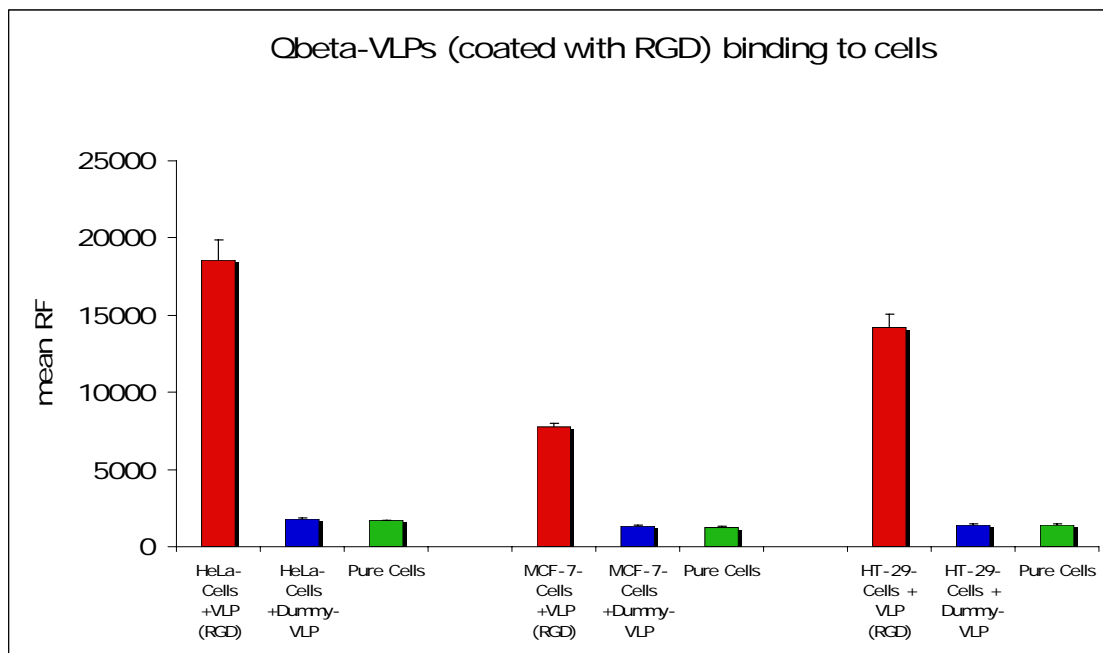
Figure 64: *Binding of the coated VLPs to different cell line derived from FACS data. The red bars symbolize the coated VLP while the blue bars symbolize a dummy VLP, the green ones symbolize the cells without any VLP.*

The strongest binding efficiency was detected for HeLa cells which is in good agreement with biochemical data for the parent peptide Cilengitide[128]. Hence, binding to MCF7 cells is less efficient compared to HeLa cells. The fact that the dummy particles do not interact with the cells further underlines target specificity due to the coating.

In addition, competition-binding assays with free affinity ligand **259** using HT29 cells showed that the free ligand competes with the coated VLPs confirming receptor-specific delivery of the VLPs to the cancer cells (figure 65).
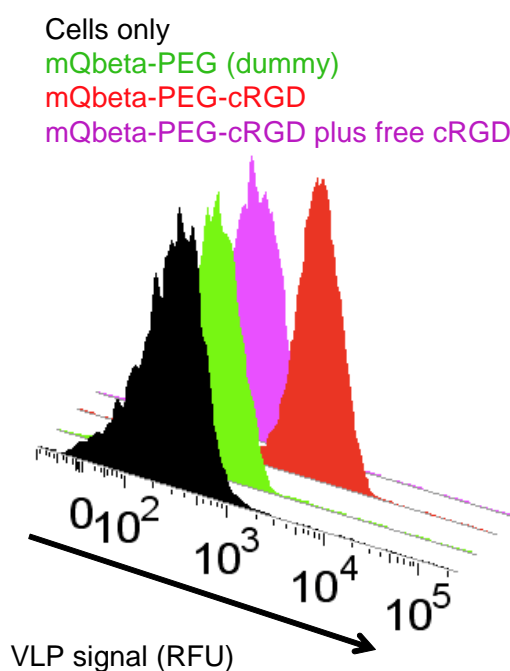
Figure 65*: Competition-binding assay using HT29 cells.*

Summing up, it was demonstrated that integrin-mediated targeting of VLPs to cancer cells is possible by using affinity ligand **259** as targeting peptide. The binding was selective towards $\alpha v\beta 3$, $\alpha v\beta 5$ and $\alpha 5\beta 1$. Further, binding was exlusively mediated by **259**, non-labeled VLPs did not interact with cells and specificity could be further confirmed in competition binding assays.

II.2.4.3 Selective α5β1 integrin ligands for surface coating

To transform one of the selective α5β1 integrin ligands into a molecule being able to be attached to the surface, a spacer and an anchor functionality have to be introduced at a position pointing out of the binding pocket. As can be seen in figure 66, the aromatic side chain of the acid residue points out of the pocket and might be used for attachment of the spacer and anchor functionality.
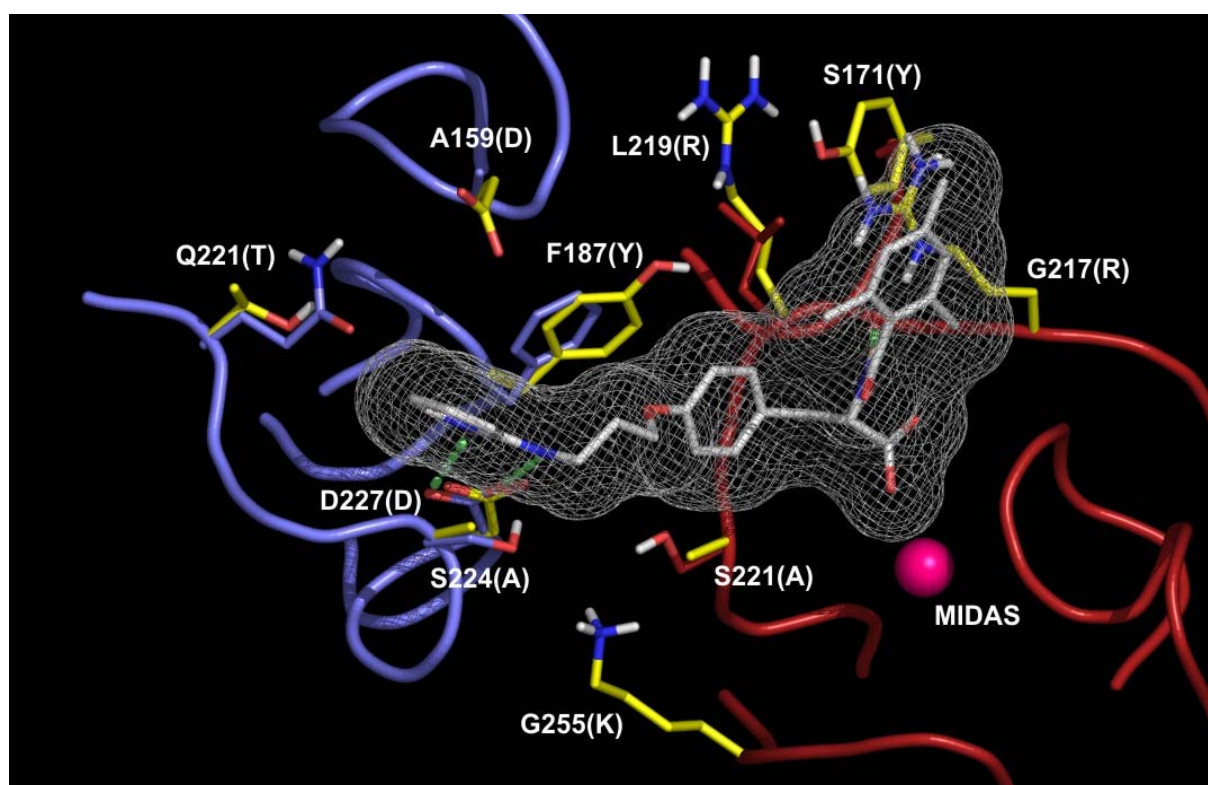
Figure 66: *Ribbon draw of the α5β1 integrin binding pocket (α5 in blue, β1 in red) with the predicted binding mode of a tyrosine based integrin ligand. .*

As lead structure for this molecule, the selective ligand **237** was chosen and the mesityl derivative in the side chain of the acid group prolonged with amino butanol, 6-aminohexanoic acid and mercaptopropionic acid which enables attachment to gold and titanium surfaces.
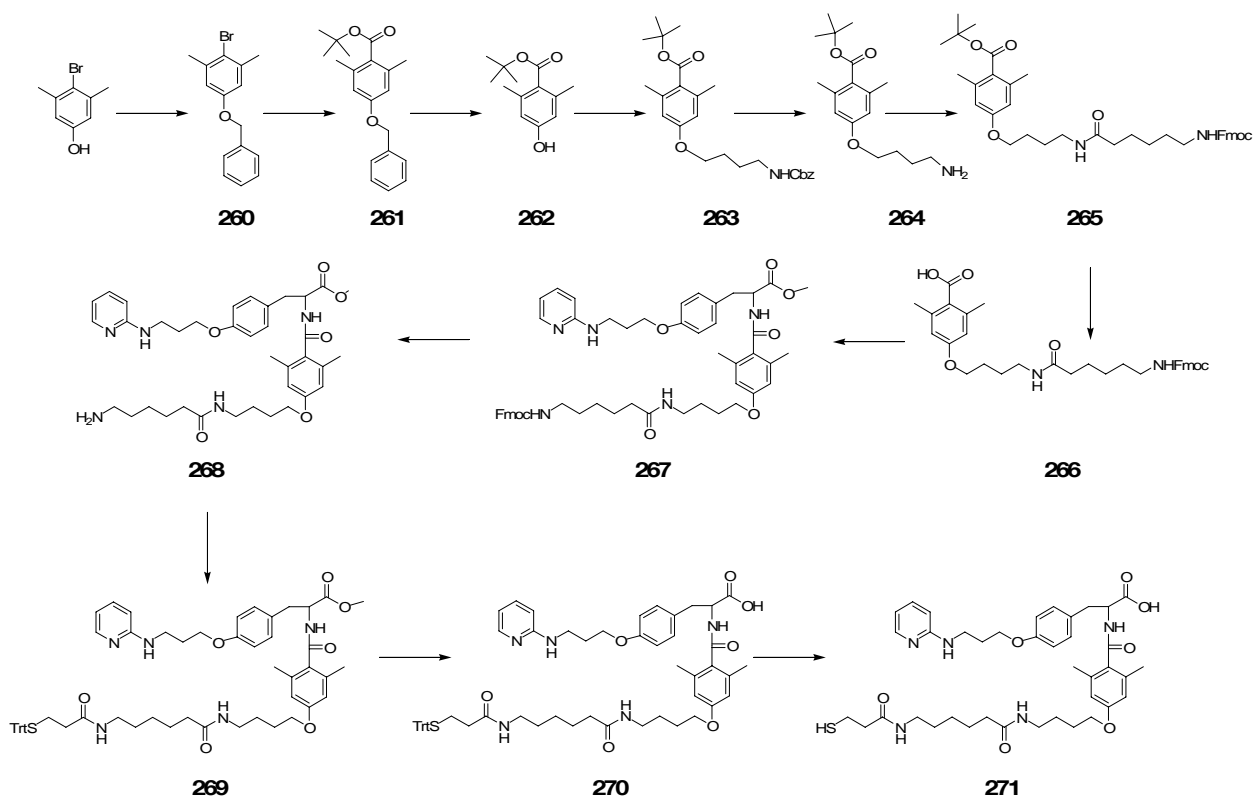
Scheme 20: *Synthesis of the surface ligand 271.*

Although a thiol functionality is prone to dimerization and not such a strong anchor as e.g. a phosphonate would be, the facile synthesis in comparison to other anchor groups led to this choice to obtain a first ligand **271** which is applicable to surface coating to investigate the importance of α5β1 in comparison to αvβ3 for attachment of osteoblasts. Biological evaluation in the group of Prof. Joachim Spatz (MPI Stuttgart) and in the group of Dr. Rainer Burgkart (Klinikum recht der Isar) are currently in progress.

III Summary

The scope of this work was the synthesis of bioactive peptides and their mimetics. Out of the eleven different topics, four topics concentrated on the influence of *N*-methylation towards cyclic penta- and hexapeptides while the other topics had the focus on the synthesis on biologically active peptides or peptidomimetics.

III.1 The Influence of N-Methylation towards Cyclic Peptides

In a first approach for basic research, a library of 60 different **N-methylated cyclic hexa-alanine-peptides** was synthesized and screened for sequences that show a preferred structure with a main conformation that is higher populated than 90%. Out of these 60 peptides, 15 compounds were found that fulfill this criterium. In a next step, all these 60 peptides were investigated towards their cell permeability via a CaCo2 assay. This project is currently still in progress but out of the so far tested compounds, seven peptides were found that show cell permeability in range comparable to testosterone.

In the next project, the influence of **N-methylated amino acids** to form β-turn structures in cyclic pentapeptides was compared to the influence of **proline** which is typically used for this purpose. It was possible to show that proline can be replaced in the (*i*), (*i+1*) and (*i+2*)-position without affecting the population of the main conformation. This enables the replacement of proline in peptides bearing this amino acid at one of these positions which has the advantage that the side-chain functionality is gained back which normally is lost due to the pyrrolidine ring of proline. This side-chain could then be used to improve the activity, selectivity or could act as a pharmacophore in the peptide.

In the third project, the **side-chain impact on N-methylated cyclic pentapeptides** towards the occurrence of a *cis*-amide bond at the position of the *N*-methylation was investigated. For this purpose, a cyclic penta-alanine of the DL_4-type was chosen as template structure with an *N*-methylation at the (*i+3*)-position. This peptide shows a 50/50 mixture of the all-*trans* conformation and the conformation bearing one *cis*-amide bond at the *N*-methylated alanine in the NMR time scale with DMSO as solvent. Variation of nine different amino acids through every five positions of the cyclic peptide revealed that the β-branched amino acids (threonine, isoleucine and valine) can shift the 50/50-mixture to an at least 75/25-mixture with the all-*trans* conformation as the preferred one if they are inserted at any position except the one of the D-residue.

The fourth project based on a cyclic pentapeptide published by N. Fujii and co-workers[130] which is active in the low nanomolar range towards the **CXCR4 receptor**. This peptide was enlarged to a cyclic hexapeptide that still showed activity in the nanomolar range. However, introduction of one to four *N*-methylations into this peptide resulted in a complete loss of activity. Another approach starting from a disulfide bridged peptide[125] led to a peptide with mild biological activity. As shortening of the peptide sequence and a D-amino acid scan did not lead to a more active compound, this approach was abolished.

III.2 Synthesis of Biologically Active Peptides or Peptidomimetics

Based on the previous work of Sebastian Knör[165], several peptides and peptidomimetics were tested for their binding affinity towards **FVIII**. For the best peptidomimetic a solution phase synthesis was developed and optimized towards an easy and economically reasonable strategy. Furthermore, evaluation of the binding mode and the enzymatic stability of the ligand was performed to ensure that the ligand is highly selective, stable towards enzymatic degradation and not binding in the B-domain which is often not present in recombinantely expressed FVIII.
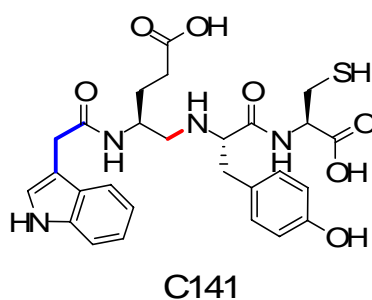
Figure 67: *The affinity ligand C141 (***195***)*.

As there was no synthesis of condensed and aromatic-ring-substituted tyrosine derivatives described in literature, a **synthesis of enantiomerically pure 3-aryl-substituted L-tyrosine analogues *via* a Suzuki-type cross coupling** reaction was developed. A second approach was used to extend the aromatic residue, in which the condensed 2-naphthylalanine analogue of tyrosine was synthesized *via* unselective hydrogenation of the corresponding α-enamide and enantioselective cleavage of the racemic mixture using acylase I as key step.

Using the homology model for α5β1[279], a new backbone for the synthesis of **highly active and selective α5β1 integrin ligands** was created. This lead to a small library of compounds with activity in the low nanomolar or even subnanomolar range and a selectivity profile towards αvβ3 of up to 10^4.
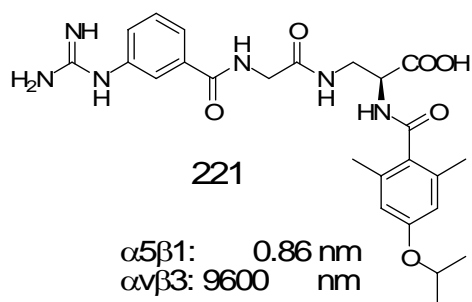
Figure 68: *The highly active and selective integrin ligand* **221**.

As the carboxylic acid functionality in all RGD-based integrin ligands is the most conserved structural feature it was tried to replace it by a **hydroxamic acid** functionality to create a complete **new class of integrin ligands**. Doing so, it was found that the replacement causes a shift of the selectivity from $\alpha5\beta1$ towards $\alpha v\beta3$ which might be due to the longer distance between the carbonyl and the hydroxyl functionality. Nevertheless, the ligands still showed activity in the low nanomolar range which might enable the synthesis of highly active and selective $\alpha v\beta3$ ligands.
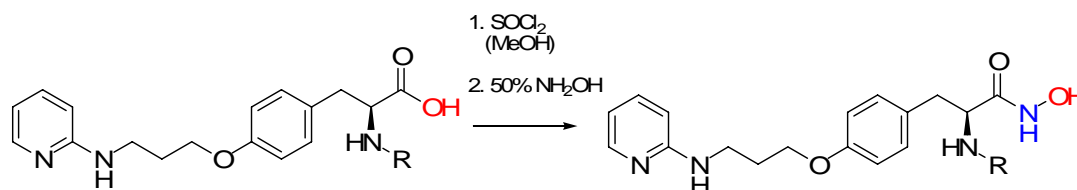
Scheme 21: *Conversion of a carboxylic into a hydroxamic acid.*

To enable further **studies of interversicle cross-linking**, a **lipopeptide** based on the sequence *cyclo*(-G-R-G-D-f-K-) was synthesized which binds towards the $\alpha IIb\beta3$ integrin receptor. Studies on coating and/or insertion into artificial membranes are currently in progress in the group of Prof. M. Tanaka at the University of Heidelberg.

In another project, a Cilengitide based peptide was used to enable **selective internalization of virus like particles (VLPs) into cancer cell lines**. For this purpose the peptide was derivatized with a PEG-spacer and an alkyne functionality so that the ligand could be attached towards the surface of the VLP via click-reaction. First biological data suggest that the goal of selective internalization might have been reached.

In the last project, a selective $\alpha5\beta1$ **integrin ligand** was transformed to be applied **for coating** of gold and titanium surfaces via a thiol anchor functionality. Biological evaluation of this compound is still in progress.

271
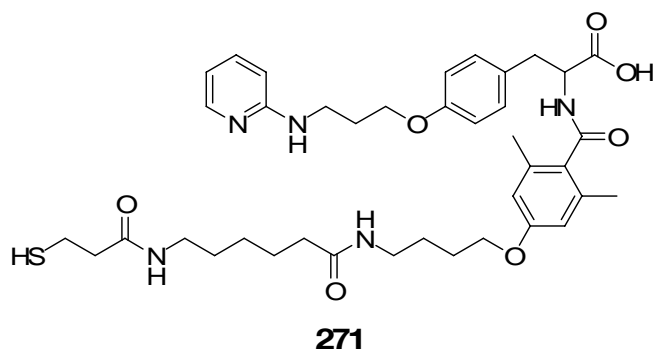
Figure 69: *The integrin ligand 271 for surface coating.*

IV Experimental Section

Wenn Sie keine Zeit mehr dazu finden,

ein Buch zu lesen oder in die Oper zu gehen,

dann arbeiten Sie zuviel!

Prof. Dr. Horst Kessler (Technische Universität München)

IV.1 Materials and Methods

Mass spectra were obtained by *electrospray ionization* (ESI) *electron impact ionization* (EI).

HPLC-ESI-MS spectra were recorded on a *Finnigan LCQ* combined with an HPLC system *Hewlett Packard HP1100* (column material Nucleosil 100 5C$_{18}$).

HPLC-purifications were performed on following systems:

(A)   *Pharmacia Basic 10 F*, pump unit P-900, Detector UV-900, autosampler A 900, Software: Unicorn, Version 3.00; column material: YMC-ODS-A 120 5-C$_{18}$ (1 µm, 250 x 4.6 mm), analytical.

(B)   *Pharmacia Basic 100 F*, pump unit P-900, Detector UV-900, Software: Unicorn, Version 3.00; column material: (1) YMC-ODS-A 120 10-C$_{18}$ (10 µm, 250 x 20 mm) semipreparative; (2) YMC-ODS 120 11-C$_{18}$ (11 µm, 250 x 30 mm), preparative.

TLC – monitoring was performed on Merck DC silica gel plates (60 F-254 on aluminum foil). Spots were detected by UV-absorption at 254 nm and/or by staining with a 5 % solution of ninhydrine in ethanol or Mo-stain (6.25 g phosphormolybdaic acid, 2.5 g cerium-(IV)-sulfate and 15 mL sulfuric acid in 235 mL water) or potassium permanganate (5% in 1N aq. NaOH).

All technical solvents were distilled prior to use or purchased as anhydrous solvents. Reagents were purchased *per synthesis* from *E. Merck, Fluka*, *Sigma*, *Aldrich, Acros or Lancaster* and were used without purifications. Trt-polystyrene resin was purchased from *PepChem* (Tübingen). Protected and unprotected amino acids – if not synthesized -, HOBt and Fmoc-Cl were purchased from *Alexis*, *Advanced Chemtech*, *Bachem*, *Neosystem*, *Novabiochem* or *Iris*. NMP for solid phase synthesis was a kind gift from *BASF*, Ludwigshafen.

Flash column chromatography was performed using silica gel 60 (63-200 µm) from *Merck* at 1-1.5 atm pressure.

Air / water-sensitive reactions were performed in flame-dried flasks under an atmosphere of argon (99.996%).

Solid phase peptide synthesis and other reactions on solid phase with less than 1 g resin were performed in syringes (*Becton-Dickinson*) equipped with a polypropylene frit (*Vetter Labortechnik*). The loaded syringes were stuck into a rubber stopper connected to the rotor of a rotary evaporator and mixed by gentle rotation.

¹H-NMR and **¹³C-NMR** spectra were recorded at 300 K on a 900 MHz Bruker Avance, 500 MHz Bruker DMX, 500 MHz Bruker AV, 360 MHz Bruker AV or a 250 MHz Bruker AC spectrometer (Bruker, Karlsruhe, Germany). Chemical shifts (δ) are given in *parts per million* (ppm) relative to trimethylsilane (TMS). Following solvent peaks were used as internal standards: DMSO-d_5: 2.50 ppm (¹H-NMR) und 39.46 ppm (¹³C-NMR); CHCl$_3$: 7.26 ppm (¹H-NMR) and 77.0 ppm (¹³C-NMR). Processing was performed using XWINNMR or TOPSPIN (Bruker) and analyzed with either XWINNMR, TOPSPIN, or SPARKY[347]. The assignment of proton and carbon resonances followed a strategy described in literature[348]. Sequential assignment was accomplished by through-bond connectivities from heteronuclear multiple bond correlation (HMBC)[349] spectra whereas *N*-methyl groups served as starting point. Connectivities were proved by interresidual scalar couplings, e.g between carbonyl carbons and adjacent amide protons. TOCSY spectra were recorded with a mixing time of 60 ms, ROESY spectra with a mixing time of 150 ms, thus avoiding unwanted effects caused by spin diffusion. Several compounds show more than one conformation that are in slow exchange at the NMR time scale. Conformational exchange was proven by detection of inverted signal signs in ROESY spectra[350]. Evidence of *cis* peptide bonds in proline containing peptides was achieved using carbon shifts in DEPT45 spectra[351]. The ratio of different conformational populations was determined via the integrals of amide and H$^\alpha$-signals in ¹H-1D spectra.

Computational methods: Proton distances were calculated according to the isolated two-spin approximation from volume integrals of ROESY spectra[352]. No ROE offset correction was performed since biasing offset effects at the field strength used in this study are rather small. The integrated volumes of ROE cross peaks were converted to proton–proton distances by the help of calibration to an averaged alanine Hα–Hβ^* distance as reference (2.45 Å for alanine; including pseudo-atom correction). Upper and lower distance restraints were obtained by adding and subtracting 10% to the calculated experimental values, thus accounting for experimental errors and simulation uncertainties. Metric matrix DG calculations were carried out with a (slightly modified version of a) distance geometry program utilizing random metrization[353]. Experimental

distance restraints which are more restrictive than the geometric distance bounds (holonomic restraints) were used to create the final distance matrix. All structure templates were first embedded in four dimensions and then partially minimized using conjugate gradient minimization followed by distance-driven dynamics (DDD)[354] wherein only distance constraints were used. The DDD simulation was carried out at 1000 K for 50 ps with a gradual reduction in temperature over the next 30 ps. The DDD procedure utilized holonomic and experimental distance constraints plus a chiral penalty function for the generation of violation energies and forces. A distance matrix was calculated from each structure, and the EMBED algorithm was used to compute Cartesian coordinates in three dimensions. 100 structures were calculated for each peptide, and > 90% of the structure bundle of each peptide did not show any significant violations (> 0.2 Å). Molecular Dynamics calculations were carried out with the program DISCOVER using the CVFF force field[355]. Structures resulting from DG calculations were placed in a cubic box with a vector length of 3.0 nm and soaked with DMSO. Intramolecular distances of the peptides were kept constant according to the experimental values. After energy minimization using steepest descent and conjugate gradient algorithms, the system was gradually heated in 50 K steps (equilibration time at each temperature was 2 ps) starting from 10 K, each by direct scaling of velocities. The system was equilibrated for 50 ps with temperature bath coupling (300 K). Configurations in the subsequent production runs (150 ps) were saved every 100 fs. Finally, 150 ps free MD simulations at 300 K were carried out in order to prove that no significant structural changes occur when no distance restraints are present during the simulation.

IV.2 General Procedures

IV.2.1 GP1 (Loading of TCP resin)

Chloro-TCP-resin (theoretical loading 1.04 mmol/g) was filled into a suitable syringe (20 mL for 1 g resin) equipped with a PP-frit and a canula. The amino acid (1.2 mmol, referring to theoretical loading) was dissolved in dry DCM (8 mL/g resin), treated with DIPEA (2.5 eq., referring to amino acid) and sucked directly into the syringe with the resin and mixed by gentle rotation for 1 h. The resin was capped by adding 0.2 mL methanol (per gram resin) and 0.2 eq. DIPEA to the reaction mixture and shaken for 15 min. The loaded resin was washed with DCM (3x), NMP (3x), NMP / methanol 1 : 1 (1x) and pure methanol (3x).

IV.2.2 GP2 (Solid phase Fmoc deprotection)

The washed and swollen resin was treated twice with a solution of piperidine (20%) in NMP (v/v), 15 min and 10 min, respectively and washed 3 times with NMP.

IV.2.3 GP3 (Solid phase peptide coupling with HOBt/TBTU)

The amino acid, HOBt and TBTU (each 2.5 eq. referring to resin loading) were dissolved in NMP (8mL/g resin). After addition of DIPEA (6.5 eq., 1.3 eq. per acid), the solution was mixed with the resin and shaken for 1 h. The mixture was discarded and the resin washed 3 times with NMP.

IV.2.4 GP4 (Solid phase peptide coupling with HOAt/HATU)

The amino acid (2 eq. referring to resin loading), HOAt (2 eq.) and HATU (2 eq.) were dissolved in NMP. After addition of DIPEA (5.2 eq., 1.3 eq. per acid), the solution was mixed with the resin and shaken for 1 h. The mixture was discarded and the resin washed 3 times with NMP.

IV.2.5 GP5 (*N*-methylation of amino acids on solid phase)

A solution of *o*-NBS-Cl (4 eq.) and collidine (10 eq.) in NMP was added to the resin-bound free amine peptides and shaken for 15 min at room temperature. The solution was discarded and the resin washed 3 times with NMP followed by dry THF (3x). A solution of triphenylphosphine (5 eq.) and methanol in THF was added to the resin and shaken for 1 min. A solution of DIAD (5 eq.) in THF was added in portions to the reaction mixture and shaken for 10 min. The resin was filtered and washed with THF (3x) and NMP (5x). For *o*-NBS deprotection, the resin was shaken for 5 min with a solution of mercaptoethanol (10 eq.) and DBU (5 eq.) in NMP. The deprotection procedure was repeated once more and the resin washed 3 times with NMP.

IV.2.6 GP6 (Cleavage of side-chain-protected peptides from TCP-resin)

The resin was swollen in DCM and then treated with a solution of 20% HFIP in DCM. After shaking for 20 min, the procedure was repeated twice and the resin finally washed with DCM. The collected solutions were concentrated *in vacuo*.

IV.2.7 GP7 (backbone cyclization of peptides using DPPA)

The linear, side-chain protected peptide was diluted with DMF to 10^{-3} - 10^{-4} M. After addition of DPPA (3 eq.) and $NaHCO_3$ (5 eq.), the mixture was stirred until all starting material was consumed (HPLC / LC-MS monitoring), usually 12 h. The solution was concentrated under reduced pressure and the cyclic peptide precipitated by addition of water. In case of an improper precipitation, water was substituted with brine. The peptide was spun down in a centrifuge, washed twice with water and dried under vacuum.

For peptides mainly containing alanine in their sequence, a precipitation is not possible and the concentrate was directly taken up in acetonitrile for HPLC purification.

IV.2.8 GP8 (backbone cyclization of peptides using PyBOP)

The linear, side-chain protected peptide was diluted with DMF to 10^{-3} - 10^{-4} M. After addition of PyBOP (2 eq.) and Collidin (5 eq.), the mixture was stirred until all starting material was consumed (HPLC / LC-MS monitoring), usually 12 h. The solution was concentrated under reduced pressure and the cyclic peptide precipitated by addition of water. In case of an improper precipitation, water was substituted with brine. The peptide was spun down in a centrifuge, washed twice with water and dried under vacuum.

IV.2.9 GP9 (backbone cyclization of peptides using HATU/HOBt)

The linear, side-chain protected peptide was diluted with DMF to 10^{-3} - 10^{-4} M. After addition of HATU (2 eq.), HOBt (2 eq.) and DIPEA (10 eq.), the mixture was stirred until all starting material was consumed (HPLC / LC-MS monitoring), usually 12 h. The solution was concentrated under reduced pressure and the cyclic peptide precipitated by addition of water. In case of an improper precipitation, water was substituted with brine. The peptide was spun down in a centrifuge, washed twice with water and dried under vacuum.

IV.2.10   GP10 (Peptide cyclization by disulfide formation)

The linear, deprotected peptide was dissolved in water / DMSO (10^{-3} M). The pH was adjusted to 8 - 8.5 by addition of $NaHCO_3$. The solution was stirred for 12 h. The solvent was evaporated and the resulting peptide purified by *reverse phase* HPLC.

IV.2.11   GP11 (*N*-Alloc deprotection on solid phase)

The dry resin was swollen with dry DCM for 10 min. The resin was then treated with a solution of *tetrakis*-triphenylphosphinepalladium (0.25 eq.) and phenylsilane (10 eq.) in dry DCM at ambient temperature. Care had to be taken due to gas evolution and the pressure had to be released from the reaction vessel from time to time. After 1.5 h of shaking, the mixture was filtered and the resin washed twice with a 0.5% solution of DDTC (sodium *N,N*-diethyldithiocarbamate) in DMF and a 0.5% solution of DIEA in DMF. The washing procedure was repeated and the resin washed five times with NMP.

IV.2.12   GP12 (Synthesis of Fmoc-NMe-alanine in solution)[44]

To a solution of 1.56g Fmoc-alanine in 100 mL toluene 1g of paraformaldehyde and 0.1g of *p*-toluene sulfonic acid were added and the mixture stirred for 30 min under reflux. The solution washed with a saturated $NaHCO_3$ solution (2x) and concentrated *in vacuo*. The resulting residue was taken up in 23 mL $CHCL_3$, 23 mL TFA and 2.3 mL triethylsilane. The mixture was stirred for 12h and the solvent removed under reduced pressure. Precipitation in ether/hexane yields the pure product.

IV.2.13 GP13 (Formation of *aza*-glycines)[313]

The amino-functionalized, dry resin was swollen with dry DCM for 5 min. The freshly prepared, dry building block **216** was dissolved in dry DCM, mixed with the resin and shaken for 90 minutes. The resin was washed with DCM (5x).

IV.2.14 GP14 (Guanidinylation)

The amino-functionalized resin was added to a solution of 10 eq. *N,N'*-bis-Boc-guanidinylpyrazole in dry DCM (10 mL / g resin) in a closed reaction vessel. The mixture was shaken over night at room temperature. The resin was filtered and washed five times with DCM. The unconsumed guanidinylpyrazole could be recycled by concentration of the filtrate and recrystallization from hexane / ethyl acetate.

IV.2.15 GP15 (Cleavage from TCP-resin and Boc-deprotection)

The resin was swollen in DCM and then treated 3 times with a mixture of DCM, TFA, water and triisopropylsilane (47.5%, 47.5%, 2.5%, 2.5%, v/v/v/v) for 30 min. The combined solutions were monitored by ESI-MS until full Boc-deprotection was observed. The solvents were evaporated under reduced pressure and the crude product directly subjected to HPLC-purification on *reverse-phase* silica gel.

IV.2.16 GP16 (Reductive cleavage of benzyl protecting groups)

The starting material (1 eq.) was dissolved in methanol. After addition of the catalyst (5 % Pd/C, 15 mg/mmol starting material), the mixture was hydrogenated (1 atm H_2) at ambient temperature. The progress of the reaction was monitored by TLC until all starting material was consumed. The catalyst was removed by filtration over Celite®, the solvent was removed and the residue purified by flash chromatography on silica gel.

IV.3 *N*-Methylated Cyclic Hexapeptides as Template Structures for Spatial Screening and Oral Bioavailability

IV.3.1 Synthesis of the *N*-Methylated Cyclic Hexapeptides

All peptides were synthesized according to general procedures GP1-4, GP6, GP7and GP12. All compounds were purified by *reversed phase* HPLC. Compounds, synthesized by Dr. Jayanta Chatterjee are written in italics. Compounds, synthesized by the author are marked in bold.

sequence	no.	Mass calc.	obsd. $(M+H^+)^+$ or $(M+Na^+)^+$	R_t (min) (10-100%)
cyclo(-Mea-A-A-A-A-A-)	**1**	440.2	441.2	6.94
cyclo(-a-MeA-A-A-A-A-)	**2**	440.2	441.0	7.84
cyclo(-a-A-MeA-A-A-A-)	**3**	440.2	441.0	7.48
cyclo(-a-A-A-MeA-A-A-)	**4**	440.2	441.4	6.93
cyclo(-a-A-A-A-MeA-A-)	**5**	440.2	441.2	7.29
cyclo(-a-A-A-A-A-MeA-)	**6**	440.2	441.0	6.88
cyclo(-Mea-MeA-A-A-A-A-)	**7**	454.3	455.6	8.95
cyclo(-Mea-A-MeA-A-A-A-)	**8**	454.3	455.5	8.04
cyclo(-Mea-A-A-MeA-A-A-)	**9**	454.3	455.5	7.98
cyclo(-Mea-A-A-A-MeA-A-)	**10**	454.3	455.3	8.24
cyclo(-Mea-A-A-A-A-MeA-)	**11**	454.3	455.4	7.64
cyclo(-a-MeA-MeA-A-A-A-)	**12**	454.3	455.5	7.67
cyclo(-a-MeA-A-MeA-A-A-)	**13**	454.3	455.3	9.23
cyclo(-a-MeA-A-A-MeA-A-)	**14**	454.3	455.5	9.02
cyclo(-a-MeA-A-A-A-MeA-)	**15**	454.3	455.3	8.05
cyclo(-a-A-MeA-MeA-A-A-)	**16**	454.3	477.5	8.16
cyclo(-a-A-MeA-A-MeA-A-)	**17**	454.3	455.3	8.53
cyclo(-a-A-MeA-A-A-MeA-)	**18**	454.3	455.6	7.92
cyclo(-a-A-A-MeA-MeA-A-)	**19**	454.3	477.2	8.54
cyclo(-a-A-A-MeA-A-MeA-)	**20**	454.3	477.5	8.47
cyclo(-a-A-A-A-MeA-MeA-)	**21**	454.3	455.5	7.88
cyclo(-Mea-MeA-MeA-A-A-A-)	**22**	468.3	491.3	8.94
cyclo(-Mea-MeA-A-MeA-A-A-)	**23**	468.3	469.5	9.38
cyclo(-Mea-MeA-A-A-MeA-A-)	**24**	468.3	469.6	9.76

cyclo(-Mea-MeA-A-A-A-MeA-)	**25**	468.3	469.3	7.96
cyclo(-Mea-A-MeA-MeA-A-A-)	**26**	468.3	469.4	9.06
cyclo(-Mea-A-MeA-A-A-MeA-)	**27**	468.3	469.3	9.83
cyclo(-Mea-A-A-MeA-MeA-A-)	**28**	468.3	469.2	9.06
cyclo(-Mea-A-A-MeA-A-MeA-)	**29**	468.3	491.5	8.29
cyclo(-Mea-A-A-A-MeA-MeA-)	**30**		not possible	
cyclo(-a-MeA-MeA-MeA-A-A-)	**31**	468.3	469.5	9.03
cyclo(-a-MeA-MeA-A-MeA-A-)	**32**	468.3	469.5	8.97
cyclo(-a-MeA-MeA-A-A-MeA-)	**33**	468.3	469.2	9.39
cyclo(-a-MeA-A-MeA-MeA-A-)	**34**	468.3	469.4	10.13
cyclo(-a-MeA-A-MeA-A-MeA-)	**35**		not possible	
cyclo(-a-MeA-A-A-MeA-MeA-)	**36**		not possible	
cyclo(-a-A-MeA-MeA-MeA-A-)	**37**	468.3	469.3	8.99
cyclo(-a-A-MeA-MeA-A-MeA-)	**38**	468.3	491.4	9.16
cyclo(-a-A-MeA-A-MeA-MeA-)	**39**		not possible	
cyclo(-a-A-A-MeA-MeA-MeA-)	**40**		not possible	
cyclo(-Mea-MeA-MeA-MeA-A-A-)	**41**	482.3	505.5	9.87
cyclo(-Mea-MeA-MeA-A-MeA-A-)	**42**	482.3	505.5	18.47*
cyclo(-Mea-MeA-MeA-A-A-MeA-)	**43**	482.3	505.4	13.95*
cyclo(-Mea-MeA-A-MeA-MeA-A-)	**44**	482.3	483.1	14.48*
cyclo(-Mea-MeA-A-MeA-A-MeA-)	**45**	482.3	483.2	11.2**
cyclo(-Mea-A-A-MeA-MeA-MeA-)	**46**	482.3	483.4	16.1*
cyclo(-Mea-A-MeA-MeA-MeA-A-)	**47**	482.3	505.5	9.64
cyclo(-Mea-A-MeA-MeA-A-MeA-)	**48**	482.3	483.2	16.32*
cyclo(-Mea-A-A-MeA-MeA-MeA-)	**49**	482.3	505.3	9.37
cyclo(-a-MeA-MeA-MeA-MeA-A-)	**50**		not possible	
cyclo(-a-MeA-MeA-MeA-A-MeA-)	**51**	482.3	483.4	11.48**
cyclo(-a-MeA-A-MeA-MeA-MeA-)	**52**	482.3	505.5	9.38
cyclo(-a-A-MeA-MeA-MeA-MeA-)	**53**	482.3	483.4	18.48*
cyclo(-a-MeA-MeA-A-MeA-MeA-)	**54**	482.3	483.3	19.96*
cyclo(-Mea-A-MeA-A-MeA-MeA-)	**55**	482.3	483.3	13.37**
cyclo(-a-MeA-MeA-MeA-MeA-MeA-)	**56**	496.3	497.2	11.53
cyclo(-Mea-A-MeA-MeA-MeA-MeA-)	**57**	496.3	497.3	12.01
cyclo(-Mea-MeA-A-MeA-MeA-MeA-)	**58**	496.3	497.2	11.72
cyclo(-Mea-MeA-MeA-A-MeA-MeA-)	**59**	496.3	497.2	12.42
cyclo(-Mea-MeA-MeA-MeA-MeA-A-)	**60**	496.3	497.3	23.01*

*(10-30% ACN)

**(10-50% ACN)

IV.3.2 Evaluation of Bioavailability via CaCo-2
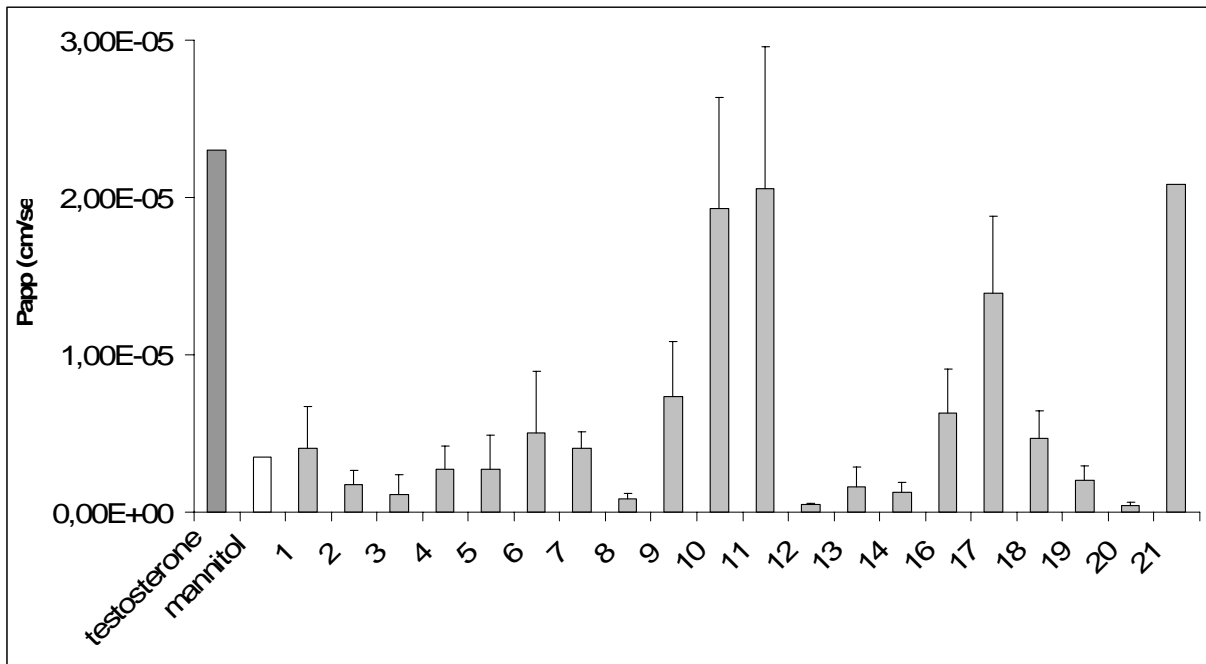
Figure 70: *Permeability in CaCo2 for the mono- and di-N-methylated cyclic hexapeptides in comparison to testosterone and mannitol.*
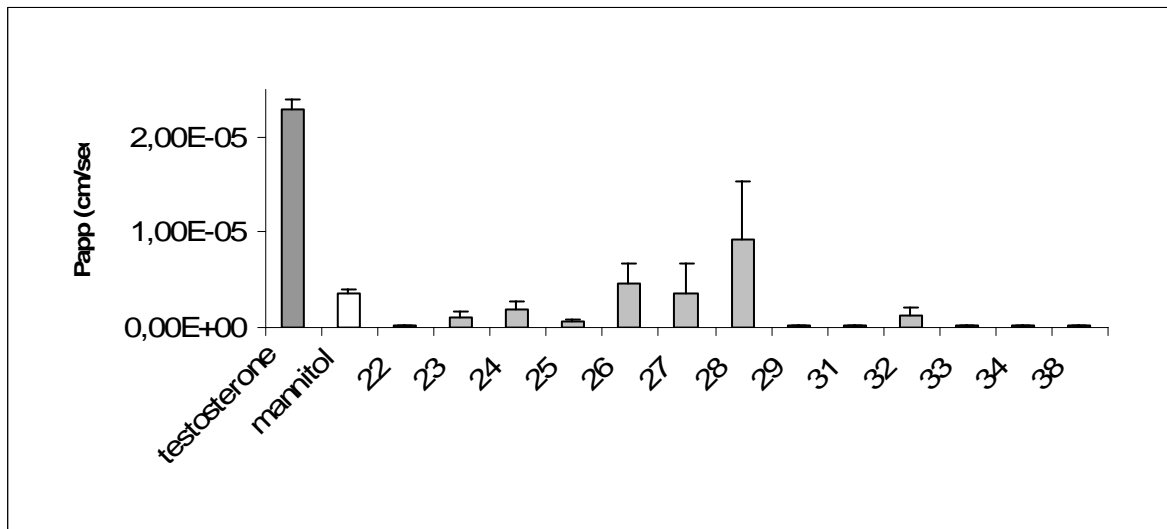
Figure 71: *Permeability in CaCo2 for the so far tested tri-N-methylated cyclic hexapeptides in comparison to testosterone and mannitol.*
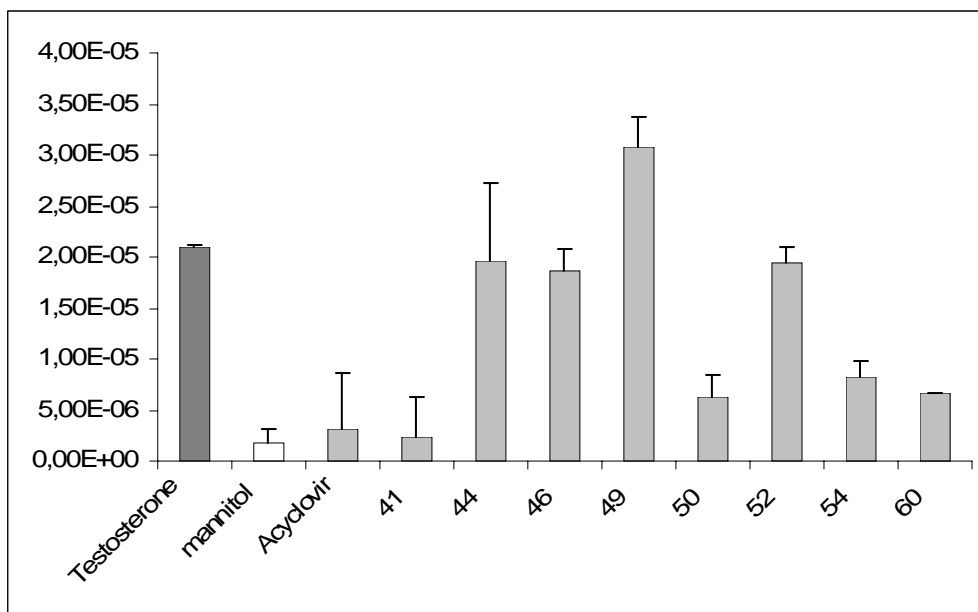
Figure 72: *Permeability in CaCo2 for the so far tested tetra- and penta-N-methylated cyclic hexapeptides in comparison to testosterone and mannitol.*

IV.4 *N-Methylated Amino Acids as Substitutes for Proline in Cyclic Pentapeptides*

All peptides were synthesized according to general procedures GP1-7, GP9 and GP12. All compounds were purified by *reversed phase* HPLC.

IV.4.1 Analytical Data

sequence	no.	Mass		R_t (min)
		calc.	obsd. (M+H$^+$)$^+$ or (M+Na$^+$)$^+$	(10-90%)
cyclo(-p-A-A-A-A-)	**61**	381.2	404.2	14.3
cyclo(-a-P-A-A-A-)	**62**	381.2	382.2	8.66
cyclo(-a-A-P-A-A-)	**63**	381.2	382.4	8.10
cyclo(-a-A-A-P-A-)	**64**	381.2	382.2	7.85
cyclo(-a-A-A-A-P-)	**65**	381.2	404.1	7.86
cyclo(-Mek-A-A-A-A-)	**66**	426.3	427.3	5.86
cyclo(-p-A-A-P-A-)	**67**	407.2	408.3	8.98
cyclo(-a-P-A-P-A-)	**68**	407.2	408.2	8.73
cyclo(-a-A-P-P-A-)	**69**	407.2	408.2	10.76
cyclo(-a-A-A-P-P-)	**70**	407.2	408.2	6.52
cyclo(-Mea-A-A-P-A-)	**71**	395.2	396.2	8.95
cyclo(-a-MeA-A-P-A-)	**72**	395.2	396.3	11.12
cyclo(-a-A-MeA-P-A-)	**73**	395.2	396.3	9.86
cyclo(-a-A-A-P-MeA-)	**74**	395.2	396.3	7.15
cyclo(-p-A-A-MeA-A-)	**75**	395.2	396.5	9.35
cyclo(-a-P-A-MeA-A-)	**76**	395.2	396.3	11.58
cyclo(-a-A-P-MeA-A-)	**77**	395.2	396.2	8.90
cyclo(-a-A-A-MeA-P-)	**78**	395.2	396.3	7.67

All *N*-methylated all-alanine peptides were synthesized by Dr. Jayanta Chatterjee. Spectroscopical data for these compounds can be found in:

J. Am. Chem. Soc. **2006**, *128*, 47, 15164-15172.

Chem. Europ. J. **2008**, *14*, 5, 1508-1517.

IV.4.2 Structure Calculation

Restraints and violations for *cyclo*(-a-P-A-A-A-) **62**:

Proton 1	Proton 2	Low Å	Upp Å	Calc Å	Viol.
1:ALA_1:CB	1:ALA_1:HN	2.020	2.870	2.733	0.000
1:ALA_1:CB	1:PRO_2:CD	2.410	3.840	4.342	0.490
1:ALA_1:HN	1:ALA_5:HN	2.060	2.520	3.813	1.240
1:PRO_2:HA	1:PRO_2:CD	2.580	3.670	3.180	0.000
1:PRO_2:HA	1:PRO_2:CG	2.030	2.820	3.103	0.254
1:PRO_2:CD	1:PRO_2:CG	1.670	3.780	1.528	-0.144
1:ALA_3:CB	1:ALA_3:HN	2.230	3.120	2.906	0.000
1:ALA_3:HN	1:ALA_5:HN	2.030	2.480	3.827	1.226
1:ALA_4:HA	1:ALA_4:CB	1.970	2.810	2.135	0.000
1:ALA_4:HA	1:ALA_4:HN	1.910	2.330	3.058	0.726
1:ALA_4:HA	1:ALA_5:HN	1.970	2.410	3.581	1.166
1:ALA_4:HN	1:ALA_5:HN	1.780	2.170	2.494	0.261
1:ALA_5:CB	1:ALA_5:HN	2.260	3.160	2.871	0.000
1:ALA_1:HA	1:PRO_2:CD	1.610	2.450	2.656	0.199
1:ALA_1:HN	1:ALA_3:HN	2.520	3.390	4.731	1.235
1:ALA_1:HN	1:ALA_5:HA	1.780	2.180	2.289	0.084
1:ALA_3:HA	1:ALA_3:CB	2.080	2.940	2.138	0.000
1:ALA_3:HA	1:ALA_4:HN	2.050	2.510	3.585	1.070
1:ALA_5:HA	1:ALA_5:CB	2.030	2.880	2.143	0.000
1:PRO_2:HA	1:ALA_3:HN	2.380	2.910	3.559	0.643
1:ALA_3:HA	1:ALA_3:HN	2.290	2.800	3.064	0.262
1:ALA_1:CB	1:ALA_1:HA	2.300	3.210	2.125	-0.179
1:PRO_2:HD1	1:PRO_2:CG	1.850	3.060	2.172	0.000
1:PRO_2:HD1	1:PRO_2:HD2	1.320	1.610	1.785	0.171
1:ALA_3:HN	1:PRO_2:HB1	2.500	3.060	2.944	0.000
1:ALA_4:HN	1:ALA_3:CB	1.920	2.750	2.908	0.132
1:ALA_4:HN	1:ALA_4:CB	2.070	2.930	2.785	0.000
1:PRO_2:HA	1:PRO_2:HB2	1.700	2.080	2.341	0.251
1:PRO_2:HA	1:PRO_2:HB1	2.220	2.710	2.920	0.192

Restraints and violations for *cyclo*(-a-A-A-P-P-) **70**:

Proton 1	Proton 2	Low Å	Upp Å	Calc Å	Viol.
1:ALA_1:HN	1:PRO_4:HA	3.360	4.100	3.126	-0.234
1:ALA_2:HN	1:ALA_1:HA	1.960	2.400	2.200	0.000
1:ALA_2:HN	1:ALA_2:HA	2.750	3.360	2.998	0.000
1:ALA_3:HN	1:ALA_2:HA	3.120	3.810	3.545	0.000
1:ALA_2:HN	1:ALA_3:HN	2.340	2.860	2.668	0.000
1:ALA_3:HN	1:ALA_3:HA	2.560	3.120	3.019	0.000
1:PRO_4:HA	1:PRO_4:HD2	3.620	5.330	3.950	0.000
1:ALA_1:HN	1:PRO_5:HA	2.050	2.510	2.300	0.000
1:PRO_5:HA	1:PRO_5:HD2	3.490	5.170	4.090	0.000
1:ALA_1:HN	1:PRO_5:HB1	2.750	4.270	2.721	-0.029
1:ALA_1:HN	1:PRO_5:HB2	2.880	4.420	3.557	0.000
1:ALA_1:HN	1:ALA_1:CB	2.420	3.460	2.705	0.000
1:ALA_1:HA	1:ALA_1:CB	2.180	3.160	2.138	-0.042
1:ALA_2:HN	1:ALA_2:CB	2.330	3.350	2.647	0.000
1:ALA_2:HA	1:ALA_2:CB	2.220	3.210	2.134	-0.086
1:ALA_3:HN	1:ALA_2:CB	3.260	4.490	2.940	-0.320
1:ALA_3:HN	1:ALA_3:CB	2.390	2.870	2.827	0.000
1:ALA_3:CB	1:ALA_3:HA	2.230	3.230	2.124	-0.106
1:ALA_3:CB	1:PRO_5:HA	4.100	5.910	6.281	0.371
1:PRO_5:HD1	1:ALA_3:CB	3.550	6.240	8.035	1.795

IV.5 *The Side-Chain Impact on N-Methylated Cyclic Pentapeptides*

All peptides were synthesized according to general procedures GP1-7, GP9 and GP12. All compounds were purified by *reversed phase* HPLC.

IV.5.1 Analytical Data

sequence	no.	Mass		R_t (min)
		calc.	obsd. $(M+H^+)^+$ or $(M+Na^+)^+$	(10-90%)
cyclo(-t-A-A-MeA-A-)	**79**	399.2	400.1	6.95
cyclo(-a-T-A-MeA-A-)	**80**	399.2	400.2	7.38
cyclo(-a-A-T-MeA-A-)	**81**	399.2	400.1	7.56
cyclo(-a-A-A-MeT-A-)	**82**	399.2	400.2	7.03
cyclo(-a-A-A-MeA-T-)	**83**	399.2	400.1	6.97
cyclo(-v-A-A-MeA-A-)	**84**	397.2	398.5	10.17
cyclo(-a-V-A-MeA-A-)	**85**	397.2	398.4	10.37
cyclo(-a-A-V-MeA-A-)	**86**	397.2	420.3	10.76
cyclo(-a-A-A-MeV-A-)	**87**	397.2	398.4	11.66
cyclo(-a-A-A-MeA-V-)	**88**	397.2	398.2	11.15
cyclo(-i-A-A-MeA-A-)	**89**	411.3	412.5	13.11
cyclo(-a-I-A-MeA-A-)	**90**	411.3	412.5	12.11
cyclo(-a-A-I-MeA-A-)	**91**	411.3	412.4	12.47
cyclo(-a-A-A-MeI-A-)	**92**	411.3	412.6	14.03
cyclo(-a-A-A-MeA-I-)	**93**	411.3	434.3	13.00
cyclo(-l-A-A-MeA-A-)	**94**	411.3	412.5	12.52
cyclo(-a-L-A-MeA-A-)	**95**	411.3	412.6	12.51
cyclo(-a-A-L-MeA-A-)	**96**	411.3	412.5	13.12
cyclo(-a-A-A-MeL-A-)	**97**	411.3	412.6	13.65
cyclo(-a-A-A-MeA-L-)	**98**	411.3	412.6	13.44
cyclo(-s-A-A-MeA-A-)	**99**	385.2	386.2	12.24
cyclo(-a-S-A-MeA-A-)	**100**	385.2	386.4	13.62
cyclo(-a-A-S-MeA-A-)	**101**	385.2	386.1	12.74
cyclo(-a-A-A-MeS-A-)	**102**	385.2	386.4	13.75
cyclo(-a-A-A-MeA-S-)	**103**	385.2	386.3	11.32

cyclo(-n-A-A-MeA-A-)	**104**	412.2	413.1	10.04
cyclo(-a-N-A-MeA-A-)	**105**	412.2	413.2	11.03
cyclo(-a-A-N-MeA-A-)	**106**	412.2	413.0	10.04
cyclo(-a-A-A-MeN-A-)	**107**	412.2	435.2	10.16
cyclo(-a-A-A-MeA-N-)	**108**	412.2	413.1	10.40
cyclo(-d-A-A-MeA-A-)	**109**	413.2	414.1	7.04
cyclo(-a-D-A-MeA-A-)	**110**	413.2	414.2	7.30
cyclo(-a-A-D-MeA-A-)	**111**	413.2	414.4	6.98
cyclo(-a-A-A-MeD-A-)	**112**	413.2	414.1	6.94
cyclo(-a-A-A-MeA-D-)	**113**	413.2	414.5	7.05
cyclo(-f-A-A-MeA-A-)	**114**	445.2	446.5	17.26
cyclo(-a-F-A-MeA-A-)	**115**	445.2	446.4	17.11
cyclo(-a-A-F-MeA-A-)	**116**	445.2	446.5	13.68
cyclo(-a-A-A-MeF-A-)	**117**	445.2	446.5	14.46
cyclo(-a-A-A-MeA-F-)	**118**	445.2	446.4	14.27
cyclo(-w-A-A-MeA-A-)	**119**	484.2	507.2	15.15
cyclo(-a-W-A-MeA-A-)	**120**	484.2	485.1	14.99
cyclo(-a-A-W-MeA-A-)	**121**	484.2	485.1	14.87
cyclo(-a-A-A-MeW-A-)	**122**	484.2	485.0	15.02
cyclo(-a-A-A-MeA-W-)	**123**	484.2	485.1	14.62

IV.6 N-Methyl Scan and Ring Enlargement of CXCR4-Binding Peptides

IV.6.1 Ring enlargement of FC131 towards a cyclic hexapeptide and *N*-methylscan thereof

All peptides were synthesized according to general procedures GP1-6, GP8, GP9 and GP12. All compounds were purified by *reversed phase* HPLC.

sequence	no.	Mass calc.	Mass obsd. (M+H$^+$)$^+$ or (M+Na$^+$)$^+$	R$_t$ (min) (10-90%)
cyclo(-Mey-R-R-Nal-A-G-)	**124**	814.4	815.8	14.48
cyclo(-y-MeR-R-Nal-A-G-)	**125**	814.4	815.7	15.43
cyclo(-y-R-MeR-Nal-A-G-)	**126**	814.4	815.7	15.37
cyclo(-y-R-R-MeNal-A-G-)	**127**	814.4	815.7	14.88
cyclo(-y-R-R-Nal-MeA-G-)	**128**	814.4	815.8	14.60
cyclo(-y-R-R-Nal-A-MeG-)	**129**	814.4	815.6	17.25
cyclo(-Mey-MeR-R-Nal-A-G-)	**130**	828.4	829.7	14.79
cyclo(-Mey-R-MeR-Nal-A-G-)	**131**	828.4	829.9	15.32
cyclo(-Mey-R-R-MeNal-A-G-)	**132**	828.4	829.8	13.92
cyclo(-Mey-R-R-Nal-MeA-G-)	**133**	828.4	829.7	16.05
cyclo(-Mey-R-R-Nal-A-MeG-)	**134**	828.4	829.7	14.99
cyclo(-y-MeR-MeR-Nal-A-G-)	**135**	828.4	829.8	14.83
cyclo(-y-MeR-R-MeNal-A-G-)	**136**	828.4	829.9	15.35
cyclo(-y-MeR-R-Nal-MeA-G-)	**137**	828.4	829.8	15.87
cyclo(-y-MeR-R-Nal-A-MeG-)	**138**	828.4	829.8	15.38
cyclo(-y-R-MeR-MeNal-A-G-)	**139**	828.4	829.7	14.25
cyclo(-y-R-MeR-Nal-MeA-G-)	**140**	828.4	829.6	14.39
cyclo(-y-R-MeR-Nal-A-MeG-)	**141**	828.4	829.8	13.97
cyclo(-y-R-R-MeNal-MeA-G-)	**142**	828.4	829.7	15.43
cyclo(-y-R-R-MeNal-A-MeG-)	**143**	828.4	829.7	14.00
cyclo(-y-R-R-Nal-MeA-MeG-)	**144**	828.4	829.7	15.13
cyclo(-Mey-MeR-MeR-Nal-A-G-)	**145**	842.3	843.8	16.01
cyclo(-Mey-MeR-R-MeNal-A-G-)	**146**	842.3	843.7	15.82
cyclo(-Mey-MeR-R-Nal-MeA-G-)	**147**	842.3	843.7	15.80

cyclo(-Mey-MeR-R-Nal-A-MeG-)	**148**	842.3	843.6	16.20
cyclo(-Mey-R-MeR-MeNal-A-G-)	**149**	842.3	843.7	16.74
cyclo(-Mey-R-MeR-Nal-MeA-G-)	**150**	842.3	843.7	16.03
cyclo(-Mey-R-MeR-Nal-A-MeG-)	**151**	842.3	843.6	14.44
cyclo(-y-MeR-R-MeNal-A-MeG-)	**152**	842.3	843.7	17.33
cyclo(-y-MeR-R-Nal-MeA-MeG-)	**153**	842.3	843.6	16.82
cyclo(-y-MeR-MeR-Nal-A-MeG-)	**154**	842.3	843.6	15.65
cyclo(-y-MeR-R-Nal-MeA-MeG-)	**155**	842.3	843.7	15.80
cyclo(-y-MeR-MeR-MeNal-A-G-)	**156**	842.3	843.7	17.37
cyclo(-Mey-R-R-Nal-MeA-MeG-)	**157**	842.3	843.9	16.58
cyclo(-Mey-R-R-MeNal-A-MeG-)	**158**	842.3	843.6	16.03
cyclo(-Mey-R-R-MeNal-MeA-G-)	**159**	842.3	843.6	15.95
cyclo(-y-R-R-MeNal-MeA-MeG-)	**160**	842.3	843.7	15.27
cyclo(-y-R-MeR-Nal-MeA-MeG-)	**161**	842.3	843.7	15.74
cyclo(-y-R-MeR-MeNal-MeA-G-)	**162**	842.3	843.6	17.23
cyclo(-y-R-MeR-MeNal-A-MeG-)	**163**	842.3	843.5	14.82
cyclo(-Mey-MeR-R-Nal-MeA-MeG-)	**164**	856.5	857.8	15.97
cyclo(-Mey-MeR-R-MeNal-A-MeG-)	**165**	856.5	857.3	17.12
cyclo(-Mey-MeR-MeR-Nal-A-MeG-)	**166**	856.5	857.6	17.32
cyclo(-Mey-MeR-R-MeNal-MeA-G-)	**167**	856.5	857.8	17.22
cyclo(-Mey-MeR-MeR-Nal-MeA-G-)	**168**	856.5	857.3	17.56
cyclo(-Mey-MeR-MeR-MeNal-A-G-)	**169**	856.5	857.2	17.84
cyclo(-Mey-R-R-MeNal-MeA-MeG-)	**170**	856.5	857.7	18.04
cyclo(-Mey-R-MeR-Nal-MeA-MeG-)	**171**	856.5	857.8	18.12
cyclo(-y-MeR-MeR-MeNal-MeA-G-)	**172**	856.5	857.6	17.99
cyclo(-Mey-R-MeR-MeNal-MeA-G-)	**173**	856.5	857.8	17.63

IV.6.2 Ring-Size Reduction Scan of T140

All peptides were synthesized according to general procedures GP136, GP6 and GP10. All compounds were purified by *reversed phase* HPLC.

| sequence | no. | Mass | | R_t (min) |
		calc.	obsd. $(M+H^+)^+$ or $(M+Na^+)^+$	(10-90%)
cyclo[4,9]-R-R-Nal-C-Y-R-R-Cit-C-R	**174**	1519.8	761.2	11.53
cyclo[3,8]-R-Nal-C-Y-R-R-Cit-C-R	**175**	1363.7	1364.4	11.37
cyclo[2,7]-Nal-C-Y-R-R-Cit-C-R	**176**	1207.6	1208.6	11.28
cyclo[3,8]-R-Nal-C-Y-R-R-Cit-C	**177**	1207.6	1208.6	10.39
cyclo[3,8]-r-Nal-C-Y-R-R-Cit-C-R	**178**	1363.7	1364.7	10.45
cyclo[3,8]-R-nal-C-Y-R-R-Cit-C-R	**179**	1363.7	1364.6	10.73
cyclo[3,8]-R-Nal-c-Y-R-R-Cit-C-R	**180**	1363.7	1364.7	10.42
cyclo[3,8]-R-Nal-C-y-R-R-Cit-C-R	**181**	1363.7	1364.8	11.20
cyclo[3,8]-R-Nal-C-Y-r-R-Cit-C-R	**182**	1363.7	1364.7	10.55
cyclo[3,8]-R-Nal-C-Y-R-r-Cit-C-R	**183**	1363.7	1364.7	10.55
cyclo[3,8]-R-Nal-C-Y-R-R-cit-C-R	**184**	1363.7	1364.7	10.80
cyclo[3,8]-R-Nal-C-Y-R-R-Cit-c-R	**185**	1363.7	1364.7	10.64
cyclo[3,8]-R-Nal-C-Y-R-R-Cit-C-r	**186**	1363.7	1364.6	10.04

IV.7 Peptidomimetics for Purification of FVIII

IV.7.1 Synthesis of the Described Compounds

Methyl (1-*tert*-butyloxycarbonyl-indol-3-yl)acetate (187)
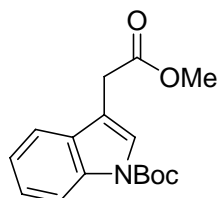
A solution of indol-3-yl acetic acid (10.2 g, 58.0 mmol, 1.0 equiv) in MeOH (500 mL) was cooled to 0°C and $SOCl_2$ (21.0 mL, 290 mmol, 5.0 equiv) was added slowly. After stirring for 4 h at room temperature, the mixture was concentrated under reduced pressure, the residue taken up in EtOAc (500 mL) and washed with saturated aqueous NH_4Cl (300 mL), saturated aqueous $NaHCO_3$ (300 mL) and brine (150 mL). After drying over Na_2SO_4, the mixture was concentrated to dryness to give the pure methyl ester as brown oil (10.8 g, 98%).

The methyl ester (10.6 g, 56.0 mmol, 1.0 equiv) was dissolved in acetonitrile (45 mL) and di-*tert*-butyl dicarbonate (37.4 g, 171 mmol, 3.0 equiv) and DMAP (1.34 g, 11.0 mmol, 0.2 equiv) were added.[186] The mixture was stirred for 2 h and the solvent removed under reduced pressure. The residue was dissolved in EtOAc (500 mL) and subsequently washed with saturated aqueous NH_4Cl (300 mL), saturated aqueous $NaHCO_3$ (300 mL) and brine (150 mL). After drying over Na_2SO_4, the solvent was removed in *vacuo* and the crude product purified by flash chromatography on silica gel (EtOAc/hexane; gradient 1:10 -> 1:2) to obtain **187** (14.0 g, 86 %; 2 steps) as a colorless solid.

Methyl (indol-3-yl)acetate

R_f = 0.3 (EtOAc/hexane 1:2)

^{1}H-NMR (360 MHz, $CDCl_3$): δ = 8.17 (s, 1H), 7.65 (d, J = 7.7 Hz, 1H), 7.29 (d, J = 7.8 Hz, 1H), 7.26-7.14 (m, 2H, H_{arom}), 7.02 (s, 1H, H_{arom}), 3.82 (s, 2H, CH_2), 3.74 (s, 3H, CH_3).

^{13}C NMR (91 MHz, $CDCl_3$): δ = 172.7, 136.0, 127.1, 123.2, 122.0, 119.5, 118.6, 111.2, 108.0, 51.9, 31.0.

HRMS (EI) calcd for $C_{11}H_{11}NO_2$ 189.07898; found 189.07883.

Methyl (1-*tert*-butyloxycarbonyl-indol-3-yl)acetate (187)

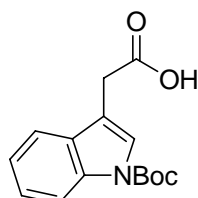RP-HPLC (10 - 100%) R_t = 27.4; 96% purity.

R_f = 0.5 (EtOAc/hexane 1:2)

mp 53°C

¹H NMR (500 MHz, CDCl₃): δ = 8.15 (d, J = 6.4 Hz, 1H), 7.57 (s, 1H), 7.52 (m, J = 7.8 Hz, 1H), 7.32 (dd, J = 7.6, 7.6 Hz, 1H), 7.24 (dd, J = 7.5, 7.5 Hz, 1H), 3.71 (s, 2H), 3.71 (s, 3H), 1.66 (s, 9H).

¹³C-NMR (91 MHz, CDCl₃): δ = 171.5, 149.6, 135.5, 130.1, 124.6, 124.5, 122.7, 119.0, 115.3, 113.1, 83.6, 52.1, 30.9, 28.2.

HRMS (EI) calcd for $C_{16}H_{19}NO_4$ 289.13141; found 289.13145.

(1-*tert*-Butyloxycarbonyl-indol-3-yl)acetic acid (188)

A solution of lithium hydroxide (LiOH*H₂O, 6.00 g, 143 mmol, 3 equiv) in H₂O (250 mL) was added to a solution of **187** (13.8 g, 47.7 mmol, 1.0 equiv) in THF (350 mL) and MeOH (150 mL). After stirring for 18 h, the mixture was concentrated in *vacuo* and a 10% aqueous solution of citric acid (300 mL) was added. The aqueous layer was extracted with EtOAc (3×200 mL) and the combined organic layers were washed with water (200 mL) and brine (200 mL) and dried over Na₂SO₄. The solvent was removed under reduced pressure and the residue purified by flash chromatography on silica gel (EtOAc/hexane gradient 1:10 -> 1:1, 1% AcOH) to yield **188** (10.9 g, 83%) as a colorless solid.

RP-HPLC (10 -> 90%) R_t = 24.5; 98% purity.

R_f = 0.6 (MeOH/CHCl₃ 1:9, 1% AcOH)

mp 117-120°C

¹H-NMR (500 MHz, CDCl₃): δ = 8.15 (s, 1H), 7.59 (s, 1H), 7.53 (dd, J = 7.8, 0.6 Hz, 1H), 7.34 (dd, J = 8.2, 7.3 Hz, 1H), 7.30-7.23 (m, 2H), 3.76 (s, 2H), 1.67 (s, 9H).

¹³C-NMR (125 MHz, CDCl₃): δ = 176.2, 149.5, 129.8, 124.8, 124.6, 122.6, 118.9, 115.3, 112.3, 83.7, 30.6, 28.1.

HRMS (EI) calcd for $C_{15}H_{17}NO_4$ 275.11576; found 275.11531.

(9H-fluoren-9-yl)methyl 4-(tert-butoxycarbonyl)-1-hydroxybutan-2-ylcarbamate (189)
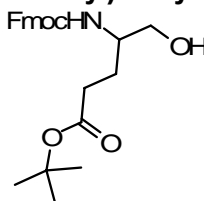
4.112 g Fmoc-Glu(O*t*-Bu)-OH (9.68 mmol) were dissolved in 70 mL dry THF under an argon atmosphere. The solution was cooled down to -10°C and 1.023 mL (1.2 equiv) N-methylmorpholine were slowly added. Afterwards, 0.710 mL methylchloroformiate (1.2 equiv) are

added and the solution stirred for 30 min. Then, 1.052 g (2.88 equiv) NaBH$_4$ in 80 mL dry MeOH were added dropwise over a period of 30 min. The solution was allowed to stir another 3 h at 0°C and 130 mL 1N HCl were addd. The resulting mixture was three times extracted with DCM and purified via flash chromatography to give 1.1 g (28%) of **189** as a colourless oil.

RP-HPLC (10 - 100%) R_t = 23.7; 99% purity.

R_f = 0.3 (EtOAc/hexane 2:1)

MS (ESI) calcd for C$_{24}$H$_{30}$NO$_5$ 412. 2; m/z 412.0 [M+H]$^+$.

(S)-*tert*-Butyl 4-(2-(1-*tert*-butyloxycarbonyl-indol-3-yl)-5-hydroxypentanoate (191)
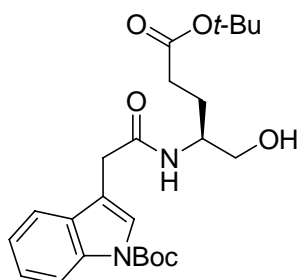
Fmoc-Glutamol(O*t*-Bu) (**189**) (1.83 g, 4.45 mmol) was dissolved in piperidine/DMF (20/80, v/v; 100 mL) and after stirring for 1 h the mixture was evaporated to dryness. The resulting crude amine **190** was taken up in DMF (250 mL) and **188** (1.23 g, 4.45 mmol, 1.0 equiv), HOBt (681 mg, 4.45 mmol, 1.0 equiv) and TBTU (1.43 g, 4.45 mmol, 1.0 equiv) were added. Then, the mixture was cooled to 0°C and DIPEA (2.25 mL, 13.2 mmol, 3.0 equiv) was added. After stirring for 18 h at room temperature, the solvent was removed in *vacuo* and the residue taken up in EtOAc (300 mL). The mixture was washed with saturated aqueous NH$_4$Cl (2×150 mL), saturated aqueous NaHCO$_3$ (2×150 mL) and brine (150 mL). After drying over Na$_2$SO$_4$, the solvent was removed under reduced pressure and the crude product purified by flash chromatography on silica gel (MeOH/CHCl$_3$; gradient 1:50 -> 1:20) to obtain **191** (1.88 g, 95%) as a hygroscopic colorless oil.

RP-HPLC (30 - 100%) R_t = 20.3; 96% purity.

R_f = 0.1 (MeOH/CHCl$_3$ 1:30), R_f = 0.3 (EtOAc/hexane 2:1)

$[\alpha]_D^{23}$ −13.2 (c 7.0, MeOH)

^{1}H-NMR (500 MHz, CDCl$_3$): δ = 8.14 (s, 1H), 7.55 (s, 1H), 7.49 (d, J = 7.8 Hz, 1H), 7.32 (dd, J = 7.3, 7.3 Hz, 1H), 7.23 (dd, J = 7.5, 7.5 Hz, 1H), 6.36 (d, J = 8.1 Hz, 1H), 5.38 (s, 1H, br), 3.96-3.87 (m, 1H), 3.67 (s, 2H), 3.56 (dd, J = 11.5, 3.7 Hz, 1H), 3.49 (dd, J = 11.4, 5.0 Hz, 1H), 2.19 (t, J = 6.9, 2H), 1.75 (dt, J = 14.0, 7.3 Hz, 1H), 1.66 (s, 9H), 1.65-1.59 (m, 1H), 1.40 (s, 9H).

^{13}C-NMR (63 MHz, CDCl$_3$): δ = 173.1, 170.9, 149.4, 135.5, 129.7, 124.8, 122.8, 118.8, 115.3, 113.6, 83.8, 80.8, 64.5, 51.6, 33.3, 31.7, 28.1, 27.9, 25.4.

HRMS (EI) calcd for C$_{24}$H$_{34}$N$_2$O$_6$ 446.24169; found 446.24164.

(S)-*tert*-Butyl 4-(2-(1-*tert*-butyloxycarbonyl-indol-3-yl)acetylamino)-4-formyl-butanoate (192)
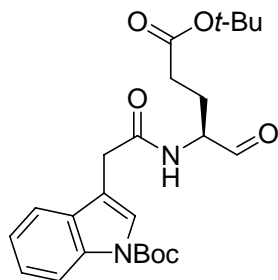
To a solution of **191** (1.2 g, 2.68 mmol, 1.0 equiv) in dry DCM (30 mL) Dess-Martin periodinane (3.41 g, 8.04 mmol, 3.0 equiv) was added in three portions over 1.5 h. The mixture was allowed to stir for another 1 h after which the suspension was diluted with DCM (30 mL) and subsequently washed with a mixture of 10% aqueous $Na_2S_2O_3$ and saturated aqueous $NaHCO_3$ (1:1, v/v; 2×30 mL), water (30 mL) and brine (30 mL). Drying over Na_2SO_4 and evaporation gave the crude aldehyde **192** (1.18 g) as a pale yellow solid which was directly used without further purification.

R_f = 0.2 (MeOH/CHCl$_3$ 1:30), R_f = 0.5 (EtOAc/hexane 2:1)

^{1}H-NMR (360 MHz, CDCl$_3$): δ = 9.44 (s, 1H), 8.11 (d, J = 7.9 Hz, 1H), 7.55 (s, 1H), 7.48 (d, J = 7.7 Hz, 1H), 7.30 (dd, J = 7.9, 7.9, 1H), 7.24-7.17 (m, 1H), 6.49 (d, J = 6.8 Hz, 1H), 4.42 (m, 1H), 3.67 (s, 2H), 2.24-2.04 (m, 3H), 1.76 (m, 1H), 1.63 (s, 9H), 1.34 (s, 9H).

^{13}C-NMR (91 MHz, CDCl$_3$): δ = 198.5, 172.1, 170.6, 149.4, 135.5, 129.6, 124.8, 122.8, 118.8, 115.3, 113.3, 83.8, 80.9, 58.2, 33.0, 30.8, 28.1, 27.9, 23.6.

HRMS (EI) calcd for $C_{24}H_{32}N_2O_6$ 444.22604; found 444.22634.

(S)-*tert*-Butyl-5-[(S)-1-methoxycarbonyl-2-(4-*tert*-butoxyphenyl)ethylamino]-4-(2-(1-*tert*-butyl-oxycarbonyl-indol-3-yl)acetylamino)-pentanoate (193)
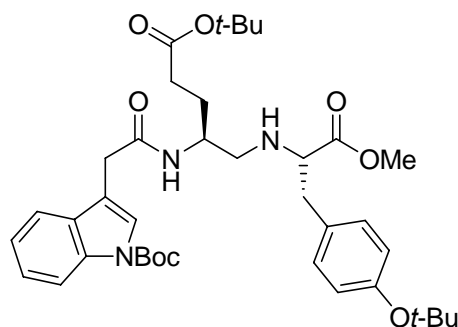
The crude aldehyde **192** (1.18 g) was dissolved in dry DCM (60 mL) and Tyr(OtBu)OMe * HCl (925 mg, 3.21 mmol, 1.2 equiv) and MgSO$_4$ (1.61 g, 13.4 mmol, 5.0 equiv) were added. After reacting for 30 min, NaB(OAc)$_3$H (3.18 g, 15.0 mmol, 5.6 equiv) was added and stirring continued for additional 18 h. Then, the mixture was diluted with saturated aqueous NaHCO$_3$ (50 mL) and after 30 min extracted with DCM (2×60 mL). The combined organic layers were dried over Na$_2$SO$_4$, the solvent was removed under reduced pressure and the crude product purified by flash

chromatography on silica gel (EtOAc/hexane gradient 1:2 - 2:1) to give **193** (1.37 g, 75% based on **191**) as a pale yellow oil.

RP-HPLC (30 - 100%) R_t = 22.5; 95% purity.

R_f = 0.5 (MeOH/CHCl$_3$ 1:30), R_f = 0.6 (EtOAc/hexane 2:1)

$[\alpha]_D^{23}$ +4.2 (c 0.3, MeOH)

^{1}H-NMR (500 MHz, MeOH-d$_4$): δ = 8.12 (d, J = 8.1 Hz, 1H), 7.65-7.58 (m, 2H), 7.32 (dd, J = 8.2, 8.2 Hz, 1H), 7.25 (dd, J = 7.5, 7.5 Hz, 1H), 7.11-7.06 (m, 2H), 6.95-6.90 (m, 2H), 4.15-4.00 (m, 2H), 3.71-3.62 (m, 5H), 3.16-2.86 (m, 4H), 2.23-2.16 (m, 2H), 1.86-1.76 (m, 1H), 1.67 (s, 9H), 1.64-1.58 (m, 1H), 1.39 (s, 9H), 1.31 (s, 9H).

^{13}C-NMR (91 MHz, CDCl$_3$): δ = 174.5, 172.5, 169.9, 153.9, 149.3, 135.4, 131.9, 129.7, 129.4, 129.3, 124.7, 124.6, 124.0, 123.9, 123.8, 122.6, 118.9, 115.2, 113.8, 83.6, 80.1, 78.0, 63.1, 51.4, 50.5, 49.0, 38.7, 33.3, 31.8, 28.6, 28.0, 27.9, 27.2.

HRMS (EI) calcd for C$_{38}$H$_{53}$N$_3$O$_8$ 679.38324; found 679.38327.

(S)-*tert*-Butyl-5-[(S)-1-((S)-1-butoxycarbonyl-2-tritylsulfanyl-ethylcarbamoyl)-2-(4-butoxyphenyl)ethylamino]-4-(2-(1-*tert*-butyloxycarbonyl-indol-3-yl)acetyl-amino)-pentanoate (194)
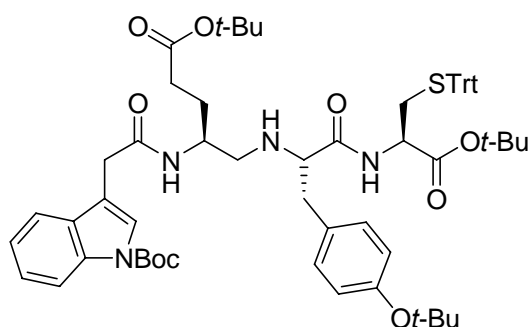
A solution of LiOH*H$_2$O (196 mg, 4.68 µmol, 3.5 equiv) in H$_2$O (5.3 mL) was added to a solution of **193** (1.06 g, 1.56 mmol, 1.0 equiv) in THF (5.3 mL) and dioxane (15.9 mL). After stirring for 1.5 h, the mixture was acidified by addition of a 10% aqueous solution of citric acid (100 mL) and the aqueous layer was extracted with EtOAc (3×100 mL). The combined organic layers were washed with water (100 mL) and brine (50 mL), dried (Na$_2$SO$_4$) and evaporated to give the crude acid (986 mg; 93% purity; RP-HPLC (20 - 100%) R_t = 23.0) as a pale yellow solid which was redissolved in DMF (55 mL). Then, Cys(Trt)O*t*Bu*HCl[356] (1.06 g, 2.34 mmol, 1.5 equiv), HOBt (232 mg, 1.72 mmol, 1.1 equiv) and TBTU (552 mg, 1.72 mmol, 1.1 equiv) were added and the mixture was cooled to 10°C. Collidine (1.03 mL, 7.80 mmol, 5.0 equiv) was added and the solution was stirred for 18 h at room temperature. After the solvent was evaporated, the residue was taken up in EtOAc (200 mL) and subsequently washed with saturated aqueous NH$_4$Cl (2×150 mL), saturated aqueous NaHCO$_3$ (2×150 mL) and brine (150 mL). After drying over Na$_2$SO$_4$, the solvent was removed under reduced pressure and the crude product purified by flash chromatography on

silica gel (EtOAc/hexane; gradient 1:4 -> 2:1) to give **194** (1.38 g, 83%) as a hygroscopic, pale yellow oil.

RP-HPLC (20 - 100%) R_t = 31.2; 97% purity.

R_f = 0.6 (EtOAc/hexane 2:1)

$[\alpha]_D^{23}$ +3.6 (c 0.6, ACN)

^{1}H-NMR (500 MHz, MeOH-d$_4$): δ = 8.12 (d, J = 8.1 Hz, 1H), 7.65-7.58 (m, 2H), 7.32 (dd, J = 8.2, 8.2 Hz, 1H), 7.25 (dd, J = 7.5, 7.5 Hz, 1H), 7.11-7.06 (m, 2H), 6.95-6.90 (m, 2H), 4.15-4.00 (m, 2H), 3.71-3.62 (m, 5H), 3.16-2.86 (m, 4H), 2.23-2.16 (m, 2H), 1.86-1.76 (m, 1H), 1.67 (s, 9H), 1.64-1.58 (m, 1H), 1.39 (s, 9H), 1.31 (s, 9H)

^{1}H-NMR (500 MHz, DMSO-d$_6$): δ = 8.95 (d, J = 7.7 Hz, 1H), 8.09 (d, J = 8.0 Hz, 1H), 8.05 (d, J = 8.2 Hz, 1H), 7.60 (d, J = 7.8 Hz, 1H), 7.57 (s, 1H), 7.38-7.27 (m, 14H), 7.27-7.20 (m, 4H), 7.10 (d, J = 8.3 Hz, 2H), 6.83 (d, J = 8.3 Hz, 2H), 4.08-4.02 (m, 1H), 4.00-3.92 (m, 1H), 3.91-3.85 (m, 1H), 3.59 (d, J = 15.5 Hz, 1H), 3.49 (d, J = 15.4 Hz, 21H), 3.09-3.01 (m, 2H), 2.93-2.86 (m, 1H), 2.84-2.80 (m, 1H), 2.57-2.52 (m, 1H), 2.39 (dd, J = 12.6, 5.2 Hz, 1H), 2.14-1.98 (m, 2H), 1.62 (s, 10H), 1.50-1.44 (m, 1H), 1.32 (s, 9H), 1.29 (s, 9H), 1.25 (s, 9H).

^{13}C-NMR (125 MHz, DMSO-d$_6$): δ = 171.3, 170.4, 168.1, 166.7, 154.1, 148.9, 143.8, 134.5, 130.0, 129.8, 128.9, 128.6, 128.0, 126.7, 124.3, 124.0, 123.4, 122.3, 119.4, 114.8, 114.5, 83.4, 81.5, 79.5, 77.6, 66.4, 60.8, 52.5, 49.7, 45.7, 34.9, 32.7, 31.9, 30.6, 28.4, 27.6, 27.5, 27.3.

MS (ESI) calcd for $C_{63}H_{78}N_4O_9S$ 1066.55; found 1067.6 [M+H]$^+$, 1089.3 [M+Na]$^+$.

5-[1-(1-Carboxy-2-mercapto-ethylcarbamoyl)-2-(4-hydroxy-phenyl)-ethylami-no]-4-(2-1H-indol-3-yl-acetylamino)-pentanoic acid (195)
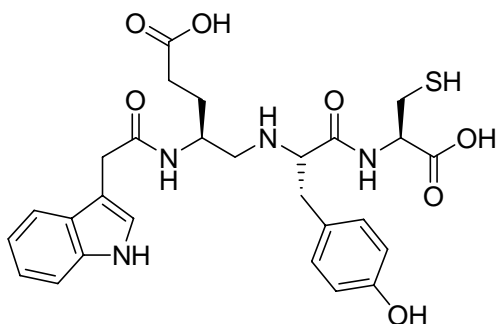
To a vigorously stirred mixture of **194** (500 mg, 0.47 mmol) in triisopropylethylsilane (1.00 mL; 10%), ethane dithiol (1.00 mL, 10%) and water (0.50 mL; 5%) trifluoroacetic acid (7.50 mL; 75%) was added slowly over 8h via a syringe pump. The mixture was stirred for additional 30 min, after which the solvent was removed in *vacuo*. The residue was dissolved in a minimum volume of acetic acid and precipitated in ice cold ether/pentane (2×20 mL) to give pure **195** (242 mg, 93%).

96% purity; RP-HPLC (10 -> 50%) R_t = 14.4

$[\alpha]_D^{23}$ –0.4 (c 0.2, MeOH/H$_2$O 2:1)

mp 135°C

Two conformers (ca. 4:1 ratio)

^{1}H-NMR (500 MHz, MeOH-d$_4$): δ = 7.58 (d, J = 7.9 Hz, 1H, 20%), 7.56 (d, J = 8.0 Hz, 1H, 80%), 7.38-7.35 (m, 1H), 7.22 (s, 1H, 20%), 7.20 (s, 1H, 80%), 7.15-7.09 (m, 1H), 7.07 (d, J = 8.5 Hz, 2H), 7.05-7.02 (m, 1H), 6.75 (d, J = 8.46 Hz, 2H), 4.54-4.46 (m, 1H), 4.20-4.14 (m, 1H, 20%), 4.12 (t, J = 7.0, 1H, 20%), 4.05 (m, 1H, 80%), 3.98 (t, J = 6.9, 1H, 80%), 3.77-3.63 (m, 2H), 3.11-3.03 (m, 2H), 3.03-2.96 (m, 2H), 2.94-2.81 (m, 2H), 2.33-2.20 (m, 2H), 1.87-1.76 (m, 1H), 1.72-1.60 (m, 1H).

^{13}C-NMR (125 MHz, MeOH-d$_4$): δ = 176.4, 176.3, 172.5, 170.4, 158.1, 138.2, 131.5, 131.5, 125.2, 125.1, 122.6, 120.0, 119.2, 116.8, 112.4, 109.0, 64.1 (80%), 63.2 (20%), 56.5 (20%), 56.3 (80%), 52.9 (80%), 52.5 (20%), 48.1, 37.5, 34.0 (20%), 33.9 (80%), 31.0 (80%), 30.9 (20%), 28.3 (20%), 28.0 (80%), 26.8.

HRMS (ESI) calcd for C$_{27}$H$_{33}$N$_4$O$_7$S 557.20700 [M+H]$^+$; found 557.20590 [M+H]$^+$, 1089.3 [M+Na]$^+$.

IV.7.2 Biological Evaluation of the Described Peptides and Peptidomimetics

Immobilization of ligands to Toyopearl AF-Epoxy-650M resin.

2.5 mg of the respective peptidic or peptidomimetic ligand were dissolved in 0.25 mL of immobilization buffer (0.2 M sodium bicarbonate, pH 10.3) and 36.0 mg of Toyopearl AF-Epoxy-650M resin (corresponding to 0.125 mL of swollen resin; *Tosoh Bioscience*, Stuttgart, Germany) were added, followed by incubation of the mixture with gentle rotation for 48 hours. Then, the resin was washed once with immobilization buffer, once with 1 M NaCl and then 3 times with binding buffer (0.01 M HEPES, 0.1 M NaCl, 5 mM CaCl$_2$, 0.01% Tween-80; pH=7.4). The achieved ligand loading was determined by measuring the UV adsorption (280 nm) of the source solution before and after the immobilization.

Ligand Stability in Human Serum

Human serum was obtained from a healthy donor according to standard procedures. Ligands were dissolved in serum (1 mg/mL), incubated for different periodes of time at 37°C and samples were subjected to Isolute-SPE-columns (*Separtis*, Grenzach-Wyhlen, Germany): Cartridges were washed with methanol and water and loaded with the test solution diluted in 1 mL of phosphate buffered saline (PBS). The cartridge was washed with 5% methanol/water (2 mL). The ligands were eluted from the column by methanol (2 mL). The solvent was removed and the residue taken up in acetonitrile/water (1:1; v/v) containing 1% trifluoroacetic acid and analyzed by HPLC and HPLC-MS^3-SRM.

Binding Studies Using Coated ToyoPearl Resins

These experiments were performed by Dr. Alexey Khrenov.

Ligand-coated resins were resuspended in binding buffer-1 (0.01 M Hepes, 0.1 M NaCl, 5 mM CaCl$_2$, 0.01% Tween-80; pH 7.4) (1:7; v/v) and aliquoted (40 µL/tube). ^{125}I-pdFVIII (100000 cpm in 10 µL) was added and the volume adjusted to 100 µL with buffer-1 containing 4% BSA. The samples were gently rocked for 2 hours, washed with binding buffer and the radioactivity of beads was measured. The radioactivity of uncoated resin was considered as background value. Binding was calculated as percentage of maximal achievable binding, as determined by immunoprecipitation of ^{125}I-FVIII with mAb 8860 (generously provided by *Baxter/Hyland Healthcare*, Glendale, CA) coated resin. Scrambled peptide ECYYEHWS was used as negative and parent peptide EYHSWEYC as positive control in each experiment.

Localization of the Binding Site in FVIII

Cloning of recombinant DNA and expression of L-[^{35}S]methionine-labeled rFVIII fragments was performed as previously described[146]. The following domain fragments were used: A1a1A2a2$_{1-758}$, A1a1$_{1-398}$, a1A2a2$_{318-758}$, B$_{741-1647}$, LC$_{1637-2332}$, a3A3C1$_{1637-2173}$, C2$_{2170-2332}$

Labeled polypeptides (3 µL) were mixed with ligand-coated resin (50 µL) and buffer-1 (350 µL). The suspension was gently rocked for 16 h at 4°C, centrifuged and washed. Bound complexes were eluted by boiling for 3 min in SDS-PAGE loading buffer (30 µL). 2 µL of radio-labeled fragments were diluted in scintillation liquid (5 mL; *Lumasafe*, Luma, Groningen, Netherlands) for radioactivity counting in a *Packard* counter (Groningen, Netherlands).

As positive control, immunoprecipitation using mAbs F7B4, F19C2, F16E11 and BO2C11 (produced at the University of Leuven [357,358]) to FVIII was performed[358].

Affinity Purification Using C141

These experiments were performed by Dr. Alexey Khrenov.

C141-coated resin (1 mL) (prepared from **195** (25 mg) and Toyopearl resin (360 mg) as described above) was packed into a glass column (*GE Healthcare*, Piscataway, NJ) and purification was performed employing a *Waters* 650E Advanced Protein Purification System at a flow-rate of 1 mL/min. Buffer-1 was used for FVIII loading (0.1 M NaCl) and and a mixture of buffer-1 and buffer-2 (1.0 M NaCl) for elution. Elution was monitored by a flow-through UV detector at 280 nm.

pdFVIII (0.5 mg), purified from Monarc-M as described above, was mixed with 55 mL of cell-conditioned 10% fetal bovine serum (FBS)-containing Delbucco's Modified Eagles Medium (DMEM) and diluted with 30 mL of buffer-1 (0.01 M Hepes, 5 mM CaCl$_2$, 0.01% Tween-80) to give a final FVIII concentration of ~6 µg mL^{-1} (~30 IU mL^{-1}) and a final salt concentration of 0.1 M NaCl. The mixture was applied onto the column, followed by subsequent washing with buffer-1 (~130 mL) until OD280 had returned to background and with a mixture of buffer-1 and buffer-2 (~8 mL;

85:15, v/v). FVIII was eluted using a mixture of buffer-1 and buffer-2 (4:6, v/v). Volume of FVIII elution peak was 12 mL (160 IU mL^{-1}; 78% yield).

For the control experiment without added medium, 0.5 mg pdFVIII were diluted in 25 mL of buffer-1 (32 IU mL^{-1}). Purification was performed in an analogous manner except that FVIII was eluted directly after washing with buffer-1 using a mixture of 20% buffer-1 and 80% buffer-2. Volume of FVIII elution peak was 3.4 mL (209 IU mL^{-1}; 89% yield).

Elution fractions were analyzed by determining OD280 and by SDS-PAGE and Western blot analysis and FVIII activity was confirmed by APTT assay.

FVIII Activity in Presence of Unbound Ligands

20 , 2 and 0.2 μg of ligand were dissolved in buffer solution (245 μL; 50 mM Tris, 9% NaCl, 1% BSA, pH 7.2) and pdFVIII (20 μL; 2 U mL^{-1}; *CAF-DCF*, Brussels, Belgium) was added. The solution was gently rocked for 2 hours at room temperature. Activity of FVIII was determined by a chromogenic assay (*Dade Behring*, Marburg, Germany), according to manufacturer's instructions. Negative and positive controls were buffer solution and buffer solution supplemented with pdFVIII, respectively.

IV.8 Asymmetric Synthesis of Condensed and Aromatic Ring-Substituted Tyrosine Derivatives

IV.8.1 Synthesis of 3-Aryl-Substituted Tyrosine Derivatives

(S)-N^α-tert-Butyloxycarbonyl-m-iodotyrosine (196)
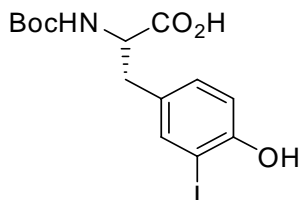
To a solution of *m*-iodo-L-tyrosine (2.16 g, 7.02 mmol, 1.0 equiv) and NEt$_3$ (1.46 mL, 10.5 mmol, 1.5 equiv) in 100 mL of dioxan/H$_2$O (1:1) at 0°C di-*tert*-butyldicarbonate (1.69 g, 7.73 mmol, 1.1 equiv) was added in small portions and the mixture was stirred for 45 min at 0°C and additional 18 h at room temperature. After the dioxane was removed under reduced pressure, the solution was acidified by addition of a 10% aqueous solution of citric acid (200 mL) and the aqueous layer was extracted with EtOAc (3×100 mL). The combined organic layers were dried over Na$_2$SO$_4$ and the solvent removed under reduced pressure to yield **196** (2.74 g, 96%) as a colorless oil which was used without further purification.

R_f = 0.15 (EtOAc/hexane 1:4, 1% AcOH)

$[\alpha]_D^{23}$ +2.4 (c 0.1, CHCl$_3$)

mp 83-85°C

^{1}H NMR (360 MHz, MeOH-d$_4$): δ = 7.53 (d, *J* = 1.3 Hz, 1H), 7.03 (dd, *J* = 8.2, 2.1 Hz, 1H), 6.73 (d, *J* = 8.2 Hz, 1H), 4.25 (dd, *J* = 8.6, 5.0 Hz, 1H), 3.02 (dd, *J* = 13.9, 4.9 Hz, 1H), 2.76 (dd, *J* = 13.8, 8.9 Hz, 1H), 1.38 (s, 9H).

^{13}C-NMR (90 MHz, MeOH-d$_4$): δ = 175.2, 157.7, 156.8, 141.0, 140.9, 131.4131.4, 115.6, 84.4, 80.6, 56.3, 37.3, 28.7.

MS (ESI) calcd for C$_{14}$H$_{18}$INO$_5$ 407.02; m/z 408.1 [M+H]$^+$, 852.9 [2M+K]$^+$, 1243.8 [3M+Na]$^+$, 1259.7 [3M+K]$^+$.

(S)-N -tert-Butyloxycarbonyl-O-benzyl-m-iodotyrosine benzyl ester (197)
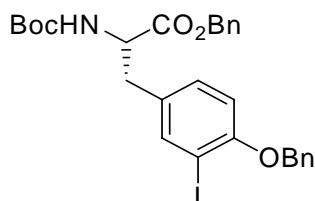
To a solution of **196** (2.74 g, 6.73 mmol, 1.0 equiv) in acetone (20 mL), K_2CO_3 (2.90 g, 21.0 mmol, 3.0 equiv) and benzyl bromide (1.38 mL, 14.4 mmol, 2.2 equiv) were added and the mixture heated under reflux for 5 h. After the solvent was evaporated, the residue was taken up in $CHCl_3$ (240 mL), washed with saturated aqueous $NaHCO_3$ (3×80 mL) and dried over Na_2SO_4 and the solvent evaporated under reduced pressure. Flash chromatography on silica gel (EtOAc/hexane 1:4) yielded **197** (3.30 g, 83%) as a colorless solid.

R_f = 0.20 (EtOAc/hexane, 1:4)

$[\alpha]_D^{23}$ +2.4 (c 6.1, $CHCl_3$)

mp 68-70°C

^{1}H-NMR (360 MHz, $CDCl_3$): δ = 7.55 (d, J = 1.1 Hz, 1H), 7.51 (m, 2H), 7.36 (m, 8H), 6.94 (d, J = 7.9 Hz, 1H), 6.69 (d, J = 8.4 Hz, 1H), 5.17 (d, J = 12.2 Hz, 1H), 5.11 (d, J = 12.2 Hz, 1H), 5.10 (s, 2H), 5.02 (d, J = 7.6 Hz, 1H), 4.57 (m, 1H), 3.08-2.88 (m, 2H), 1.44 (s, 9H).

^{13}C-NMR (90 MHz, $CDCl_3$): δ = 171.4, 156.3, 154.9, 140.2, 136.5, 135.1, 130.5, 130.2, 128.6, 128.52, 128.49, 128.47, 127.9, 126.9, 112.5, 86.8, 80.0, 70.9, 67.2, 54.5, 36.9, 28.3.

HRMS (EI) calcd for $C_{28}H_{30}INO_5$ 587.11687; found 587.11707.

(S)-*N*$^\alpha$-*tert*-Butyloxycarbonyl-*O*-benzyl-*m*-phenyltyrosine benzyl ester (198)
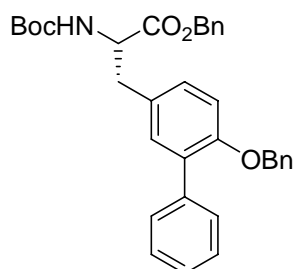
To a solution of **197** (3.30 g, 5.62 mmol, 1.0 equiv) in degassed DME/H_2O (6:1; 40 mL) the appropriate phenyl boronic acid (1.03 g, 8.43 mmol, 1.5 equiv) and Na_2CO_3 (1.20 g, 11.2 mmol, 2.0 equiv) was added. After five vacuum/argon cycles, $Pd(OAc)_2$ (63 mg, 281 µmol, 5 mol%) and P(*o*-tolyl)$_3$ (171 mg, 562 µmol, 10 mol%) were added and the mixture heated to 80°C until complete conversion (3-8 h). After the reaction mixture was cooled to room temperature, it was passed through a short column with a bottom layer of silica gel (40-63 µm) and a top layer of $NaHCO_3$ using EtOAc as eluent. The solvent was removed under reduced pressure and the crude product purified by flash chromatography (EtOAc/hexane 1:4) to achieve **198** (2.75 g, 91%) as a pale yellow solid.

R_f = 0.25 (EtOAc/hexane, 1:4)

$[\alpha]_D^{23}$ +2.6 (c 0.6, $CHCl_3$)

mp 111-113°C

^{1}H-NMR (360 MHz, CDCl$_3$): δ = 7.54 (d, J = 7.5 Hz, 2H), 7.40 (dd, J = 7.4, 7.4 Hz, 2H), 7.38-7.26 (m, 11H), 7.09 (s, 1H), 6.94 (d, J = 7.4 Hz, 1H), 6.87 (d, J = 8.1 Hz, 1H), 5.15 (d, J = 12.3, 1H), 5.10 (d, J = 12.3, 1H), 5.06-5.00 (m, 3H), 4.67-4.61 (m, 1H), 3.13-3.02 (m, 2H), 1.41 (s, 9H).

^{13}C-NMR (63 MHz, CDCl$_3$): δ = 171.7, 155.1, 154.6, 138.1, 137.1, 135.0, 132.0, 131.2, 130.3, 129.5, 129.2, 128.5, 128.43, 128.40, 128.37, 127.8, 127.5, 126.9, 126.7, 113.4, 80.0, 70.4, 67.1, 54.5, 37.3, 28.2.

HRMS (EI) calcd for C$_{34}$H$_{35}$NO$_5$ 537.25153; found 537.25207.

General procedure for synthesis of 3-aryl-substituted tyrosine analogues 199-207

To a solution of **197** (1.0 equiv) in degassed DME/H$_2$O (6:1; 7 mL/mmol) the appropriate aryl boronic acid (1.5 equiv) and Na$_2$CO$_3$ (2.0 equiv) was added. After five vacuum/argon cycles Pd(OAc)$_2$ (5 mol%) and P(o-tolyl)$_3$ (10 mol%) were added and the mixture heated to 80°C until complete conversion (3-8 h). After the reaction mixture was cooled to room temperature, it was passed through a short column with a bottom layer of silica gel (40-63 μm) and a top layer of NaHCO$_3$ using EtOAc as eluent. The solvent was removed under reduced pressure and the crude product purified by flash chromatography using an appropriate mixture of EtOAc and hexane as eluent.

(S)-N$^\alpha$-tert-Butyloxycarbonyl-O-benzyl-m-(p-tolyl)tyrosine benzyl ester (199)
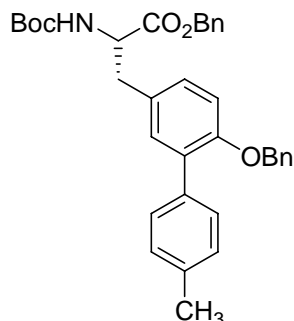
Pale yellow solid; Yield 93%.

R_f = 0.25 (EtOAc/hexane, 1:4)

[α]$_D^{23}$ +3.0 (c 1.3, CHCl$_3$)

mp 97-101°C

^{1}H-NMR (250 MHz, CDCl$_3$): δ = 7.45-7.38 (m, 2H), 7.34-7.16 (m, 12H), 7.06 (d, J = 1.3 Hz, 1H), 6.89 (d, J = 8.5 Hz, 1H), 6.82 (d, J = 8.4 Hz, 1H), 5.12 (d, J = 12.3 Hz, 1H), 5.06 (d, J = 12.4 Hz, 1H), 5.05-4.95 (m, 3H), 4.60 (m, 1H), 3.13-2.90 (m, 2H), 2.36 (s, 3H), 1.39 (s, 9H).

^{13}C-NMR (63 MHz, CDCl$_3$): δ = 171.8, 155.0, 154.7, 137.2, 136.6, 135.2, 135.1, 131.9, 131.1, 129.4, 128.9, 128.6, 128.5, 128.42, 128.37, 127.5, 126.8, 113.4, 79.9, 70.4, 67.1, 54.51, 37.4, 28.3, 21.2.

HRMS (EI) calcd for C$_{35}$H$_{37}$NO$_5$ 551.26715; found 551.26702.

(S)-*N*^α-tert-Butyloxycarbonyl-*O*-benzyl-*m*-(*m*-tolyl)tyrosine benzyl ester (200)
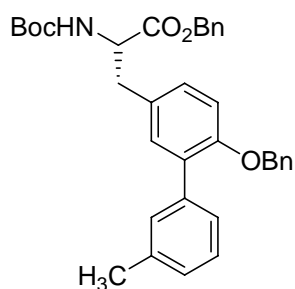
Pale yellow solid; Yield 79%.

R_f = 0.25 (EtOAc/hexane, 1:4)

$[\alpha]_D^{23}$ +2.9 (c 2.8, CHCl$_3$)

mp 78-82°C

^{1}H-NMR (250 MHz, CDCl$_3$): δ = 7.36-7.21 (m, 13H), 7.14-7.04 (m, 2H), 6.92 (d, J = 8.7 Hz, 1H), 6.85 (d, J = 8.3 Hz, 1H), 5.13 (d, J = 12.2 Hz, 1H), 5.07 (d, J = 12.6 Hz, 1H), 5.05-4.99 (m, 3H), 4.61 (m, 1H), 3.12-2.98 (m, 2H), 2.36 (s, 3H), 1.39 (s, 9H).

^{13}C-NMR (63 MHz, CDCl$_3$): δ = 171.8, 155.1, 154.7, 138.0, 137.3, 137.2, 135.1, 132.0, 131.4, 130.3, 129.1, 128.53, 128.45, 128.37, 127.8, 127.7, 127.5, 126.8, 126.7, 113.4, 80.0, 70.5, 67.1, 54.6, 37.4, 28.3, 28.1, 21.5.

HRMS (EI) calcd for C$_{35}$H$_{37}$NO$_5$ 551.26715; found 551.26682.

(S)-*N*^α-tert-Butyloxycarbonyl-*O*-benzyl-*m*-(*o*-tolyl)tyrosine benzyl ester (201)

Pale yellow oil; Yield 70%.

R_f = 0.25 (EtOAc/hexane, 1:4)

$[\alpha]_D^{23}$ +2.6 (c 1.9, CHCl$_3$)

^{1}H-NMR (250 MHz, CDCl$_3$): δ = 7.30-7.20 (m, 10H), 7.20-7.17 (m, 2H), 7.17-7.12 (m, 2H), 6.93 (d, J = 8.5 Hz, 1H), 6.90-6.81 (m, 2H), 5.14 (d, J = 12.2 Hz, 1H), 5.08 (d, J = 12.4 Hz, 1H) 5.03-4.95 (m, 3H), 4.60 (m, 1H), 3.13-2.92 (m, 2H), 1.39 (s, 9H).

^{13}C-NMR (63 MHz, CDCl$_3$): δ = 171.7, 155.0, 154.8, 138.3, 137.3, 136.6, 135.1, 132.2, 131.7, 130.0, 129.5, 129.2, 128.5, 128.4, 128.3, 128.1, 127.4, 127.3, 126.5, 125.3, 113.2, 79.9, 70.3, 67.1, 54.5, 37.4, 28.3, 20.1.

HRMS (EI) calcd for C$_{35}$H$_{37}$NO$_5$ 551.26715; found 551.26764.

(S)-N^α-tert-Butyloxycarbonyl-O-benzyl-m-(3-hydroxyphenyl)tyrosine benzyl ester (202)
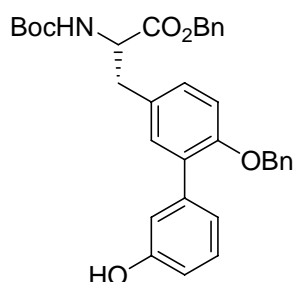
Pale yellow solid; Two rotamers (ca. 4:1 ratio); Yield 80%.

R_f = 0.21 (EtOAc/hexane, 1:4)

$[\alpha]_D^{23}$ +3.8 (c 0.9, CHCl$_3$)

mp 65-68°C

^{1}H-NMR (250 MHz, CDCl$_3$): δ = 7.33-7.15 (m, 11H), 7.11-6.95 (m, 3H), 6.89 (dd, J = 8.3, 1.7 Hz, 1H), 6.82 (s, 1H), 6.78 (m, 1H), 5.53 (s, 1H), 5.15-5.00 (m, 3H), 4.98 (s, 2H), 4.60 (m, 1H), 4.60 (m, 1H), 3.11-2.90 (m, 2H), 1.38 (s, 9H), 1.29 (s, 9H).

^{13}C-NMR (63 MHz, CDCl$_3$): δ = 171.8, 155.4, 155.2, 154.6, 139.6, 137.1, 135.0, 131.8, 130.9, 129.2, 128.9, 128.5, 128.3, 127.5, 126.7, 121.8, 116.5, 113.9, 113.5, 80.1, 70.5, 67.1, 54.5, 37.3, 28.2.

HRMS (EI) calcd for C$_{34}$H$_{35}$NO$_6$ 553.24644; found 553.24703.

(S)-N^α-tert-Butyloxycarbonyl-O-benzyl-m-(3-chlorophenyl)tyrosine benzyl ester (203)
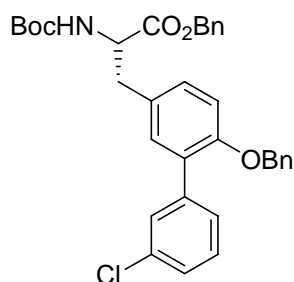
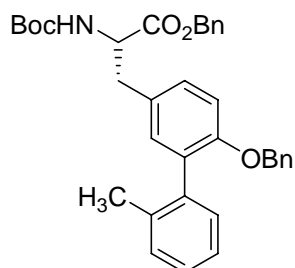Pale yellow oil; Yield 39%.

R_f = 0.38 (EtOAc/hexane, 1:4)

$[\alpha]_D^{23}$ +3.0 (c 0.5, CHCl$_3$)

^{1}H-NMR (250 MHz, CDCl$_3$): δ = 7.55 (m, 1H), 7.42-7.22 (m, 13H), 7.05 (d, J = 1.7 Hz, 1H), 6.98 (d, J = 8.3 Hz, 1H), 6.88 (d, J = 8.3 Hz, 1H), 5.17 (d, J = 12.3 Hz, 1H), 5.10 (d, J = 12.5 Hz, 1H), 5.04-4.97 (m, 3H), 4.64 (m, 1H), 3.20-2.92 (m, 2H), 1.42 (s, 9H).

^{13}C-NMR (63 MHz, CDCl$_3$): δ = 171.7, 155.0, 154.5, 139.9, 136.9, 135.1, 133.7, 131.8, 129.9, 129.7, 129.1, 128.6, 128.54, 128.46, 128.4, 127.73, 127.68, 127.0, 126.8, 113.3, 80.0, 70.5, 67.1, 54.5, 37.4, 28.3.

HRMS (EI) calcd for C$_{34}$H$_{34}$ClNO$_5$ 571.21255; found 571.21109.

(S)-N$^\alpha$-tert-Butyloxycarbonyl-O-benzyl-m-(4-fluorophenyl)tyrosine benzyl ester (204)
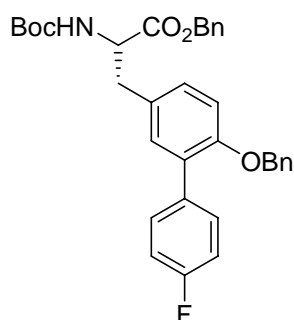
Pale yellow solid; Yield 94%.

R_f = 0.25 (EtOAc/hexane, 1:4)

$[\alpha]_D^{23}$ +1.3 (c 1.7, CHCl$_3$)

mp 108-110°C

^{1}H-NMR (250 MHz, CDCl$_3$): δ = 7.54-7.45 (m, 2H), 7.36-7.25 (m, 10H), 7.12-7.03 (m, 3H), 6.96 (d, J = 8.4Hz, 1H), 6.88 (d, J = 8.4 Hz, 1H), 5.17 (d, J = 12.2 Hz, 1H), 5.10 (d, J = 12.4 Hz, 1H), 5.04 (m, 3H), 4.64 (m, 1H), 3.20-2.95 (m, 2H), 1.42 (s, 9H).

^{13}C-NMR (63 MHz, CDCl$_3$): δ = 171.7, 163.9, 160.0, 155.0, 154.6, 137.0, 135.1, 134.11, 134.06, 131.9, 131.2, 131.1, 130.2, 129.4, 128.5, 128.43, 128.37, 127.7, 126.8, 114.9, 114.6, 113.3, 79.9, 70.5, 67.1, 54.5, 37.4, 28.3.

HRMS (EI) calcd for C$_{34}$H$_{34}$FNO$_5$ 555.24210; found 555.24184.

(S)-N$^\alpha$-tert-Butyloxycarbonyl-O-benzyl-m-(4-carboxyphenyl)tyrosine benzyl ester (205)

Pale yellow solid; Two rotamers (ca. 7:3 ratio); Yield 92%.

R_f = 0.35 (EtOAc/hexane 1:4, 1% AcOH)

$[\alpha]_D^{23}$ −10.5 (c 0.02, CHCl$_3$)

^{1}H-NMR (250 MHz, CDCl$_3$): δ = 9.53 (s, 1 H), 8.12 (d, J = 7.9 Hz, 2H), 7.63 (d, J = 8.0 Hz, 2H), 7.39-7.22 (m, 10H), 7.11 (s, 1H), 6.99 (d, J = 8.4 Hz, 1H), 6.90 (d, J = 8.2 Hz, 1H), 5.20-5.08 (m, 2H), 5.08-5.04 (m, 3H), 4.66 (m, 1H), 4.38 (m, 1H), 3.20-3.01 (m, 2H), 1.42 (s, 9H), 1.32 (s, 9H).

^{13}C-NMR (125 MHz, CDCl$_3$): δ = 171.8, 171.3, 155.1, 154.7, 143.9, 136.8, 135.1, 132.0, 131.9, 129.93, 129.88, 129.7, 129.6, 128.7, 128.6, 128.5, 127.8, 127.7, 126.9, 126.8, 113.3, 80.1, 70.6, 67.2, 54.5, 37.5, 28.3.

MS (ESI) m/z 604.4 [M+Na]⁺, 1185.1 [2M+Na]⁺.

(S)-*N*$^{\alpha}$-tert-Butyloxycarbonyl-*O*-benzyl-*m*-(2-furanyl)tyrosine benzyl ester (206)
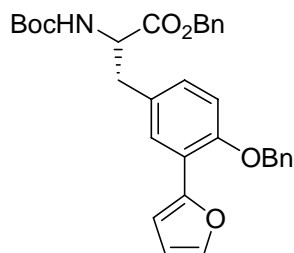
Pale yellow solid; Yield 99%.

R_f = 0.38 (EtOAc/hexane, 1:4)

$[\alpha]_D^{23}$ +7.1 (c 0.3, CHCl$_3$)

mp 97-100°C

^{1}H-NMR (250 MHz, CDCl$_3$): δ = 7.67 (d, *J* = 0.4 Hz, 1H), 7.52-7.36 (m, 6H), 7.35-7.30 (m, 5H), 6.93-6.86 (m, 3H), 6.44 (dd, *J* = 3.4, 1.8 Hz, 1H), 5.17-5.12 (m, 4 H), 5.05 (d, *J* = 7.0 Hz, 1H), 4.64 (m, 1H), 3.17-3.01 (m, 2H), 1.44 (s, 9H).

^{13}C-NMR (63 MHz, CDCl$_3$): δ = 171.7, 155.0, 153.5, 149.9, 141.0, 136.7, 135.2, 128.61, 128.57, 128.49, 128.43, 128.3, 128.2, 128.1, 127.6, 126.9, 120.1, 112.3, 111.8, 110.3, 79.9, 70.5, 67.1, 54.6, 54.6, 37.5, 28.3.

HRMS (EI) calcd for C$_{32}$H$_{33}$NO$_6$ 527.23079; found 527.23086.

(S)-*N*$^{\alpha}$-tert-Butyloxycarbonyl-*O*-benzyl-*m*-(3-thienyl)tyrosine benzyl ester (207)

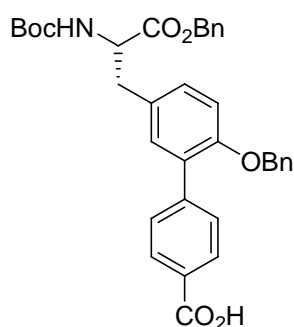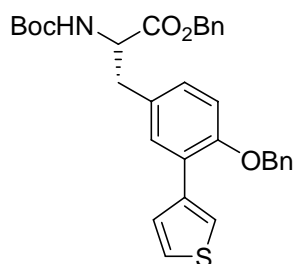Pale yellow solid; Yield 45%.

R_f = 0.37 (EtOAc/hexane, 1:4)

$[\alpha]_D^{23}$ 0.0 (c 1.2, CHCl$_3$)

mp 115-117°C

^{1}H-NMR (250 MHz, CDCl$_3$): δ = 7.57 (dd, *J* = 3.0, 1.3 Hz, 1H), 7.41 (dd, *J* = 5.1, 1.3 Hz, 1H), 7.39-7.34 (m, 4H), 7.34-7.23 (m, 8H), 6.95-6.84 (m, 2H), 5.15 (d, *J* = 12.2 Hz, 1H), 5.09 (d, *J* = 12.3 Hz, 1H), 5.07 (s, 2H), 5.02 (m, 1H), 4.63 (m, 1H), 3.17-2.96 (m, 2H), 1.41 (s, 9H).

^{13}C-NMR (63 MHz, CDCl$_3$): δ = 171.7, 155.0, 154.7, 137.9, 136.9, 135.1, 130.8, 128.9, 128.52, 128.49, 128.45, 128.37, 127.8, 127.1, 125.5, 124.3, 123.4, 113.2, 79.9, 70.6, 67.1, 54.5, 37.4, 28.3.

HRMS (EI) calcd for $C_{32}H_{33}NO_5S$ 543.20794; found 543.20752.

IV.8.2 Enantionselective Synthesis of 4-Hydroxynaphthyl Alanine

4-(*tert*-Butyldimethylsilyloxy)naphthalene-1-carbaldehyde (208)
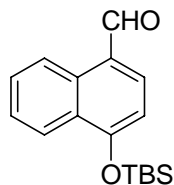
This compound has been synthesized by Dr. Sebastian Knör.

A solution of 4-hydroxynaphthalene-1-carbaldehyde (1.13 g, 6.56 mmol, 1.0 equiv) in dry THF (30 mL) was cooled to 0°C and sequentially imidazole (0.86 g, 12.6 mmol, 1.9 equiv) and *tert*-butyldimethylsilyl chloride (TBSCl) (1.72 g, 11.4 mmol, 1.7 equiv) were added. After stirring at room temperature for 18 h the reaction mixture was filtered and the solvent evaporated. The residue was taken up in EtOAc (100 mL) and washed with saturated aqueous NH_4Cl (40 mL), water (40 mL) and brine (40 mL) and dried over Na_2SO_4. The solvent was removed under reduced pressure and the residue purified by flash chromatography on silica gel (EtOAc/ hexane 1:20) yielding **208** (1.69 g, 88%) as a pale yellow solid.

R_f = 0.26 (EtOAc/hexane, 1:10)

mp 87-91°C

^{1}H-NMR (500 MHz, CDCl$_3$): δ = 10.23 (s, 1H), 9.31 (d, J = 8.5 Hz, 1H), 8.28 (d, J = 8.4 Hz, 1H), 7.87 (d, J = 7.9 Hz, 1H), 7.69 (dd, J = 7.4, 7.4 Hz, 1H), 7.58 (dd, J = 7.6, 7.6 Hz, 1H), 6.95 (d, J = 7.9 Hz, 1H), 1.11 (s, 9H), 0.37 (s, 6H).

^{13}C-NMR (63 MHz, CDCl$_3$): δ = 192.1, 158.0, 139.0, 132.5, 129.4, 127.7, 126.2, 125.2, 124.9, 122.9, 111.3, 25.7, 18.4, –4.2.

HRMS (EI) calcd for $C_{17}H_{22}O_2Si$ 286.13892; found 286.13885.

(*Z*)-Methyl 2-(benzyloxycarbonyl)amino-3-(1-(*tert*-butyldimethylsilyloxy) naphthalene-4-yl) acrylate (209)
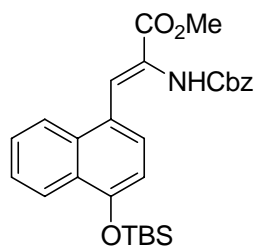
This compound has been synthesized by Dr. Sebastian Knör.

(MeO)₂P(O)CH(NHCbz)CO₂Me (1.10 g, 3.33 mmol, 1.5 equiv) was dissolved in dry CH_2Cl_2 (3 mL) and DBU (432 µL, 2.89 mmol, 1.3 equiv) was added. The mixture was stirred for 10 min at 0°C. Then, a solution of **208** (635 mg, 2.22 mmol, 1.0 equiv) in dry CH_2Cl_2 (3 mL) was added slowly *via* syringe and the reaction mixture was warmed to room temperature over 18 h. After the solvent was removed under reduced pressure, the residue was dissolved in EtOAc (50 mL), quickly washed with saturated aqueous NH_4Cl (2×20 mL) and brine (20 mL) and dried over Na_2SO_4. The solvent was evaporated and the crude product purified by flash chromatography on silica gel (EtOAc/hexane 1:4, 1% NEt₃) yielding **209** (948 mg, 87%) as a pale yellow oil.

R_f = 0.33 (EtOAc/hexane, 1:2)

¹H-NMR (360 MHz, CDCl₃): δ = 8.28-8.20 (m, 1H), 7.95-7.88 (m, 1H), 7.81 (s, 1H), 7.56-7.47 (m, 3H), 7.34-7.27 (m, 3H), 7.27-7.20 (m, 2H), 6.81 (d, J = 8.0 Hz, 1H), 6.25 (s, 1H), 5.06 (s, 2H), 3.86 (s, 3H), 1.11 (s, 9H), 0.32 (s, 6H).

¹³C-NMR (90 MHz, CDCl₃): δ = 165.6, 153.9, 153.0, 135.85, 133.0, 128.4, 128.1, 128.1, 128.1, 127.9, 127.3, 127.0, 125.5, 125.4, 123.9, 123.2, 123.2, 111.9, 67.3, 52.6, 25.8, 18.4, –4.2.

HRMS (EI) calcd for $C_{28}H_{33}NO_5Si$ 491.21280; found 491.21264.

(R/S)-N$^\alpha$-Acetyl-1-(4-*tert*-butyldimethylsilyloxy)naphthylalanine methyl ester (210)
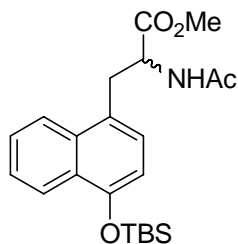
To a solution of **209** (0.28 g, 0.57 mmol, 1 equiv) in degassed MeOH (30 mL) palladium on charcoal (5% Pd/C, 0.12 g, 10mol% Pd) was added. Hydrogenation was carried out at 1 bar hydrogen pressure for 2 h. After the catalyst was removed by filtration, the solvent was removed under reduced pressure and the residue dissolved in dry DCM (10 mL). Ac₂O (60 µL, 0.68 mmol, 1.2 equiv) and NEt₃ (0.12 mL, 0.85 mmol, 1.5 equiv) were added and the mixture stirred for additional 18 h. The solvent was removed under reduced pressure, the residue taken up with EtOAc (50 mL) and subsequently washed with saturated aqueous NaHCO₃ (2×50 mL) and brine (50 mL) and dried over Na₂SO₄. After the solvent was removed under reduced pressure, the crude product was purified by flash chromatography on silica gel (EtOAc/hexane 1:1, 1% NEt₃) yielding **210** (194 mg, 76%) as a colorless solid.

R_f = 0.16 (EtOAc/hexane 1:1, 1% NEt₃)

mp 50-55°C

¹H-NMR (250 MHz, CDCl₃): δ = 8.24 (d, J = 7.9 Hz, 1H), 8.01 (d, J = 7.8 Hz, 1H), 7.57-7.43 (m, 2H), 7.08 (d, J = 7.8 Hz, 1H), 6.77 (d, J = 7.7 Hz, 1H), 5.99 (d, J = 7.7 Hz, 1H), 4.97 (m, 1H), 3.61 (s,

3H), 3.45 (dd, *J* = 13.9, 6.8 Hz, 1H), 3.45 (dd, *J* = 14.4, 6.1 Hz, 1H), 1.93 (s, 3H), 1.09 (s, 9H), 0.28 (s, 6H).

^{13}C-NMR (63 MHz, CDCl$_3$): δ = 172.4, 169.6, 151.2, 133.4, 128.1, 127.2, 126.4, 124.9, 124.7, 123.4, 123.2, 111.8, 53.2, 52.1, 34.6, 25.8, 23.0, 18.4, –4.2.

HRMS (EI) calcd for C$_{20}$H$_{23}$NO$_5$ 357.15762; found 357.15622.

(*R*)-*N*$^\alpha$-Acetyl-1-(4-hydroxy)naphthylalanines (212) and
(*S*)-1-(4-hydroxy)-naphthylalanine methyl ester (211)

To a solution of **210** (100 mg, 249 µmol, 1.0 equiv) in dry THF (7 mL) at 0°C tetrabutylammonium fluoride (82.5 mg, 261 µmol, 1.05 equiv) was added. After stirring for 15 min, a solution of lithium hydroxide (41.8 mg, 996 µmol, 4 equiv) in water (1.5 mL) was added and stirring was continued for additional 2 h at room temperature until complete conversion (TLC control). Thereafter, the solvent was removed under reduced pressure and the residue dissolved in water (10 mL) and adjusted to pH 7-8 by addition of 1N HCl. Acylase I (50 mg) was added and the mixture was stirred at 37°C until no further conversion was observed (2-3 h, HPLC monitoring). Additional acylase I (50 mg) was added and stirring continued for 1 h. The mixture was diluted with water (20 mL), acidified to pH 1 by addition of 1N HCl and extracted with EtOAc (5×20 mL).

The organic phase was dried over Na$_2$SO$_4$, the solvent removed under reduced pressure and the residue further purified by a short column of silica (MeOH/CHCl$_3$ 1:3, 1% AcOH) to give **212** (31 mg, 46%) as a colorless solid.

The aqueous phase was concentrated under reduced pressure and dried. The residue was suspended in dry MeOH (30 mL) and SOCl$_2$ (1 mL) was added drop wise at 0°C. After stirring for 24 h at room temperature the mixture was concentrated under reduced pressure, diluted with 1N NaOH (30 mL) and extracted with EtOAc (5×20 mL). The organic phase was dried over Na$_2$SO$_4$, the solvent removed under reduced pressure and the residue further purified by a short column of silica (MeOH/CHCl$_3$ 1:9, 1% NEt$_3$) to obtain a pale yellow oil which was dissolved in Et$_2$O and a minimum volume of dioxane. Addition of a 1M solution of HCl in ether (2 mL) gave **211** as a colorless solid which was filtered of and dried in *vacuo*.

(*S*)-1-(4-Hydroxy)naphthylalanine methyl ester (211)
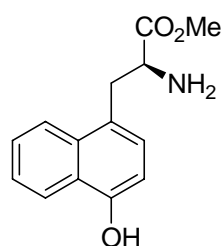
R_f = 0.50 (MeOH/CHCl$_3$ 1:9, 1% NEt$_3$)

$[\alpha]_D^{23}$ +5.2 (c 0.6, MeOH)

mp (**211***HCl) >240°C

^{1}H-NMR (250 MHz, CDCl$_3$): δ = 8.30 (d, J = 8.3 Hz, 1H), 7.94 (d, J = 8.3 Hz, 1H), 7.59 (dd, J = 7.5, 7.5 Hz, 1H), 7.48 (dd, J = 7.4, 7.4 Hz, 1H), 7.21 (d, J = 7.6 Hz, 1H), 6.80 (d, J = 7.6 Hz, 1H), 4.31 (dd, J = 7.4, 7.4 Hz, 1H), 3.80-3.63 (m, 4H), 3.41 (dd, J = 14.5, 8.5 Hz, 1H).

^{13}C-NMR (226 MHz, CDCl$_3$): δ = 175.8, 154.4, 134.3, 129.2, 127.5, 125.5, 124.2, 108.3, 56.1, 52.6, 38.3.

HRMS (EI) calcd for C$_{14}$H$_{15}$NO$_3$ 245.10519; found 245.10519.

(*R*)-*N* -Acetyl-1-(4-hydroxy)naphthylalanine (212)
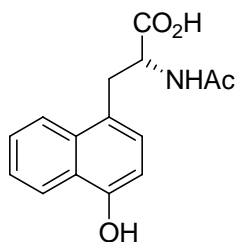
R_f = 0.31 (MeOH/CHCl$_3$ 1:1, 0.1% TFA)

$[\alpha]_D^{23}$ −1.7 (c 0.5, MeOH); mp 130-134°C

^{1}H-NMR (500 MHz, MeOH-d$_4$): δ = 8.23 (d, J = 8.3 Hz, 1H), 8.05 (d, J = 8.5 Hz, 1H), 7.51 (dd, J = 7.6, 7.6 Hz, 1H), 7.42 (dd, J = 7.5, 7.5 Hz, 1H), 7.17 (d, J = 7.7 Hz, 1H), 6.73 (d, J = 7.7 Hz, 1H), 4.74 (dd, J = 8.9, 5.2 Hz, 1H), 3.63 (dd, J = 14.3, 5.1 Hz, 1H), 3.21 (dd, J = 14.3, 9.0 Hz, 1H), 1.85 (s, 3H).

^{13}C-NMR (125 MHz, MeOH-d$_4$): δ = 175.4, 173.1, 154.0, 134.4, 128.8, 127.3, 126.8, 125.2, 125.1, 124.3, 124.0, 108.2, 55.0, 35.5, 22.3.

HRMS (EI) calcd for C$_{15}$H$_{15}$NO$_4$ 273.10010; found 273.10083.

IV.9 Integrin Ligands

IV.9.1 Synthesis of Highly Active and Selective α5β1 Integrin Ligands

1-bromo-2,6-dimethyl-4-isopropoxybenzene (213)
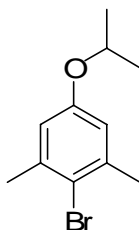
4-bromo-3,5-dimethylphenol (1.0 g, 5.0 mmol, 1 eq.) was dissolved in 60 mL dry DMF. After addition of K_2CO_3 (4.2 g, 15.0 mmol, 3 eq.), 2-bromopropane (3.1 g, 25.0 mmol, 5 eq.) and potassium iodide (2.5 g, 15.0 mmol, 3 eq.), the mixture was heated to $120°C$ and stirred for 8 h. After cooling to room temperature, DMF was removed under reduced pressure, the residue taken up in ethyl acetate, washed with water and brine, dried over Na_2SO_4, filtered and concentrated *in vacuo*. The crude product was purified by flash chromatography on silica gel (hexane/ethyl acetate 8:2) to give **213** (0.86 g, 3.5 mmol, 70%) as colorless oil.

RP-HPLC (10-100%): R_t = 30.67 min.

^{1}H-NMR (250 MHz, CDCl$_3$): δ = 6.69 (s, 2H), 4.53 (sept, ^3J = 6.1 Hz, 1H), 2.42 (s, 6H), 1.36 (d, ^3J = 6.1 Hz, 6H).

^{13}C-NMR (63 MHz, DMSO): δ = 156.3, 138.9, 117.9, 115.8, 69.9, 23.9, 22.0.

MS (EI): calcd for $C_{11}H_{15}BrO$ 242.0; found 242.2.

2,6-dimethyl-4-isopropoxybenzoic acid (214).
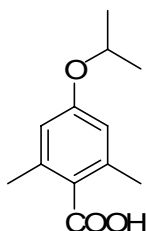
To a cooled (-78°C) solution of **213** in dry THF (0.86 g, 3.5 mmol, 1 eq.) *n*BuLi (1.6 M in THF, 2.6 mL, 4.2 mmol, 1.2 eq.) was added under an argon atmosphere. The resulting white suspension was stirred for 30 min. After addition of crushed dry ice (~10 g), the cooling bath was removed and the reaction mixture allowed to warm to room temperature. The mixture was acidified with 1M HCl and extracted with ethyl acetate. The organic layers were washed with brine, dried over Na_2SO_4, filtered and concentrated. Recrystallization from DCM / hexane gave 0.47 g (2.28 mmol, 65 %) of colorless crystals.

RP-HPLC (10-100%, 30 min): R_t = 19.42 min.

^{1}H-NMR (250 MHz, DMSO): δ = 12.78 (bs, 1H), 6.61 (s, 2H), 4.60 (sept, ^3J = 6.0 Hz, 1H), 2.25 (s, 6H), 1.24 (d, ^3J = 6.0 Hz, 6H).

^{13}C-NMR (62.9 MHz, DMSO): δ = 170.4, 157.3, 136.1, 127.3, 114.3, 68.8, 21.7, 19.8.

MS (EI): calcd for $C_{12}H_{16}O_3$ 208.1; found 208.1.

5-(9*H*-fluoren-9-yloxy)-1,3,4-oxadiazolidin-2-one (215)[313]
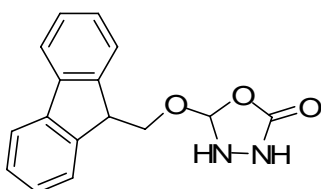
Fmoc-hydrazine hydrochloride (0.33 g, 1.28 mmol, 1 eq.) was suspended in 25 mL of DCM/saturated NaHCO$_3$ solution (1/1) in an ice-bath for five minutes under vigorous stirring. Stirring was stopped and the layers were allowed to separate for additional five minutes. 2 mL of a 1.9 M solution of phosgene in toluene (3.80 mmol, 3.0 eq.) were injected into the lower, organic phase and stirring was restarted for ten minutes. The organic layer was separated, the aqueous layer extracted twice with 10 mL DCM and the combined organic layers dried over Na$_2$SO$_4$, filtered and the filtrate concentrated under reduced pressure. The crude product was thoughtfully dried under vacuum and used without further purification. Yield: 0.32 g (1.13 mmol, 89%) of a colorless solid.

^{1}H-NMR (250 MHz, CDCl$_3$): δ = 7.77 (m, 2H), 7.61 (m, 2H), 7.37 (m, 4H), 4.51 (t, ^3J = 7.4 Hz, 1H), 4.40 (s, 2H).

Preparation of 3-[*N*-(*N*'-(3-(guanidylbenzoyl)-hydrazino)carbonyl]amino-2-(*S*)-(2,6-dimethyl-4-isopropoxybenzamido)propionic acid (217)
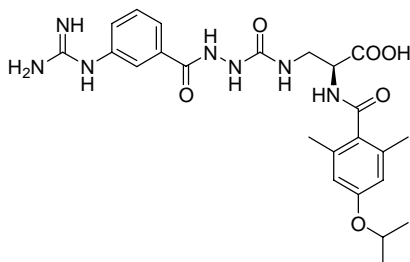
The title compound was synthesized from β-*N*-Alloc-α-*N*-Fmoc-diaminoproanoic acid according to following reaction sequence: a) Loading of 200 mg resin (theroretical loading 104 µmol, real loading ~67 µmol, GP1); b) Fmoc deprotection (GP2); c) Coupling of 2,6-dimethyl-4-isopropoxybenzoic acid with HATU (GP4), d) Alloc-deprotection (GP11); e) Formation of *aza*-glycine (GP13); f) Fmoc-deprotection (GP2); g) Coupling of *N*-Fmoc-3-aminobenzoic acid with

HATU (GP4); h) Fmoc-deprotection (GP2); i) Guadinylation (GP14), followed by cleavage from the resin (GP15). HPLC-purification yielded 6.3 mg (12.2 μmol, 9%) as colorless solid (TFA salt).

^{1}H-NMR (500 MHz, DMSO): δ = 10.21 (s, 1H), 9.94 (s, 1H), 8.33 (bs, 1H), 8.27 (s, 1H), 7.76 (d, *J* = 7.7 Hz, 1H), 7.7 (s, 1H), 7.54 (s, 1H), 7.41 (d, *J* = 7.8 Hz, 1H), 6.56 (s, 2H), 6.53 (bs, 1H), 4.59 (m, 1H), 4.38-4.34 (m, 1H), 3.57-3.52 (m, 1H), 2.20 (s, 6H), 1.23 (d, *J* = 5.9 Hz, 6H).

^{13}C-NMR (226.3 MHz, DMSO): δ = 172.9, 170.1, 166.4, 159.1, 157.8, 156.6, 136.9, 136.5, 134.9, 131.5, 130.7, 128.4, 126.2, 124.3, 115.0, 69.6, 54.1, 41.3, 22.7, 19.9.

HR-MS (ESI) cacld for $C_{24}H_{32}N_7O_6^+$ 514.2414; found: 514.2418.

Preparation of 3-[*N*-(*N*'-(3-(guanidylpropylcarbonyl)-hydrazino)carbonyl]amino-2-(*S*)-(2,6-dimethyl-4-isopropoxybenzamido)propionic acid (218)

The title compound was synthesized from β-*N*-Alloc-α-*N*-Fmoc-diaminoproanoic acid according to following reaction sequence: a) Loading of 100 mg resin (theroretical loading 104 μmol, real loading ~62 μmol, GP1); b) Fmoc deprotection (GP2); c) Coupling of 2,6-dimethyl-4-isopropoxybenzoic acid with HATU (GP4), d) Alloc-deprotection (GP11); e) Formation of *aza*-glycine (GP13); f) Fmoc-deprotection (GP2); g) Coupling of *N*-Fmoc-4-aminobutanoic acid with TBTU (GP3); h) Fmoc-deprotection (GP2); i) Guadinylation (GP14), followed by cleavage from the resin (GP15). HPLC-purification yielded 3.8 mg (6.9 μmol, 11%) as colorless solid (TFA salt).

^{1}H-NMR (500 MHz, DMSO): δ = 10.21 (s, 1H), 9.94 (s, 1H), 8.33 (bs, 1H), 8.27 (s, 1H), 7.76 (d, *J* = 7.7 Hz, 1H), 7.7 (s, 1H), 7.54 (s, 1H, Ar-*H*), 7.41 (d, *J* = 7.8 Hz, 1H), 6.56 (s, 2H), 6.53 (bs, 1H), 4.59 (m, 1H), 4.38-4.34 (m, 1H), 3.57-3.52 (m, 1H), 2.20 (s, 6H), 1.23 (d, *J* = 5.9 Hz, 6H).

^{13}C-NMR (226.3 MHz, DMSO): δ = 172.9, 170.1, 166.4, 159.1, 157.8, 156.6, 136.9, 136.5, 134.9, 131.5, 130.7, 128.4, 126.2, 124.3, 115.0, 69.6, 54.1, 41.3, 22.7, 19.9.

HR-MS (ESI) cacld for $C_{21}H_{34}N_7O_6^+$ 480.2571; found: 480.2583.

Preparation of 3-[*N*-(*N'*-(2-(guanidylethylcarbonyl)-hydrazino)carbonyl]amino-2-(*S*)-(2,6-dimethyl-4-isopropoxybenzamido)propionic acid (219)

The title compound was synthesized from β-*N*-Alloc-α-*N*-Fmoc-diaminoproanoic acid according to following reaction sequence: a) Loading of 200 mg resin (threoretical loading 104 μmol, real loading ~67 μmol, GP1); b) Fmoc deprotection (GP2); c) Coupling of 2,6-dimethyl-4-isopropoxybenzoic acid with HATU (GP4), d) Alloc-deprotection (GP11); e) Formation of *aza*-glycine (GP13); f) Fmoc-deprotecti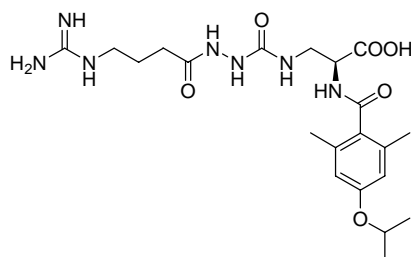on (GP2); g) Coupling of *N*-Fmoc-3-aminopropanoic acid with TBTU (GP3); h) Fmoc-deprotection (GP2); i) Guadinylation (GP14), followed by cleavage from the resin (GP15). HPLC-purification yielded 5.3 mg (11.4 μmol, 9%) as colorless solid (TFA salt).

^{1}H-NMR (900 MHz, DMSO): δ = 9.65 (s, 1H), 8.36 (bs, 1H), 8.06 (bs, 1H), 7.40 (s, 1H), 6.57 (s, 2H), 6.50 (bs, 1H), 4.59 (m, 1H), 4.37 (m, 1H), 3.50-3.46 (m, 2H), 2.51 (m, 2H), 2.37 (m, 2H), 2.19 (s, 6H), 1.23 (d, *J* = 5.7 Hz, 6H).

^{13}C-NMR (226.3 MHz, DMSO): δ = 136.3, 122.7, 115.0, 69.4, 56.8, 37.4, 35.3, 22.3, 19.6.

HR-MS (ESI) calcd for $C_{20}H_{32}N_7O_6^+$ 466.2414; found: 466.3540.

Preparation of 3-[*N*-(*N'*-(3-(guanidylpropylcarbonyl)-aminomethylen)carbonyl]amino-2-(*S*)-(2,6-dimethyl-4-isopropoxybenzamido)propionic acid (220)
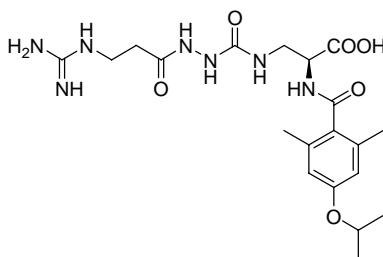

The title compound was synthesized from β-*N*-Alloc-α-*N*-Fmoc-diaminoproanoic acid according to following reaction sequence: a) Loading of 200 mg resin (threoretical loading 104 μmol, real loading ~67 μmol, GP1); b) Fmoc deprotection (GP2); c) Coupling of 2,6-dimethyl-4-isopropoxybenzoic acid with HATU (GP4), d) Alloc-deprotection (GP11); e) Coupling of Fmoc-glycine with TBTU (GP3); f) Fmoc-deprotection (GP2); g) Coupling of *N*-Fmoc-4-aminobutanoic acid with TBTU (GP3); h) Fmoc-deprotection (GP2); i) Guadinylation (GP14), followed by cleavage from the resin (GP15). HPLC-purification yielded 4.8 mg (9.4 μmol, 7%) as colorless solid (TFA salt).

^{1}H-NMR (900 MHz, DMSO): δ = 9.84 (s, 1H), 8.78 (bs, 1H), 8.05 (s, 1H), 7.76 (d, J = 7.7 Hz, 1H), 7.73 (s, 1H), 7.53 (m, 1H), 7.50 (s, 2H), 7.38 (d, J = 7.6 Hz, 1H), 6.58 (s, 2H), 4.59 (m, 1H), 3.88 (m, 1H), 3.84 (m, 1H), 3.48 (m, 2H), 3.42 (m, 2H), 2.19 (s, 6H), 1.23 (d, J = 5.9 Hz, 6H).

^{13}C-NMR (226.3 MHz, DMSO): δ = 169.6, 167.8, 167.0, 166.2, 157.5, 156.1, 136.3, 136.0, 131.2, 130.1, 125.6, 123.8, 117.3, 114.5, 69.3, 52.4, 43.0, 40.6, 22.2, 19.6.

HR-MS (ESI) calcd for $C_{22}H_{35}N_6O_6^+$ 479.2618; found: 479.3580.

Preparation of 3-[*N*-(*N*'-(3-(guanidylbenzoyl)-aminomethylen)carbonyl]amino-2-(*S*)-(2,6-dimethyl-4-isopropoxybenzamido)propionic acid (221)
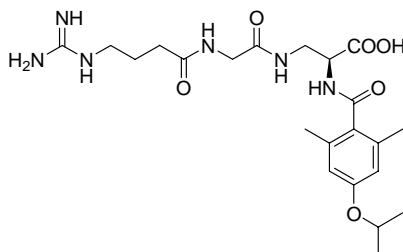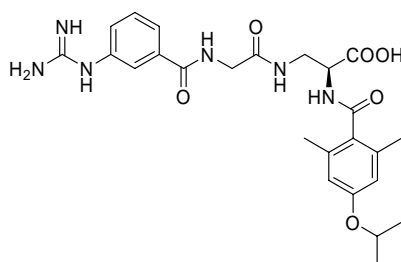

The title compound was synthesized from β-*N*-Alloc-α-*N*-Fmoc-diaminoproanoic acid according to following reaction sequence: a) Loading of 200 mg resin (theroretical loading 104 μmol, real loading ~67 μmol, GP1); b) Fmoc deprotection (GP2); c) Coupling of 2,6-dimethyl-4-isopropoxybenzoic acid with HATU (GP4), d) Alloc-deprotection (GP11); e) Coupling of Fmoc-glycine with TBTU (GP3); f) Fmoc-deprotection (GP2); g) Coupling of *N*-Fmoc-3-aminobenzoic acid with HATU (GP4); h) Fmoc-deprotection (GP2); i) Guadinylation (GP14), followed by cleavage from the resin (GP15). HPLC-purification yielded 6.2 mg (12.9 μmol, 10%) as colorless solid (TFA salt).

^{1}H-NMR (900 MHz, DMSO): δ = 8.32 (d, J = 7.7 Hz, 1H), 8.12 (t, 1H, J = 5.7 Hz, 1H), 7.92 (t, 1H, J = 5.7 Hz, 1H), 7.52 (bs, 1H), 7.28 (bs, 1H), 6.57 (s, 2H), 4.59 (m, 1H), 4.50 (m, 1H), 3.70 (m, 1H'), 3.63 (m, 1H'), 3.51 (m, 2H), 3.10 (dd, J = 6.7 Hz, J = 13.2 Hz, 2H), 2.19 (s, 6H), 2.18 (t, 2H), 1.69 (m, 2H), 1.23 (d, J = 6.0 Hz, 6H).

^{13}C-NMR (226.3 MHz, DMSO): δ = 172.5, 172.2, 169.9, 169.7, 157.4, 157.2, 136.3, 130.9, 114.6, 69.3, 52.3, 42.4, 40.8, 32.4, 25.1, 22.3, 19.6.

HR-MS (ESI) calcd for $C_{25}H_{33}N_6O_6^+$ 513.2462; found: 513.2469.

IV.9.2 Hydroxamic Acids as a New Class of Integrin Ligands

General Procedures for the synthesis of hydroxamic acids:

Boc-deprotection: The ligand precursor (**227** or **228**) was dissolved in 3 mL dioxane. 1 ml concentrated hydrochloric acid was added and the reaction mixture stirred for 1 h at room temperature. The solvents were evaporated.

Acylation:

a) by benzoyl chloride: The amine hydrochloride was re-dissolved in dioxane. 3 eq. NaHCO₃ were added, followed by 1.1 eq. benzoyl chloride. The mixture was stirred for 0.5 h and evaporated to dryness.

b) by sulfonic acid chlorides: The amine hydrochloride was dissolved in dry DCM. 5 eq. of DIPEA were added, followed by 1.2 eq. of the sulfonic acid chloride. The mixture was stirred over night and then evaporated to dryness.

c) by other aromatic carboxylic acids: The amine hydrochloride was dissolved in DMF. 1.2 eq. of the aromatic carboxylic acid and 1.2 eq. of HATU were added, followed by 5 eq. DIPEA. The mixture was stirred over night and then evaporated to dryness.

Saponification/aminolysis: The residue was dissolved in THF (0.1 M). 10 eq. of 50% aqueous NH₂OH solution were added, followed by 1 eq. LiOH. The resulting mixture was stirred at room temperature for 24h under HPLC-monitoring. After total consumption of the starting material, the solvents were evaporated and the product purified by RP-HPLC to give the desired hydroxamic acids along with the carboxylic acids as TFA salts.

Methyl 4-(4-benzyloxyphenyl)-3-(*S*)-(*tert*.butyloxycarbonylamino) butanoate (222)
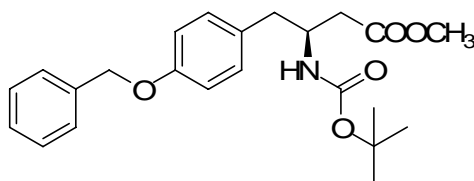
1. Preparation of diazomethane:

A 100 mL Erlenmeyer flask was filled with 35 mL of 40% aqueous KOH solution and 50 mL of diethyl ether and cooled to -5 - 0°C. 5.3 g *N*-methyl nitroso urea were added in portions keeping the temperature below 0°C at any time. After 1.5 h, the mixture was carefully converted into a separating funnel, the layers were separated and the organic layer dried for 3 h over KOH.

2. Preparation of 1-diazo-2-oxo-4-(4-benzyloxyphenyl)-3-(S)-(tert.butyloxycarbonyl)butane

A solution of Boc-Tyr(OBn)-OH (3.71 g, 10.0 mmol, 1 eq.) in 35 mL dry THF under an argon atmosphere was cooled to -15°C. After addition of TEA (2.9 mL, 20 mmol, 2 eq.) and ethyl chloroformate (1.05 mL, 11 mmol, 1.1 eq.), the colorless suspension was stirred for 0.5 h at -5°C. Subsequently, the reaction flask was opened and the freshly prepared diazomethane solution was

added carefully via a PP pipette. The yellow suspension was stirred at -15 - -5°C for 1 h. The reaction was quenched by addition of acetic acid (0.5 mL), followed by diethyl ether and saturated NaHCO$_3$ solution. The layers were separated and the organic layer washed with saturated NH$_4$Cl solution and brine, dried with Na$_2$SO$_4$, filtered and evaporated. The crude diazoketone was purified by flash column chromatography on silica gel (hexane/ethyl acetate 4:1) to give a yellow solid (3.91 g, 9.89 mmol, 99%).

HPLC (10-100%, 30 min): R$_t$ = 25.60 min.

^{1}H-NMR (250 MHz, CDCl$_3$): δ = 7.45-7.30 (m, 5H), 7.10 (d, ^3J = 8.5 Hz, 2H), 6.91 (d, ^3J = 8.5 Hz, 2H), 5.19 (bs, 1H), 5.03 (s, 1H), 5.04 (m, 2H), 4.36 (m, 1H), 2.96 (d, ^3J = 6.7 Hz, 2H), 1.42 (s, 9H).

3. Preparation of Methyl 4-(4-benzyloxyphenyl)-3-(S)-(tert.butyloxycarbonylamino) butanoate (223)

The diazoketone (3.91 g, 9.89 mmol, 1 eq.) was dissolved in 150 mL abs. MeOH and cooled to -25°C. Silver benzoate (228 mg, 1 mmol, 0.1 eq.) was dissolved in triethylamine (5.5 mL, 40 mmol, 4 eq.) and added dropwise to the diazoketon. The mixture was allowed to warm to room temperature over night. After evaporation of the solvent, the residue was taken up in ethyl acetate, washed with sat. NaHCO$_3$, 5% aqueous citric acid and brine, dried over Na$_2$SO$_4$ and filtered. After evaporation, the crude product was purified by flash column chromatography on silica gel (hexane/ethyl acetate 2:1) to give 3.94 g (9.87 mmol, 99%) of a colorless solid.

HPLC (10-100%, 30 min): R$_t$ = 26.41 min.

^{1}H-NMR (250 MHz, CDCl$_3$): δ = 7.45 - 7.29 (m, 5H), 7.09 (d, ^3J = 8.6 Hz, 2H), 6.91 (d, ^3J = 8.6 Hz, 2H), 5.05 (s, 2H), 4.11 (m, 1H), 4.94 (bs, 1H), 3.68 (s, 3H), 2.86 (dd, ^2J = 13.6 Hz, ^3J = 6.5 Hz, 1H), 2.75 (dd, ^2J = 13.6 Hz, ^3J = 7.6 Hz, 1H), 2.52 (dd, ^2J = 15.7 Hz, ^3J = 5.6 Hz, 1H), 2.43 (dd, ^2J = 15.7 Hz, ^3J = 5.7 Hz, 1H), 1.42 (s, 9H).

^{13}C-NMR (125 MHz, DMSO): δ = 172.0, 157.6, 155.1, 137.1, 130.3, 130.0, 128.5, 127.8, 127.3, 114.9, 79.3, 70.0, 51.5, 49.0, 39.5, 37.6, 28.3.

MS (ESI) calcd for C$_{23}$H$_{29}$NO$_5$ 399.2; found 422.2 [m+Na$^+$]$^+$, 366.4 [m+Na$^+$-^{t}Bu]$^+$, 300.4 [m+H$^+$-Boc]$^+$.

MS (EI): calcd. for C$_{23}$H$_{29}$NO$_5$ 399.2; found 399.1.

Methyl 4-(4-hydroxyphenyl)-3-(*S*)-(*tert*.butyloxycarbonylamino) butanoate, (Boc-β-Tyr-OMe) (223)
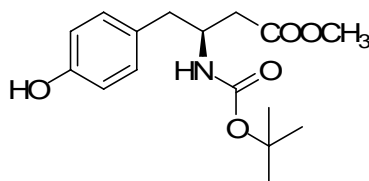
Benzyl ether **222** (3.94 g, 9.87 mmol) was hydrogenated according to GP16 (400 mg 5% Pd/C). After filtration over Celite® and evaporation of the solvents, the product was purified by flash

chromatography on silica gel (hexane / ethyl acetate 2 : 1) to give **223** (2.21 g, 7.14 mmol, 71%) as colorless solid.

HPLC (10-100%, 30 min): R_t = 18.54 min.

^{1}H-NMR (250 MHz, CDCl$_3$): δ = 7.15 (bs, 1H), 6.97 (d, ^3J = 8.3 Hz, 2H), 6.75 (d, ^3J = 8.4 Hz, 2H), 5.16 (d, ^3J = 7.6 Hz, 1H), 4.10 (m, 1H), 2.81 (dd, ^2J = 12.9 Hz, ^3J = 5.0 Hz, 1H), 2.68 (dd, ^2J = 13.3 Hz, ^3J = 7.7 Hz, 1H), 2.49 (dd, ^2J = 15.9 Hz, ^3J = 5.5 Hz, 1H), 2.39 (dd, ^2J = 15.8 Hz, ^3J = 6.1 Hz, 1H), 1.40 (s, 9H).

^{13}C-NMR (125 MHz, DMSO): δ = 172.3, 155.5, 155.1, 130.3, 128.7, 115.4, 79.8, 51.7, 49.1, 39.6, 37.5, 28.3.

MS (ESI) calcd. for C$_{16}$H$_{23}$NO$_5$ 309.2; found 310.2 [m+H$^+$].

3-(pyridin-2-ylamino)-1-(*tert.*butyldiphenylsilyloxy)propane (224)
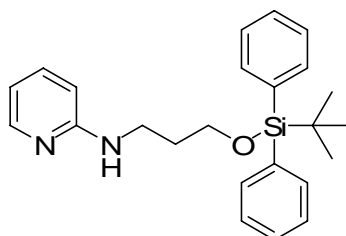
1. Preparation of 3-(pyridine-2-ylamino)propan-1-ol

2-Bromopyridine (5.2 g, 33 mmol) was dissolved in 3-aminopropan-1-ol (6.0 g, 80 mmol) and heated in a sealed glass tube to 140°C over night. After cooling to room temperature, the reaction mixture was directly subjected to column chromatography on silica gel. Purification by flash chromatography on silica gel (DCM/MeOH 95 : 5) gave 4.8 g (31.5 mmol, 95%) of a light brown oil.

HPLC (10-50%, 30 min): R_t = 8.75 min.

^{1}H-NMR (250 MHz, CDCl$_3$): δ = 7.99 (dd, ^3J = 5.1 Hz, ^4J = 1.0 Hz, 1H); 7.34 (ddd, ^3J = 8.6 Hz, ^3J = 7.1 Hz, ^4J = 1.9 Hz, 1H); 6.51 (ddd, ^3J = 7.0 Hz, ^3J = 5.2 Hz, ^4J = 0.8 Hz, 1H); 6.37 (d, ^3J = 8.4 Hz, 1H); 4.70 (bs, 1H); 4.60 (bs, 1H); 3.63 (m, 2H); 3.49 (dd, ^2J = 12.2 Hz, ^3J = 6.2 Hz, 2H); 1.73 (m, 2H).

^{13}C-NMR (75 MHz, CDCl$_3$): δ = 159.0, 147.4, 136.5, 111.2, 107.8, 58.7, 37.9, 32.4.

MS (ESI) calcd. for C$_8$H$_{12}$N$_2$O 152.1; found 153.0 [m+H$^+$].

*2. Preparation of 3-(pyridin-2-ylamino)-1-(tert.butyldiphenylsilyloxy)propane (**224**)*

To an ice-cooled solution of 3-(pyridine-2-ylamino)propan-1-ol (1.56 g, 10.3 mmol)in dry DCM (~0.1 - 0.2 M) imidazole (1.96 g, 28.8 mmol) followed by TBDPS chloride (3.5 mL, 13.4 mmol) was added under argon atmosphere. The resulting suspension was stirred at ambient temperature over night (TLC monitoring). The solvent was removed in vacuo and the resulting mixture directly

applied onto a silica gel. Purification by flash chromatography (hexane/ethyl acetate 7:3 + 1% TEA) gave 3.54 g (9.05 mmol, 88%) of a colorless oil.

HPLC (10-100%, 30 min): R_t = 23.68 min.

^{1}H-NMR (250 MHz, CDCl$_3$): δ = 8.08 (d, ^3J = 4.1 Hz, 1H), 7.69 (m, 4H), 7.70-7.68 (m, 7H), 6.54 (t, ^3J = 6.0 Hz, 1H), 6.33 (d, ^3J = 8.4 Hz, 1H), 3.82 (t, ^3J = 5.7 Hz, 2H), 3.44 (q, ^3J = 6.2 Hz, 2H), 1.87 (m, 2H), 1.10 (s, 9H).

^{13}C-NMR (63 MHz, CDCl$_3$): δ = 158.7, 147.9, 137.2, 135.5, 133.5, 129.6, 127.7, 112.4, 106.8, 62.1, 39.5, 31.9, 26.9, 19.1.

MS (ESI) calcd. for C$_{24}$H$_{30}$N$_2$OSi 390.2; found 391.2 [m+H$^+$]$^+$.

3-(*N-tert.*butyloxycarbonyl-*N*-pyridin-2-ylamino)1-(*tert.*butyldiphenylsilyloxy)propane (225)
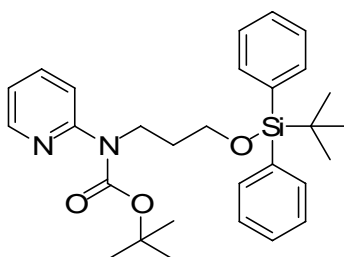
3-(pyridin-2-ylamino)-1-(tert.butyldiphenylsilyloxy)propane (**224**) (616 mg, 1.58 mmol) was dissolved in dry THF (~0.2 M). Boc-anhydride (379 mg, 1.73 mmol) was added, followed by TEA (657 μL, 4.74 mmol) and DMAP (20 mg, 0.16 mmol). Stirring was continued until the TLC indicated total consumption of the starting material (usually over night). The solvents were evaporated and the reaction mixture purified directly by flash column chromatography (hexane/ethyl acetate 8:2 + 1% TEA) to give **225** (696 mg, 1.42 mmol, 90%) as colorless oil.

HPLC (10-100%, 30 min): R_t = 25.38 min.

^{1}H-NMR (250 MHz, CDCl$_3$): δ = 8.37 (dd, ^3J = 5.0 Hz, ^4J = 1.6 Hz, 1H), 7.71 - 7.53 (m, 6H), 7.46-7.33 (m, 6H), 7.00 (ddd, ^3J = 6.6 Hz, ^3J = 4.9 Hz, ^4J = 1.5 Hz, 1H), 4.12 (m, 2H), 3.72 (t, ^3J = 6.3 Hz, 2H), 1.94 (m, 2H), 1.50 (s, 9H), 1.05 (s, 9H).

^{13}C-NMR (62.9 MHz, CDCl$_3$): δ = 154.7, 154.2, 147.6, 136.8, 135.5, 133.8, 129.5, 127.5, 120.1, 119.4, 80.8, 61.9, 44.3, 32.0, 28.3, 26.8, 19.1.

MS (ESI) calcd. for C$_{29}$H$_{38}$N$_2$O$_3$Si 490.3; found 513.2 [m+Na$^+$]$^+$, 391.4 [m+H$^+$-Boc]$^+$.

4-*N*-(pyridin-2-yl)-*N*-(*tert.*butyloxycarbonyl)aminobutan-1-ol (226)
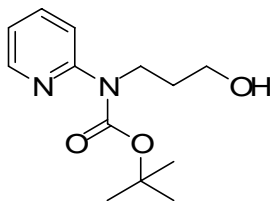
The TBDPS-protected alcohol (666 mg, 1.36 mmol) was dissolved in THF (~0.2 M). TBAF (473 mg, 1.50 mmol) was added and the reaction stirred for 12 h at ambient temperature. The solvents were evaporated and the alcohol purified directly by flash column chromatography (hexane/ethyl acetate 2:1) to give **226** (220 mg, 0.87 mmol, 63%) as light brown oil.

HPLC (10-100%, 30 min): R_t = 12.52 min.

^{1}H-NMR (250 MHz, CDCl$_3$): δ = 8.16 (dt, ^3J = 4.9 Hz, ^4J = 1.2 Hz), 7.49 (m, 2H), 6.87 (dd, ^3J = 8.8 Hz, ^3J = 4.5 Hz, 1H), 5.24 (t, ^3J = 6.8 Hz, 1H), 3.83 (t, ^3J = 6.0 Hz, 2H), 3.51 (q, ^3J = 6.2 Hz, 2H), 1.78 (m, 2H), 1.38 (s, 9H).

^{13}C-NMR (62.9 MHz, CDCl$_3$): δ = 155.0, 153.7, 146.6, 137.0, 119.3, 119.1, 81.1, 57.7, 44.0, 31.1, 27.9.

MS (ESI) calcd. for C$_{13}$H$_{20}$N$_2$O$_3$ 252.1; found 253.3 [m+H$^+$].

Methyl-4-[4-(3-*N*-pyridin-2-yl-3-*N*-(*tert.*butyloxycarbonylamino)propoxy)phenyl]-3-(*S*)-(tert.butyloxycarbonylamino) butanoate (227)
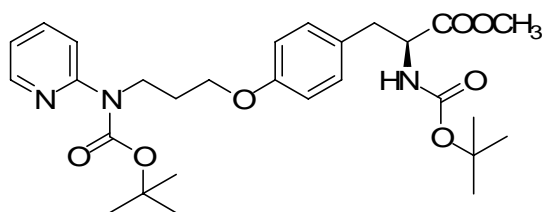
In a dried flask, Boc-Tyr-OMe (1.17 g, 3.97 mmol), the aminoalcohol **226** (1.2 g, 4.76 mmol) and tributylphosphine (1.3 mL, 5.16 mmol) were dissolved in dry THF (0.05 - 0.1 M) and stirred at 0°C under argon. Azodicarboxylic dipiperidid (ADDP, 1.3 g, 5.16 mmol) was dissolved in dry THF (0.2 M) and added dropwise to the reaction mixture over a period of 4 h. The resulting light yellow suspension was allowed to warm to room temperature overnight. After addition of silica gel and evaporation of the THF, the product was purified by flash column chromatography (DCM/ethyl acetate 7:3) to give **227** (418 mg, 790 µmol, 40%) as a colorless foam.

HPLC (10-100%, 30 min): R_t = 24.25 min.

^{1}H-NMR (250 MHz, CDCl$_3$): δ = 8.31 (dt, ^3J = 4.8 Hz, ^4J = 1.3 Hz, 1H), 7.59 - 7.57 (m, 2H), 7.00-6.94 (m, 3H), 6.74 (d, ^3J = 8.6 Hz, 2H), 4.96 (d, ^3J = 7.8 Hz, 1H), 4.51 (m, 1H), 4.12 (t, ^3J = 7.0 Hz, 2H), 3.96 (t, ^3J = 6.3 Hz, 2H), 3.68 (s, 3H), 2.98 (m, 2H), 2.10 (m, 2H), 1.47 (s, 9H), 1.40 (s, 9H).

^{13}C-NMR (62 MHz, CDCl$_3$): δ = 172.3, 158.0, 155.0, 154.4, 154.1, 147.6, 136.8, 130.1, 127.6, 119.8, 119.4, 114.3, 82.0, 81.0, 79.8, 65.5, 44.0, 37.3, 28.8, 28.2, 28.1.

MS (ESI) calcd. for C$_{28}$H$_{39}$N$_3$O$_7$ 529.3; found 530.1 [m+H$^+$]$^+$.

(S)-3-*tert*-Butoxycarbonylamino-4-{4-[3-(*tert*-butoxycarbonyl-pyridin-2-yl-amino)-propoxy]-phenyl}-butyric acid methyl ester (228)

In a dried flask, Boc-β-Tyr-OMe (**223**) (261 mg, 825 μmol), the aminoalcohol **226** (152 mg, 1.0 mmol) and tributylphosphine (264 μL, 1.07 mmol) were dissolved in dry THF (0.05 - 0.1 M) and stirred at 0°C under argon. Azodicarboxylic dipiperidid (ADDP, 269 mg, 1.07 mmol) was dissolved in dry THF (0.2 M) and added dropwise to the reaction mixture in 4 h time. The resulting light yellow suspension was allowed to warm to room temperature overnight. After addition of silica gel and evaporation of the THF, the product was purified by flash column chromatography (DCM/ethyl acetate 2:1) to give **228** (106 mg, 244 μmol, 30%) as a colorless foam.

HPLC (10-100%, 30 min): R_t = 23.86 min.

^{1}H-NMR (250 MHz, CDCl$_3$): δ = 8.03 (d, ^3J = 7.6 Hz, 1H); 7.36 (m, 1H); 7.06 (d, ^3J = 8.4 Hz, 2H); 6.80 (d, ^3J = 8.4 Hz, 2H); 6.52 (dd, ^3J = 5.2 Hz, ^3J = 6.9 Hz, 1H); 6.37 (d, ^3J = 8.4 Hz, 1H); 5.05 (bs, 1H), 4.95 (bs, 1H); 4.08 (m, 1H); 4.05 (t, ^3J = 5.9 Hz, 2H); 3.65 (s, 3H); 3.46 (m, 2H); 2.84 (m, 2H); 2.71 (dd, ^2J = 13.6 Hz, ^3J = 7.7 Hz, 1H), 2.44 (m, 2H); 2.07 (m, 2H); 1.39 (s, 18H, ^{t}Bu).

^{13}C-NMR (63 MHz, CDCl$_3$): δ = 178.0, 158.6, 157.5, 155.0, 147.8, 137.4, 130.2, 129.8, 114.4, 112.6, 106.6, 79.2, 65.7, 51.6, 48.9, 39.4, 39.3, 37.3, 29.0, 28.3.

MS (ESI) calcd. for C$_{29}$H$_{41}$N$_3$O$_7$ 543.3; found 566.1 [m+Na]$^+$, 444.1 [m+H-Boc]$^+$.

2-(*S*)-Benzamido-3-(4-(3-pyridin-2-ylaminopropoxy)phenyl)propionic acid (229) and

N-hydroxy-(2-(*S*)-benzamido-3-(4-(3-pyridin-2-ylaminopropoxy)phenyl))-propionamide (230)
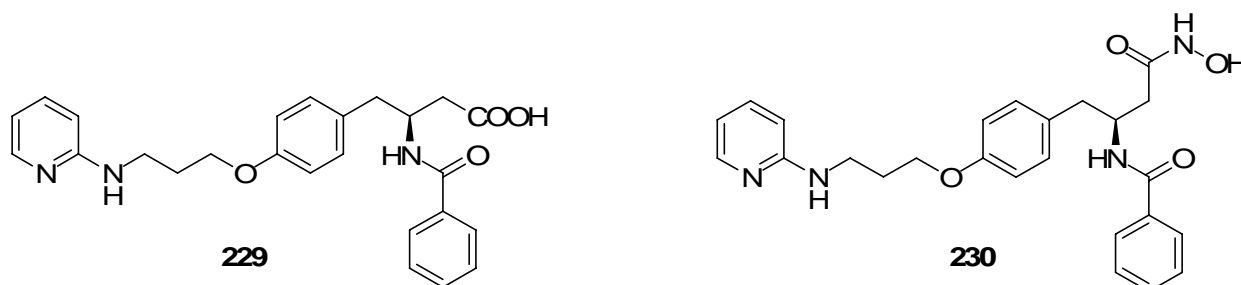
Both compounds were prepared from methyl 2-(*S*)-*tert.*butyloxycarbonylamino-3-(4-(3-pyridin-2-ylaminopropoxy)phenyl)propionate (**227**) (19 mg, 45 μmol) according to the GP. Yield after purification: 2.15 mg (5.1 μmol, 11 %) **229** and 1.99 mg (4.6 μmol, 10%) **230**.

Analytical data **229**:

^{1}H-NMR (500 MHz, DMSO): δ = 13.32 (bs, 1H), 12.77 (bs, 1H), 8.71 (bs, 1H), 8.66 (d, J = 8.2 Hz, 1H), 7.89 (d, J = 6.1 Hz, 1H), 7.83 (t, J = 7.9 Hz, 1H), 7.80 (d, J = 7.5 Hz, 2H), 7.52 (t, J = 7.3 Hz,

1H), 7.45 (t, *J* = 7.6 Hz, 2H), 7.23 (d, *J* = 8.5 Hz, 2H), 7.00 (d, *J* = 9.0 Hz, 1H), 6.83 (d, *J* = 8.6 Hz, 2H), 6.80 (t, *J* = 6.8 Hz, 1H), 4.57 (m, 1H), 4.01 (t, *J* = 6.0 Hz, 2H), 3.45 (t, *J* = 6.2 Hz, 2H), 3.12 (dd, *J* = 13.8 Hz, *J* = 4.3 Hz, 1H), 3.00 (dd, 1H, *J* = 13.7 Hz, *J* = 10.9 Hz, 1H), 2.01 (m, 2H).

^{13}C-NMR (125 MHz, DMSO): δ = 173.1, 166.2, 156.8, 152.9, 142.4, 136.5, 133.8, 131.2, 130.1, 129.9, 128.1, 127.2, 114.0, 112.7, 111.7, 64.6, 54.3, 39.4, 38.5, 35.4, 27.6.

HR-MS (ESI) calcd. for $C_{24}H_{26}N_3O_4^+$ 420.1918; found 420.1909.

Analytical data **230**:

^{1}H-NMR (500 MHz, DMSO): δ = 10.78 (s, 1H), 8.60 (d, *J* = 6.7 Hz, 1H), 7.89 (d, *J* = 9.8 Hz, 1H), 7.81 (m, 3H), 7.51 (t, *J* = 7.0 Hz, 1H), 7.44 (t, *J* = 7.5 Hz, 2H), 7.24 (d, *J* = 8.6 Hz, 2H), 6.99 (d, *J* = 8.2 Hz, 1H), 6.81 (m, 3H), 4.54 (m, 1H), 4.01 (t, *J* = 6.0 Hz, 2H), 3.45 (t, *J* = 6.2 Hz, 2H), 2.96 (m, 2H), 2.01 (m, 2H).

^{13}C-NMR (125 MHz, DMSO): δ = 171.3, 162.7, 160.5, 159.3, 146.1, 142.2, 137.7, 134.6, 132.4, 129.5, 121.9, 120.3, 114.1, 103.1, 85.1, 71.2, 68.9, 67.9, 65.1, 42.3, 33.1.

HR-MS (ESI) calcd. for $C_{24}H_{27}N_4O_4^+$ 435.2027; found 435.2011.

2-(*S*)-(2,4,6-trimethylbenzamido)-3-(4-(3-pyridin-2-ylaminopropoxy)phenyl)propionic acid (231) and

N-hydroxy-(2-(*S*)-(2,4,6-trimethylbenzamido)-3-(4-(3-pyridin-2-ylaminopropoxy) phenyl))propionamide (232)
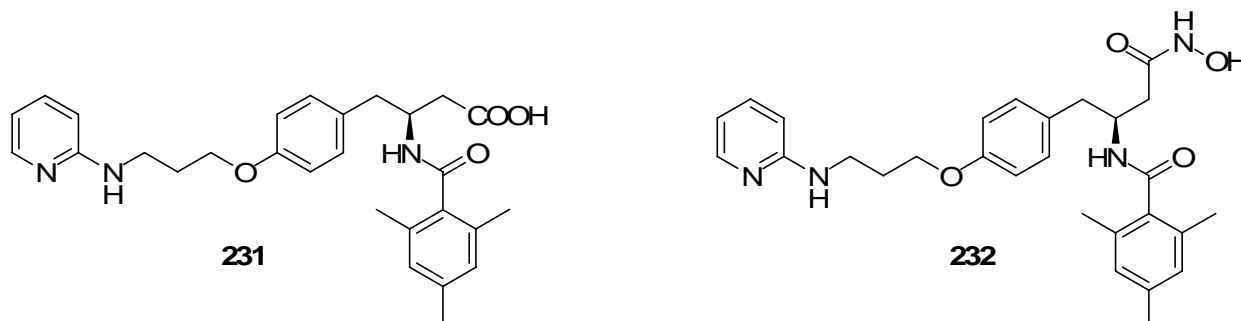
Both compounds were prepared from methyl 2-(*S*)-*tert.*butyloxycarbonylamino-3-(4-(3-pyridin-2-ylaminopropoxy)phenyl)propionate (**227**) (8.6 mg, 20 μmol) according to GP. Yield after purification: 2.81 mg (5.90 μmol, 30 %) **231** and 0.94 mg (1.97 μmol, 10%) **232**.

Analytical data **231**:

^{1}H-NMR (500 MHz, DMSO): δ = 15-12 (bs, 1H), 8.86 (bs, 1H), 8.47 (d, *J* = 7.6 Hz, 1H), 7.93 (m, 1H), 7.89 (m, 1H), 7.21 (d, *J* = 7.0 Hz, 2H), 7.06 (d, *J* = 8.1 Hz, 1H), 6.85 (d, *J* = 6.6 Hz, 3H), 6.75 (s, 2H), 4.62 (m, 1H), 4.05 (m, 2H), 3.48 (m, 2H), 3.10 (d, *J* = 13.3 Hz, 1H), 2.79 (t, *J* = 12.2 Hz, 1H), 2.20 (s, 3H, CH₃), 2.05 (m, 2H), 1.93 (s, 6H).

^{13}C-NMR (125 MHz, DMSO): δ = 173.1, 169.1, 156.9, 152.8, 142.7, 136.9, 136.1, 135.3, 133.7, 130.0, 127.3, 114.1, 113.1, 111.8, 64.7, 53.4, 38.6, 35.4, 27.5, 20.5, 18.4.

HR-MS (ESI) calcd. for $C_{27}H_{32}N_3O_4^+$ 462.2387; found 462.2382.

Analytical data **232**:

¹H-NMR (500 MHz, DMSO): ¹H-NMR (500 MHz, DMSO): δ = 10.70 (d, *J* = 12.2 Hz, 1H), 8.36 (d, *J* = 8.5 Hz, 1H), 8.32 (m, *J* = 8.4 Hz,1H), 7.94 (d, *J* = 5.0 Hz, 1H), 7.20 (m, 1H), 7.08 (d, *J* = 8.2 Hz, 1H), 6.85 (d, *J* = 8.7 Hz, 1H), 6.75 (d, *J* = 7.2 Hz, 2H), 6.65 (d, *J* = 8.4 Hz, 1H), 4.53 (m, 1H), 4.04 (m, 2H), 2.78 (m, 2H), 2.19 (s, 3H), 2.02 (m, 2H), 1.94 (s, 6H).

¹³C-NMR (125 MHz, DMSO): δ = 180.2, 178.2, 172.9, 162.3, 160.3, 158.9, 157.1, 146.6, 145.2, 133.8, 86.9, 84.5, 83.9, 71.3, 70.6, 68.7, 63.3 43.1, 41.7, 30.7, 29.7.

HR-MS (ESI) calcd. for $C_{27}H_{33}N_4O_4^+$ 477.2496; 477.2479.

2-(*S*)-(phenylsulfonamido)-3-(4-(3-pyridin-2-ylaminopropoxy)phenyl)propionic acid (233) and *N*-hydroxy-(2-(*S*)-(phenylsulfonamido)-3-(4-(3-pyridin-2-ylaminopropoxy)phenyl))propionamide (234)
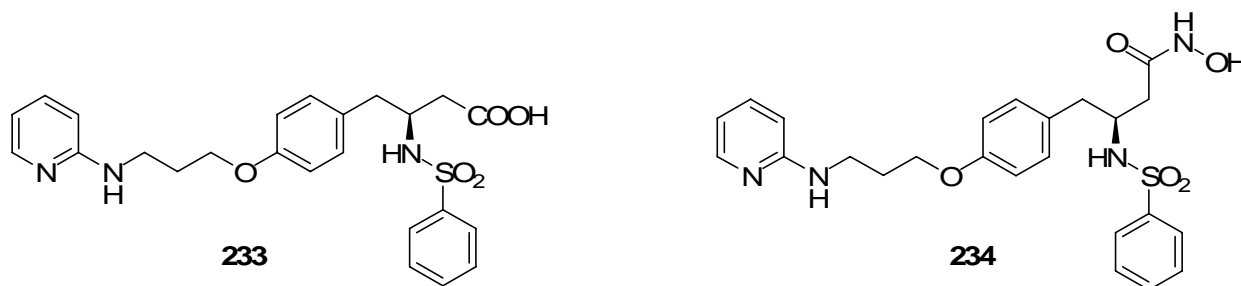
Both compounds were prepared from methyl 2-(*S*)-*tert.*butyloxycarbonylamino-3-(4-(3-pyridin-2-ylaminopropoxy)phenyl)propionate (**227**) (25 mg, 53 μmol) according to the GP. Yield after purification: 12 mg (26 μmol, 50 %) **233** and 7.5 mg (16 μmol, 30%) **234**.

Analytical data **233**:

¹H-NMR (500 MHz, DMSO): δ = 12.74 (bs, 1H), 8.70 (bs, 1H), 8.22 (d, *J* = 9.0 Hz, 1H), 7.92 (d, *J* = 5.6 Hz, 1H), 7.85 (ddd, *J* = 8.4 Hz, *J* = 7.2 Hz, *J* = 1.4 Hz, 1H), 7.58 (dd, *J* = 8.2 Hz, *J* = 1.0 Hz, 2H), 7.53 (tt, *J* = 7.4 Hz, *J* = 1.1 Hz, 1H), 7.43 (t, *J* = 7.7 Hz, 2H), 7.03 (d, *J* = 8.6 Hz, 3H), 6.82 (t, *J* = 6.4 Hz), 6.76 (d, *J* = 8.6 Hz, 2H), 4.03 (t, *J* = 6.1 Hz), 3.82 (dt, *J* = 9.0 Hz, *J* = 5.7 Hz, 1H), 3.49 (t, *J* = 6.3 Hz, 1H), 2.87 (dd, *J* = 13.8 Hz, *J* = 5.6 Hz, 1H), 2.63 (dd, *J* = 13.8 Hz, *J* = 9.0 Hz, 1H), 2.05 (m, 2H).

¹³C-NMR (125 MHz, DMSO): δ = 172.1, 157.0, 153.1, 142.3, 141.0, 136.7, 131.9, 130.1, 128.6, 126.1, 114.0, 112.8, 111.8, 64.6, 57.5, 39.4, 38.5, 36.9, 27.6.

HR-MS (ESI) calcd. for $C_{23}H_{26}N_3O_5S^+$ 456.2387; found 456.1588.

Analytical data **234**:

¹H NMR (500 MHz, DMSO): δ = 10.58 (s, 1H), 8.84 (br s, 1H), 8.16 (d, *J* = 9.0 Hz, 1H), 7.93 (d, *J* = 5.0 Hz, 1H), 7.57 (m, 1H), 7.52 (m, 1H), 7.42 (t, *J* = 7.7 Hz, 1H), 6.95 (d, *J* = 8.0 Hz, 1H), 6.72 (d, *J* = 8.9 Hz, 1H), 4.01 (m, 2H), 3.45 (m, 2H), 2.71 (m, 1H), 2.55 (m, 1H), 2.02 (m, 2H).

¹³C NMR (125 MHz, DMSO): δ = 171.9, 158.6, 150.8, 146.2, 142.7, 136.8, 129.8, 127.8, 125.8, 125.1, 129.7, 84.5, 72.4, 69.6, 68.4, 57.1, 49.8, 41.5, 31.6.

HR-MS (ESI) calcd. for $C_{23}H_{27}N_4O_5S^+$ 471.1697; found 471.1704.

2-(*S*)-(2,4,6-trimethylphenylsulfonamido)-3-(4-(3-pyridin-2-ylaminopropoxy)phenyl)propionic acid (235) and

***N*-hydroxy-(2-(*S*)-(2,4,6-trimethylphenylsulfonamido)-3-(4-(3-pyridin-2-ylaminopropoxy)-phenyl))propionamide (236)**
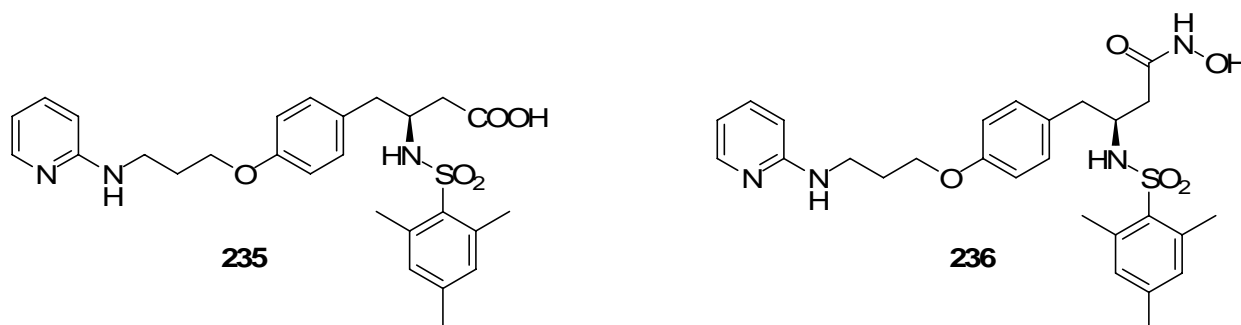
Both compounds were prepared from methyl 2-(*S*)-*tert.*butyloxycarbonylamino-3-(4-(3-pyridin-2-ylaminopropoxy)phenyl)propionate (**227**) (25 mg, 58 µmol), 2,4,6-timethylphenylsulfonic acid chloride (14.5 mg, 70 µmol) and DIPEA (50 µL, 290 µmol) according to the GP. Yield after purification: 6.6 mg (13.3 µmol, 23 %) **235** and 3.27 mg (6.4 µmol, 11 %) **236**.

Analytical data **235**:

^{1}H-NMR (500 MHz, DMSO): δ = 8.86 (bs, 1H), 8.00 (d, *J* = 9.5 Hz, 1H), 7.93 (d, *J* = 6.1 Hz, 1H), 7.88 (t, *J* = 8.0 Hz, 1H), 7.06 (d, *J* = 9.0 Hz, 1H), 6.96 (d, *J* = 8.4 Hz, 2H), 6.85 (s, 2H), 6.85 (m, 1H), 6.65 (d, *J* = 8.4 Hz, 2H), 4.02 (t, *J* = 6.1 Hz, 2H), 3.70 (dt, *J* = 5.3 Hz, *J* = 9.4 Hz, 1H), 3.49 (t, *J* = 6.4 Hz, 2H), 2.85 (dd, *J* = 13.8 Hz, *J* = 5.2 Hz, 1H), 2.66 (dd, *J* = 13.8 Hz, *J* = 9.6 Hz, 1H), 2.41 (s, 6H), 2.21 (s, 3H), 2.05 (m, 2H).

^{13}C-NMR (125 MHz, DMSO): δ = 172.4, 156.9, 152.8, 142.7, 140.8 , 138.0, 136.1 134.4, 131.2, 129.7, 128.7, 113.8, 113.0, 111.8, 64.5, 57.0, 38.6, 36.7, 27.6, 22.4, 20.2.

HR-MS (ESI) calcd. for $C_{26}H_{32}N_3O_5S^+$ 498.2057; found 498.2049.

Analytical data **236**:

^{1}H-NMR (500 MHz, DMSO): δ =10.54 (s, 1H), 8.84 (s, 1H), 7.89 (m, 2H), 7.80 (d, *J* = 9.3 Hz, 2H), 6.87 (d, *J* = 7.2 Hz, 3H), 6.79 (s, 2H), 6.60 (d, *J* = 8.6 Hz, 2H), 3.98 (m, 2H), 3.61 (m, 1H), 3.44 (m, 2 H), 2.67 (m, 1H), 2.61 (m, 1H), 2.38 (s, 6H), 2.18 (s, 3H), 2.02 (m, 3H), 1.22 (m, 2H).

^{13}C-NMR (225 MHz, DMSO): δ =138.6, 135.2, 131.7, 130.2, 114.2, 112.2, 65.6, 55.7, 38.1, 23.5, 20.8.

HR-MS (ESI) calcd. for $C_{26}H_{33}N_4O_5S^+$ 513.2166; found 513.2179.

2-(*S*)-(2,6-dimethyl-4-isopropoxybenzamido)-3-(4-(3-pyridin-2-ylaminopropoxy)phenyl) propionic acid (237) and

2-(*S*)-(2,6-dimethyl-4-isopropoxybenzamido)-3-(4-(3-pyridin-2-ylaminopropoxy)phenyl)-propanehydroxamic acid (238)
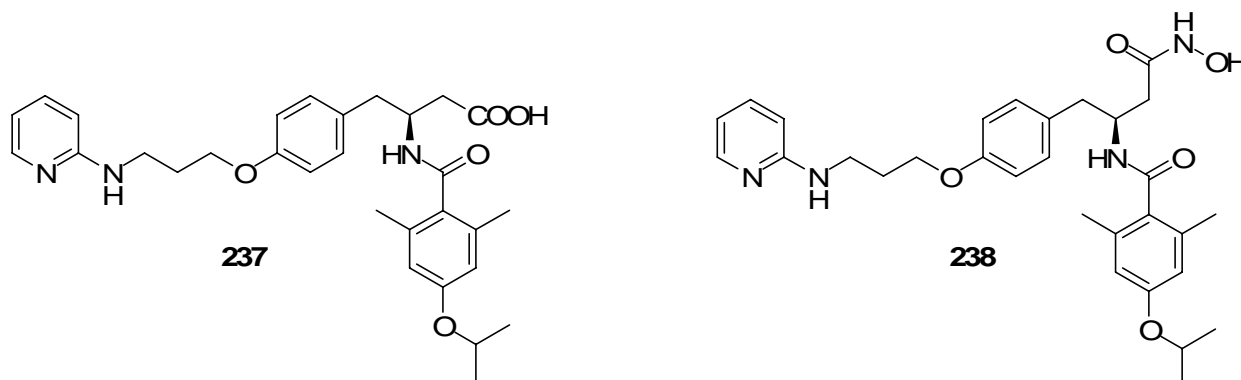
These compounds have been synthesized by Dr. Dominik Heckmann.

Both compounds were prepared from methyl 2-(*S*)-*tert.*butyloxycarbonylamino-3-(4-(3-pyridin-2-ylaminopropoxy)phenyl)propionate (**227**) (25 mg, 58 μmol), 2,6-dimethyl-4-isopropoxybenzoic acid **214** (14 mg, 70 μmol), HATU (24 mg, 70 μmol) and DIPEA (50 μL, 290 μmol) according to the GP. Yield after purification: 4.1 mg (8.2 μmol, 14 %) **237** and 2.71 mg (5.2 μmol, 9 %) **238**.

Analytical data **237**:

^{1}H-NMR (500 MHz, DMSO): δ = 12.70 (bs), 8.74 (bs), 8.45 (d, *J* = 8.3 Hz, 1H), 7.92 (d, *J* = 5.8 Hz, 1H), 7.86 (t, *J* = 7.7 Hz, 1H), 7.20 (d, *J* = 8.3 Hz, 2H), 7.03 (d, *J* = 8.9 Hz, 1H), 6.85 (d, *J* = 8.3 Hz, 2H), 6.83 (t, *J* = 6.7 Hz, 1H), 6.50 (s, 2H), 4.60 (m, 1H), 4.55 (m, 1H), 4.05 (t, *J* = 5.1 Hz, 2H), 3.47 (m, 2H), 3.09 (dd, *J* = 13.8 Hz, *J* = 3.5 Hz, 1H), 2.79 (dd, *J* = 13.4 Hz, *J* = 11.7 Hz, 1H), 2.04 (m, 2H), 1.94 (s, 6H).

^{13}C-NMR (125 MHz, DMSO): δ = 173.1, 169.0, 156.9, 156.7, 152.9, 142.5, 136.6, 135.5, 130.7, 130.0, 130.0, 114.1, 113.8, 113.1, 111.8, 68.7, 64.7, 53.4, 39.4, 38.5, 27.5, 21.7, 18.7.

HR-MS (ESI) calcd. for $C_{27}H_{32}N_3O_5^+$ 506.2649; found 506.2645.

Analytical data **238**:

^{1}H-NMR (500 MHz, DMSO): δ = 10.69 (s, 1H), 8.34 (d, *J* = 8.5 Hz, 1H), 7.92 (d, *J* = 5.7 Hz, 1H), 7.88 (d, *J* = 7.9 Hz, 1H), 7.21 (d, *J* = 5.0 Hz, 2H), 7.05 (d, *J* = 5.9 Hz, 1H), 6.85 (m, 3H), 6.49 (s, 2H), 4.55 (m, 2H), 4.05 (m, 2H), 3.48 (m, 2H), 2.82 (m, 2H), 2.05 (m, 2H), 1.92 (m, 6H), 1.22 (d, *J* = 3.0 Hz, 6H).

^{13}C-NMR (125 MHz, DMSO): δ =179.4, 176.7, 159.8, 158.5, 146.3, 133.6, 129.6, 86.3, 84.5, 68.1, 67.5, 62.8, 45.5, 41.5, 30.1, 29.4.

HR-MS (ESI) calcd. for $C_{27}H_{33}N_4O_5^+$ 521.2758; found 521.2763.

3-(*S*)-benzamido-4-(4-(3-pyridin-2-ylaminopropoxy)phenyl)butanoic acid (239) and

***N*-hydroxy-(3-(*S*)-benzamido-4-(4-(3-pyridin-2-ylaminopropoxy)phenyl))butyramide (240)**
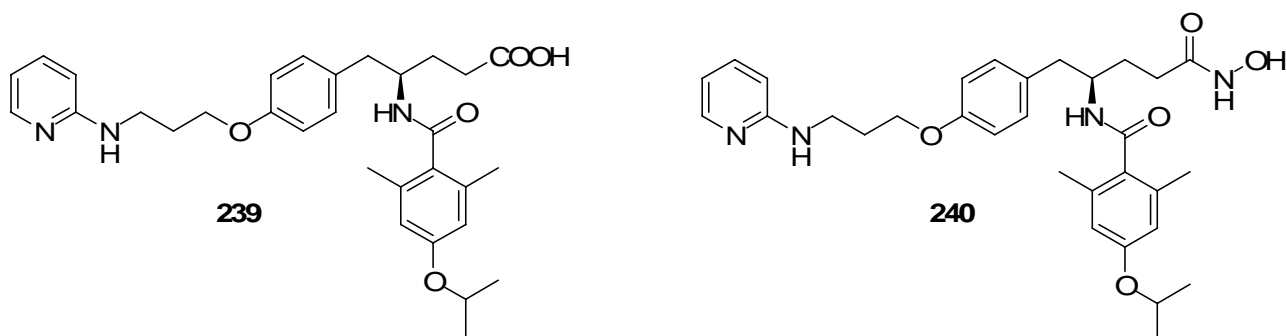
Both compounds were prepared from methyl 3-(*S*)-*tert.*butyloxycarbonylamino-4-(4-(3-pyridin-2-ylaminopropoxy)phenyl)butylate (**228**) (19 mg, 44 μmol) according to the GP. Yield after purification: 2 mg (5 μmol, 12 %) **239** and 2 mg (5 μmol, 11 %) **240**.

Analytical data **239**:

^{1}H-NMR (500 MHz, DMSO): δ = 12.26 (bs, 1H), 8.82 (bs, 1H), 8.32 (d, 1H, *J* = 8.4 Hz, 1H), 7.91 (d, *J* = 6.1 Hz, 1H), 7.85 (t, *J* = 7.9 Hz, 1H), 7.76 (d, *J* = 7.2 Hz, 2H), 7.50 (t, *J* = 7.3 Hz, 1H), 7.44 (t, *J* = 7.5 Hz, 2H), 7.14 (d, *J* = 8.5 Hz, 2H), 7.03 (d, *J* = 9.0 Hz), 6.83 (d, *J* = 8.5 Hz, 2H), 6.81 (t, *J* = 6.5 Hz, 1H), 4.44 (m, 1H), 4.02 (t, *J* = 6.0 Hz, 2H), 3.47 (t, *J* = 6.5 Hz, 2H), 2.82 (dd, *J* = 13.6 Hz, *J* = 8.0 Hz, 1H), 2.76 (dd, *J* = 13.6 Hz, *J* = 5.9 Hz, 1H), 2.53 (dd, *J* = 15.5 Hz, *J* = 7.7 Hz, 1H), 2.44 (dd, *J* = 15.4 Hz, *J* = 6.2 Hz, 1H), 2.02 (m, 2H).

^{13}C-NMR (125 MHz, DMSO): δ = 172.3, 165.5, 156.7, 152.9, 142.6, 136.3, 134.6, 130.9, 130.8, 130.0, 128.0, 127.0, 114.1, 112.9, 111.7, 64.6, 48.3, 38.8, 38.7, 38.5, 27.6.

HR-MS (ESI) calcd. for $C_{25}H_{28}N_3O_4^+$ 434.2074; found 434.2076.

Analytical data **240**:

^{1}H-NMR (500 MHz, DMSO): δ = 10.43 (s, 1H), 8.77 (bs, 1H), 8.23 (d, *J* = 6.8 Hz, 1H), 7.89 (d, *J* = 6.8 Hz, 1H), 7.75 (d, *J* = 6.8 Hz, 2H), 7.50 (t, *J* = 7.2 Hz, 1H), 7.44 (t, *J* = 7.5 Hz, 2H), 7.13 (d, *J* = 8.5 Hz, 2H), 6.92 (d, *J* = 6.9 Hz, 1H), 6.82 (d, *J* = 9.8 Hz, 2H), 6.76 (t, *J* = 6.5 Hz, 1H), 4.43 (m, 1H), 4.01 (t, *J* = 6.0 Hz, 2H), 3.43 (m, 2H), 2.76 (m, 2H), 2.30 (m, 1H), 2.22 (m, 1H), 2.01 (m, 2H).

^{13}C-NMR (125 MHz, DMSO): δ = 170.7, 166.2, 159.9, 158.7, 152.4, 149.8, 149.3, 133.7, 124.4, 114.9, 107.1, 102.9, 86.5, 84.2, 71.3, 70.1, 68.3, 67.3, 63.6, 41.6, 32.9, 31.3.

HR-MS (ESI) calcd. for $C_{25}H_{29}N_4O_4^+$ 449.2183; found 449.2190.

Methyl-2-(*S*)-phenylsulfonamido-3-(4-(3-pyrimidin-2-ylaminopropoxy)phenyl)propionate (241b)
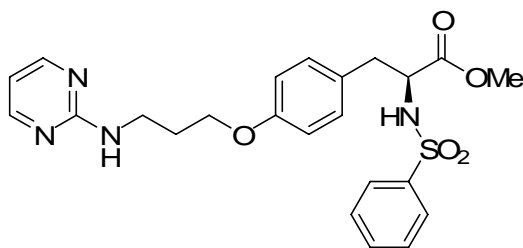
This compound was synthesized by Dr. Dominik Heckmann.

To a solution of methyl 2-(*S*)-*tert.*butoxycarbonylamino-3-(4-(3-pyrimidin-2-ylaminopropoxy) phenyl)propionate (**241**) (1.0 g, 2.33 mmol) in 30 mL dioxane 10 mL concentrated hydrochloric acid was added. The mixture was stirred for 1 h at room temperature, the solvents evaporated *in vacuo* and the resulting amine hydrochloride taken up in 20 mL dry DCM. Phenylsulfonic acid chloride (493 mg, 2.79 mmol) and triethylamine (1.62 mL, 11.65 mmol) were added and the resulting mixture stirred over night at room temperature. The mixture was diluted with DCM and washed with sat. NaHCO$_3$ solution and brine. The organic phase was dried over Na$_2$SO$_4$, the solvent evaporated and the crude product purified by column chromatography on silica gel (DCM/Ethyl acetate 4:1) to give the title compound (794 mg, 1.69 mmol, 73%) as a colourless solid.

^{1}H-NMR (500 MHz, CDCl$_3$): δ = 8.26 (d, *J* = 3.0 Hz, 2H), 7.75 (d, *J* = 7.8 Hz, 2H), 7.52 (t, *J* = 7.3 Hz, 1H), 7.43 (t, *J* = 7.0 Hz, 2H), 6.94 (d, *J* = 8.4 Hz, 2H), 6.73 (d, *J* = 8.5 Hz, 2H), 6.50 (dt, *J* = 4.8 Hz, *J* = 1.9 Hz, 1H), 5.99 (d, *J* = 9.2 Hz, 1H), 5.73 (bs, 1H), 4.21 (m, 1H, C*H*), 4.01 (t, *J* = 5.2 Hz, 2H), 3.60 (m, 2H), 3.43 (s, 3H), 2.97 (d, *J* = 5.6 Hz, 2H), 2.08 (m, 2H).

^{13}C-NMR (125 MHz, DMSO): δ = 171.4, 162.3, 158.1, 158.0, 139.9, 132.6, 130.3, 128.9, 127.0, 114.5, 110.4, 65.6, 56.8, 52.2, 38.6, 38.6, 29.0.

MS (ESI) calcd. for C$_{23}$H$_{26}$N$_4$O$_5$S 470.2; found 471.3 [m+H]$^+$.

Methyl-2-(*S*)-phenylsulfonamido-3-(4-(3-(tetrahydropyrimidin-2(1*H*)-ylideneamino)phenyl) propionate (242)
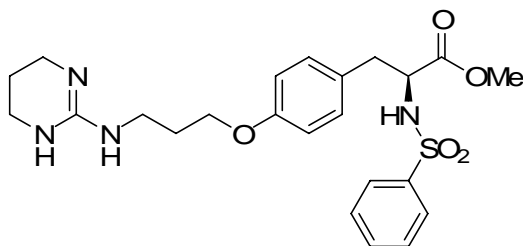
600 mg (1.28 mmol) methyl 2-(*S*)-phenylsulfonamido-3-(4-(3-pyrimidin-2-ylamino-propoxy)phenyl)propionate (**241b**) was dissolved in 20 mL methanol and 1 mL acetic acid. The mixture was hydrogenated (100 mg 5% Pd/C, 25 atm H$_2$) at room temperature, until the HPLC

showed total consumption of starting material. The catalyst was removed by filtration over Celite and the filtrate evaporate to give 612 mg (1.14 mmol, 90%) of the crude **242** as a colorless solid (acetate). A sample of 120 mg was purified by preparative HPLC for analytical data and biological testing.

^{1}H-NMR (500 MHz, DMSO): δ = 8.45 (d, J = 9.0 Hz, 1H), 7.81 (bs, 1H), 7.77 (bs, 1H), 7.61-7.57 (m, 3H), 7.49 (t, J = 7.7 Hz, 2H), 7.39 (bs, 1H), 7.03 (d, J = 8.4 Hz, 2H), 6.78 (d, J = 8.5 Hz, 2H), 3.96 (t, J = 6.0 Hz, 2H), 3.90 (m, 1H), 3.30 (s, 3H), 3.22 (m, 6H), 2.85 (dd, J = 13.7 Hz, J = 6.4 Hz, 1H), 2.69 (dd, J = 13.7 Hz, J = 8.8 Hz, 1H), 1.91 (m, 2H), 1.79 (m, 2H).

^{13}C-NMR (125 MHz, DMSO): δ = 171.0, 157.1, 152.6, 140.6, 132.1, 130.1, 128.8, 128.2, 126.2, 114.1, 64.5, 57.5, 51.5, 38.0, 37.4, 36.7, 28.1, 19.6.

HR-MS (ESI) calcd. for $C_{23}H_{31}N_5O_4S^+$ 475.2091; found 475.2014.

N-hydroxy-(2-(*S*)-phenylsulfonamido-3-(4-(3-(tetrahydropyrimidin-2(1*H*)-ylideneamino) phenyl))propionamide (243)
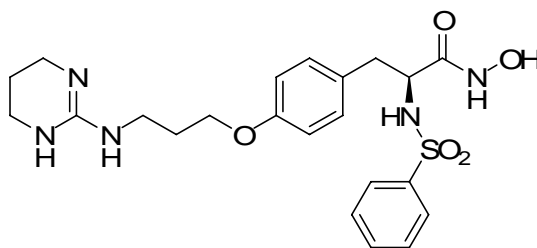
This compound was synthesized by Dr. Dominik Heckmann.

200 mg (372 μmol) of **242** were dissolved in 5 mL methanol. 250 μL (3.72 mmol) of 50% aqueous NH$_2$OH solution and 10 mg potassium cyanide were added and the mixture stirred at room temperature (HPLC monitoring). After five days, the solvents were evaporated and the title compound purified by RP-HPLC to give 24.3 mg (51 μmol, 14%) of a colourless solid.

^{1}H-NMR (500 MHz, DMSO): δ = 10.57 (s, 1H), 8.83 (s, 1H), 8.15 (d, J = 9.0 Hz, 1H), 7.73 (bs, 2H), 7.59 (d, J = 7.3 Hz, 2H), 7.54 (t, J = 7.4 Hz, 1H), 7.43 (t, J = 7.7 Hz, 2H), 7.34 (bs, 1H), 6.96 (d, J = 8.5 Hz, 2H), 6.73 (d, J = 8.6 Hz, 2H), 3.95 (t, J = 6.0 Hz, 2H), 3.73 (dt, J = 8.6 Hz, J = 6.9 Hz, 1H), 3.25-3.22 (m, 6H), 2.72 (dd, J = 13.7 Hz, J = 6.4 Hz, 1H), 2.51-2.47 (m, 1H), 1.92 (m, 2H), 1.79 (m, 2H).

^{13}C-NMR (125 MHz, DMSO): δ = 166.7, 156.9, 152.6, 141.3, 131.8, 130.0, 128.8, 128.6, 126.0, 113.9, 64.4, 55.6, 38.0, 37.5, 37.4, 28.2, 19.6.

HR-MS (ESI) calcd. for $C_{22}H_{30}N_5O_5S^+$ 476.1962; found 476.1966.

2-(*S*)-phenylsulfonamido-3-(4-(3-(tetrahydropyrimidin-2(1*H*)-ylideneamino)phenyl)propionic acid (244)
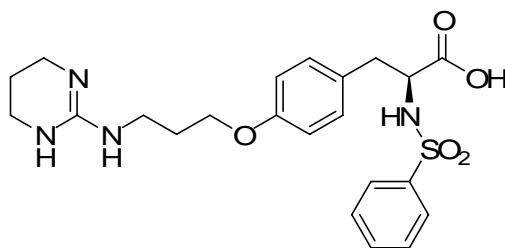
32 mg (67.5 μmol) **242** was dissolved in 4 mL methanol / water 3:1. 15.5 mg (675 μmol) LiOH were added and the mixture stirred over night at room temperature. The solvents were evaporated and the title compound purified by RP-HPLC to give 12 mg (25.6 μmol, 38%) of a colourless solid.

^{1}H-NMR (500 MHz, DMSO): δ = 12.66 (bs), 8.21 (d, *J* = 9.0 Hz, 1H), 7.80 (bs, 2H), 7.57 (d, *J* = 7.9 Hz, 2H), 7.53 (t, *J* = 7.4 Hz, 1H), 7.46-7.41 (m, 3H), 7.02 (d, *J* = 8.5 Hz, 2H), 6.74 (d, *J* = 8.6 Hz, 2H), 3.95 (t, *J* = 6.1 Hz, 2H), 3.80 (dt, *J* = 9.0 Hz, *J* = 5.7 Hz, 1H), 3.22 (m, 6H), 2.86 (dd, *J* = 13.8 Hz, *J* = 5.6 Hz, 1H), 2.69 (dd, *J* = 13.7 Hz, *J* = 9.0 Hz, 1H), 1.91 (m, 2H), 1.78 (m, 2H).

^{13}C-NMR (125 MHz, DMSO): δ = 172.1, 157.0, 152.6, 141.0, 131.9, 130.1, 128.7, 126.1, 114.0, 64.5, 57.6, 38.0, 37.4, 36.9, 28.1, 19.6.

HR-MS (ESI) calcd. for $C_{22}H_{28}N_4O_5S^+$ 461.1775; found 461.1856.

2-(*S*)-phenylsulfonamido-3-(4-(3-(tetrahydropyrimidin-2(1*H*)-ylideneamino)phenyl) propionylamide (245)
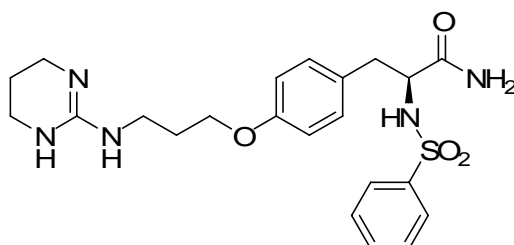
10 mg (21.7 μmol) **244** was dissolved in 4 mL DMF and coupled to a Rink-amide-resin using 6 mg HOBt (43.4 μmol), 14 mg TBTU (43.4 μmol) and 28 mg DIPEA (217 μmol). Cleavage from the resin was performed using 95 % TFA/ 2.5 % H$_2$O/ 2.5 % TIPS for 1h, to give 2 mg (4.3 μmol, 20%) of a colourless solid.

^{1}H-NMR (500 MHz, DMSO): δ =7.90 (d, *J* = 9.2 Hz), 7.69 (bs, 2H), 7.59 (d, *J* = 8.1 Hz), 7.54 (t, *J* = 7.6 Hz, 1H), 7.42 (t, *J* = 8.0 Hz, 2H), 7.30 (m, 2H), 7.05 (d, *J* = 8.3 Hz, 2H), 6.93 (s, 1H), 6.75 (d, *J* = 9.0 Hz, 2H), 3.96 (t, *J* = 6.2 Hz, 2H), 3.85 (m, 1H), 3.23 (m, 7H), 2.79 (m, 1H), 2.56 (m, 1H), 1.92 (m, 2H), 1.79 (m, 2H).

^{13}C-NMR (125 MHz, DMSO): δ = 170.1, 158.7, 157.1, 152.8, 141.3, 132.2, 130.4, 129.6, 128.9, 126.4, 114.0, 84.5, 72.2, 69.7, 69.1, 68.1, 66.4, 57.9, 57.2, 45.7, 42.7, 41.4, 39.8, 32.0, 31.7, 31.2, 25.6.

HR-MS (ESI) calcd. for $C_{22}H_{29}N_5O_4S^+$ 460.2019; found 460.2019.

N-Amino-(2-(*S*)-phenylsulfonamido-3-(4-(3-(tetrahydropyrimidin-2(1*H*)-ylideneamino)phenyl)) propionamide (246)
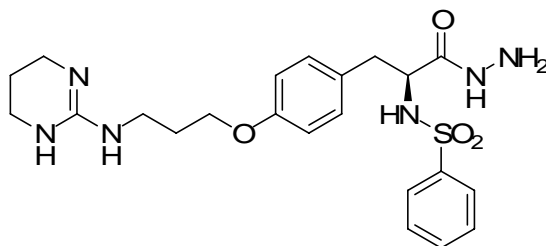
10 mg (21.7 μmol) **244** was dissolved in 4 mL DMF and coupled to 4 mg (26.4 μmol) hydrazinecarboxylic acid *tert*-butyl ester using 6 mg HOBt (43.4 μmol), 14 mg TBTU (43.4 μmol) and 28 mg DIPEA (217 μmol). The solvent was evaporated and the crude product was dissolved in ethyl acetate and washed with saturated $NaHCO_3$. After evaporation of the solvent, deprotection was performed using 95 % TFA/ 2.5 % H_2O/ 2.5 % TIPS for 1h, to give 8 mg (17.4 μmol, 80%) of a colourless solid after HPLC purification.

^{1}H-NMR (500 MHz, DMSO): δ =9.04 (s, 1H), 8.08 (d, *J* = 8.8 Hz, 1H), 7.70 (s, 2H), 7.58 (d, *J* = 7.5 Hz, 1H), 7.54 (t, *J* = 7.2 Hz, 1H), 7.44 (t, *J* = 8.3 Hz, 2H), 7.30 (t, *J* = 5.0 Hz, 1H), 6.99 (m, 2H), 6.74 (d, *J* = 8.5 Hz, 2H), 3.96 (t, *J* = 5.6 Hz, 3H), 3.83 (m, 1H), 3.23 (m, 7H), 2.71 (m, 1H), 2.54 (m, 1H), 1.92 (m, 2H), 1.80 (m, 2H).

^{13}C-NMR (125 MHz, DMSO): δ = 178.7, 160.2, 158.8, 158.7, 158.3, 141.8, 133.9, 84.4, 72.2, 69.7, 69.4, 69.2, 68.1, 66.4, 57.1, 45.8, 41.4, 26.9.

HR-MS (ESI) calcd. for $C_{22}H_{31}N_6O_4S^+$ 475.2122; found 475.2127.

N-Methyl-*N*-hydroxy-(2-(*S*)-phenylsulfonamido-3-(4-(3-*N*-(tetrahydropyrimidin-2(1*H*)-ylidene) aminopropoxy)phenyl))propionamide (247)
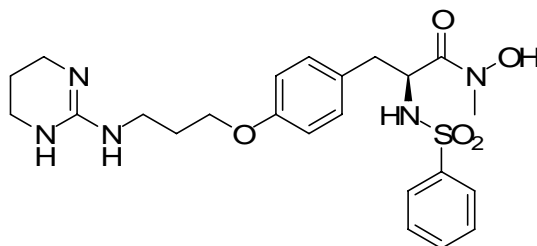
The title compound was prepared from **242** (27 mg, 57.6 μmol), *N*-methylhydroxylamine hydrochlorid (14 mg, 173 μmol) as described for **243**. The reaction proceeded with low reaction rates and was terminated after 7 days at ~40% conversion. Yield after HPLC purification: 1.3 mg (2.7 μmol, 5%) of a light brown solid.

^{1}H-NMR (500 MHz, DMSO): δ = 10.13 (s, 1H), 7.90 (d, *J* = 9.7 Hz, 1H), 7.74 (s, 2H), 7.52 (d, *J* = 7.8 Hz, 2H), 7.40 (t, *J* = 7.4 Hz, 2H), 7.36 (t, *J* = 5.2 Hz, 1H), 7.05 (d, *J* = 8.2 Hz, 2H), 6.77 (d,

J = 8.2 Hz, 2H), 4.56 (m, 1H), 4.05 (t, *J* = 5.7 Hz, 2H), 3.26-3.18 (m, 6H), 2.91 (s, 3H), 2.82 (dd, *J* = 13.7 Hz, 1H), 2.53 (m, 1H), 1.97-1.89 (m, 2H), 1.80 (m, 2H,).

^{13}C-NMR (125 MHz, DMSO): δ = 170.2, 156.8, 152.5, 141.0, 131.7, 130.1, 129.5, 128.4, 126.1, 113.9, 64.4, 54.2, 38.0, 37.4, 36.4, 35.7, 28.2, 19.6.

HR-MS (ESI) calcd. for $C_{23}H_{32}N_5O_5S^+$ 490.2129; found 490.2122.

IV.9.3 Integrin Ligands for Surface Coating

IV.9.3.1   Integrin Ligands for Interversicle Cross-Linking

cyclo(-G-R(Pbf)-G-D(tBu)-f-K(Cbz)-) (248)

The title compound was synthesized according to the general procedures GP1-3, GP6 and GP9 to give 0.68g of **248**.

RP-HPLC (10-100%, 30 min): R_t = 22.88 min.

MS (ESI) calcd. for $C_{54}H_{74}N_{10}O_{13}S$ 1102.5; found 1103.2 $[M+H^+]^+$.

cyclo(-G-R(Pbf)-G-D(tBu)-f-K-) (249)

The title compound was synthesized according to the general procedure GP16 to give 0.11g of **249** after HPLC purification.

RP-HPLC (10-100%, 30 min): R_t = 17.05 min.

MS (ESI) calcd. for $C_{46}H_{68}N_{10}O_{11}S$ 968.5; found 969.3 $[M+H^+]^+$.

Tetradecanoic acid 2-mercapto-1-tetradecanoyloxymethyl-ethyl ester (250)
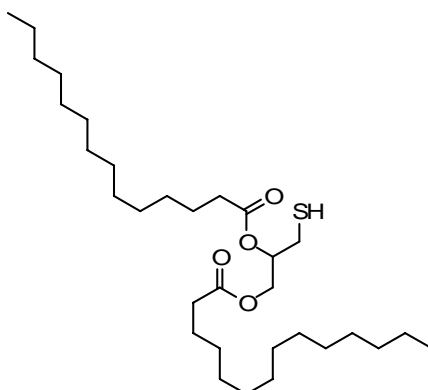
0.1 g of tetradecanoic acid 2-*tert*-butyldisulfanyl-1-tetradecanoyloxymethyl-ethyl ester were dissolved in 5 mL of a 1:1 solution of CF_3CH_2OH and Et_2O. After addition of 0.05 mL water, 0.06 mL of PBu_3 were added. After 8 h, the solvent was removed under reduced pressure and the residue taken up in TFE/cyclo hexane 1:1. Separation of the layers and evaporation of the solvent (cyclo hexane) gives the crude product, which is directly used without any further purification.

(2-{6-[2-(2,5-Dioxo-2,5-dihydro-pyrrol-1-yl)-acetylamino]-hexanoylamino}-acetylamino)-acetic acid (251)
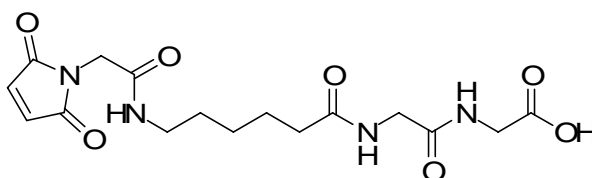
The title compound was synthesized according to the general procedures GP1-3 and GP6 to give 0.31g of **251**.

RP-HPLC (0-50%, 30 min): R_t = 13.70 min.

MS (ESI) calcd. for $C_{16}H_{22}N_4O_7$ 382.1; found 419.2 [M+Na$^+$]$^+$.

Tetradecanoic acid 2-{1-[2-(5-{[(carboxymethyl-carbamoyl)-methyl]-carbamoyl}-pentyl-carbamoyl)-ethyl]-2,5-dioxo-pyrrolidin-3-ylsulfanyl}-1-tetradecanoyloxymethyl-ethyl ester (252).
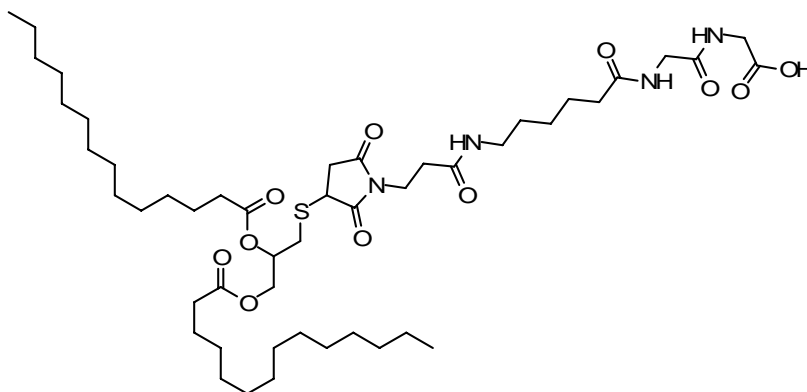
50 mg of **250** were dissolved in dry, degassed DMF under argon atmosphere. After addition of 56 mg of **251**, the solution was allowed to stir for 30 min. The solution was concentrated under reduced pressure and the residue was taken up in ethyl acetate/brine 1:1. Evaporation of the organic layer gave 87 mg of the crude product **252**, which was used without further purification.

MS (ESI) calcd. for $C_{48}H_{84}N_4O_{11}S$ 924.6; found 925.4 [M+H$^+$]$^+$.

cyclo(G-R-G-D-F-K(Tetradecanoic acid 2-{1-[2-(5-{[(carboxymethyl-carbamoyl)-methyl]-carbamoyl}-pentylcarbamoyl)-ethyl]-2,5-dioxo-pyrrolidin-3-ylsulfanyl}-1-tetradecanoyloxy methyl-ethyl ester)-) (253)
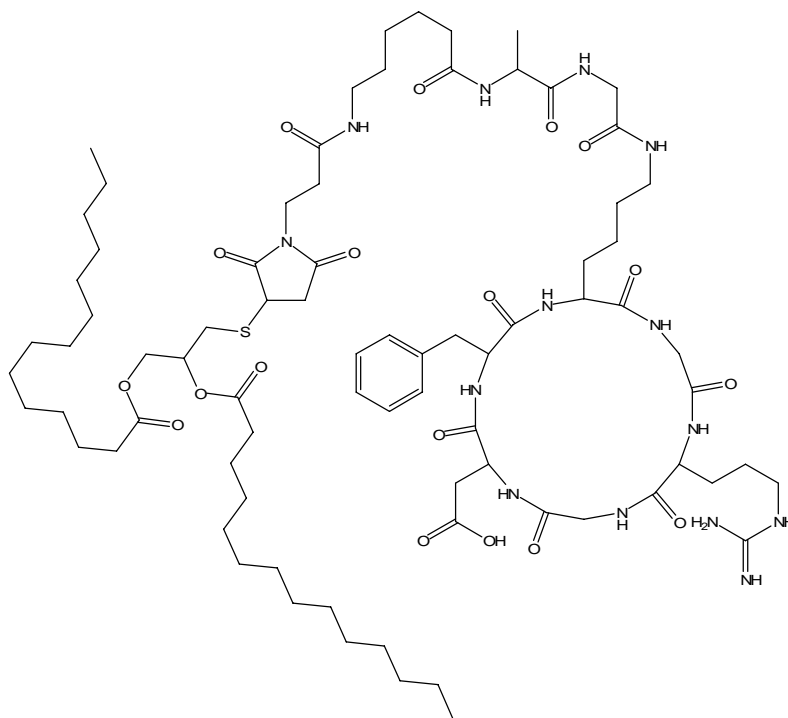
To a solution of 30 mg **252** in DMF, 38 mg **249** (1.2 eq), 25 mg HATU (2 eq) and 20 μL DIPEA (4 eq) were added. After 12 h, the solvent was removed under reduced pressure. The residue was taken up in ethyl acetate and washed with sat. NH₄Cl and sat. NaHCO₃. After evaporation of the solvent, the residue was taken up in 95% TFA, 2.5% TIPS and 2.5% water. After 2.5 h, the solvent was removed under reduced pressure and the residue taken up in ACN. Evaporation of the solvent led to 5.5 mg of the pure product **253**.

RP-HPLC (10-100%, 30 min): R_t = 30.11 min.

MS (ESI) calcd. for $C_{77}H_{126}N_{14}O_{18}S$ 1566.9; found 1567.8 $[M+H^+]^+$.

IV.9.3.2 Synthesis of Cilengitide-Coated Virus Like Particles

cyclo(-f-MeK-R(Pbf)-G-D-(tBu)-) (254)

The title compound was synthesized according to general procedures GP1-6, GP9 and GP16 to give 76 mg of **254** after HPLC purification for 1g of loaded resin.

RP-HPLC (10-100%, 30 min): R_t = 18.94 min.

MS (ESI) calcd. for $C_{45}H_{67}N_9O_{10}S$ 925.5; found 926.4 $[M+H^+]^+$.

3-(2-(2-(2-(2-(2-(2-(2-(2-(2-(2-azidoethoxy)ethoxy)ethoxy)ethoxy)ethoxy)ethoxy)ethoxy)ethoxy)ethoxy)ethoxy)prop-1-yne (255)
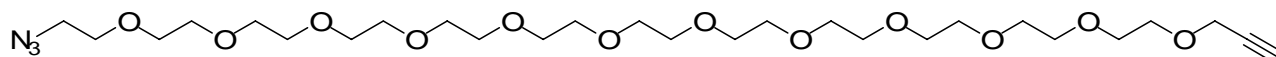
50 mg of NaH were dissolved in dry DMF under an argon atmosphere and stirred for 5 min. Afterwards, the 500 mg of the azido-PEG$_{11}$ (2-(2-(2-(2-(2-(2-(2-(2-(2-(2-(2-azidoethoxy)ethoxy)ethoxy)ethoxy)ethoxy)ethoxy)ethoxy)ethoxy)ethoxy)ethoxy)ethanol) were added and the solution again stirred for 5 min. Then, 0.1 mL of propargylbromide were added and the solution was allowed to stir for 12h at room temperature. The solvent was removed under reduced pressure and the crude product purified via C-18 flash chromatography (ACN/water 10%->100% ACN) to give 320 mg of **255**.

MS (ESI) calcd. for $C_{27}H_{51}N_3O_{12}$ 609.3; found 610.3 $[M+H^+]^+$.

2-(2-(2-(2-(2-(2-(2-(2-(2-(2-(2-(prop-2-ynyloxy)ethoxy)ethoxy)ethoxy)ethoxy)ethoxy)ethoxy)ethoxy)ethoxy)ethoxy)ethoxy)ethanamine (256)
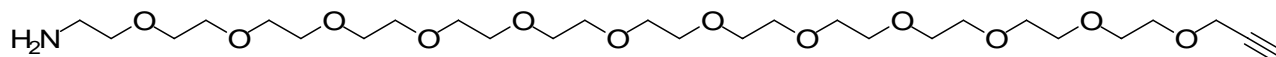
To a solution of 15 mL dry THF under argon atmosphere 320 mg of **255** and 1.5g of triphenyl posphine were added and the solution allowed to stir for 12h. After addition of 15 mL of water, the solution was stirred for additional 15 min and the solvent removed under reduced pressure. The residue was taken up in ethyl acetate/water 1:1 and the two layers were separated. The water layer was concentrated under reduced pressure to give **256** in quantitative yield.

MS (ESI) calcd. for $C_{27}H_{53}NO_{12}$ 583.4; found 584.3 $[M+H^+]^+$.

3-(2-(2-(2-(2-(2-(2-(2-(2-(2-(2-(2-(prop-2-ynyloxy)ethoxy)ethoxy)ethoxy)ethoxy)ethoxy) ethoxy)ethoxy)ethoxy)ethoxy)ethoxy)ethylcarbamoyl)propanoic acid (257)
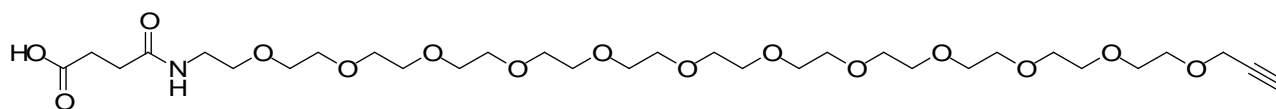
To a solution of 10 mL dry ACN and 100 mg of **256**, 250 mg succinic anhydride and 0.5 mL DIPEA were added. The solution was allowed to stir for 10 h. The solvent was removed under reduced pressure and the crude product purified via C-18 flash column chromatography (ACN/water 0%->60% ACN) to give 78 mg of **257**.

MS (ESI) calcd. for $C_{31}H_{57}NO_{15}$ 683.4; found 684.3 $[M+H^+]^+$.

cyclo(-f-MeK(3-(2-(2-(2-(2-(2-(2-(2-(2-(2-(2-(2-(prop-2-ynyloxy)ethoxy)ethoxy)ethoxy) ethoxy)ethoxy)ethoxy)ethoxy)ethoxy)ethoxy)ethoxy)ethylcarbamoyl)propanoic acid)-R(Pbf)-G-D(tBu)-) (258)
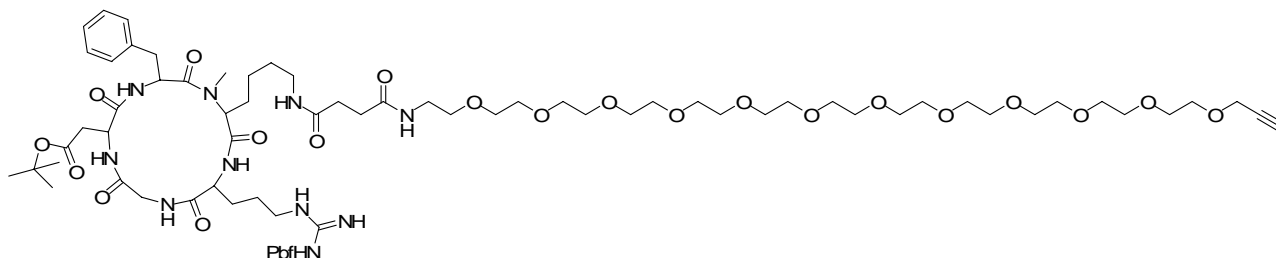
5 mg of **254** and 5.6 mg **257** were dissolved in 5 mL DMF. After addition of 2.5 mg HCTU and 10 μL DIPEA the solution was allowed to stir for 16h. The solvent was removed under reduced pressure and the crude product used without further purification.

RP-HPLC (0-95%, 20 min): R_t = 9.45 min.

cyclo(-f-MeK(3-(2-(2-(2-(2-(2-(2-(2-(2-(2-(2-(2-(prop-2-enyloxy)ethoxy)ethoxy)ethoxy) ethoxy)ethoxy)ethoxy)ethoxy)ethoxy)ethoxy)ethoxy)ethylcarbamoyl)propanoic acid)-R-G-D-) (259)
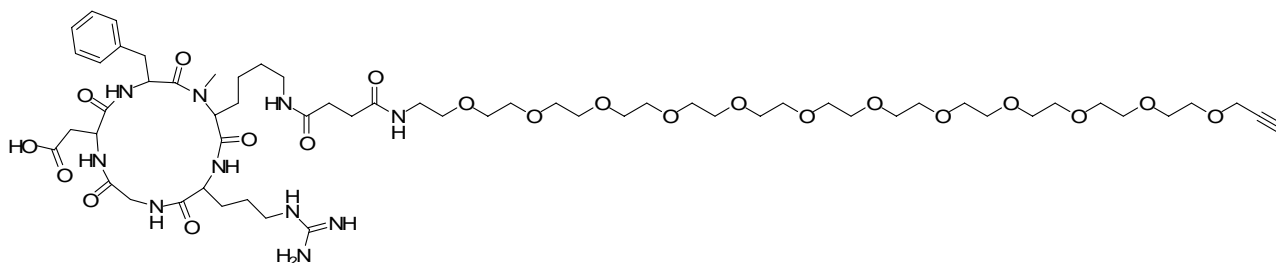
The crude product of **258** was dissolved in 5 mL TFA/TIPS/water (95/2.5/2.5) and allowed to stir for 2h. The solution was concentrated under reduced pressure and the residue precipitated into cold ether. HLPC-purification of the precipitate gave 5 mg of **259**.

RP-HPLC (0-95%, 20 min): R_t = 8.89 min.

MS (ESI) calcd. for $C_{59}H_{98}N_{10}O_{21}$ 1282.7; found 642.4 $1/2[M+H^+]^+$.

Preparation of the Qβ-virus like particles (VLPs)

Starting from 5g of bacteriophage Qβ cell pellet, the pellet was re-suspended in 20 mL of distilled water and 5 mL of lysis buffer (1x TBS, 2mM EDTA) and sonicated for 6 minutes. Afterwards, the sample was centrifuged at 14k rpm for 10 minutes. The precipitate was discarded and 10% (w/v) PEG 8000 and 2.9g NaCl were added to the supernatant. The solution was allowed to stand for 30 min and afterwards centrifuged at 10k rpm for 10 min. The supernatant was discarded and the precipitate re-suspended in 15 mL of 0.1M Tris buffer at pH 8. The solution was again centrifuged at 14k rpm for 10 min and the supernatant collected. Centrifugation at 42k rpm for 4 h using a sucrosie cushion resulted in ultra-pellets which were resuspended in 2mL phosphate buffer per pellet. The samples were given on a 10-40% sucrose gradient and centrifuged at 28k rpm for 5 h. The virus band was collected and ultrapelleted at 42k rpm for 4 h. The pellets were resuspended in 0.1M phosphate buffer at pH 7 and stored at 0°C. Purity and protein concentration were determined using Lowry assay and FPLC.

Attachment of Alexa568 on virus like particles

0.2 eq. of Alexa568-NHS ester were dissolved in DMSO and slowly added to 0.74 mM/L of the VLP. The reaction was allowed to run for 12h at 0°C. Afterwards, the sample was purified by a 10-40% sucrose gradient, which was performed at 28k rpm for 4 h. The virus band was collected and ultracentrifuged at 49k rpm for 2 h. The pellets were resuspended in 0.1M HEPES buffer pH 8 to give a final virus like particle concentration of ~ 20 mg/mL.

Linker attachment to the virus like particle

2 eq of 5-(3-azidopropylamino)-5-oxopentanoic acid NHS ester were dissolved in DMSO and added to 0.74 mM/L of the VLP. The reaction was allowed to run for 12h at 0°C. Afterwards, the sample was purified by a 10-40% sucrose gradient, which was run at 28k rpm for 4 h. The virus band was collected and ultracentrifuged at 49k rpm for 2 h. The pellets were resuspended in 0.1M HEPES buffer pH 8 to give a final virus like particle concentration of ~ 20 mg/mL.

Attachment of the Cilengitide derivative (259) on the VLP

In a 2 mL eppendorf tube, 100 μL of Qβ-Azide (2 mg/mL) were added followed by 810 mL HEPES 0.1M pH 8 and 10 μL of **259** (1.5 eq). Afterwards, a premixed $CuSO_4$ and TBTA-OH solution (1:2; 0.5 mM) was added, followed by addition of 50 μL sodium ascorbate solution (5 mM). The tube was shaken for 1.5 h and the crude product purified by FPLC to give the coated virus like particle with 1-4 attached molecules of **259** per unit.

MALDI-TOF: uncoated VLP: ~15-16000

                    1x **259** attached: ~ 18000

                    2x **259** attached: ~ 19000

                    3x **259** attached: ~ 20000

                    4x **259** attached: ~ 21000
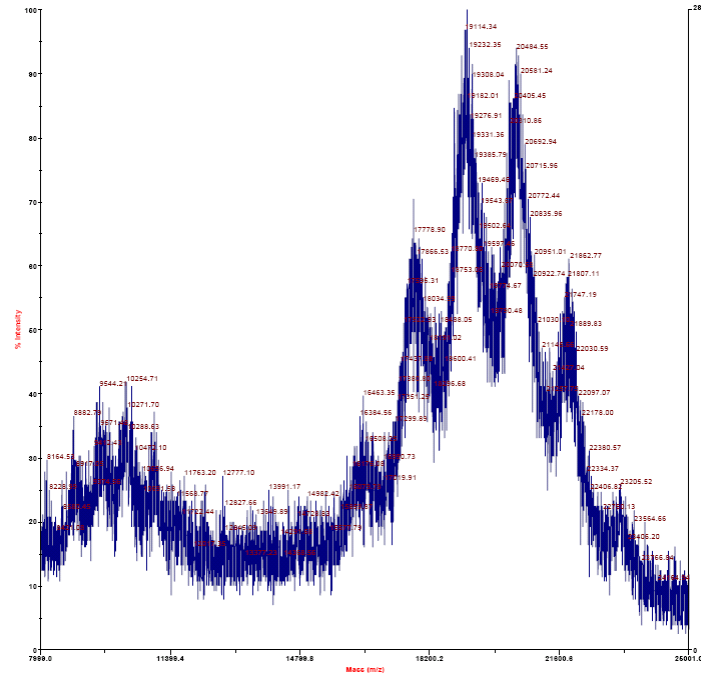
Figure 73: *MALDI-spectrum of the VLP coated with **259**.*

IV.9.4 Selective α5β1 integrin ligands for surface coating

1-((4-bromo-3,5-dimethylphenoxy)methyl)benzene (260)
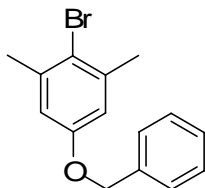
4-bromo-3,5-dimethylphenole (2.37g, 11.8 mmol) were dissolved in 50 mL dry DMF and cooled down to 0°C. 1.2 eq (14.2 mmol, 1.2 equiv) NaH were added and the solution allowed to stir for 30 min. After addition of 1.68 mL (14.2 mmol, 1.2 equiv) benzylbromide the solution was stirred for another 1.5 h at room temperature. After addition of 30 mL saturated aqueous NH_4Cl, the solution was extracted with ether and the organic layer washed with brine. The solvent was removed under reduced pressure to give **260** (3.06 g, 89%) as yellow crystals.

RP-HPLC (10-100%) R_t = 31.13 min.

R_F = 0.63 (H/EtOAc 9:1)

^{1}H-NMR (250 MHz, DMSO): δ = 7.41 (m, 5H), 6.89 (s, 2H), 5.07 (s, 2H), 2.32 (s, 6H).

^{13}C-NMR (63 MHz, CDCl$_3$): δ = 157.3, 139.1, 136.8, 128.6, 128.0, 127.4, 118.5, 114.7, 70.0, 24.0.

tert-Butyl 4-(benzyloxy)-2,6-dimethylbenzoate (261)
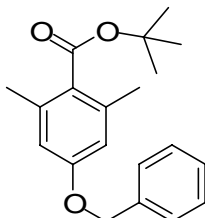
The arylbromide **260** (0.50 g, 1.7 mmol) was dissolved in 10 mL dry THF and cooled down to -78°C. Then, *n*-Butyllithium (2,5 M in hexan, 0.82 mL, 2.1 mmol, 1.2 equiv) were added and the solution allowed to stir for 30 min. After addition of Boc$_2$O (375 mg, 1.7 mmol, 1 equiv) the solution was again stirred for 30 min before it was allowed to come to room temperature within 1h. The mixture was acidified with 1 N HCl and extracted with EtOAc. The organic layer was washed with brine and the organic solvent removed under reduced pressure. The crude product was purified via flash chromatography to give **261** (330 mg, 1.03 mmol, 61%) as a white solid.

RP-HPLC (10-100%) R_t = 29.67 min.

R_F = 0.48 (H/EtOAc 9:1)

^{1}H-NMR (250 MHz, DMSO): δ = 7.42 (m, 5H), 6.72 (s, 2H), 5.10 (s, 2H), 2.22 (s, 6H), 1.52 (s, 9H).

^{13}C-NMR (90 MHz, DMSO): δ = 169.1, 158.1, 136.8, 136.7, 128.3, 127.8, 127.7, 127.4, 113.6, 80.8, 69.9, 27.7, 19.3.

tert-Butyl 4-hydroxy-2,6-dimethylbenzoate (262)
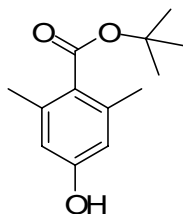
261 (290 mg, 0.93 mmol) was dissolved in methanol (50 mL). After addition of the catalyst (10% Pd/C, 30 mg) the solution was allowed to stir for 12h under an atmosphere of H_2 at 1 atm. The catalyst was filtered off via Celite and the solvent removed under reduced pressure to give **262** (182 mg, 0.82 mmol, 88%) as a pale yellow solid.

RP-HPLC (10-100%) R_t = 21.19 min.

R_F = 0.9 (H/EtOAc 1:2)

^{1}H-NMR (250 MHz, DMSO): δ = 9.51 (s, 1H), 6.23 (s, 2H), 2.17 (s, 6H), 1.51 (s, 9H).

benzyl 4-(4-(tert-butoxycarbonyl)-3,5-dimethylphenoxy)butylcarbamate (263)
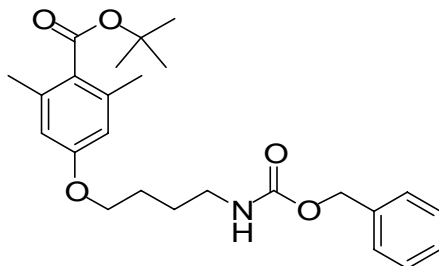
262 (168 mg, 0.76 mmol), 4-(benzyloxycarbonylamino)-butan-1-ol (186 mg, 0.83 mmol, 1.1 equiv) and tri-*n*-butylphosphin (198 mg, 0.98 mmol, 1.3 equiv) were dissolved in 10 mL dry THF and stirred at 0°C. ADDP (248 mg, 0.98 mmol, 1.3 equiv) in 5 mL dry THF were added dropwise over 5 h. The mixture was stirred for 12 h t come to room temperature and the crude product purified via flash chromatography to give 263 (210 mg, 0.47 mmol, 63%) as a white solid.

RP-HPLC (10-100%) R_t = 28.24 min.

^{1}H-NMR (250 MHz, DMSO): δ = 7.34 (m, 5H), 6.61 (s, 2H), 5.01 (s, 2H), 3.94 (t, ^3J = 6.1 Hz, 2H), 3.05 (m, 2H), 2.22 (s, 6H), 1.68 (m, 2H),1.52 (m, 2H), 1.52 (s, 9H).

^{13}C-NMR (90 MHz, DMSO): δ = 169.2, 158.4, 137.2, 135.8, 128.2, 127.6, 127.5, 127.5, 113.2, 80.75, 66.9, 65.0, 25.9, 25.9, 27.7, 19.3.

tert-Butyl 4-(4-aminobutoxy)-2,6-dimethylbenzoate (264)
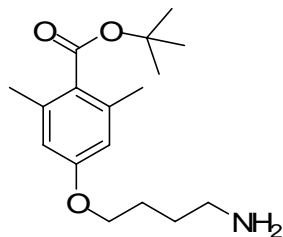
263 (195 mg, 0.44 mmol) were dissolved in methanol (40 mL). After addition of the catalyst (10% Pd/C, 30 mg) the solution was allowed to stir for 12h under an atmosphere of H_2 at 1 atm. The catalyst was filtered off via Celite and the solvent removed under reduced pressure to give **264** (119 mg, 0.41 mmol, 92%) as a pale yellow oil.

RP-HPLC (10-100%) R_t = 17.21 min.

R_F = 0 (H/EtOAc 4:1)

^{1}H-NMR (250 MHz, DMSO): δ = 6.61 (s, 2H), 3.94 (t, ^3J = 6.4 Hz, 2H), 2.55 (m, 2H), 2.22 (s, 6H), 1.69 (m, 2H),1.52 (s, 9H), 1.47 (m, 2H).

tert Butyl-4-{4-[6-(*N*-((9*H*-fluoren-9-yl)methoxy)carbonylamino)hexanamido]butoxy}-2,6-dimethylbenzoat (265)
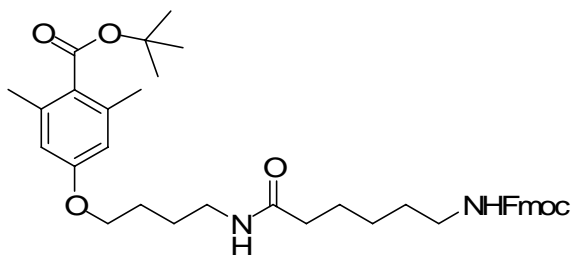
To a solution of **264** (119 mg, 0.39 mmol) and 6-(9-Fluorenylmethoxycarbonylamino)hexanoic acid (275 mg, 0.77 mmol, 2 equiv) in dry DMF (40 mL) a solution of HATU (177 mg, 0.47 mmol, 1.2 equiv) and DIPEA (0.26 mL, 1.55 mmol, 4 equiv) in 37 mL dry DMF was slowly added and allowed to stir for 12h. After removal of the solvent under reduced pressure, the residue was taken up in EtOAc and washed with brine. Purification via prep. RP-HPLC gave **265** (207 mg, 0.33 mmol, 85%) as a pale yellow oil.

RP-HPLC (10-100%) R_t = 29.10 min.

R_F = 0.5 (EtOAc)

MS (ESI) calcd. for $C_{38}H_{49}N_2O_6$ 629.8; found 629.3 $[M+H^+]^+$.

4-{4-[6-(*N*-((9*H*-fluoren-9-yl)methoxy)carbonylamino)hexanamido]butoxy}-2,6-dimethyl-benzoic acid (266)
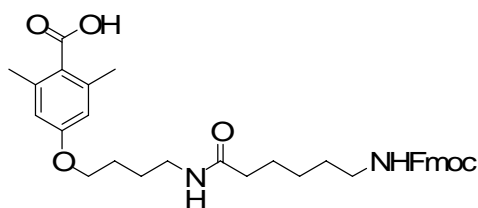
265 (122 mg, 0.19 mmol) were dissolved in 50% TFA in DCM (5 mL) and stirred for 1 h. The solvent was removed under reduced pressure to give **266** (72 mg, 0.126 mmol, 93%) as pale yellow oil.

RP-HPLC (10-100%) R_t = 22.75 min.

R_F = 0.15 (EtOAc)

MS (ESI) calcd. for $C_{34}H_{41}N_2O_6$ 573.3; found 573.1 $[M+H^+]^+$.

2-(4-{4-[6-(9H-Fluoren-9-ylmethoxycarbonylamino)-hexanoylamino]-butoxy}-2,6-dimethyl-benzoylamino)-3-{4-[3-(pyridin-2-ylamino)-propoxy]-phenyl}-propionic acid methyl ester (267)
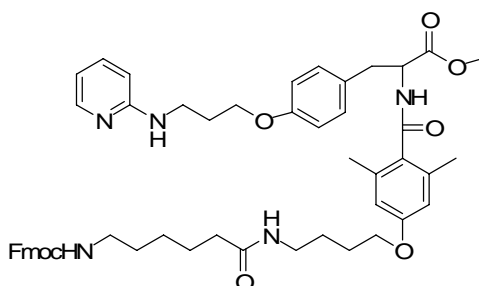
To a solution of 52 mg **227** (0.09 mmol) in 5 mL DCM 5 mL TFA were given and the solution allowed to stir for 2 h. The solvent was removed under reduced pressure and the residue taken up in 5 mL DMF. After addition of 50 mg **266** (0.08 mmol, 0.9 equiv) a solution of 56 mg HATU (1.5 equiv), 20 mg HOAt (1.5 equiv) and 0.2 mL DIPEA (10 equiv) in 5 mL DMF were slowly added. The solution was allowed to stir for 14 h. The solvent was removed under reduced pressure and the residue taken up in EtOAc and washed with saturated NH_4Cl, $NaHCO_3$ solution and brine. Removal of the solvent under reduced pressure gave **267** as crude product which was used without further purification.

RP-HPLC (10-100%) Rt = 26.95 min.

MS (ESI) calcd. for $C_{52}H_{62}N_5O_8$ 884.5; found 884.5 $[M+H^+]^+$.

2-{4-[4-(6-Amino-hexanoylamino)-butoxy]-2,6-dimethyl-benzoylamino}-3-{4-[3-(pyridin-2-ylamino)-propoxy]-phenyl}-propionic acid methyl ester (268)
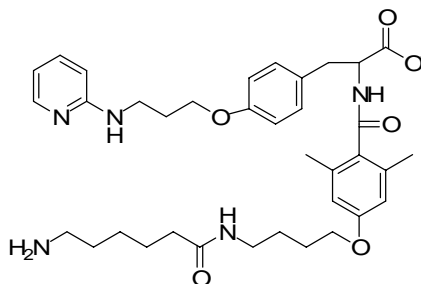
The crude product **267** was dissolved in 8 mL DMF and 2 mL piperidine were added. The solution was allowed to stir for 2 h. The solvent was removed under reduced pressure to give **268** as crude product which was directly used without further purification.

MS (ESI) calcd. for $C_{37}H_{52}N_5O_6$ 662.4; found 662.4 $[M+H^+]^+$.

2-(2,6-Dimethyl-4-{4-[6-(3-tritylsulfanyl-propionylamino)-hexanoylamino]-butoxy}-benzoylamino)-3-{4-[3-(pyridin-2-ylamino)-propoxy]-phenyl}-propionic acid methyl ester (269)
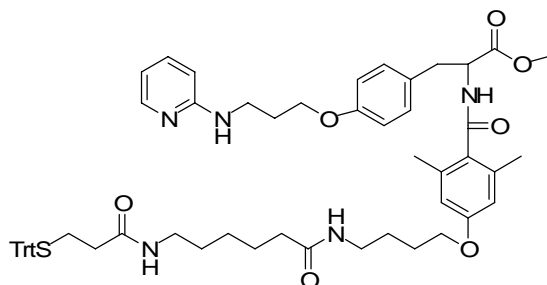
To a solution of 64 mg **268** (0.1 mmol) in 5 mL DMF slowly a solution of 27 mg 3-(tritylthio)propanoic acid (0.08 mmol, 0.8 equiv), 41 mg TBTU (0.13 mmol, 1.3 equiv) and 0.17 mL DIPEA (1 mmol, 10 equiv) in 5 mL DMF were added. After 10 h the solvent was removed under reduced pressure and the residue purified via prep. RP-HPLC to give 13 mg of **269** (0.01 mmol,13%).

RP-HPLC (10-100%) Rt = 22.61 min.

MS (ESI) calcd. for $C_{59}H_{70}N_5O_7S$ 992.5; found 992.4 $[M+H^+]^+$.

2-(2,6-Dimethyl-4-{4-[6-(3-tritylsulfanyl-propionylamino)-hexanoylamino]-butoxy}-benzoylamino)-3-{4-[3-(pyridin-2-ylamino)-propoxy]-phenyl}-propionic acid (270)
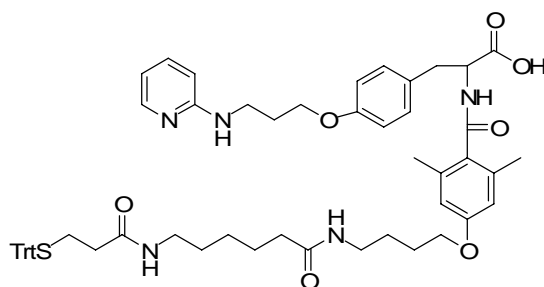
To a solution of 13 mg **269** (0.01 mmol) in 5 mL THF and 5 mL H$_2$O 3 mg LiOH (0.05 mmol, 5 equiv) were added and the solution stirred for 1 h. The solvent was removed under reduced pressure and the crude product purified via prep. RP-HPLC to give 9 mg **270** (0.009 mmol, 70%).

RP-HPLC (10-100%) Rt = 21.91 min.

MS (ESI) calcd. for C$_{58}$H$_{67}$N$_5$O$_7$S 978.5; found 978.5 [M+H$^+$]$^+$.

2-(4-{4-[6-(3-Mercapto-propionylamino)-hexanoylamino]-butoxy}-2,6-dimethyl-benzoyl-amino)-3-{4-[3-(pyridin-2-ylamino)-propoxy]-phenyl}-propionic acid (271)
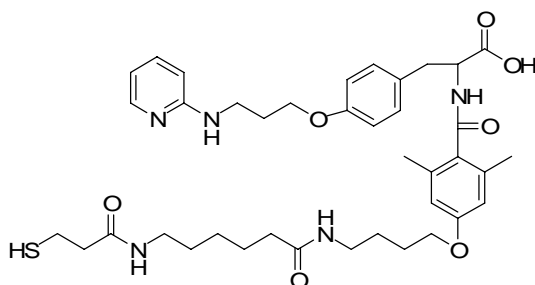
To a solution of 9 mg **270** (0.009 mmol) in 1 mL TIPS and 1 mL H$_2$O 8mL TFA were slowly added. After 1 h the solvent was removed under reduced pressure and the crude product purified via prep. RP-HPLC to give 2.7 mg **271** (0.004 mmol, 44%).

RP-HPLC (10-100%) Rt = 14.44 min.

MS (ESI) calcd. for C$_{39}$H$_{54}$N$_5$O$_7$S 736.4; found 736.5 [M+H$^+$]$^+$.

V References

> And as soon as you finished reading this scroll,
>
> you will tie a stone to it and throw it into the middle of the Euphrates.
>
> Jeremiah 51:63 (New American Standard Bible)

1   Evans, B. E.; Rittle, K. E.; Bock, M. G.; DiPardo, R. M.; Freidinger, R. M.; Whitter, W. L.; Lundell, G. F.; Veber, D. F.; P. S. Anderson; Methods for drug discovery: development of potent, selective, orally effective cholecystokinin antagonists, *J. Med. Chem.* **1988**, *31*, 2235-2246.

2   Maclean, D.; Baldwin, J. J.; Ivanov, V. T.; Kato, Y.; Shaw, A.; Schneider, P.; Gordon, E. M.; Glossary of Terms Used in Combinatorial Chemistry, *Pure Appl. Chem.* **1999**, *71*, 2349-2365.

3   Müller, G.; Medicinal chemistry of target family-directed masterkeys, *Drug Disc. Today* **2003**, *8*, 681-691.

4   Nicolaou, K. C.; Pfefferkorn, J. A.; Roecker, A. J.; Cao, G.-Q.; Barluenga, S.; Mitchell, H. J.; Natural Product-like Combinatorial Libraries Based on Privileged Structures. 1. General Principles and Solid-Phase Synthesis of Benzopyrans, *J. Am. Chem. Soc.* **2000**, *122*, 9939–9953.

5   Horton, D. A.; Bourne, G. T.; Smythe, M. L.; Exploring privileged structures: The combinatorial synthesis of cyclic peptides, *Molec. Divers.* **2000**, *5*, 289-304.

6   Gurrath, M.; Müller, G.; KESSLER, H.; Aumailley, M.; Timpl, R.; Conformation/activity studies of rationally designed potent anti-adhesive RGD peptides, *Eur J Biochem* **2004**, *210*, 911-921.

7   Pierschbacher, M. D.; Ruoslahti, E.; Cell attachment activity of fibronectin can be duplicated by small synthetic fragments of the molecule, *Nature* **1984**, *309*, 30-3.

8   Haubner, R.; Gratias, R.; Diefenbach, B.; Goodman, S. L.; Jonczyk, A.; Kessler, H.; Structural and Functional Aspects of RGD-Containing Cyclic Pentapeptides as Highly Potent and Selective Integrin V3 Antagonists, *J Am Chem Soc* **1996**, *118*, 7461-7472.

9   Lipinski, C. A.; Lombardo, F.; Dominy, B. W.; Feeney, P. J.; Experimental and computational approaches to estimate solubility and permeability in drug discovery and development settings, *Adv Drug Deliv Rev* **2001**, *46*, 3-26.

10   Veber, D. F.; Johnson, S. R.; Cheng, H. Y.; Smith, B. R.; Ward, K. W.; Kopple, K. D.; Molecular properties that influence the oral bioavailability of drug candidates, *J Med Chem* **2002**, *45*, 2615-23.

11   Rügger, A.; Kuhn, M.; Lichti, H.; Loosli, H. R.; Huguenin, R.; Quiquerez, C.; von Wartburg, A.; [Cyclosporin A, a Peptide Metabolite from Trichoderma polysporum (Link ex Pers.) Rifai, with a remarkable immunosuppressive activity], *Helv. Chim. Acta* **1976**, *59*, 1075-92.

12   Lindholm, A.; Factors influencing the pharmacokinetics of cyclosporine in man, *Ther Drug Monit* **1991**, *13*, 465-77.

13   Loosli, H.-R.; Kessler, H.; Oschkinat, H.; Weber, H.-P.; Petcher, T. J.; Widmer, A.; Peptide conformations. Part 31. The conformation of cyclosporin a in the crystal and in solution Helvetica Chimica Acta, *Helv. Chim. Acta* **1985**, *68*, 682-704.

14   Kessler, H.; Conformation and Biological Activity of Cyclic Peptides, *Angew. Chem. Int. Ed. Engl.* **1982**, *21*, 512-523.

15   Fischer, E.; Lipschitz, W.; Optisch-aktlve N-Monomethyl-Derivate von Alanin, Leucin, Phenylalanin und Tyrosin, *Ber. dt. chem. Ges.* **1915**, *48*, 360-378.

16   Tonelli, A.; The effects of isolated N-methylated residues on the conformational characteristics of polypeptides, *Biopolymers* **1976**, *15*, 1615-22.

17   Chatterjee, J.; Gilon, C.; Hoffman, A.; Kessler, H.; N-Methylation: A New Perspective in Peptide Medicinal Chemistry, *Accounts Chem. Res.* **2008**, *41*, 1331-1342.

18   Chatterjee, J.; Mierke, D.; Kessler, H.; N-methylated cyclic pentaalanine peptides as template structures, *J Am Chem Soc* **2006**, *128*, 15164-72.

19   Gilon, C.; Halle, D.; Chorev, M.; Selinger, Z.; Byk, G.; Backbone cyclization: A new method for conferring conformational constraint on peptides, *Biopolymers* **1991**, *31*, 745-50.

20   Fischer, E.; *Chem. Ber.* **1894**, *3*, 2985-2993.

21   Fischer, E.; *J. Chem. Soc.* **1907**, *91*, 1749-1765.

22   Deber, C. M.; Madison, V.; Blout, E. R.; *Accounts Chem. Res.* **1976**, *9*, 106-113.

23   Koshland, D. E., Jr.; Correlation of Structure and Function in Enzyme Action, *Science* **1963**, *142*, 1533-41.

24   Koshland, D. E.; *Proc. Nat. Acad. Sci. U.S.A.* **1958**, *44*, 98-104.

25   Charpentier, B.; Dor, A.; Roy, P.; England, P.; Pham, H.; Durieux, C.; Roques, B. P.; Synthesis and binding affinities of cyclic and related linear analogues of CCK8 selective for central receptors, *J. Med. Chem.* **1989**, *32*, 1184-90.

26   Al-Obeidi, F.; Castrucci, A. M.; Hadley, M. E.; Hruby, V. J.; Potent and prolonged acting cyclic lactam analogues of alpha-melanotropin: design based on molecular dynamics, *J. Med. Chem.* **1989**, *32*, 2555-61.

27   Veber, D. F.; Holly, F. W.; Nutt, R. F.; Bergstrand, S. J.; Brady, S. F.; Hirschmann, R.; Glitzer, M. S.; Saperstein, R.; Highly active cyclic and bicyclic somatostatin analogues of reduced ring size, *Nature* **1979**, *280*, 512-4.

28   Kessler, H. In *Vorlesung "Industrielle Wirkstoffforschung"*, 2005.

29   Kishore, R.; Raghothama, S.; Balaram, P.; Cystine peptides: the intramolecular antiparallel beta-sheet conformation of a 20-membered cyclic peptide disulfide, *Biopolymers* **1987**, *26*, 873-91.

30   Toniolo, C.; Structure of conformationally constrained peptides: from model compounds to bioactive peptides, *Biopolymers* **1989**, *28*, 247-57.

31   Gilon, C.; Mang, C.; Lohof, E.; Friedler, A.; Kessler, H. In *Methods of Organic Chemistry (Houben-Weyl)*; Büchel, K. H., Falbe, J., Hagemann, H., Hanack, M., Klamann, D., Kreher, R., Kropf, H., Regitz, M., Schaumann, E., Eds.; Georg Thieme Verlag: Stuttgart, 2003; Vol. E 22; pp 461-542.

32   Richardson, J. S.; The anatomy and taxonomy of protein structure, *Adv. Protein Chem.* **1981**, *34*, 167-339.

33   Venkatachalam, C. M.; Stereochemical criteria for polypeptides and proteins. V. Conformation of a system of three linked peptide units, *Biopolymers* **1968**, *6*, 1425-36.

34   Cornish-Bowden, A.; *Eur. J. Biochem.* **1984**, *138*, 9-37.

35   Kurz, M., Technische Universität München, 1991.

36   Schwyzer, R.; Carrión, J. P.; Gorup, B.; Nolting, H.; Tun-Kyi, A.; Verdoppelungserscheinungen beim Ringschlus von Peptiden; Relative Bedeutung der sterischen Hinderung und der Assoziation über Wasserstoff-Brücken bei Tripeptiden. Spektroskopische Versuche zur Konformationsbestimmung, *Hel. Chim. Acta.* **1964**, *47*, 441-464.

37   Mierke, D. F.; Kurz, M.; Kessler, H.; Flexibility and Calculations of an Ensemble of Molecules, *J. Am. Chem. Soc.* **1994**, *116*, 1042-1049.

38   Weide, T.; Modlinger, A.; Kessler, H.; Spatial Screening for the Identification of the Bioactive Conformation of Integrin Ligands, *Top. Curr. Chem.* **2007**, *272*, 1-50.

39   Nikiforovich, G. V.; Kövér, K. E.; Zhang, W.-J.; Marshall, G. R.; Cyclopentapeptides as Flexible Conformational Templates, *J. Am. Chem. Soc.* **2000**, *122*, 3262-3273.

40   Heller, M.; Sukopp, M.; Tsomaia, N.; John, M.; Mierke, D. F.; Reif, B.; Kessler, H.; The conformation of cyclo(-D-Pro-Ala4-) as a model for cyclic pentapeptides of the DL4 type, *J Am Chem Soc* **2006**, *128*, 13806-14.

41   Matter, H.; Kessler, H.; Structures, Dynamics and Biological Activities of 15 Cyclic Hexapeptide Analogues of the Alpha-Amylase Inhibitor Tendamistat (Hoe-467) in Solution, *J. Am. Chem. Soc.* **1995**, *117*, 3347-3359.

42   Lindenberg, H.; Ueber Methylamidopropionsäure und die Bildung von Homokreatin, *J. Prakt. Ch.* **1875**, *12*, 244-259.

43   Aurelio, L.; Brownlee, R. T.; Hughes, A. B.; Synthetic preparation of N-methyl-alpha-amino acids, *Chem. Rev.* **2004**, *104*, 5823-46.

44   Freidinger, R. M.; Hinkle, J. S.; Perlow, D. S.; Arison, B. H.; Synthesis of 9-Fluorenylmethyloxycarbonyl-Protected N-Alkyl Amino Acids by Reduction of Oxazolidinones, *J. Org. Chem.* **1983**, *48*, 77-81.

45   Miller, S. C.; Scanlan, T. S.; Site-Selective N-Methylation of Peptides on Solid Support, *J. Am. Chem. Soc.* **1997**, *119*, 2301-2302.

46   Miller, S. C.; Scanlan, T. S.; oNBS-SPPS: A New Method for Solid-Phase Peptide Synthesis, *J. Am. Chem. Soc.* **1998**, *120*, 2690-2691.

47   Biron, E.; Chatterjee, J.; Kessler, H.; Optimized selective N-methylation of peptides on solid support, *J Pept Sci* **2006**, *12*, 213-9.

48   Chatterjee, J.; Mierke, D. F.; Kessler, H.; Conformational preference and potential templates of N-methylated cyclic pentaalanine peptides, *Chemistry Eur. J.* **2008**, *14*, 1508-17.

49   Kessler, H.; Detection of Hindered Rotation and Inversion by NMR Spectroscopy, *Angew. Chem. Int. Ed.* **1970**, *9*, 219-235.

50   Gurrath, M.; Muller, G.; Kessler, H.; Aumailley, M.; Timpl, R.; Conformation/activity studies of rationally designed potent anti-adhesive RGD peptides, *Eur J Biochem* **1992**, *210*, 911-21.

51   Chatterjee, J.; Ovadia, O.; Zahn, G.; Marinelli, L.; Hoffman, A.; Gilon, C.; Kessler, H.; Multiple N-methylation by a designed approach enhances receptor selectivity, *J Med Chem* **2007**, *50*, 5878-81.

52   Veber, D. F.; Freidlinger, R. M.; Perlow, D. S.; Paleveda, W. J., Jr.; Holly, F. W.; Strachan, R. G.; Nutt, R. F.; Arison, B. H.; Homnick, C.; Randall, W. C.; Glitzer, M. S.; Saperstein, R.; Hirschmann, R.; A potent cyclic hexapeptide analogue of somatostatin, *Nature* **1981**, *292*, 55-8.

53   Biron, E.; Chatterjee, J.; Ovadia, O.; Langenegger, D.; Brueggen, J.; Hoyer, D.; Schmid, H. A.; Jelinek, R.; Gilon, C.; Hoffman, A.; Kessler, H.; Improving oral bioavailability of peptides by multiple N-methylation: somatostatin analogues, *Angew Chem Int Ed Engl* **2008**, *47*, 2595-9.

54   Kang, Y. K.; Jhon, J. S.; Preferred conformations of a linear RGD tripeptide, *J Pept Res* **2000**, *56*, 360-72.

55   Venkatachalapathi, Y. V.; Balaram, P.; Temperature Dependence of Peptide NH Chemical Shifts in Benzene: Delineation of Solvent-Shielded and Exposed Amide Protons, *Biopolymers* **1981**, *20*, 625-628.

56   Fresno, M. d.; Alsina, J.; Royo, M.; Barany, G.; Albericio, F.; Solid-phase synthesis of diketopiperazines, useful scaffolds for combinatorial chemistry, *Tet. Let.* **1998**, *39*, 2639-2642.

57   Artursson, P.; Cell cultures as models for drug absorption across the intestinal mucosa, *Crit Rev Ther Drug Carrier Syst* **1991**, *8*, 305-30.

58   Artursson, P.; Palm, K.; Luthman, K.; Caco-2 monolayers in experimental and theoretical predictions of drug transport, *Adv Drug Deliv Rev* **2001**, *46*, 27-43.

59   Matsumoto, S.; Saito, H.; Inui, K.; Transcellular transport of oral cephalosporins in human intestinal epithelial cells, Caco-2: interaction with dipeptide transport systems in apical and basolateral membranes, *J Pharmacol Exp Ther* **1994**, *270*, 498-504.

60   Hunter, J.; Jepson, M. A.; Tsuruo, T.; Simmons, N. L.; Hirst, B. H.; Functional expression of P-glycoprotein in apical membranes of human intestinal Caco-2 cells. Kinetics of vinblastine secretion and interaction with modulators, *J Biol Chem* **1993**, *268*, 14991-7.

61   Ingels, F. M.; Augustijns, P. F.; Biological, pharmaceutical, and analytical considerations with respect to the transport media used in the absorption screening system, Caco-2, *J Pharm Sci* **2003**, *92*, 1545-58.

62   Anderson, J. M.; Molecular structure of tight junctions and their role in epithelial transport, *News Physiol Sci* **2001**, *16*, 126-30.

63   Shin, K.; Fogg, V. C.; Margolis, B.; Tight junctions and cell polarity, *Annu Rev Cell Dev Biol* **2006**, *22*, 207-35.

64   Mitic, L. L.; Van Itallie, C. M.; Anderson, J. M.; Molecular physiology and pathophysiology of tight junctions I. Tight junction structure and function: lessons from mutant animals and proteins, *Am J Physiol Gastrointest Liver Physiol* **2000**, *279*, G250-4.

65   Arrieta, M. C.; Bistritz, L.; Meddings, J. B.; Alterations in intestinal permeability, *Gut* **2006**, *55*, 1512-20.

66   Lee, D. B.; Jamgotchian, N.; Allen, S. G.; Abeles, M. B.; Ward, H. J.; A lipid-protein hybrid model for tight junction, *Am J Physiol Renal Physiol* **2008**, *295*, F1601-12.

67   Balda, M. S.; Matter, K.; Tight junctions at a glance, *J Cell Sci* **2008**, *121*, 3677-82.

68   Laufer, B.; Chatterjee, J.; Frank, A. O.; Kessler, H.; Can N-methylated amino acids serve as substitutes for prolines in conformational design of cyclic pentapeptides?, *J Pept Sci* **2009**, *15*, 141-6.

69   Mierke, D. F.; Kurz, M.; Kessler, H.; Peptide Flexibility and Calculations of an Ensemble of Molecules, *J Am Chem Soc* **1994**, *116*, 1042-1049.

70   Zhang, X.; Nikiforovich, G. V.; Marshall, G. R.; Conformational templates for rational drug design: flexibility of cyclo(D-Pro1-Ala2-Ala3-Ala4-Ala5) in DMSO solution, *J Med Chem* **2007**, *50*, 2921-5.

71   Brandts, J. F.; Halvorson, H. R.; Brennan, M.; Consideration of the Possibility that the slow step in protein denaturation reactions is due to cis-trans isomerism of proline residues, *Biochemistry* **1975**, *14*, 4953-63.

72   Chalmers, D. K.; Marshall, G. R.; Pro-D-NMe-Amino Acid and D-Pro-NMe-Amino Acid: Simple, Efficient Reverse-Turn Constraints, *J Am Chem Soc* **1995**, *117*, 5927-5937.

73   Takeuchi, Y.; Marshall, G. R.; Conformational Analysis of Reverse-Turn Constraints by N-Methylation and N-Hydroxylation of Amide Bonds in Peptides and Non-Peptide Mimetics, *J Am Chem Soc* **1998**, *120*, 5363-5372.

74   Karle, I. L.; Conformation of the Cyclic Pentapeptide Gly-L-Pro-L-Ser-D-Ala-L-Pro in the Crystalline State and an Example of Rotational "Isomerism" between Analogues, *J Am Chem Soc* **1979**, *101*, 181-184.

75   Robinson, J. A.; b-Hairpin Peptidomimetics: Design, Structures and Biological Activities, *Accounts Chem. Res.* **2008**.

76   Rose, G. D.; Gierasch, L. M.; Smith, J. A.; Turns in peptides and proteins, *Adv Protein Chem* **1985**, *37*, 1-109.

77   Torchia, D. A.; Bovey, F. A.; A Nuclear Magnetic Resonance Study of Poly(L-proline) in Aqueous and Aqueous Salt Solutions, *Macromolecules* **1971**, *4*, 246-251.

78   Kessler, H.; Müller, A.; Eine ungewöhnliche Konformation des cyclischen Pentapeptids cyclo(-Pro-Pro-Phe-Phe-Gly-) in DMSO, *Liebigs Ann. Chem.* **1986**, *1986*, 1687-1704.

79   Francart, C.; Wieruszeski, J.-M.; Tartar, A.; Lippens, G.; Structural and Dynamic Characterization of Pro Cis/Trans Isomerization in a Small Cyclic Peptide, *J Am Chem Soc* **1996**, *118*, 7019-7027.

80   Che, Y.; Marshall, G. R.; Impact of cis-proline analogs on peptide conformation, *Biopolymers* **2006**, *81*, 392-406.

81   Keller, M.; Sager, C.; Dumy, P.; Schutkowski, M.; Fischer, G. S.; Mutter, M.; Enhancing the Proline Effect: Pseudo-Prolines for Tailoring Cis/Trans Isomerization, *J. Am. Chem. Soc.* **1998**, *120*, 2714-2720.

82   Owens, N. W.; Braun, C.; O'Neil, J. D.; Marat, K.; Schweizer, F.; Effects of Glycosylation of (2S,4R)-4-Hydroxyproline on the Conformation, Kinetics, and Thermodynamics of Prolyl Amide Isomerization, *J Am Chem Soc* **2007**, *129*, 11670-11671.

83   Biron, E.; Kessler, H.; Convenient synthesis of N-methylamino acids compatible with Fmoc solid-phase peptide synthesis, *J. Org. Chem.* **2005**, *70*, 5183-9.

84   Mahalakshmi, R.; Sengupta, A.; Raghothama, S.; Shamala, N.; Balaram, P.; Tryptophan rich peptides: influence of indole rings on backbone conformation, *Biopolymers* **2007**, *88*, 36-54.

85   Russell, S. J.; Blandl, T.; Skelton, N. J.; Cochran, A. G.; Stability of cyclic beta-hairpins: asymmetric contributions from side chains of a hydrogen-bonded cross-strand residue pair, *J Am Chem Soc* **2003**, *125*, 388-95.

86   Meng, H. Y.; Thomas, K. M.; Lee, A. E.; Zondlo, N. J.; Effects of i and i+3 residue identity on cis-trans isomerism of the aromatic(i+1)-prolyl(i+2) amide bond: implications for type VI beta-turn formation, *Biopolymers* **2006**, *84*, 192-204.

87   Demmer, O.; Dijkgraaf, I.; Schottelius, M.; Wester, H. J.; Kessler, H.; Introduction of functional groups into peptides via N-alkylation, *Org Lett* **2008**, *10*, 2015-8.

88   Kwon, Y. U.; Kodadek, T.; Quantitative evaluation of the relative cell permeability of peptoids and peptides, *J Am Chem Soc* **2007**, *129*, 1508-9.

89   Dechantsreiter, M. A.; Mathä, B.; Jonczyk, A.; Goodman, S. L.; Kessler, H. In *Proc. 24th Euroopean Peptide Symposium*; Ramage, R., Epton, R., Eds.; Mayflower Scientific Ltd.: Kingswinford, 1998; pp 329-331.

90   Haviv, F.; Fitzpatrick, T. D.; Swenson, R. E.; Nichols, C. J.; Mort, N. A.; Bush, E. N.; Diaz, G.; Bammert, G.; Nguyen, A.; Rhutasel, N. S.; et al.; Effect of N-methyl substitution of the peptide bonds in luteinizing hormone-releasing hormone agonists, *J Med Chem* **1993**, *36*, 363-9.

91   Wormser, U.; Laufer, R.; Hart, Y.; Chorev, M.; Gilon, C.; Selinger, Z.; Highly selective agonists for substance P receptor subtypes, *Embo J* **1986**, *5*, 2805-8.

92   Ron, D.; Gilon, C.; Hanani, M.; Vromen, A.; Selinger, Z.; Chorev, M.; N-methylated analogs of Ac[Nle28,31]CCK(26-33): synthesis, activity, and receptor selectivity, *J Med Chem* **1992**, *35*, 2806-11.

93   Baysal, C.; Meirovitch, H.; Ab initio prediction of the solution structures and populations of a cyclic pentapeptide in DMSO based on an implicit solvation model, *Biopolymers* **2000**, *53*, 423-33.

94   Kessler, H.; Griesinger, C.; Lautz, J.; Müller, A.; van Gunsteren, W. F.; Berendsen, H. J. C.; Conformational Dynamics Detected by Nuclear Magnetic Resonance NOE Values and J Coupling Constants, *J Am Chem Soc* **1988**, *110*, 3393-3396.

95   Wester, H.-J.; Koglin, N.; Schwaiger, M.; Kessler, H.; Laufer, B.; Demmer, O.; Anton, M., 2007.

96   Zlotnik, A.; Yoshie, O.; Chemokines: a new classification system and their role in immunity, *Immunity* **2000**, *12*, 121-7.

97   Rossi, D.; Zlotnik, A.; The biology of chemokines and their receptors, *Annu. Rev. Immunol.* **2000**, *18*, 217-42.

98   Balkwill, F.; Cancer and the chemokine network, *Nat. Rev. Cancer* **2004**, *4*, 540-50.

99   Horuk, R.; Chemokine receptors, *Cytokine Growth Factor Rev.* **2001**, *12*, 313-35.

100   Murdoch, C.; CXCR4: chemokine receptor extraordinaire, *Immunol. Rev.* **2000**, *177*, 175-84.

101   Balkwill, F.; The significance of cancer cell expression of the chemokine receptor CXCR4, *Semin. Cancer Biol.* **2004**, *14*, 171-9.

102   Nomura, H.; Nielsen, B. W.; Matsushima, K.; Molecular cloning of cDNAs encoding a LD78 receptor and putative leukocyte chemotactic peptide receptors, *Int. Immunol.* **1993**, *5*, 1239-49.

103   Loetscher, M.; Geiser, T.; O'Reilly, T.; Zwahlen, R.; Baggiolini, M.; Moser, B.; Cloning of a human seven-transmembrane domain receptor, LESTR, that is highly expressed in leukocytes, *J. Biol. Chem.* **1994**, *269*, 232-7.

104   Hori, T.; Sakaida, H.; Sato, A.; Nakajima, T.; Shida, H.; Yoshie, O.; Uchiyama, T.; Detection and delineation of CXCR-4 (fusin) as an entry and fusion cofactor for T-tropic [correction of T cell-tropic] HIV-1 by three different monoclonal antibodies, *J. Immunol.* **1998**, *160*, 180-8.

105   Bleul, C. C.; Farzan, M.; Choe, H.; Parolin, C.; Clark-Lewis, I.; Sodroski, J.; Springer, T. A.; The lymphocyte chemoattractant SDF-1 is a ligand for LESTR/fusin and blocks HIV-1 entry, *Nature* **1996**, *382*, 829-33.

106   Oberlin, E.; Amara, A.; Bachelerie, F.; Bessia, C.; Virelizier, J. L.; Arenzana-Seisdedos, F.; Schwartz, O.; Heard, J. M.; Clark-Lewis, I.; Legler, D. F.; Loetscher, M.; Baggiolini, M.; Moser, B.; The CXC chemokine SDF-1 is the ligand for LESTR/fusin and prevents infection by T-cell-line-adapted HIV-1, *Nature* **1996**, *382*, 833-5.

107   Ganju, R. K.; Brubaker, S. A.; Meyer, J.; Dutt, P.; Yang, Y.; Qin, S.; Newman, W.; Groopman, J. E.; The alpha-chemokine, stromal cell-derived factor-1alpha, binds to the transmembrane G-protein-coupled CXCR-4 receptor and activates multiple signal transduction pathways, *J. Biol. Chem.* **1998**, *273*, 23169-75.

108   Feng, Y.; Broder, C. C.; Kennedy, P. E.; Berger, E. A.; HIV-1 entry cofactor: functional cDNA cloning of a seven-transmembrane, G protein-coupled receptor, *Science* **1996**, *272*, 872-7.

109   Moore, J. P.; Kitchen, S. G.; Pugach, P.; Zack, J. A.; The CCR5 and CXCR4 coreceptors--central to understanding the transmission and pathogenesis of human immunodeficiency virus type 1 infection, *AIDS Res. Hum. Retroviruses* **2004**, *20*, 111-26.

110   Scotton, C. J.; Wilson, J. L.; Milliken, D.; Stamp, G.; Balkwill, F. R.; Epithelial cancer cell migration: a role for chemokine receptors?, *Cancer Res.* **2001**, *61*, 4961-5.

111   Scotton, C. J.; Wilson, J. L.; Scott, K.; Stamp, G.; Wilbanks, G. D.; Fricker, S.; Bridger, G.; Balkwill, F. R.; Multiple actions of the chemokine CXCL12 on epithelial tumor cells in human ovarian cancer, *Cancer Res.* **2002**, *62*, 5930-8.

112   Zeelenberg, I. S.; Ruuls-Van Stalle, L.; Roos, E.; The chemokine receptor CXCR4 is required for outgrowth of colon carcinoma micrometastases, *Cancer Res.* **2003**, *63*, 3833-9.

113   Piovan, E.; Tosello, V.; Indraccolo, S.; Cabrelle, A.; Baesso, I.; Trentin, L.; Zamarchi, R.; Tamamura, H.; Fujii, N.; Semenzato, G.; Chieco-Bianchi, L.; Amadori, A.; Chemokine receptor expression in EBV-associated lymphoproliferation in hu/SCID mice: implications for CXCL12/CXCR4 axis in lymphoma generation, *Blood* **2005**, *105*, 931-9.

114   Koshiba, T.; Hosotani, R.; Miyamoto, Y.; Ida, J.; Tsuji, S.; Nakajima, S.; Kawaguchi, M.; Kobayashi, H.; Doi, R.; Hori, T.; Fujii, N.; Imamura, M.; Expression of stromal cell-derived factor 1 and CXCR4 ligand receptor system in pancreatic cancer: a possible role for tumor progression, *Clin. Cancer Res.* **2000**, *6*, 3530-5.

115   Chen, T.; Triplett, J.; Dehner, B.; Hurst, B.; Colligan, B.; Pemberton, J.; Graff, J. R.; Carter, J. H.; Transforming growth factor-beta receptor type I gene is frequently mutated in ovarian carcinomas, *Cancer Res.* **2001**, *61*, 4679-82.

116   Müller, A.; Homey, B.; Soto, H.; Ge, N.; Catron, D.; Buchanan, M. E.; McClanahan, T.; Murphy, E.; Yuan, W.; Wagner, S. N.; Barrera, J. L.; Mohar, A.; Verastegui, E.; Zlotnik, A.; Involvement of chemokine receptors in breast cancer metastasis, *Nature* **2001**, *410*, 50-6.

117   Geminder, H.; Sagi-Assif, O.; Goldberg, L.; Meshel, T.; Rechavi, G.; Witz, I. P.; Ben-Baruch, A.; A possible role for CXCR4 and its ligand, the CXC chemokine stromal cell-derived factor-1, in the development of bone marrow metastases in neuroblastoma, *J. Immunol.* **2001**, *167*, 4747-57.

118 Han, Y.; He, T.; Huang, D. R.; Pardo, C. A.; Ransohoff, R. M.; TNF-alpha mediates SDF-1 alpha-induced NF-kappa B activation and cytotoxic effects in primary astrocytes, *J. Clin. Invest.* **2001**, *108*, 425-35.

119 Libura, J.; Drukala, J.; Majka, M.; Tomescu, O.; Navenot, J. M.; Kucia, M.; Marquez, L.; Peiper, S. C.; Barr, F. G.; Janowska-Wieczorek, A.; Ratajczak, M. Z.; CXCR4-SDF-1 signaling is active in rhabdomyosarcoma cells and regulates locomotion, chemotaxis, and adhesion, *Blood* **2002**, *100*, 2597-606.

120 Zeelenberg, I. S.; Ruuls-Van Stalle, L.; Roos, E.; Retention of CXCR4 in the endoplasmic reticulum blocks dissemination of a T cell hybridoma, *J. Clin. Invest.* **2001**, *108*, 269-77.

121 Retz, M.; Sidhu, S. S.; Lehmann, J.; Tamamura, H.; Fujii, N.; Basbaum, C.; New HIV-drug inhibits in vitro bladder cancer migration and invasion, *Eur. Urol.* **2005**, *48*, 1025-30.

122 Masuda, M.; Nakashima, H.; Ueda, T.; Naba, H.; Ikoma, R.; Otaka, A.; Terakawa, Y.; Tamamura, H.; Ibuka, T.; Murakami, T.; et al.; A novel anti-HIV synthetic peptide, T-22 ([Tyr5,12,Lys7]-polyphemusin II), *Biochem. Biophys. Res. Commun.* **1992**, *189*, 845-50.

123 Murakami, T.; Zhang, T. Y.; Koyanagi, Y.; Tanaka, Y.; Kim, J.; Suzuki, Y.; Minoguchi, S.; Tamamura, H.; Waki, M.; Matsumoto, A.; Fujii, N.; Shida, H.; Hoxie, J. A.; Peiper, S. C.; Yamamoto, N.; Inhibitory mechanism of the CXCR4 antagonist T22 against human immunodeficiency virus type 1 infection, *J. Virol.* **1999**, *73*, 7489-96.

124 Taichman, R. S.; Cooper, C.; Keller, E. T.; Pienta, K. J.; Taichman, N. S.; McCauley, L. K.; Use of the stromal cell-derived factor-1/CXCR4 pathway in prostate cancer metastasis to bone, *Cancer Res.* **2002**, *62*, 1832-7.

125 Tamamura, H.; Xu, Y.; Hattori, T.; Zhang, X.; Arakaki, R.; Kanbara, K.; Omagari, A.; Otaka, A.; Ibuka, T.; Yamamoto, N.; Nakashima, H.; Fujii, N.; A low-molecular-weight inhibitor against the chemokine receptor CXCR4: a strong anti-HIV peptide T140, *Biochem. Biophys. Res. Commun.* **1998**, *253*, 877-82.

126 Tamamura, H.; Hiramatsu, K.; Mizumoto, M.; Ueda, S.; Kusano, S.; Terakubo, S.; Akamatsu, M.; Yamamoto, N.; Trent, J. O.; Wang, Z.; Peiper, S. C.; Nakashima, H.; Otaka, A.; Fujii, N.; Enhancement of the T140-based pharmacophores leads to the development of more potent and bio-stable CXCR4 antagonists, *Org. Biomol. Chem.* **2003**, *1*, 3663-9.

127 Tamamura, H.; Hiramatsu, K.; Kusano, S.; Terakubo, S.; Yamamoto, N.; Trent, J. O.; Wang, Z.; Peiper, S. C.; Nakashima, H.; Otaka, A.; Fujii, N.; Synthesis of potent CXCR4 inhibitors possessing low cytotoxicity and improved biostability based on T140 derivatives, *Org. Biomol. Chem.* **2003**, *1*, 3656-62.

128 Dechantsreiter, M. A.; Planker, E.; Mathä, B.; Lohof, E.; Hölzemann, G.; Jonczyk, A.; Goodman, S. L.; Kessler, H.; N-Methylated cyclic RGD peptides as highly active and selective alpha(V)beta(3) integrin antagonists, *J. Med. Chem.* **1999**, *42*, 3033-40.

129 Haubner, R.; Finsinger, D.; Kessler, H.; Stereoisomeric Peptide Libraries and Peptidomimetics for Designing Selective Inhibitors of the [alpha] v [beta] 3 Integrin for a New Cancer Therapy, *Angew. Chem. Int. Ed.* **1997**, *36*, 1374-1389.

130 Fujii, N.; Oishi, S.; Hiramatsu, K.; Araki, T.; Ueda, S.; Tamamura, H.; Otaka, A.; Kusano, S.; Terakubo, S.; Nakashima, H.; Broach, J. A.; Trent, J. O.; Wang, Z. X.; Peiper, S. C.; Molecular-size reduction of a potent CXCR4-chemokine antagonist using orthogonal combination of conformation- and sequence-based libraries, *Angew. Chem. Int. Ed. Engl.* **2003**, *42*, 3251-3.

131 Tamamura, H.; Mizumoto, M.; Hiramatsu, K.; Kusano, S.; Terakubo, S.; Yamamoto, N.; Trent, J. O.; Wang, Z.; Peiper, S. C.; Nakashima, H.; Otaka, A.; Fujii, N.; Topochemical exploration of potent compounds using retro-enantiomer libraries of cyclic pentapeptides, *Org. Biomol. Chem.* **2004**, *2*, 1255-7.

132 Laufer, B. Master's Thesis, Technische Universität München, 2006.

133 Trent, J. O.; Wang, Z. X.; Murray, J. L.; Shao, W.; Tamamura, H.; Fujii, N.; Peiper, S. C.; Lipid bilayer simulations of CXCR4 with inverse agonists and weak partial agonists, *J. Biol. Chem.* **2003**, *278*, 47136-44.

134   Knor, S.; Khrenov, A. V.; Laufer, B.; Saenko, E. L.; Hauser, C. A.; Kessler, H.; Development of a peptidomimetic ligand for efficient isolation and purification of factor VIII via affinity chromatography, *J Med Chem* **2007**, *50*, 4329-39.

135   Knor, S.; Khrenov, A.; Laufer, B.; Benhida, A.; Grailly, S. C.; Schwaab, R.; Oldenburg, J.; Beaufort, N.; Magdolen, V.; Saint-Remy, J. M.; Saenko, E. L.; Hauser, C. A.; Kessler, H.; Efficient factor VIII affinity purification using a small synthetic ligand, *J Thromb Haemost* **2008**, *6*, 470-7.

136   Vehar, G. A.; Keyt, B.; Eaton, D.; Rodriguez, H.; O'Brien, D. P.; Rotblat, F.; Oppermann, H.; Keck, R.; Wood, W. I.; Harkins, R. N.; et al.; Structure of human factor VIII, *Nature* **1984**, *312*, 337-342.

137   Wang, W.; Wang, Y. J.; Kelner, D. N.; Coagulation factor VIII: structure and stability, *Int. J. Pharm.* **2003**, *259*, 1-15.

138   Toole, J. J.; Pittman, D. D.; Orr, E. C.; Murtha, P.; Wasley, L. C.; Kaufman, R. J.; A large region (approximately equal to 95 kDa) of human factor VIII is dispensable for in vitro procoagulant activity, *Proc. Natl. Acad. Sci. USA* **1986**, *83*, 5939-5942.

139   Khrenov, A. V.; Ananyeva, N. M.; Saenko, E. L.; Role of the B domain in proteolytic inactivation of activated coagulation factor VIII by activated protein C and activated factor X, *Blood Coagul. Fibrin.* **2006**, *17*, 379-88.

140   Fay, P. J.; Anderson, M. T.; Chavin, S. I.; Marder, V. J.; The size of human factor-VIII heterodimers and the effects produced by thrombin, *Biochim. Biophys. Acta* **1986**, *871*, 268-278.

141   Lenting, P. J.; van Mourik, J. A.; Mertens, K.; The life cycle of coagulation factor VIII in view of its structure and function, *Blood* **1998**, *92*, 3983-3996.

142   Fay, P. J.; Activation of factor VIII and mechanisms of cofactor action, *Blood Rev.* **2004**, *18*, 1-15.

143   Graw, J.; Brackmann, H. H.; Oldenburg, J.; Schneppenheim, R.; Spannagl, M.; Schwaab, R.; Haemophilia A: from mutation analysis to new therapies, *Nat. Rev. Genet.* **2005**, *6*, 488-501.

144   Stoylova, S. S.; Lenting, P. J.; Kemball-Cook, G.; Holzenburg, A.; Electron crystallography of human blood coagulation factor VIII bound to phospholipid monolayers, *J. Biol. Chem.* **1999**, *274*, 36573-8.

145   Saenko, E. L.; Scandella, D.; The acidic region of the factor VIII light chain and the C2 domain together form the high affinity binding site for von willebrand factor, *J Biol Chem* **1997**, *272*, 18007-14.

146   Jacquemin, M.; Benhida, A.; Peerlinck, K.; Desqueper, B.; Vander Elst, L.; Lavend'homme, R.; d'Oiron, R.; Schwaab, R.; Bakkus, M.; Thielemans, K.; Gilles, J. G.; Vermylen, J.; Saint-Remy, J. M.; A human antibody directed to the factor VIII C1 domain inhibits factor VIII cofactor activity and binding to von Willebrand factor, *Blood* **2000**, *95*, 156-63.

147   Wise, R. J.; Dorner, A. J.; Krane, M.; Pittman, D. D.; Kaufman, R. J.; The role of von Willebrand factor multimers and propeptide cleavage in binding and stabilization of factor VIII, *J Biol Chem* **1991**, *266*, 21948-55.

148   Kaufman, R. J.; Pipe, S. W.; Regulation of factor VIII expression and activity by von Willebrand factor, *Thromb Haemost* **1999**, *82*, 201-8.

149   Weiss, H. J.; Sussman, II; Hoyer, L. W.; Stabilization of factor VIII in plasma by the von Willebrand factor. Studies on posttransfusion and dissociated factor VIII and in patients with von Willebrand's disease, *J Clin Invest* **1977**, *60*, 390-404.

150   Over, J.; Sixma, J. J.; Bruine, M. H.; Trieschnigg, M. C.; Vlooswijk, R. A.; Beeser-Visser, N. H.; Bouma, B. N.; Survival of 125iodine-labeled Factor VIII in normals and patients with classic hemophilia. Observations on the heterogeneity of human Factor VIII, *J Clin Invest* **1978**, *62*, 223-34.

151   Fay, P. J.; Activation of factor VIII and mechanisms of cofactor action, *Blood Rev* **2004**, *18*, 1-15.

152   Shen, B. W.; Spiegel, P. C.; Chang, C. H.; Huh, J. W.; Lee, J. S.; Kim, J.; Kim, Y. H.; Stoddard, B. L.; The tertiary structure and domain organization of coagulation factor VIII, *Blood* **2008**, *111*, 1240-7.

153   Wise, R. J.; Dorner, A. J.; Krane, M.; Pittman, D. D.; Kaufman, R. J.; The role of von-Willebrand-factor multimers and propeptide cleavage in binding and stabilization of Factor-VIII, *J. Biol. Chem.* **1991**, *266*, 21948-21955.

154   Saenko, E. L.; Scandella, D.; The acidic region of the factor VIII light chain and the C2 domain together form the high affinity binding site for von Willebrand factor, *J. Biol. Chem.* **1997**, *272*, 18007-18014.

155   Fay, P. J.; Coumans, J. V.; Walker, F. J.; von-Willebrand-factor mediates protection of factor-VIII from activated protein-C-catalyzed inactivation, *J. Biol. Chem.* **1991**, *266*, 2172-2177.

156   Nesheim, M.; Pittman, D. D.; Giles, A. R.; Fass, D. N.; Wang, J. H.; Slonosky, D.; Kaufman, R. J.; The effect of plasma von-Willebrand-factor on the binding of human factor-VIII to thrombin-activated human platelets, *J. Biol. Chem.* **1991**, *266*, 17815-17820.

157   Koppelman, S. J.; Koedam, J. A.; Vanwijnen, M.; Stern, D. M.; Nawroth, P. P.; Sixma, J. J.; Bouma, B. N.; Von-Willebrand-factor as a regulator of intrinsic-factor-X activation, *J. Lab. Clin. Med.* **1994**, *123*, 585-593.

158   Davie, E. W.; Ratnoff, O. D.; Waterfall Sequence for Intrinsic Blood Clotting, *Science* **1964**, *145*, 1310-2.

159   Butenas, S.; Mann, K. G.; Blood coagulation, *Biochemistry (Mosc)* **2002**, *67*, 3-12.

160   Adams, T. E.; Huntington, J. A.; Thrombin-cofactor interactions: structural insights into regulatory mechanisms, *Arterioscler Thromb Vasc Biol* **2006**, *26*, 1738-45.

161   Bishop, P.; Lawson, J.; Recombinant biologics for treatment of bleeding disorders, *Nat Rev Drug Discov* **2004**, *3*, 684-94.

162   Tankersley, D. L.; Finlayson, J. S.; Kinetics of activation and autoactivation of human factor XII, *Biochemistry* **1984**, *23*, 273-9.

163   Zhuo, R.; Siedlecki, C. A.; Vogler, E. A.; Autoactivation of blood factor XII at hydrophilic and hydrophobic surfaces, *Biomaterials* **2006**, *27*, 4325-32.

164   Silverberg, M.; Dunn, J. T.; Garen, L.; Kaplan, A. P.; Autoactivation of human Hageman factor. Demonstration utilizing a synthetic substrate, *J Biol Chem* **1980**, *255*, 7281-6.

165   Knör, S. Ph. D., Technische Universität München, 2007.

166   Bolton-Maggs, P. H.; Pasi, K. J.; Haemophilias A and B, *Lancet* **2003**, *361*, 1801-9.

167   Huntington, J. A.; Baglin, T. P.; Targeting thrombin--rational drug design from natural mechanisms, *Trends Pharmacol Sci* **2003**, *24*, 589-95.

168   Lenting, P. J.; van Mourik, J. A.; Mertens, K.; The life cycle of coagulation factor VIII in view of its structure and function, *Blood* **1998**, *92*, 3983-96.

169   Panteleev, M. A.; Ovanesov, M. V.; Kireev, D. A.; Shibeko, A. M.; Sinauridze, E. I.; Ananyeva, N. M.; Butylin, A. A.; Saenko, E. L.; Ataullakhanov, F. I.; Spatial propagation and localization of blood coagulation are regulated by intrinsic and protein C pathways, respectively, *Biophys J* **2006**, *90*, 1489-500.

170   Graw, J.; Brackmann, H. H.; Oldenburg, J.; Schneppenheim, R.; Spannagl, M.; Schwaab, R.; Haemophilia A: from mutation analysis to new therapies, *Nat Rev Genet* **2005**, *6*, 488-501.

171   Jacquemin, M.; De Maeyer, M.; D'Oiron, R.; Lavend'Homme, R.; Peerlinck, K.; Saint-Remy, J. M.; Molecular mechanisms of mild and moderate hemophilia A, *J Thromb Haemost* **2003**, *1*, 456-63.

172   Oldenburg, J.; Ananyeva, N. M.; Saenko, E. L.; Molecular basis of haemophilia A, *Haemophilia* **2004**, *10 Suppl 4*, 133-9.

173   Klinge, J.; Ananyeva, N. M.; Hauser, C. A.; Saenko, E. L.; Hemophilia A--from basic science to clinical practice, *Semin Thromb Hemost* **2002**, *28*, 309-22.

174 Saenko, E. L.; Ananyeva, N.; Kouiavskaia, D.; Schwinn, H.; Josic, D.; Shima, M.; Hauser, C. A.; Pipe, S.; Molecular defects in coagulation Factor VIII and their impact on Factor VIII function, *Vox Sang* **2002**, *83*, 89-96.

175 Mannucci, P. M.; Hemophilia: treatment options in the twenty-first century, *J Thromb Haemost* **2003**, *1*, 1349-55.

176 Hoots, W. K.; The future of plasma-derived clotting factor concentrates, *Haemophilia* **2001**, *7 Suppl 1*, 4-9.

177 Farrugia, A.; Safety and supply of haemophilia products: worldwide perspectives, *Haemophilia* **2004**, *10*, 327-33.

178 Mannucci, P. M.; Treatment of hemophilia: recombinant factors only? No, *J Thromb Haemost* **2003**, *1*, 216-7.

179 Gitschier, J.; Wood, W. I.; Goralka, T. M.; Wion, K. L.; Chen, E. Y.; Eaton, D. H.; Vehar, G. A.; Capon, D. J.; Lawn, R. M.; Characterization of the human factor VIII gene, *Nature* **1984**, *312*, 326-30.

180 Wood, W. I.; Capon, D. J.; Simonsen, C. C.; Eaton, D. L.; Gitschier, J.; Keyt, B.; Seeburg, P. H.; Smith, D. H.; Hollingshead, P.; Wion, K. L.; et al.; Expression of active human factor VIII from recombinant DNA clones, *Nature* **1984**, *312*, 330-7.

181 Toole, J. J.; Knopf, J. L.; Wozney, J. M.; Sultzman, L. A.; Buecker, J. L.; Pittman, D. D.; Kaufman, R. J.; Brown, E.; Shoemaker, C.; Orr, E. C.; et al.; Molecular cloning of a cDNA encoding human antihaemophilic factor, *Nature* **1984**, *312*, 342-7.

182 Pipe, S. W.; Saint-Remy, J. M.; Walsh, C. E.; New high-technology products for the treatment of haemophilia, *Haemophilia* **2004**, *10 Suppl 4*, 55-63.

183 Betts, J. P.; Recombinant factor VIII may not abolish risk of new variant CJD from factor VIII, *Bmj* **1998**, *316*, 1385.

184 Azzi, A.; De Santis, R.; Morfini, M.; Zakrzewska, K.; Musso, R.; Santagostino, E.; Castaman, G.; TT virus contaminates first-generation recombinant factor VIII concentrates, *Blood* **2001**, *98*, 2571-3.

185 (UKHCDO), U. K. H. C. D. O.; Guidelines on the selection and use of therapeutic products to treat haemophilia and other hereditary bleeding disorders, *Haemophilia* **2003**, *9*, 1-23.

186 Barbara, J.; Flanagan, P.; Blood transfusion risk: protecting against the unknown, *Bmj* **1998**, *316*, 717-8.

187 Cuatreca.P; Wilchek, M.; Anfinsen, C. B.; Selective enzyme purification by affinity chromatography, *Proc. Natl. Acad. Sci. USA* **1968**, *61*, 636-643.

188 Mejan, O.; Fert, V.; Delezay, M.; Delaage, M.; Cheballah, R.; Bourgois, A.; Immunopurification of human factor VIII/vWF complex from plasma, *Thromb. Haemost.* **1988**, *59*, 364-71.

189 Fass, D. N.; Knutson, G. J.; Katzmann, J. A.; Monoclonal antibodies to porcine factor VIII coagulant and their use in the isolation of active coagulant protein, *Blood* **1982**, *59*, 594-600.

190 Addiego, J. E.; Gomperts, E.; Liu, S. L.; Bailey, P.; Courter, S. G.; Lee, M. L.; Neslund, G. G.; Kingdon, H. S.; Griffith, M. J.; Treatment of Hemophilia-A with a highly purified factor-VIII concentrate prepared by anti-FVIIIc immunoaffinity chromatography, *Thromb. Haemost.* **1992**, *67*, 19-27.

191 Eriksson, R. K.; Fenge, C.; Lindner-Olson, E.; Ljungqvist, C.; Rosenquist, J.; Smeds, A. L.; Ostlin, A.; Charlebois, T.; Leonard, M.; Kelley, B. D.; Ljungqvist, A.; The manufacturing process for B-domain deleted recombinant factor VIII, *Semin. Hematol.* **2001**, *38*, 24-31.

192 Boedeker, B. G.; The manufacturing of the recombinant factor VIII, Kogenate, *Transfus Med. Rev.* **1992**, *6*, 256-60.

193 Gomperts, E.; Lundblad, R.; Adamson, R.; The manufacturing process of recombinant factor VIII, recombinate, *Transfus Med. Rev.* **1992**, *6*, 247-51.

194 Jakubik, J. J.; Vicik, S. M.; Tannatt, M. M.; Kelley, B. D.; West Nile Virus inactivation by the solvent/detergent steps of the second and third generation manufacturing processes for B-domain deleted recombinant factor VIII, *Haemophilia* **2004**, *10*, 69-74.

195   Jiang, R.; Monroe, T.; McRogers, R.; Larson, P. J.; Manufacturing challenges in the commercial production of recombinant coagulation factor VIII, *Haemophilia* **2002**, *8*, 1-5.

196   Jack, G. W.; Beer, D. J.; Immunoaffinity chromatography, *Methods Mol. Biol.* **1996**, *59*, 187-196.

197   Scopes, R. K. *Protein purification: Principles and Practice*; 3rd ed.; Springer: New York, 1994.

198   Roque, A. C.; Lowe, C. R.; Taipa, M. A.; Antibodies and genetically engineered related molecules: production and purification, *Biotechnol. Prog.* **2004**, *20*, 639-654.

199   Labrou, N. E.; Design and selection of ligands for affinity chromatography, *J. Chromatogr. B Analyt. Technol. Biomed. Life Sci.* **2003**, *790*, 67-78.

200   Lowe, C. R.; Lowe, A. R.; Gupta, G.; New developments in affinity chromatography with potential application in the production of biopharmaceuticals, *J. Biochem. Biophys. Methods* **2001**, *49*, 561-574.

201   Clonis, Y. D.; Affinity chromatography matures as bioinformatic and combinatorial tools develop, *J. Chromatogr. A* **2006**, *1101*, 1-24.

202   Kelley, B. D.; Tannatt, M.; Magnusson, R.; Hagelberg, S.; Booth, J.; Development and validation of an affinity chromatography step using a peptide ligand for cGMP production of factor VIII, *Biotechnol. Bioeng.* **2004**, *87*, 400-412.

203   Kelley, B. D.; Booth, J.; Tannatt, M.; Wub, Q. L.; Ladner, R.; Yuc, J.; Potter, D.; Ley, A.; Isolation of a peptide ligand for affinity purification of factor VIII using phage display, *J. Chromatogr. A* **2004**, *1038*, 121-130.

204   Amatschek, K.; Necina, R.; Hahn, R.; Schallaun, E.; Schwinn, H.; Josic, D.; Jungbauer, A.; Affinity chromatography of human blood coagulation factor VIII on monoliths with peptides from a combinatorial library, *J. High Resolut. Chromatogr.* **2000**, *23*, 47-58.

205   Pflegerl, K.; Hahn, R.; Berger, E.; Jungbauer, A.; Mutational analysis of a blood coagulation factor VIII-binding peptide, *J. Pept. Sci.* **2002**, *59*, 174-182.

206   Pflegerl, K.; Hahn, R.; Berger, E.; Jungbauer, A.; Mutational analysis of a blood coagulation factor VIII-binding peptide, *J Pept Res* **2002**, *59*, 174-82.

207   Huang, P. Y.; Baumbach, G. A.; Dadd, C. A.; Buettner, J. A.; Masecar, B. L.; Hentsch, M.; Hammond, D. J.; Carbonell, R. G.; Affinity purification of von Willebrand factor using ligands derived from peptide libraries, *Bioorgan. Med. Chem.* **1996**, *4*, 699-708.

208   Sewald, N.; Jakubke, H.-D. *Peptides: Chemistry and Biology*; WILEY-VCH Verlag GmbH: Weinheim, 2002.

209   Zervas, L.; Photaki, I.; On cysteine and cystine peptides .1. New S-protecting groups for cysteine, *J. Am. Chem. Soc.* **1962**, *84*, 3887-3897.

210   Siedler, F.; Weyher, E.; Moroder, L.; Cysteine racemization in peptide synthesis: a new and easy detection method, *J. Pept. Sci.* **1996**, *2*, 271-275.

211   Goodman, M.; Levine, L.; Peptide synthesis via active esters . 4 . Racemization + ring-opening reactions of optically active oxazolones, *J. Am. Chem. Soc.* **1964**, *86*, 2918-2922.

212   Henkel, B.; Zhang, L. S.; Bayer, E.; Investigations on solid-phase peptide synthesis in N-to-C direction (inverse synthesis), *Liebigs Ann.-Recl.* **1997**, 2161-2168.

213   Steglich, W.; Hofle, G.; N,N-Dimethyl-4-pyridinamine, a very effective acylation catalyst, *Angew. Chem. Int. Edit.* **1969**, *8*, 981.

214   Davies, H. M. L.; Townsend, R. J.; Catalytic asymmetric cyclopropanation of heteroaryldiazoacetates, *J. Org. Chem.* **2001**, *66*, 6595-6603.

215   Micuch, P.; Seebach, D.; Preparation of beta(2)-homotryptophan derivatives for beta-peptide synthesis, *Helv. Chim. Acta* **2002**, *85*, 1567-1577.

216   Hilton, S. T.; Ho, T. C. T.; Pljevaljcic, G.; Jones, K.; A new route to spirooxindoles, *Org. Lett.* **2000**, *2*, 2639-2641.

217   Tidwell, T. T.; Oxidation of alcohols by activated dimethyl-sulfoxide and related reactions - an update, *Synthesis-Stuttgart* **1990**, 857-870.

218   Mancuso, A. J.; Huang, S. L.; Swern, D.; Oxidation of long-chain and related alcohols to carbonyls by dimethyl-sulfoxide activated by oxalyl chloride, *J. Org. Chem.* **1978**, *43*, 2480-2482.

219   Denis, J. N.; Correa, A.; Greene, A. E.; Direct, highly efficient synthesis from (S)-(+)-phenylglycine of the taxol and taxotere side-chains, *J. Org. Chem.* **1991**, *56*, 6939-6942.

220   Blaskovich, M. A.; Lajoie, G. A.; Synthesis of a chiral serine aldehyde equivalent and Its conversion to chiral alpha-amino-acid derivatives, *J. Am. Chem. Soc.* **1993**, *115*, 5021-5030.

221   Grigg, R.; MacLachlan, W. S.; MacPherson, D. T.; Sridharan, V.; Suganthan, S.; Thornton-Pett, M.; Zhang, J.; Pictet-Spengler/palladium catalyzed allenylation and carbonylation processes, *Tetrahedron* **2000**, *56*, 6585-6594.

222   Gryko, D.; Chalko, J.; Jurczak, J.; Synthesis and reactivity of N-protected-alpha-amino aldehydes, *Chirality* **2003**, *15*, 514-541.

223   Dess, D. B.; Martin, J. C.; Readily accessible 12-I-5 oxidant for the conversion of primary and secondary alcohols to aldehydes and ketones, *J. Org. Chem.* **1983**, *48*, 4155-4156.

224   Dess, D. B.; Martin, J. C.; A useful 12-I-5 triacetoxyperiodinane (the Dess-Martin periodinane) for the slective oxidation of primary or secondary alcohols and a variety of related 12-I-5 species, *J. Am. Chem. Soc.* **1991**, *113*, 7277-7287.

225   Masiukiewicz, E.; Rzeszotarska, B.; An improved synthesis of tert-butyl N-alpha-tert-butoxy carbonyl-L-(S-trityl)cysteinate, *Org. Prep. Proced. Int.* **1999**, *31*, 571-572.

226   Pearson, D. A.; Blanchette, M.; Baker, M. L.; Guindon, C. A.; Trialkylsilanes as scavengers for the trifluoroacetic-acid deblocking of protecting groups in peptide-synthesis, *Tetrahedron Lett.* **1989**, *30*, 2739-2742.

227   Knor, S.; Laufer, B.; Kessler, H.; Efficient enantioselective synthesis of condensed and aromatic-ring-substituted tyrosine derivatives, *J Org Chem* **2006**, *71*, 5625-30.

228   Strable, E.; Prasuhn, D. E., Jr.; Udit, A. K.; Brown, S.; Link, A. J.; Ngo, J. T.; Lander, G.; Quispe, J.; Potter, C. S.; Carragher, B.; Tirrell, D. A.; Finn, M. G.; Unnatural amino acid incorporation into virus-like particles, *Bioconjug Chem* **2008**, *19*, 866-75.

229   Trabocchi, A.; Scarpi, D.; Guarna, A.; Structural diversity of bicyclic amino acids, *Amino Acids* **2008**, *34*, 1-24.

230   Hanessian, S.; Auzzas, L.; The practice of ring constraint in peptidomimetics using bicyclic and polycyclic amino acids, *Acc Chem Res* **2008**, *41*, 1241-51.

231   Goodman, M.; Shao, H.; Peptidomimetic building blocks for drug discovery: An overview, *Pure Appl. Chem.* **1996**, *68*, 1303-1308.

232   Jeng, A. Y.; Savage, P.; Beil, M. E.; Bruseo, C. W.; Hoyer, D.; Fink, C. A.; Trapani, A. J.; CGS 34226, a thiol-based dual inhibitor of endothelin converting enzyme-1 and neutral endopeptidase 24.11, *Clin Sci (Lond)* **2002**, *103 Suppl 48*, 98S-101S.

233   Dechantsreiter, M. A.; Planker, E.; Matha, B.; Lohof, E.; Holzemann, G.; Jonczyk, A.; Goodman, S. L.; Kessler, H.; N-Methylated cyclic RGD peptides as highly active and selective alpha(V)beta(3) integrin antagonists, *J Med Chem* **1999**, *42*, 3033-40.

234   Wang, W.; Zhang, J.; Xiong, C.; Hruby, V. J.; Design and synthesis of hydrophobic, bulky x2-constrained phenylalanine and naphthylalanine derivatives, *Tet. Let.* **2002**, *43*, 2137-2140.

235   Burk, M. J.; Lee, J. R.; Martinez, J. P.; A Versatile Tandem Catalysis Procedure for the Preparation of Novel Amino Acids and Peptides, *J. Am. Chem. Soc.* **1994**, *116*, 10847-10848.

236   Kotha, S.; Lahiri, K.; Application of the Suzuki-Miyaura cross-coupling reaction for the modification of phenylalanine peptides, *Biopolymers* **2003**, *69*, 517-528.

237   Burk, M. J.; Gross, M. F.; Harper, T. G. P.; Kalberg, C. S.; Lee, J. R.; Martinez, J. P.; Asymmetric catalytic routes to chiral building blocks of medicinal interest, *Pure Appl. Chem.* **1996**, *68*, 37-44.

238   Birnbaum, S. M.; Levintow, L.; Kingsley, R. B.; Greenstein, J. P.; Specificity of amino acid acylases, *J Biol Chem* **1952**, *194*, 455-70.

239   Tamkun, J. W.; DeSimone, D. W.; Fonda, D.; Patel, R. S.; Buck, C.; Horwitz, A. F.; Hynes, R. O.; Structure of integrin, a glycoprotein involved in the transmembrane linkage between fibronectin and actin, *Cell* **1986**, *46*, 271-82.

240   Pytela, R.; Pierschbacher, M. D.; Ruoslahti, E.; A 125/115-kDa cell surface receptor specific for vitronectin interacts with the arginine-glycine-aspartic acid adhesion sequence derived from fibronectin, *Proc Natl Acad Sci U S A* **1985**, *82*, 5766-70.

241   Pytela, R.; Pierschbacher, M. D.; Ruoslahti, E.; Identification and isolation of a 140 kd cell surface glycoprotein with properties expected of a fibronectin receptor, *Cell* **1985**, *40*, 191-8.

242   Hynes, R. O.; Integrins: bidirectional, allosteric signaling machines, *Cell* **2002**, *110*, 673-87.

243   Suzuki, S.; Argraves, W. S.; Pytela, R.; Arai, H.; Krusius, T.; Pierschbacher, M. D.; Ruoslahti, E.; cDNA and amino acid sequences of the cell adhesion protein receptor recognizing vitronectin reveal a transmembrane domain and homologies with other adhesion protein receptors, *Proc Natl Acad Sci U S A* **1986**, *83*, 8614-8.

244   Jin, H.; Varner, J.; Integrins: roles in cancer development and as treatment targets, *Br J Cancer* **2004**, *90*, 561-5.

245   Clemetson, K. J.; Clemetson, J. M.; Integrins and cardiovascular disease, *Cell Mol Life Sci* **1998**, *54*, 502-13.

246   Yusuf-Makagiansar, H.; Anderson, M. E.; Yakovleva, T. V.; Murray, J. S.; Siahaan, T. J.; Inhibition of LFA-1/ICAM-1 and VLA-4/VCAM-1 as a therapeutic approach to inflammation and autoimmune diseases, *Med Res Rev* **2002**, *22*, 146-67.

247   Humphries, M. J.; McEwan, P. A.; Barton, S. J.; Buckley, P. A.; Bella, J.; Mould, A. P.; Integrin structure: heady advances in ligand binding, but activation still makes the knees wobble, *Trends Biochem Sci* **2003**, *28*, 313-20.

248   Nermut, M. V.; Green, N. M.; Eason, P.; Yamada, S. S.; Yamada, K. M.; Electron microscopy and structural model of human fibronectin receptor, *Embo J* **1988**, *7*, 4093-9.

249   Xiong, J. P.; Stehle, T.; Diefenbach, B.; Zhang, R.; Dunker, R.; Scott, D. L.; Joachimiak, A.; Goodman, S. L.; Arnaout, M. A.; Crystal structure of the extracellular segment of integrin alpha Vbeta3, *Science* **2001**, *294*, 339-45.

250   Xiong, J. P.; Stehle, T.; Zhang, R.; Joachimiak, A.; Frech, M.; Goodman, S. L.; Arnaout, M. A.; Crystal structure of the extracellular segment of integrin alpha Vbeta3 in complex with an Arg-Gly-Asp ligand, *Science* **2002**, *296*, 151-5.

251   Bork, P.; Doerks, T.; Springer, T. A.; Snel, B.; Domains in plexins: links to integrins and transcription factors, *Trends Biochem Sci* **1999**, *24*, 261-3.

252   Rocco, M.; Rosano, C.; Weisel, J. W.; Horita, D. A.; Hantgan, R. R.; Integrin conformational regulation: uncoupling extension/tail separation from changes in the head region by a multiresolution approach, *Structure* **2008**, *16*, 954-64.

253   Lee, J. O.; Rieu, P.; Arnaout, M. A.; Liddington, R.; Crystal structure of the A domain from the alpha subunit of integrin CR3 (CD11b/CD18), *Cell* **1995**, *80*, 631-8.

254   Xiao, T.; Takagi, J.; Coller, B. S.; Wang, J. H.; Springer, T. A.; Structural basis for allostery in integrins and binding to fibrinogen-mimetic therapeutics, *Nature* **2004**, *432*, 59-67.

255   Legler, D. F.; Wiedle, G.; Ross, F. P.; Imhof, B. A.; Superactivation of integrin alphavbeta3 by low antagonist concentrations, *J Cell Sci* **2001**, *114*, 1545-53.

256   Arnaout, M. A.; Mahalingam, B.; Xiong, J. P.; Integrin structure, allostery, and bidirectional signaling, *Annu Rev Cell Dev Biol* **2005**, *21*, 381-410.

257   Luo, B. H.; Carman, C. V.; Springer, T. A.; Structural basis of integrin regulation and signaling, *Annu Rev Immunol* **2007**, *25*, 619-47.

258   Lau, T. L.; Kim, C.; Ginsberg, M. H.; Ulmer, T. S.; The structure of the integrin alphaIIbbeta3 transmembrane complex explains integrin transmembrane signalling, *Embo J* **2009**.

259   Hoefling, M.; Kessler, H.; Gottschalk, K.-E.; The Transmembrane Structure of Integrin aIIbb3 - Significance to Signal Transduction, *Angew. Chem. Int. Ed.* **2009**, *ASAP*.

260   Arndt, T.; Arndt, U.; Reuning, U.; Kessler, H.; Weber, G. F., Ed.: Norfolk, 2005; pp 93-141.

261   Karin, M.; Cao, Y.; Greten, F. R.; Li, Z. W.; NF-kappaB in cancer: from innocent bystander to major culprit, *Nat Rev Cancer* **2002**, *2*, 301-10.

262   Cheresh, D. A.; Stupack, D. G.; Integrin-mediated death: an explanation of the integrin-knockout phenotype?, *Nat Med* **2002**, *8*, 193-4.

263   Reedquist, K. A.; Ross, E.; Koop, E. A.; Wolthuis, R. M.; Zwartkruis, F. J.; van Kooyk, Y.; Salmon, M.; Buckley, C. D.; Bos, J. L.; The small GTPase, Rap1, mediates CD31-induced integrin adhesion, *J Cell Biol* **2000**, *148*, 1151-8.

264   Zhang, Z.; Vuori, K.; Wang, H.; Reed, J. C.; Ruoslahti, E.; Integrin activation by R-ras, *Cell* **1996**, *85*, 61-9.

265   Diaz-Gonzalez, F.; Forsyth, J.; Steiner, B.; Ginsberg, M. H.; Trans-dominant inhibition of integrin function, *Mol Biol Cell* **1996**, *7*, 1939-51.

266   Heckmann, D. Ph. D., Technische Universität München, 2007.

267   Müller, G.; Gurrath, M.; Kessler, H.; Pharmacophore refinement of gpIIb/IIIa antagonists based on comparative studies of antiadhesive cyclic and acyclic RGD peptides, *J Comput Aided Mol Des* **1994**, *8*, 709-30.

268   Pankov, R.; Yamada, K. M.; Fibronectin at a glance, *J Cell Sci* **2002**, *115*, 3861-3.

269   Potts, J. R.; Campbell, I. D.; Fibronectin structure and assembly, *Curr Opin Cell Biol* **1994**, *6*, 648-55.

270   Hynes, R. O.; A reevaluation of integrins as regulators of angiogenesis, *Nat Med* **2002**, *8*, 918-21.

271   Gibson, C.; Sulyok, G. A.; Hahn, D.; Goodman, S. L.; Holzemann, G.; Kessler, H.; Nonpeptidic alpha(v)beta(3) Integrin Antagonist Libraries: On-Bead Screening and Mass Spectrometric Identification without Tagging The authors acknowledge technical assistance from M. Urzinger, B. Cordes, M. Kranawetter, and A. Schroder. Financial support of the Fonds der Chemischen Industrie and the Deutsche Forschungsgemeinschaft is gratefully acknowledged, *Angew Chem Int Ed Engl* **2001**, *40*, 165-169.

272   Goodman, S. L.; Holzemann, G.; Sulyok, G. A.; Kessler, H.; Nanomolar small molecule inhibitors for alphav(beta)6, alphav(beta)5, and alphav(beta)3 integrins, *J Med Chem* **2002**, *45*, 1045-51.

273   Hutchinson, J. H.; Halczenko, W.; Brashear, K. M.; Breslin, M. J.; Coleman, P. J.; Duong le, T.; Fernandez-Metzler, C.; Gentile, M. A.; Fisher, J. E.; Hartman, G. D.; Huff, J. R.; Kimmel, D. B.; Leu, C. T.; Meissner, R. S.; Merkle, K.; Nagy, R.; Pennypacker, B.; Perkins, J. J.; Prueksaritanont, T.; Rodan, G. A.; Varga, S. L.; Wesolowski, G. A.; Zartman, A. E.; Rodan, S. B.; Duggan, M. E.; Nonpeptide alphavbeta3 antagonists. 8. In vitro and in vivo evaluation of a potent alphavbeta3 antagonist for the prevention and treatment of osteoporosis, *J Med Chem* **2003**, *46*, 4790-8.

274   Hartman, G. D.; Egbertson, M. S.; Halczenko, W.; Laswell, W. L.; Duggan, M. E.; Smith, R. L.; Naylor, A. M.; Manno, P. D.; Lynch, R. J.; Zhang, G.; et al.; Non-peptide fibrinogen receptor antagonists. 1. Discovery and design of exosite inhibitors, *J Med Chem* **1992**, *35*, 4640-2.

275   Marugan, J. J.; Manthey, C.; Anaclerio, B.; Lafrance, L.; Lu, T.; Markotan, T.; Leonard, K. A.; Crysler, C.; Eisennagel, S.; Dasgupta, M.; Tomczuk, B.; Design, synthesis, and biological evaluation of novel potent and selective alphavbeta3/alphavbeta5 integrin dual inhibitors with improved bioavailability. Selection of the molecular core, *J Med Chem* **2005**, *48*, 926-34.

276   Smallheer, J. M.; Weigelt, C. A.; Woerner, F. J.; Wells, J. S.; Daneker, W. F.; Mousa, S. A.; Wexler, R. R.; Jadhav, P. K.; Synthesis and biological evaluation of nonpeptide integrin antagonists containing spirocyclic scaffolds, *Bioorg Med Chem Lett* **2004**, *14*, 383-7.

277   Tamhane, U. U.; Gurm, H. S.; The chimeric monoclonal antibody abciximab: a systematic review of its safety in contemporary practice, *Expert Opin Drug Saf* **2008**, *7*, 809-19.

278 Reardon, D. A.; Nabors, L. B.; Stupp, R.; Mikkelsen, T.; Cilengitide: an integrin-targeting arginine-glycine-aspartic acid peptide with promising activity for glioblastoma multiforme, *Expert Opin Investig Drugs* **2008**, *17*, 1225-35.

279 Marinelli, L.; Meyer, A.; Heckmann, D.; Lavecchia, A.; Novellino, E.; Kessler, H.; Ligand binding analysis for human alpha5beta1 integrin: strategies for designing new alpha5beta1 integrin antagonists, *J Med Chem* **2005**, *48*, 4204-7.

280 Kerr, J. S.; Slee, A. M.; Mousa, S. A.; The alpha v integrin antagonists as novel anticancer agents: an update, *Expert Opin Investig Drugs* **2002**, *11*, 1765-74.

281 Cheresh, D. A.; Spiro, R. C.; Biosynthetic and functional properties of an Arg-Gly-Asp-directed receptor involved in human melanoma cell attachment to vitronectin, fibrinogen, and von Willebrand factor, *J Biol Chem* **1987**, *262*, 17703-11.

282 Aumailley, M.; Gurrath, M.; Muller, G.; Calvete, J.; Timpl, R.; Kessler, H.; Arg-Gly-Asp constrained within cyclic pentapeptides. Strong and selective inhibitors of cell adhesion to vitronectin and laminin fragment P1, *FEBS Lett* **1991**, *291*, 50-4.

283 Brooks, P. C.; Montgomery, A. M.; Rosenfeld, M.; Reisfeld, R. A.; Hu, T.; Klier, G.; Cheresh, D. A.; Integrin alpha v beta 3 antagonists promote tumor regression by inducing apoptosis of angiogenic blood vessels, *Cell* **1994**, *79*, 1157-64.

284 Eliceiri, B. P.; Klemke, R.; Stromblad, S.; Cheresh, D. A.; Integrin alphavbeta3 requirement for sustained mitogen-activated protein kinase activity during angiogenesis, *J Cell Biol* **1998**, *140*, 1255-63.

285 Scatena, M.; Almeida, M.; Chaisson, M. L.; Fausto, N.; Nicosia, R. F.; Giachelli, C. M.; NF-kappaB mediates alphavbeta3 integrin-induced endothelial cell survival, *J Cell Biol* **1998**, *141*, 1083-93.

286 Stromblad, S.; Becker, J. C.; Yebra, M.; Brooks, P. C.; Cheresh, D. A.; Suppression of p53 activity and p21WAF1/CIP1 expression by vascular cell integrin alphaVbeta3 during angiogenesis, *J Clin Invest* **1996**, *98*, 426-33.

287 Stupack, D. G.; Puente, X. S.; Boutsaboualoy, S.; Storgard, C. M.; Cheresh, D. A.; Apoptosis of adherent cells by recruitment of caspase-8 to unligated integrins, *J Cell Biol* **2001**, *155*, 459-70.

288 Byzova, T. V.; Goldman, C. K.; Pampori, N.; Thomas, K. A.; Bett, A.; Shattil, S. J.; Plow, E. F.; A mechanism for modulation of cellular responses to VEGF: activation of the integrins, *Mol Cell* **2000**, *6*, 851-60.

289 Bader, B. L.; Rayburn, H.; Crowley, D.; Hynes, R. O.; Extensive vasculogenesis, angiogenesis, and organogenesis precede lethality in mice lacking all alpha v integrins, *Cell* **1998**, *95*, 507-19.

290 Taverna, D.; Moher, H.; Crowley, D.; Borsig, L.; Varki, A.; Hynes, R. O.; Increased primary tumor growth in mice null for beta3- or beta3/beta5-integrins or selectins, *Proc Natl Acad Sci U S A* **2004**, *101*, 763-8.

291 Reynolds, L. E.; Wyder, L.; Lively, J. C.; Taverna, D.; Robinson, S. D.; Huang, X.; Sheppard, D.; Hynes, R. O.; Hodivala-Dilke, K. M.; Enhanced pathological angiogenesis in mice lacking beta3 integrin or beta3 and beta5 integrins, *Nat Med* **2002**, *8*, 27-34.

292 Simon, K. O.; Nutt, E. M.; Abraham, D. G.; Rodan, G. A.; Duong, L. T.; The alphavbeta3 integrin regulates alpha5beta1-mediated cell migration toward fibronectin, *J Biol Chem* **1997**, *272*, 29380-9.

293 Kim, S.; Bakre, M.; Yin, H.; Varner, J. A.; Inhibition of endothelial cell survival and angiogenesis by protein kinase A, *J Clin Invest* **2002**, *110*, 933-41.

294 Kim, S.; Harris, M.; Varner, J. A.; Regulation of integrin alpha vbeta 3-mediated endothelial cell migration and angiogenesis by integrin alpha5beta1 and protein kinase A, *J Biol Chem* **2000**, *275*, 33920-8.

295 Kim, S.; Bell, K.; Mousa, S. A.; Varner, J. A.; Regulation of angiogenesis in vivo by ligation of integrin alpha5beta1 with the central cell-binding domain of fibronectin, *Am J Pathol* **2000**, *156*, 1345-62.

296   Stragies, R.; Osterkamp, F.; Zischinsky, G.; Vossmeyer, D.; Kalkhof, H.; Reimer, U.; Zahn, G.; Design and synthesis of a new class of selective integrin alpha5beta1 antagonists, *J Med Chem* **2007**, *50*, 3786-94.

297   Heckmann, D.; Meyer, A.; Marinelli, L.; Zahn, G.; Stragies, R.; Kessler, H.; Probing integrin selectivity: rational design of highly active and selective ligands for the alpha5beta1 and alphavbeta3 integrin receptor, *Angew Chem Int Ed Engl* **2007**, *46*, 3571-4.

298   Lopez-Garcia, M.; Kessler, H. In *Handbook of Biomineralization*; Bäuerlein, E., Behrens, P., Epple, M., Eds.; Wiley-VCH: Weinheim, 2007; Vol. 3; pp 109-123.

299   Castner, D. G.; Ratner, B. D.; Biomedical Surface Science: Foundations of Frontiers, *Surface Science* **2002**, *500*, 28-60.

300   Gray, J. J.; The interaction of proteins with solid surfaces, *Curr. Opin. Struct. Biol.* **2004**, *14*, 110-115.

301   Roach, P.; Farrar, D.; Perry, C. C.; Interpretation of protein adsorption: surface-induced conformational changes, *J. Am. Chem. Soc.* **2005**, *127*, 8168-8173.

302   Matsuura, T.; Hosokawa, R.; Okamoto, K.; Kimoto, T.; Akagawa, Y.; Diverse mechanisms of osteoblast spreading on hydroxyapatite and titanium, *Biomaterials* **2000**, *21*, 1121-7.

303   Thull, R.; Surface functionalization of materials to initiate auto-compatibilization in vivo, *Materialwiss. Werkst.* **2001**, *32*, 949-952.

304   Kantlehner, M.; Schaffner, P.; Finsinger, D.; Meyer, J.; Jonczyk, A.; Diefenbach, B.; Nies, B.; Holzemann, G.; Goodman, S. L.; Kessler, H.; Surface coating with cyclic RGD peptides stimulates osteoblast adhesion and proliferation as well as bone formation, *Chembiochem* **2000**, *1*, 107-14.

305   Auernheimer, J.; Zukowski, D.; Dahmen, C.; Kantlehner, M.; Enderle, A.; Goodman, S. L.; Kessler, H.; Titanium implant materials with improved biocompatibility through coating with phosphonate-anchored cyclic RGD peptides, *Chembiochem* **2005**, *6*, 2034-40.

306   Pechy, P.; Rotzinger, F. P.; Nazeeruddin, M. K.; Kohle, O.; Zakeeruddin, S. M.; Humphrybaker, R.; Gratzel, M.; Preparation of Phosphonated Polypyridyl Ligands to Anchor Transition-Metal Complexes on Oxide Surfaces - Application for the Conversion of Light to Electricity with Nanocrystalline Tio2 Films (Pg 65, 1995), *J. Chem. Soc. Chem. Commun.* **1995**, 1093-1093.

307   Mammen, M.; Choi, S. K.; Whitesides, G. M.; Polyvalent interactions in biological systems: Implications for design and use of multivalent ligands and inhibitors, *Angew. Chem. Int. Ed.* **1998**, *37*, 2755-2794.

308   Auernheimer, J.; Zukowski, D.; Dahmen, C.; Kantlehner, M.; Enderle, A.; Goodman, S. L.; Kessler, H.; Titanium implant materials with improved riocompatibility through coating with phosphonate-anchored cyclic RGD peptides, *ChemBioChem* **2005**, *6*, 2034-2040.

309   Heckmann, D.; Meyer, A.; Laufer, B.; Zahn, G.; Stragies, R.; Kessler, H.; Rational design of highly active and selective ligands for the alpha5beta1 integrin receptor, *Chembiochem* **2008**, *9*, 1397-407.

310   Meyer, A.; Auernheimer, J.; Modlinger, A.; Kessler, H.; Targeting RGD recognizing integrins: drug development, biomaterial research, tumor imaging and targeting, *Curr Pharm Des* **2006**, *12*, 2723-47.

311   Sulyok, G. A.; Gibson, C.; Goodman, S. L.; Holzemann, G.; Wiesner, M.; Kessler, H.; Solid-phase synthesis of a nonpeptide RGD mimetic library: new selective alphavbeta3 integrin antagonists, *J Med Chem* **2001**, *44*, 1938-50.

312   Carmeliet, P.; Integrin indecision, *Nat Med* **2002**, *8*, 14-6.

313   Gibson, C.; Goodman, S. L.; Hahn, D.; Hoelzemann, G.; Kessler, H.; Novel solid-phase synthesis of azapeptides and azapeptoids via Fmoc-strategy and its application in the synthesis of RGD-mimetics, *J. Org. Chem.* **1999**, *64*, 7388-7394.

314   Heckmann, D.; Laufer, B.; Marinelli, L.; Limongelli, V.; Novellino, E.; Zahn, G.; Stragies, R.; Kessler, H.; Breaking the Dogma of the Metal-Coordinating Carboxylate Group in

Integrin Ligands: Introducing Hydroxamic Acids to the MIDAS to Tune Potency and Selectivity, *Angew Chem Int Ed Engl* **2009**.

315   Dayam, R.; Aiello, F.; Deng, J.; Wu, Y.; Garofalo, A.; Chen, X.; Neamati, N.; Discovery of small molecule integrin alphavbeta3 antagonists as novel anticancer agents, *J Med Chem* **2006**, *49*, 4526-34.

316   Coleman, P. J.; Askew, B. C.; Hutchinson, J. H.; Whitman, D. B.; Perkins, J. J.; Hartman, G. D.; Rodan, G. A.; Leu, C. T.; Prueksaritanont, T.; Fernandez-Metzler, C.; Merkle, K. M.; Lynch, R.; Lynch, J. J.; Rodan, S. B.; Duggan, M. E.; Non-peptide alpha(v)beta(3) antagonists. Part 4: potent and orally bioavailable chain-shortened RGD mimetics, *Bioorg Med Chem Lett* **2002**, *12*, 2463-5.

317   Humphries, M. J.; Integrin structure, *Biochem Soc Trans* **2000**, *28*, 311-39.

318   Griffith, D.; Krot, K.; Comiskey, J.; Nolan, K. B.; Marmion, C. J.; Monohydroxamic acids and bridging dihydroxamic acids as chelators to ruthenium(III) and as nitric oxide donors: syntheses, speciation studies and nitric oxide releasing investigations, *Dalton Trans* **2008**, 137-47.

319   Tam, S. S.; Lee, D. H.; Wang, E. Y.; Munroe, D. G.; Lau, C. Y.; Tepoxalin, a novel dual inhibitor of the prostaglandin-H synthase cyclooxygenase and peroxidase activities, *J Biol Chem* **1995**, *270*, 13948-55.

320   Seebach, D.; Ciceri, P. E.; Overhand, M.; Jaun, B.; Rigo, D.; Oberer, L.; Hommel, U.; Amstutz, R.; Widmer, H.; Probing the Helical Secondary Structure of Short-Chain beta-Peptides, *Hel. Chim. Acta.* **1996**, *79*, 2043-2066.

321   Brandley, B. K.; Schnaar, R. L.; Covalent attachment of an Arg-Gly-Asp sequece peptide to derivatizable polyacrylamide surfaces: Support of fibroblast adhesion and long-term growth, *Anal. Biochem.* **1988**, *172*, 270-278.

322   Massia, S. P.; Hubbell, J. A.; An RGD Spacing of 440 nm Is Sufficient for Integrin avb3-Mediated Fibroblast Spreading and 140 nm for Focal Contact and Stress Fiber Formation, *J. Cell Biol.* **1991**, *114*, 1089-1100.

323   Roberts, C.; Chen, C. S.; Mrksich, M.; Martichonok, V.; Ingber, D. E.; Whitesides, G. M.; Using Mixed Self-Assembled Monolayers Presenting RGD and (EG)3OH Groups To Characterize Long-Term Attachment of Bovine Capillary Endothelial Cells to Surfaces, *J. Am. Chem. Soc.* **1998**, *120*, 6548-6555.

324   Hu, B.; Finsinger, D.; Peter, K.; Guttenberg, Z.; Barmann, M.; Kessler, H.; Escherich, A.; Moroder, L.; Bohm, J.; Baumeister, W.; Sui, S. F.; Sackmann, E.; Intervesicle cross-linking with integrin alpha IIb beta 3 and cyclic-RGD-lipopeptide. A model of cell-adhesion processes, *Biochemistry* **2000**, *39*, 12284-94.

325   Marchi-Artzner, V.; Lorz, B.; Hellerer, U.; Kantlehner, M.; Kessler, H.; Sackmann, E.; Selective adhesion of endothelial cells to artificial membranes with a synthetic RGD-lipopeptide, *Chemistry* **2001**, *7*, 1095-101.

326   Carpino, L. A.; Sadat-Aalaee, D.; Chao, H. G.; DeSelm, R. H.; [(9-Fluorenylmethyl)oxy]carbonyl (FMOC) amino acid fluorides. Convienient new peptide coupling reagents applicable to the FMOC/tert-butyl strategy for solution and solid-phase syntheses., *J. Am. Chem. Soc.* **1990**, *112*, 9651-9652.

327   Merrifield, B.; Solid Phase Synthesis (Nobel lecture), *Angew. Chem. Int. Ed. Engl.* **1985**, *24*, 799-810.

328   Carpino, L. A.; El-Faham, A.; Albericio, F.; Racemization Studies During Solid-Phase Peptide Synthesis Using Azabenzotriazole-Based Coupling Reagents, *Tet. Let.* **1994**, *35*, 2279-2282.

329   Wang, Q.; Lin, T.; Tang, L.; Johnson, J. E.; Finn, M. G.; Icosahedral virus particles as addressable nanoscale building blocks, *Angew Chem Int Ed Engl* **2002**, *41*, 459-62.

330   Manchester, M.; Steinmetz, N. F.; Viruses and nanotechnology. Preface, *Curr Top Microbiol Immunol* **2009**, *327*, v-vi.

331 Jennings, G. T.; Bachmann, M. F.; The coming of age of virus-like particle vaccines, *Biol Chem* **2008**, *389*, 521-36.

332 Roy, P.; Noad, R.; Virus-like particles as a vaccine delivery system: myths and facts, *Hum Vaccin* **2008**, *4*, 5-12.

333 Jennings, G. T.; Bachmann, M. F.; Immunodrugs: therapeutic VLP-based vaccines for chronic diseases, *Annu Rev Pharmacol Toxicol* **2009**, *49*, 303-26.

334 Ludwig, C.; Wagner, R.; Virus-like particles-universal molecular toolboxes, *Curr Opin Biotechnol* **2007**, *18*, 537-45.

335 Steinmetz, N. F.; Manchester, M.; PEGylated viral nanoparticles for biomedicine: the impact of PEG chain length on VNP cell interactions in vitro and ex vivo, *Biomacromolecules* **2009**, *10*, 784-92.

336 Triantafilou, K.; Takada, Y.; Triantafilou, M.; Mechanisms of integrin-mediated virus attachment and internalization process, *Crit Rev Immunol* **2001**, *21*, 311-22.

337 Wickham, T. J.; Mathias, P.; Cheresh, D. A.; Nemerow, G. R.; Integrins alpha v beta 3 and alpha v beta 5 promote adenovirus internalization but not virus attachment, *Cell* **1993**, *73*, 309-19.

338 Nemerow, G. R.; Stewart, P. L.; Role of alpha(v) integrins in adenovirus cell entry and gene delivery, *Microbiol Mol Biol Rev* **1999**, *63*, 725-34.

339 Weigel-Kelley, K. A.; Yoder, M. C.; Srivastava, A.; Alpha5beta1 integrin as a cellular coreceptor for human parvovirus B19: requirement of functional activation of beta1 integrin for viral entry, *Blood* **2003**, *102*, 3927-33.

340 Simonet, M.; Riot, B.; Fortineau, N.; Berche, P.; Invasin production by Yersinia pestis is abolished by insertion of an IS200-like element within the inv gene, *Infect Immun* **1996**, *64*, 375-9.

341 Cowan, C.; Jones, H. A.; Kaya, Y. H.; Perry, R. D.; Straley, S. C.; Invasion of epithelial cells by Yersinia pestis: evidence for a Y. pestis-specific invasin, *Infect Immun* **2000**, *68*, 4523-30.

342 Wong, K. W.; Isberg, R. R.; Emerging views on integrin signaling via Rac1 during invasin-promoted bacterial uptake, *Curr Opin Microbiol* **2005**, *8*, 4-9.

343 Krukonis, E. S.; Isberg, R. R.; Integrin beta1-chain residues involved in substrate recognition and specificity of binding to invasin, *Cell Microbiol* **2000**, *2*, 219-30.

344 Kozlovska, T. M.; Cielens, I.; Dreilinna, D.; Dislers, A.; Baumanis, V.; Ose, V.; Pumpens, P.; Recombinant RNA phage Q beta capsid particles synthesized and self-assembled in Escherichia coli, *Gene* **1993**, *137*, 133-7.

345 Kaltgrad, E.; O'Reilly, M. K.; Liao, L.; Han, S.; Paulson, J. C.; Finn, M. G.; On-virus construction of polyvalent glycan ligands for cell-surface receptors, *J Am Chem Soc* **2008**, *130*, 4578-9.

346 Wang, Q.; Kaltgrad, E.; Lin, T.; Johnson, J. E.; Finn, M. G.; Natural supramolecular building blocks. Wild-type cowpea mosaic virus, *Chem Biol* **2002**, *9*, 805-11.

347 Goddard, T. D.; Kneller, D. G.; University of California: San Francisco, USA.

348 Kessler, H.; Schmitt, W. In *Encyclopedia of Nuclear Magnetic Resonance*; Grant, D. M., Harris, R. K., Eds.; Wiley: New York, 1995.

349 Bax, A.; Summers, M. F.; 1H and 13C Assignments from Sensitivity-Enhanced Detection of Heteronuclear Multiple-Bond Connectivity by 2D Multiple Quantum NMR, *J Am Chem Soc* **1986**, *108*, 2093-2094.

350 Kessler, H.; Gehrke, M.; Griesinger, C.; Two-Dimensional NMR Spectroscopy: Background and Overview of the Experiments [New Analytical Methods, *Angew Chem Int Ed Engl* **1988**, *27*, 490-536.

351 Howarth, O. W.; Lilley, D. M.; Carbon-13-NMR of Peptides and Proteins, *Progress in NMR Spectroscopy* **1978**, *12*, 1-40.

352   Kessler, H.; Griesinger, C.; Kerssebaum, R.; Wagner, K.; Ernst, R. R.; Separation of Cross-Relaxation and J Cross-Peaks in 2D Rotating-Frame NMR Spectroscopy, *J Am Chem Soc* **1987**, *102*, 607-609.

353   Havel, T. F.; An evaluation of computational strategies for use in the determination of protein structure from distance constraints obtained by nuclear magnetic resonance, *Prog Biophys Mol Biol* **1991**, *56*, 43-78.

354   Mierke, D. F.; Geyer, A.; Kessler, H.; Coupling constants and hydrogen bonds as experimental restraints in a distance geometry refinement protocol, *Int J Pept Protein Res* **1994**, *44*, 325-31.

355   Mierke, D.; Kessler, H.; Molecular Dynamics with Dimethyl Sulfoxide as a Solvent. Conformation of a Cyclic Hexapeptide, *J Am Chem Soc* **1991**, *113*, 9466-9470.

356   Masiukiewicz, E.; Rzeszotarska, B.; AN IMPROVED SYNTHESIS OF tert-BUTYL N(alpha)-tert-BUTOXYCARBONYL-L-(S-TRITYL)CYSTEINATE, *Org. Prep. Proc. Int.* **1999**, *31*, 571-572.

357   Villard, S.; Grailly, S.; Benhida, A.; Saint-Remy, J.-M.; Granier, C. In *Peptides 2000, Proceedings of the European Peptide Symposium*; Martinez, J., Fehrentz, J.-A., Eds.; Editions EDK: Paris, 2000; pp 905-906.

358   Jacquemin, M.; Benhida, A.; Peerlinck, K.; Desqueper, B.; Elst, L. V.; Lavend'homme, R.; d'Oiron, R.; Schwaab, R.; Bakkus, M.; Thielemans, K.; Gilles, J. G.; Vermylen, J.; Saint-Remy, J. M.; A human antibody directed to the factor VIIIC1 domain inhibits factor VIII cofactor activity and binding to von Willebrand factor, *Blood* **2000**, *95*, 156-163.